

FINAL REPORT

Mechanisms and Permanence of Sequestered Pb and As in
Soils: Impact on Human Bioavailability

SERDP Project ER-1742

DECEMBER 2016

Dr. Nicholas Basta
Brooke Stevens
Shane Whitacre
The Ohio State University

Dr. Kirk Scheckel
Aaron Betts
**U.S. EPA, ORD/
National Risk Management Research Laboratory**

Dr. Karen Bradham
**U.S. EPA, ORD/
National Exposure Research Laboratory**

Dr. David Thomas
**U.S. EPA, ORD/National Health and Environmental
Effects Research Laboratory**

Dr. Chris Schadt
Biosciences Division, Oak Ridge National Laboratory

Distribution Statement A
This document has been cleared for public release



Page Intentionally Left Blank

This report was prepared under contract to the Department of Defense Strategic Environmental Research and Development Program (SERDP). The publication of this report does not indicate endorsement by the Department of Defense, nor should the contents be construed as reflecting the official policy or position of the Department of Defense. Reference herein to any specific commercial product, process, or service by trade name, trademark, manufacturer, or otherwise, does not necessarily constitute or imply its endorsement, recommendation, or favoring by the Department of Defense.

Page Intentionally Left Blank

REPORT DOCUMENTATION PAGE					Form Approved OMB No. 0704-0188
<p>The public reporting burden for this collection of information is estimated to average 1 hour per response, including the time for reviewing instructions, searching existing data sources, gathering and maintaining the data needed, and completing and reviewing the collection of information. Send comments regarding this burden estimate or any other aspect of this collection of information, including suggestions for reducing the burden, to the Department of Defense Executive Service Directorate (0704-0188). Respondents should be aware that notwithstanding any other provision of law, no person shall be subject to any penalty for failing to comply with a collection of information if it does not display a currently valid OMB control number.</p> <p>PLEASE DO NOT RETURN YOUR FORM TO THE ABOVE ORGANIZATION.</p>					
1. REPORT DATE (DD-MM-YYYY) 31-05-2016		2. REPORT TYPE Final		3. DATES COVERED (From - To) 05/27/2010 - 11/27/2015	
4. TITLE AND SUBTITLE Mechanisms and Permanence of Sequestered Pb and As in Soils: Impact on Human Bioavailability			5a. CONTRACT NUMBER NA		
			5b. GRANT NUMBER NA		
			5c. PROGRAM ELEMENT NUMBER NA		
6. AUTHOR(S) Basta, Nicholas (PI) Stevens, Brooke; Whitaere, Shane; Scheckel, Kirk ; Betts, Aaron; Bradham, Karen; Schadt, Chris; Thomas, Dave; Chaney, Rufus			5d. PROJECT NUMBER ER-1742		
			5e. TASK NUMBER NA		
			5f. WORK UNIT NUMBER NA		
7. PERFORMING ORGANIZATION NAME(S) AND ADDRESS(ES) The Ohio State University, School of Natural Resources, 2021 Coffey Rd., Columbus OH 43210 USEPA, NRMRL, Cincinnati, OH 45224-1702; USEPA NERL, Research Triangle Park, NC 27711; USEPA NHEERL, Research Triangle Park, NC 27711; Oak Ridge National Laboratory, Oak Ridge, TN 37831-6038; USDA ARS, BARC, Beltsville MD 20705			8. PERFORMING ORGANIZATION REPORT NUMBER NA		
9. SPONSORING/MONITORING AGENCY NAME(S) AND ADDRESS(ES) Strategic Environmental Research and Development Program (SERDP) 4800 Mark Center Drive, Suite 17D08, Alexandria, VA 22350-3605			10. SPONSOR/MONITOR'S ACRONYM(S) SERDP		
			11. SPONSOR/MONITOR'S REPORT NUMBER(S) ER-1742		
12. DISTRIBUTION/AVAILABILITY STATEMENT Available for public release; distribution is unlimited					
13. SUPPLEMENTARY NOTES					
14. ABSTRACT Results from ER-1742 provide site managers/risk assessors the following defensible science to implement bioavailability. All of the IVBA methods can be used to predict RBA As. The CAB was more accurate for low RBA As soils and for soils with high reactive Al and Fe oxides. Non-CAB methods underpredicted RBA As for these soils. IVBA methods using gastric extraction provide a more conservative RBA As. Equations to predict RBA As from an IVBA method that has a valid IVIVC with one animal model. Arsenic speciation alone is not predictive of IVBA or RBA As. However, As speciation is very important to provide useful information to decide whether to consider adjusting for bioavailability in a risk assessment. Results from ER-1742 show sequestered Pb in P-treated soil is stable. Neither biological fungal treatments or chemical acidification ($\text{pH} > 3$) affected Pb mobility, bioaccessibility or bioavailability in P-treated soils. Low bioavailability mineral forms of Pb formed from P treatment in Joplin contaminated soil has remained stable over a long period of time (> 10 y). The Pb minerals in the P treated soil are stable to acid inputs (i.e., natural or fertilizer, acid rain, etc) to very acidic soil $\text{pH} \geq 3$.					
15. SUBJECT TERMS Bioavailability, bioaccessibility, arsenic, lead, site cleanup, risk assessment, soil remediation, contaminant speciation, metals					
16. SECURITY CLASSIFICATION OF: a. REPORT U		17. LIMITATION OF ABSTRACT UU		18. NUMBER OF PAGES	19a. NAME OF RESPONSIBLE PERSON Nicholas Basta
b. ABSTRACT U		c. THIS PAGE U			19b. TELEPHONE NUMBER (Include area code) 614-292-6282

Page Intentionally Left Blank

Table of Contents

List of Figures	iv
List of Tables	vi
Acronyms and Abbreviations	viii
Abstract	1
Objectives	3
Background	4
Materials and Methods.....	8
Task 1: Study Soils	10
Task 2: Speciation of As in Soils by Advanced Spectroscopy	15
Task 3: In Vivo Bioavailability	20
Task 4: In Vitro Arsenic Bioaccessibility.....	23
Task 5: Cross-correlation and Statistical Analysis	27
Task 6: Mechanisms and Permanence of Sequestered Pb in Soils: Impact on Human Bioavailability.....	28
Task 7: Bioavailability and Technology Transfer	33
Results and Discussion	35
Task 1: Study Soils	35
Task 2: Speciation of As in Soils by Advanced Spectroscopy	43
Task 3: In Vivo Bioavailability	61
Task 4: In Vitro Arsenic Bioaccessibility.....	68
Task 5: Cross-correlation and Statistical Analysis	72
Task 6: Mechanisms and Permanence of Sequestered Pb in Soils: Impact on Human Bioavailability.....	80
Task 7: Bioavailability and Technology Transfer	98
Conclusions and Implications for Future Research/Implementation.....	100
Literature Cited	106
Appendix A. Supporting Data	114
Appendix A.1 Tables and Figures Cited in Results and Discussion	114
Appendix A.2 Typical Experimental Design for Juvenile Swine Bioassay	139
Appendix B. List of Scientific and Technical Publications	145

List of Figures

	Page
Figure 1. Technical approach experimental design of ER-1742. Mechanism of sequestered As in soils and impact on human bioavailability	9
Figure 2. Technical approach experimental design of ER-1742. Biological and chemical processes and long-term permanence of Pb-contaminated soils	10
Figure 3. Map of soil source locations for all study soils	13
Figure 4. Arsenic fractionation by sequential extraction procedure. All results are expressed as a percentage of total soil As in each SEP fraction	44
Figure 5. Energy positions of arsenic standards grouped by oxidation and coordinated elements	46
Figure 6. As soil groupings determined via PCA analysis	52
Figure 7. Principle component analysis and groupings identified using Fe XANES species groups	62
Figure 8. Relationship between mice % RBA vs total As concentration (mg/kg) for soils < 1000 mg As/kg	64
Figure 9. Relationship between swine % RBA vs total As concentration (mg/kg) for soils <1000 mg As/kg	65
Figure 10. Percent RBA for 14 soils determined using both the adult mouse and juvenile swine models	66
Figure 11. Comparison of 90% confidence intervals for 14 soils determined using both the adult mouse and juvenile swine bioassays	67
Figure 12. Percentage of juvenile swine RBA recovered by adult mouse bioassay	68
Figure 13. Simple linear regression of soils dosed to both mice and swine. Dashed line is a 1:1 unity line. Solid is Swine %RBA vs Mice % RBA linear regression	68
Figure 14. Representative photomicrograph (100X) of monolayer exposure to diluted aqueous fraction for 4 h. Domes and areas of detached cells in cultures incubated for 4 h with diluted (1:4) aqueous fraction from control and 225 soil	71
Figure 15. LDH activity in spent media after exposure to diluted aqueous fraction generated during digestion of control solution and soil 225. Data are mean \pm SD, n = 3 per treatment	72
Figure 16. Monolayers of cell at 2-day post-confluence As was taken up at >70% confluence and 11-day post-confluence (panel A) and cell uptake of As during different stages of cell confluence showed time- and dose-dependent manner (panel B)	72
Figure 17. IVIVC for adult mouse % RBA vs % IVBA for gastric phases. IVIVC are labeled accordingly (A) Glycine (B) PBET (C) UBM (D) OSU IVG (E) CAB	75
Figure 18. IVIVC for juvenile swine % RBA vs % IVBA for gastric phases. Figure label designations are the same as described in Figure 17	76

Figure 19. IVIVC for adult mouse % RBA vs % IVBA for intestinal phases. Figure label designations are the same as described in Figure 17	78
Figure 20. IVIVC for juvenile swine % RBA vs % IVBA for intestinal phases. Figure label designations are the same as described in Figure 17	79
Figure 21. IVIVC for adult mouse % RBA vs % IVBA for gastric phases using the Bayesian approach. Dashed lines are 95% model prediction interval	80
Figure 22. Approximate sampling transects of the firing range at the Oak Ridge National Laboratory with B for the firing backstop, F for the forested transect, and G for the grassy transect	82
Figure 23. Organic acid secretion by <i>A. niger</i> and each soil fungal isolate into either 1% Czapek Dox broth (A) or 1% malt extract broth (B) determined via HPLC analysis of the supernatant after 120 h of incubation at 30°C on a rotary shaker.....	84
Figure 24. Hyphal growth (bars) and zone of clearing (points) for each isolate grown on malt extract agar for 120 h at 21°C with Pb carbonate incorporated into the medium at the equivalent of 2.5 mM (A), 10 mM (B), or 18.5 mM (C)	86
Figure 25. Proportion (%) of hits for each isolate's LSU rRNA gene sequence within the 454 pyrosequence data from each soil sample ($\geq 97\%$ identity), calculated as the number of hits for an isolate in a sample over the total number of fungal sequences for that sample	87
Figure 26. SPLP Pb results for ORNL treatments	89
Figure 27. SPLP Pb results for Joplin treatments	90
Figure 28. OSU-IVG IVBA Pb results for ORNL soil treatments	91
Figure 29. OSU-IVG IVBA Pb results for Joplin soil treatments	92
Figure 30. In vitro extractable Pb with U.S. EPA 1340 pH 1.5, U.S. EPA 1340 pH 2.5, and OSU-IVG along with mouse RBA Pb for control and P treated (with and without fungus) ORNL	94
Figure 31. In vitro extractable Pb with U.S. EPA 1340 pH 1.5, U.S. EPA 1340 pH 2.5, and OSU-IVG along with mouse RBA Pb for control and P treated (with and without fungus) Joplin soils	94
Figure 32. IVIVC (with 95% confidence intervals) of ORNL and Joplin no treatment controls and P treatments (with and without fungus) with the U.S. EPA 1340 pH 1.5 (A), U.S. EPA 1340 pH 2.5 (B), U.S. EPA 1340 pH 1.5 for control soils and U.S. EPA 1340 pH 2.5 for P treatments (C), and OSU-IVG pH 2.5 (D)	95
Figure 33. Pb Species in ORNL soil treatments; organic bound, mineral bound, pyromorphite, Pb carbonate, and Pb sulfate	96
Figure 34. Pb Species in Joplin soil treatments; organic bound, mineral bound, pyromorphite, Pb carbonate, Pb sulfate, and galena	97
Figure 35. Pb solubility across pH for control and P-treated ORNL soil	98
Figure 36. Pb solubility across pH for control and P-treated Joplin soils	98

List of Tables

	Page
Table 1. Source and geographic locations of 27 As-contaminated study soils	12
Table 2. List of natural and synthetic As-bearing minerals used for linear combination fits (LCF) to predict As phases in the soil samples	18
Table 3. List of natural and synthetic Fe-bearing minerals used for linear combination fits (LCF) to predict Fe phases in the soil samples	19
Table 4. Animal models utilized for the assessment of As relative bioavailability in contaminated soil	21
Table 5. Human gastric and intestinal physiological parameters including pH, Time in hours (h), soil:solution ratio (g:mL), ascorbic acid (AA) secretion rate, as well as sodium chloride (NaCl), pancreatin, and bile concentrations	24
Table 6. Extraction parameters for in vitro bioaccessibility methods used in this study	25
Table 7. Selection of in vitro bioaccessibility method for this study – parameters and published references	26
Table 8. Total elemental content determined using microwave-assisted acid digestion U.S. EPA Method 3051a	37
Table 9. Soil content of major elemental constituents expressed on an oxide basis	39
Table 10. Soil properties relevant to As solubility and bioaccessibility	41
Table 11. Comparison of total As determined by U.S. EPA 3051a and INAA for study soils .	42
Table 12. Arsenic K-edge e0 positions and % of oxidation from LC	47
Table 13. As species groupings determined via LCF for As EXAFS and XANES	48
Table 14. Results of LCF from As EXAFS and XANES	50
Table 15. Principle component coefficients for As EXAFS and XANES species groups	52
Table 16. Comparison of oxidation state from Mössbauer and Fe XAS LCF models	54
Table 17. Mössbauer room temperature (298K) oxidation and coordination result	56
Table 18. Mössbauer results showing the increase in magnetic ordering with decreasing temperature in selected soils	58
Table 19. Iron species groupings from iron linear combination fitting of K-edge XANES summary	59
Table 20. Fe LCF of K-edge XANES summary	60
Table 21. Principle component coefficients for Fe XANES species groups	61
Table 22. Adult mice and juvenile swine RBA values with 90% confidence intervals for all study soils	63
Table 23. Comparison of study soils that were dosed to both swine and mice	66

Table 24. Bioaccessibility results for all soils in the study	70
Table 25. Protein content of wells with Caco-2 cells after exposure to diluted aqueous fraction from simulated digestion of soil. Data are mean \pm SD, n = 3 per treatment	71
Table 26. Considerations for applying in vitro methods to predict RBA As	81
Table 27. Laboratory-determined values for moisture, pH, and heavy metals commonly found at shooting ranges for the homogenized and sieved soils collected from the abandoned ORNL firing range on 2 July 2010	83
Table 28. Relative bioavailable Pb for ORNL and Joplin sites and treatments	93

Acronyms and Abbreviations

ABA	Absolute bioavailability
Al	Aluminum
APS	Advanced Photon Source
ARS	Agricultural Research Service
As	Arsenic
CZ	Czapek Dox
DoD	Department of Defense
DOE	Department of Energy
ESTCP	Environmental Security Technology Certification Program
EXAFS	Extended x-ray absorption fine structure spectroscopy
Fe	Iron
GCMS	Gas chromatography - mass spectrometry
GE	Gastric extractable
GI	Gastrointestinal
HDPE	High density polyethylene
HHRA	Human health risk assessment
ICP-MS	Inductively coupled plasma - mass spectrometry
ICP-OES	Inductively coupled plasma – optical emission spectrometry
IE	Intestinal extractable
IRIS	Integrated Risk Information System
IVBA	In vitro bioaccessibility
IVG	In vitro gastrointestinal
LCF	Linear combination fitting
LDH	Lactate dehydrogenase
MCL	Maximum contaminant level
ME	Malt extract
Mn	Manganese
NERL	National Exposure Research Laboratory
NHEERL	National Health and Environmental Effects
NRC	National Research Council
NRMRL	National Risk Management Research Laboratory
OAH	Oxaloacetate acetylhydrolase
ORNL	Oak Ridge National Laboratory
OSU	Ohio State University
OTU	Operational taxonomic unit
P	Phosphorus
Pb	Lead
PBET	Physiologically Based Extraction Test
PBPK	Physiologically based pharmacokinetic
PBS	Phosphate buffered saline
PCR	Polymerase chain reaction
PIMS	Phosphate-induced metal stabilization

QPCR	Quantitative polymerase chain reaction
RBA	Relative bioavailability
RBALP	Relative bioaccessibility leaching procedure
rDNA	Recombinant DNA
rRNA	Recombinant RNA
S	Sulfur
SBRC	Solubility Bioaccessibility Research Consortium assay(<i>SBRC</i>)
SERDP	Strategic Environmental Research & Development Program
SPLP	Synthetic precipitation leaching procedure
SRM	Standard reference materials
TRW	Technical Review Workgroup
UBM	Unified BARGE Method
U.S. EPA	U.S. Environmental Protection Agency
XAFS	X-ray absorption fine structure spectroscopy
XANES	X-ray near edge structure spectroscopy
XAS	X-ray absorption spectroscopy
XRF	X-ray fluorescence
ZOC	Zone of clearing

Abstract

Objectives

Arsenic is one of the most common contaminants of concern exceeding risk criteria because soil ingestion is the primary human health risk driver at many DoD sites. Use of contaminant total content instead of bioavailability is often overly conservative and can result in costly and unnecessary soil remedial action. Bioavailability-based in situ remediation of Pb-contaminated soil by using inexpensive and widely available phosphorus soil amendments is a proven technology. This technology has been used to remediate soil on firing ranges of DoD sites by reducing Pb bioavailability and exposure. Concern over the long-term effect of key biological and chemical processes on bioavailability of sequestered Pb is a barrier for implementation of this successful technology. The specific objectives of ER-1742 were to (1) conduct a comprehensive study to link the binding mechanism of As in soil (i.e., speciation) with in vitro and in vivo methods used to predict current and potential future bioavailability of soil As to humans, and (2) evaluate the effect of key biological and chemical processes on the permanence of binding and bioavailability of Pb in untreated and treated (i.e., remediated) soils.

Technical Approach

Bioaccessibility, Bioavailability, and Chemical Speciation of Arsenic in Soils

Twenty-seven As contaminated soils that represent a wide variety of properties and As sources from DoD installations, industrial sites (mining, smelting, and glass production), residential and agricultural sites were studied. Contaminant binding mechanisms were determined via speciation using As and Fe XAS EXAFS and Mössbauer spectroscopy by U.S. EPA NRMRL. Relative bioavailability (RBA) of As was determined by the adult mouse bioassay by U.S. EPA NHEERL / NERL and the juvenile swine bioassay by the Univ. of Missouri. In vitro bioaccessible (IVBA) As was determined by the OSU, UBM, PBET, CAB and U.S. EPA Method 9200 IVBA methods by The Ohio State University. In vivo in vitro correlations (IVIVC) were used to evaluate the ability of IVBA methods to predict RBA.

Mechanisms and Permanence of Sequestered Pb in Soils: Impact on Human Bioavailability

Key biological and chemical processes were evaluated for soils from two contaminated sites which were remediated by P soil amendment; A firing range at the Oak Ridge National Laboratory and a Pb-smelter impacted site in Joplin, MO. Soils were incubated with fungus that has the potential to increase Pb bioavailability and mobility. Soils were subjected to soil chemical acidification. Fungal treatments were evaluated pre- and post-incubation by determining (1) IVBA Pb by OSU IVG and U.S. EPA 1340 pH 2.5, (2) RBA Pb from mouse bioassays, (3) Pb speciation by XAS EXAFS, and (4) mobility using SPLP U.S. EPA Method 1312. The effect of soil chemical acidification was determined by measuring dissolved Pb from liquid solid partitioning extraction across pH 1 – 13 (U.S. EPA Method 1313).

Results

Bioaccessibility, Bioavailability, and Chemical Speciation of Arsenic in Soils

Total soil As ranged from 162 to 12,500 mg/kg with a median value of 464 mg/kg. The most abundant As species was As(V) adsorbed to Fe oxides. Other As species included As (-III) metal sulfides, As (III) sulfides, As (III) oxides, As (III) adsorbed to Fe/ Al oxides, lead arsenates, and hydrous ferric arsenates (HFA). RBA As ranged from 6.37 to 81.2%. IVBA As ranged from <1% to 100%. Median and mean IVBA As followed the trend CAB (pH 1.5) >

UBM (pH 1.2) \approx OSU (pH 1.8) \approx PBET (pH 1.8) \approx Glycine (pH 1.5). In vivo-in vitro correlation (IVIVC) analysis showed all of the IVBA methods were predictive of RBA for both the mice and swine bioassays. Linear regression coefficient of determination (r^2) values for IVIVC using mouse RBA were OSU IVG (0.89) \geq UBM (0.84), PBET = Glycine (0.82) \geq CAB (0.74) and using the swine method were OSU IVG (0.73) \geq UBM (0.67), PBET (0.63) \geq Glycine (0.60) \geq CAB (0.54). Swine RBA As was greater than mouse RBA As. However, variability in RBA As is larger for swine than mouse. CAB was more accurate for low RBA As soils and for soils with high reactive Al and Fe oxides. Despite As(V) adsorbed to mineral surfaces being a major component of most soils (>50%), these soils ranged from ~20-80% in IVBA As and widely ranged in RBA As. Arsenic speciation alone is not predictive of IVBA or RBA As. However, As speciation is very important to provide information on IVBA or RBA As results and/or determine *a priori* if a bioavailability-based risk assessment is justified.

Mechanisms and Permanence of Sequestered Pb in Soils: Impact on Human Bioavailability

Fungi isolated from soil produced low molecular weight organic acids (LMWOA) and dissolved PbCO_3 in laboratory medium. However, the LMWOA-isolated fungus inoculated into study soils (ORNL, Joplin) has no effect on Pb solubility, mobility and bioavailability. Soil treatment with P produced Pb minerals, including Pb pyromorphite, that were much more stable to LMWOA than PbCO_3 . Soluble Pb sharply increased at pH < 4 for the untreated control soil and pH < 3 for the P-treated soil. The P-treatment extended the insolubility of Pb from pH 4 to pH 3.

Benefits

Results from ER-1742 provide site managers and risk assessors the following defensible science to implement bioavailability. All of the IVBA methods can be used to predict RBA As. The CAB was accurate for low RBA As soils and for soils with high reactive Al and Fe oxides. Non-CAB methods underpredicted RBA As for several soils with high concentrations of reactive Al and Fe oxides. IVBA methods using gastric extraction provide a more conservative RBA As. Predictive equations can be used to predict RBA As for all IVBA gastric extraction methods. Arsenic speciation alone is not predictive of IVBA or RBA As. However, As speciation is very important to provide useful information to decide whether to consider adjusting for bioavailability in a risk assessment. Arsenic species with low RBA As are excellent candidates for exposure adjustment using in vitro extraction methods (i.e., IVBA) or in vivo data from animal models (i.e., RBA).

Results from ER-1742 show sequestered Pb in P-treated soil is stable. Neither biological fungal treatments or chemical acidification (pH > 3) affected Pb mobility, bioaccessibility or bioavailability in P-treated soils. Low bioavailability mineral forms of Pb formed from P treatment in Joplin contaminated soil has remained stable over a long period of time (>10 y). The Pb minerals in the P treated soil are stable to acid inputs (i.e., natural or fertilizer, acid rain, etc.) to very acidic soil pH \geq 3. Pb contaminated soils with large amounts of sulfidic waste (i.e., mining waste) should be treated with adequate alkaline soil amendments (i.e., agricultural limestone) to neutralize excessive amounts of future acidity and maintain soil pH > 4.

A major finding of our study is U.S. EPA method 1340 is not suitable for evaluating the bioaccessibility and bioavailability of P treated soils. A modified Method 1340, extracting solution of pH 2.5 instead of 1.5, or another method (i.e., OSU IVG) should be used to evaluate IVBA and RBA Pb in soil treated with P. These results are consistent with findings reviewed by

Henry et al. (2015). Limited studies have reported U.S. EPA method does not accurately measure reduction in IVBA Pb or RBA Pb in P-treated soil and recommend changing the extraction pH from 1.5 to 2.5 in U.S. EPA Method 1340. The ability of U.S.EPA Method 1340 with an extraction pH of 2.5 to predict RBA Pb in soils treated with phosphorus and other soil amendments known to reduce RBA Pb should be researched. Research should be conducted with procedures outlined by the U.S. EPA Technical Review Workgroup (U.S. EPA, 2007a) and other committees focused on acceptable methodologies for regulatory acceptance including the Interstate Technology and Regulatory Council (ITRC) “Bioavailability in Contaminated Soil” workgroup.

Objectives

Project ER-1742 is in response to the research needs within the Strategic Environmental Research and Development Program (SERDP) Environmental Restoration Focus Area “Mechanisms of Contaminant Interaction with Soil Components and its Impact on the Bioavailability of Contaminants,” ERSO-10-03. This project addressed the “soils critical priority need” regarding the “mechanisms of interaction of contaminants with soil components” specifically identified by the SERDP and ESTCP Expert Panel Workshop on Research and Development Needs for Understanding the Bioavailability of Contaminants in Soils and Sediments (SERDP, 2008). The panel identified five overarching issues that future research and development activities must address to realize the use of bioavailability in human health risk assessment (HHRA). Our proposal addressed three of the five overarching issues: (1) need for the weight-of-evidence assessments, (2) improving the technology transfer process, and (3) challenges with biological assessments and modeling uptake.

The specific objectives of ER-1742 were to:

- Conduct a comprehensive study to link the binding mechanism of As in soil (i.e., speciation) with in vitro and in vivo methods used to predict current and potential future bioavailability of soil As to humans.
- Evaluate the effect of key biological and chemical processes on the permanence of binding and bioavailability of Pb in untreated and treated (i.e., remediated) soils.
- Perform technology transfer from the project via the U.S. EPA Bioavailability Technical Review Workgroup Committee.

Background

Lead (Pb) and arsenic (As) are the most common metals exceeding risk criteria because soil ingestion is the primary human health risk driver at many DoD sites contaminated with toxic metals. Exposure assessment is used to quantify the amount of chemical received as a dose following exposure to contaminated site soils. Exposure must be quantified considering the magnitude, frequency, and duration of exposure for the receptors and pathways selected for quantitative evaluation. For incidental ingestion, the following formula is used to quantify average daily chemical intake (U.S. EPA, 1989):

$$CDI = \frac{(CS)(IR)(CF)(BIO)(EF)(ED)}{(BW)(AT)} \quad (1)$$

where CDI = chemical daily intake ($\text{mg kg}^{-1}\text{d}^{-1}$); CS = chemical concentration in soil (mg kg^{-1}); IR = ingestion rate (mg soil d^{-1}); CF = conversion factor ($10^{-6} \text{ kg mg}^{-1}$); BIO = bioavailable fraction ingested from contaminated source (unitless); EF = exposure frequency (days y^{-1}); ED = exposure duration (y); BW = body weight (kg); and AT = averaging time (average exposure period - days, typically 70 y).

The CS variable, chemical concentration in soil, is a site-specific value measured by performing total metals analysis. The underlying assumption, in quantifying metal intake by the above formula, is that some or all of the soil contaminant (i.e., Pb or As measured) by the total metal analysis is quantified as the absorbed dose. However, there is an inherent problem with the above assumption. For an adverse health effect to be realized, the chemical toxicant (in this case, the metal) must be dissolved for Pb or As absorption to occur. Forms of Pb or As found in contaminated soils may not be soluble under conditions associated with human ingestion.

It is well known that Pb and As react with soil components to form insoluble sorbed or mineral phases ranging from weakly bound and potentially bioavailable (i.e., bioaccessible) forms to strongly bound and non-bioavailable forms (Chaney et al., 2008). Many studies have shown soil can decrease Pb or As bioaccessibility and/or bioavailability (Scheckel et al., 2009). There have been many studies on human bioaccessibility of Pb and As in soil (Ruby et al., 1999; Zia et al., 2011). Bioaccessible As was correlated with swine bioavailability (Rodriguez et al., 2003; Basta et al., 2007a) and inversely correlated with As as Fe minerals (i.e., scorodite) or sorbed to Fe oxide surfaces (Basta et al., 2007b). However, the effect of soil type and chemistry is very limited.

Previous research on contaminant bioaccessibility has predominantly focused on soils contaminated with mining and smelting waste associated with ore extraction. Most studies have focused on smelter-contaminated soils with high contaminant concentrations and contaminant solid phases (i.e., slag) unique to smelter-contaminated sites. The chemistry of As in low level contaminated non-smelter soils will likely be very different than high level contaminated smelter soils. Most contaminated soils subject to risk assessment at DoD sites will not contain As solid wastes found at smelter sites. Therefore, research is needed to investigate As bioaccessibility for DoD soils contaminated with As.

Contaminant solid phase speciation of metals is an approach that can accurately characterize the form and relative bioaccessibility in soil and mining and smelting waste. Advanced spectroscopic methods that accurately characterize specific forms (i.e., species) of Pb

and As sorbed to soils and waste materials have been reported (Ryan et al., 2004; Scheckel and Ryan, 2004). Several excellent spectroscopic methods are available that are capable of determining metal speciation, but the most authoritative approach involves the application of synchrotron methods such as x-ray absorption spectroscopy (XAS). Information gleamed from XAS experiments provides an in situ look at the current chemical form of a metal and can be used to predict the long-term fate of the metal and its potential bioavailability based on known solubility products.

Mechanisms of Sequestered As in Soils and Impact on Human Bioavailability

Soil properties and contaminant speciation greatly affect bioavailability but neither soil properties or speciation methods are used to determine exposure in a human health risk assessment (HHRA). The RBA term in the CDI risk equation (above) is determined using appropriate animal bioassays or from in vitro gastrointestinal methods correlated with these animal bioassays. Determining RBA As or RBA Pb requires knowledge of the amount of soil As or Pb dose that is absorbed into the systemic circulation. To date, the most suitable methods for evaluating As RBA involve the measurement of As in urine, blood, and/or feces following the administration of contaminated soil to animals such as swine, monkeys, and mice (Basta and Juhasz, 2014). The juvenile swine and primate models are costly, ranging from \$25,000-100,000 per soil; and the time required is approximately 3-6 months. Risk assessments that adjust for metal bioavailability may reduce the burden of unnecessary and costly remedial action. Even small adjustments in oral bioavailability can result in significant impacts on estimated risks and cleanup goals. Specifically, the Framework for Metals Risk Assessment and the Office of Solid Waste and Emergency Response have recognized the need to develop bioavailability tools (U.S. EPA, 2007a). Because of the large number of contaminated sites that may need to be evaluated, faster and less expensive in vivo and in vitro models are desirable. The mouse model, developed by U.S. EPA scientists, are a less expensive in vivo model for evaluating the bioavailability of As-contaminated soils. The in vivo techniques represent RBA As or Pb, however, these techniques are costly, time consuming, and are not conducive to rapid and routine screening of contaminated sites. To overcome these disadvantages, in vitro methods were developed that simulate the GI biochemistry of the human GI tract and that act as a surrogate for the in vivo techniques. The science of contaminant bioaccessibility has matured and several IVG methods have been reported. Guidance has been issued by U.S. EPA for the Relative Bioavailability Leaching Procedure (RBALP) of Drexler and Brattin (2007) for calculating RBA Pb in HHRA. However, guidance has not been issued by U.S. EPA for any in vitro methods for calculation of RBA As. Several in vitro methods, including the OSU IVG for As (Basta and Juhasz, 2014; Basta et al., 2007a), have met the U.S. EPA requirement that an IVG method used for HHRA must be correlated with an acceptable in vivo model (U.S. EPA, 2007a). However, further investigation is needed to demonstrate which of these methods are accurate predictors of RBA as for a wide range of soil and wastes on DoD and other contaminated sites.

A major objective of ER-1742 is to comprehensively evaluate the ability of in vitro gastrointestinal methods with currently published IVIVC to predict RBA for a wide range of soils and contaminant sources representative of As-contaminated soils DoD installations. We have selected the soils from previous U.S. EPA, SERDP, and ESTCP studies to represent a range of binding mechanisms and hence range of As bioavailability to humans.

Biological and Chemical Processes and Long-term Permanence of Pb-contaminated Soils Remediated by In Situ Soil Amendments

Excavation and replacement of contaminated soil is very expensive and ecologically destructive. A cost effective alternative remedial option is *in situ* soil amendments that reduce contaminant bioavailability. Such “bioavailability-based remediation” does not remove the soil contaminant but reduces its bioavailability and potential exposure and risk. Extensive research has shown a variety of soil amendments can successfully reduce Pb bioavailability. The subject has been comprehensively reviewed (Scheckel et al., 2013; Hettiarachchi and Pierzynski, 2004). Uncertainty in the long-term permanence of reduced Pb bioavailability in soil remediated by soil amendments is a major barrier to acceptance of this bioavailability-based remediation technology. Lead is the most common metal soil contaminant at DoD installations and many DOE and U.S. EPA cleanup sites. In situ remediation of Pb bioavailability using soil amendments would greatly reduce the burden of unnecessary and costly remedial action because soil excavation and replacement is one of the most expensive cleanup costs.

Biological and chemical processes may affect the stability of the Pb species with reduced bioavailability and hence the permanence of the sequestered Pb. Soil pH is a “master variable” that often governs many soil chemical and biological processes. Lead bioavailability is greatly increased under strongly acidic conditions ($\text{pH} < 4$). Although the effect of soil pH on Pb solubility/adsorption in soil is well known, little is known of their quantitative effect on Pb speciation or human bioavailability. Metal-reducing bacteria and fungi may also impart biological processes that affect the long-term stability of soil-metal complexes for Pb in both unamended and amended soils. Certain fungi and soil microorganisms have been shown to disrupt the solubility of soil-metal precipitates. Solubilization of inorganic nutrients from minerals is essential for soil microbial survival. Many species of fungi may be able to transform relatively stable, insoluble, phosphate-bound forms of Pb (such as pyromorphite) into highly soluble and bioavailable derivatives (Sayer et al., 1995, 1999). In the soil environment, the solubilization of inorganic nutrients and micronutrients from insoluble mineral forms is essential for microbial growth and survival. Therefore, many microorganisms have various mechanisms for accomplishing this. Of particular importance to this proposal, many species of free-living and symbiotic fungi are now known to be capable of transforming relatively stable, insoluble, phosphate-bound forms of Pb (such as pyromorphite) into soluble and bioavailable derivatives (Sayer et al., 1995, 1999). The primary mechanism for such transformations seems to be the overproduction and excretion of oxalic acid (and to a lesser extent citric acid) by aerobic fungi that may be present in soils (Strasser et al., 1994; Gadd, 1999). The presence of significant oxalate in the soil environment also may influence the bioavailability of As in contaminated soils. Oxalate effectively compete for solid phase sorption sites associated with As, therefore releasing the contaminant into the pore water as a free ion. In turn, oxalic acid production and secretion in fungi appears to be ultimately dependent upon the expression level of the oxaloacetate acetylhydrolase (OAH) gene (Ruijter et al., 1999; Han et al., 2007). However, only a very limited number of laboratory model species have been studied for this process in detail, and none in species specifically isolated from Pb-contaminated soils.

A major objective of ER-1742 is to determine the effect of soil chemical and biological processes known to have potential to mobilize Pb sequestered from *in situ* soil amendment remediation.

Research in this project is being conducted to determine the relationship between chemical contaminant molecular speciation and solid phase binding mechanisms with in vivo and in vitro models used to estimate human bioavailability for unamended and amended soils. Our goal is to provide science and technology transfer to increase the confidence level of site managers to incorporate site-specific bioavailability measures into site management decisions based on technically defensible cleanup goals while ensuring protection of human health and the environment.

Materials and Methods

The transdisciplinary, multi-institutional, experimental design of ER-1742 is summarized in Fig. 1 and Fig 2. Our research team is composed of eight members: Dr. Nicholas T. Basta (Lead Principal Investigator, PI), The Ohio State University (OSU); Dr. Kirk Scheckel (co-PI), U.S. EPA NRMRL, Dr. Karen Bradham (co-PI), U.S. EPA NERL, Dr. David Thomas (co-PI), U.S. EPA NHREEL, Dr. Philip Jardine, deceased (co-PI), University of Tennessee at Knoxville; Dr. Christopher Schadt (co-PI), Oak Ridge National Laboratory (ORNL); Dr. Mark Failla (co-PI), The Ohio State University, and Dr. Rufus Chaney, USDA ARS. The study design of ER-1742 is divided into two separate efforts: (1) mechanism of sequestered As in soils and impact on human bioavailability of 29 As-contaminated soils (Fig. 1) and (2) the effect of biological and chemical processes on long-term permanence or sequestered Pb (Fig 2).

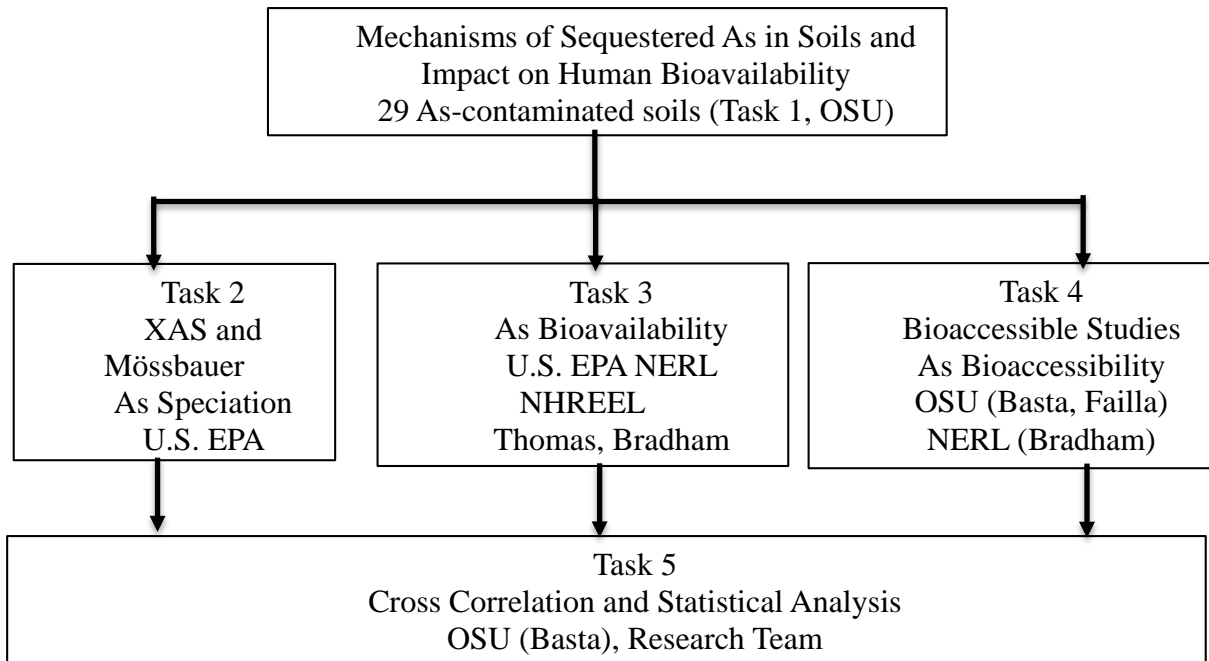


Figure 1. Technical approach experimental design of ER-1742. Mechanism of sequestered As in soils and impact on human bioavailability.

A total of 29 soils, many from DoD facilities with known sequestration properties for As, were processed and distributed from OSU (Fig. 1). Contaminated soil from two sites where the soil was treated to reduce Pb bioavailability was studied. Contaminant binding mechanisms of Pb and As were determined via surface chemical speciation using advanced spectroscopic techniques by U.S. EPA NRMRL personnel. Bioavailability of Pb and As were determined by using two in vivo bioassays models, the adult mouse model (U.S. EPA NHEERL and NERL), and the juvenile swine model (Univ. of Missouri, OSU). Bioaccessible As was determined by five in vitro gastrointestinal methods (OSU, UBM, PBET, CAB and U.S. EPA Method 9200 method (U.S. EPA NERL).

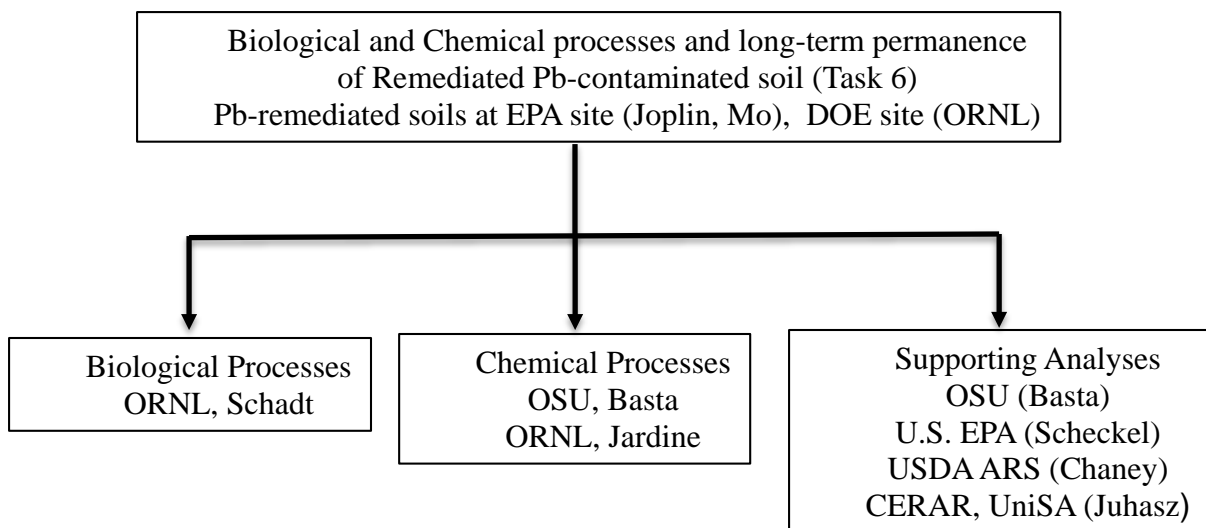


Figure 2. Technical approach experimental design of ER-1742. Biological and chemical processes and long-term permanence of Pb-contaminated soils

The effect of key biological and chemical processes on the permanence of binding and bioavailability of Pb in untreated and treated (i.e., remediated) soils was determined in Task 6 (Fig. 2). Biological treatment experiments were conducted by Dr. Schadt of Oak Ridge National Laboratory. Chemical treatment studies were conducted by OSU and Dr. Jardine of ORNL. Supporting analyses of biological process studies were provided by OSU, U.S. EPA, the Centre for Environmental Risk Assessment and Remediation (CERAR) and the University of South Australia (UniSA) by Dr. Juhasz. Dr. Juhasz conducted mouse bioassay studies to determine bioavailability of Pb in soils from Dr. Schadt.

The technology imparted by this research will be transferred to the regulatory community. Technology transfer is described in Task 7.

Bioaccessibility, Bioavailability, and Chemical Speciation of Arsenic in Soils

Task 1: Study Soils

Soil physical and chemical properties impact the solubility and chemistry of metal(loids) and minerals in soil systems. These properties are unique to each soil and are conserved when the soil is incidentally ingested by humans. To better understand and evaluate the binding mechanisms that impact arsenic contaminated soils when they are ingested by humans the soil physical and chemical properties need to be evaluated.

Twenty-seven arsenic (As) containing soils that represent a wide variety of As sources (Table 1) were collected, homogenized and sieved to <250 µm and distributed to collaborators. Soils were collected from military installations (Department of Defense), industrial sites (mining, smelting, and glass production), residential and agricultural sites. Many of the previously listed collection locations are U.S. EPA superfund or other U.S. EPA research sites. Contamination sources included pesticides, herbicides, rodenticides, Au and Cu mining, and smelting of ores (Cu, Pb, and Zn) (Table 1). Three soils that were spiked with sodium arsenate and aged for at least 12 months were also included in this study. The study soils represented a range of geographical locations and soil type (Figure 3).

Homogenization of the 27 soils was done by mixing air dried soil in an HDPE rotary mixer and analysis via microwave assisted digestion (McClure, 2001). Homogenization analysis was done by dividing the soils into eight equal units then three subsamples from each unit were analyzed, resulting in a total of 24 samples. The means of each unit were calculated and ANOVA tests performed to ensure homogenization. ANOVA testing resulting with no difference within units and between units at a 95% confidence level ($\alpha = 0.05$). The units were combined into one container for laboratory use and distribution to collaborators for all further analysis and animal dosing. One of the 27 soils was NIST SRM 2710A (Montana Soil II) and was not homogenized because homogenization was done prior to certification at NIST. Nineteen soils were dosed using the adult mouse model to determine relative bioavailable As (RBA As). Twenty two soils were dosed using the juvenile swine model to determine relative bioavailable As (RBA As). Fourteen soils were dosed to both the mouse and swine models, descriptions and results regarding animal dosing is presented later in this report.

Table 1. Source and geographic locations of 27 As-contaminated study soils.

ID	General Source	Specific Source	Geographic Location
1	Pesticide	Herbicide and Rodenticide	Hawaii
2	Pesticide	Herbicide	Hawaii
3	Pesticide	Pesticide	California
6	Mining	Gold Mining	Australia
7	Pesticide - Orchard	Pesticide	Pennsylvania
8	Smelter	Copper Smelter	Washington
9	Tailings	Tailings from a Mine Site	Utah
10	Tailings	Tailings from a Mine or Smelter Site	Arizona
11	Mining	Residential Area near Mining	Arizona
12	Mining	Slag from Copper Mining	Utah
13	Mining	Calcine Material from Copper Mining	Utah
14	Spiked	Sodium Arsenate, Weathered	Oklahoma
15	Spiked	Sodium Arsenate, Weathered	Iowa
16	Spiked	Sodium Arsenate, Weathered	Oklahoma
17	SRM	Mining/ Tailings	Montana
18	Pesticide - Orchard	Sprayed Lead Arsenate Pesticide	North Carolina
19	Pesticide - Orchard	Sprayed Lead Arsenate Pesticide	North Carolina
20	Pesticide - Orchard	Sprayed Lead Arsenate Pesticide	North Carolina
21	Pesticide - Orchard	Sprayed Lead Arsenate Pesticide	North Carolina
29	Glass Manufacturing	Manufacturing Site	Illinois
30	Glass Manufacturing	Residential Area near Manufacturing	Illinois
33	Mining	Gold Mining	California
34	Mining	Gold Mining	California
35	Mining	Gold Mining	California
36	Mining	Gold Mining	California
37	Mining	Gold Mining	California
38	Mining	Gold Mining	California

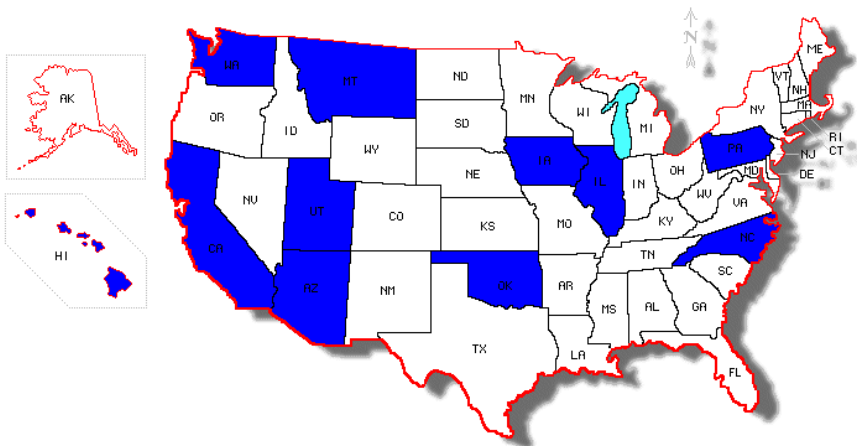


Figure 3. Map of soil source locations for all study soils.

Total Elemental Content

Total elemental content was determined using three different methods. The commonly used microwave assisted acid digestion (U.S. EPA Method 3051a) with subsequent analysis by inductively coupled plasma optical emission spectroscopy (ICP-OES; U.S. EPA Method 6010c) was used to determine metal contaminants and trace elements.

Major elemental content (Si, Al, Fe, Mn, Mg, Ca, Na, K, Ti, P, and V) were determined via fusion analysis. Major elemental analysis of the study soils was done by mixing 0.75g of sieved soil (<250 um) soil with a mixture of lithium metaborate, lithium tetraborate, and lithium bromide (9.75g). Samples were fused in Pt crucibles and poured into Pt molds for casting. Casted samples were analyzed via x-ray fluorescence (XRF) and reported as major element oxides (Norris and Hutton, 1969).

Direct soil analysis for conducted for trace and major elements using was performed with modifications to the U.S. EPA 6200 method using an Olympus X-5000 portable XRF. Each sieved sample (<250um) was placed in a plastic bag and placed over the XRF detector with approximately 0.2 – 0.5 cm soil thickness. Each sample was analyzed in triplicate (1 minute per analysis) for a total of 3 minutes. The three analyses were averaged and reported as one replicate. Mean values were calculated from three replicates. Prior to analysis calibration was preformed using the calibration standard and a standard reference material (NIST 2711a) was also analyzed to ensure proper calibration.

Soil Arsenic Content

Total arsenic content of the soil was determined using three different methods; microwave assisted acid digestion (U.S. EPA Method 3051A), x-ray fluorescence, and instrumental neutron activation analysis (INAA). Microwave assisted acid digestion and x-ray fluorescence were each performed as described above. Instrumental neutron activation analysis (INAA) was performed on sieved soils (<250 um) at the Department of Nuclear Engineering at North Carolina State University in Raleigh, North Carolina as described in Bradham et al. (2011). The mean As mass

detection limit was 0.035 µg (Bradham et al, 2011). Soil arsenic concentrations determined via INAA was available for 21 of the 27 soils.

Major Soil Properties

Soil pH and Electrical Conductivity (EC): A 10.0 g sample of soil was shaken at a 1:1 soil: solution ratio with deionized water for 30 minutes on an agitation device. After 30 minutes the sample was allowed to stand for 10 minutes and the pH of the solution was measured (Thomas, 1996). The EC of the same mixture was measured (Rhodes, 1996).

Soil Texture (Sand, Silt, Clay %): A 2.0 g sample of soil sieved to < 250 um was weighed into a glass bottle and dispersion solution was added and placed on an agitator overnight. The samples were then mixed with an automatic mixer and allowed to settle. A 1.0 mL pipet was used to remove the suspended clay fraction and it was placed into a crucible. The clay fraction was oven dried overnight at 100 °C. The sand and silt fractions were sieved retaining the sand fraction. The sand fraction was allowed to dry overnight at 100 °C. The percent clay and percent sand were calculated from the dried masses. The percent silt was calculated by difference. Each component is reported in terms of a percent of the total soil mass (%) (Kilmer et al 1949, Gee and Bauder, 1986).

Oxalate Extractable (As, Fe, Al, Mn, and P): Amorphous and poorly crystalline phases of Fe, Al, and Mn oxides were determined using an acid ammonium oxalate extraction (McKeague and Day, 1966). A 0.25 g sample of sieved soil (< 250um) was placed into 50 mL centrifuge tubes and extracted with 0.2 M ammonium oxalate solution buffered to pH 2.0. Soils were shaken in darkness for 4 hours with the extraction solution. After extraction the samples were centrifuged and a subsample of the supernatant was analyzed for As, Fe, Al, Mn, and P using ICP – OES.

Cation Exchange Capacity (Exchangeable Bases): A 1.0 g subsample of sieved sample (<250 um) was shaken with 20 mL of 0.1M BaCl₂ for 2 hours in a 50 mL centrifuge tube. After 2 hours the samples were centrifuged at 10,000 g for 10 minutes and the supernatant was removed for analysis via ICP – OES. The total Ca, Mg, Fe, K, Al, and Mn (in mg/kg) extracted from each soil were summed at the cation exchange capacity (CEC) or exchangeable bases on the soil surface. (Hendershot and Duquette, 1986).

Calcium Carbonate Equivalent: 1.0 M HCl (40.0 mL) was added 1.0 g of sieved soil (<250 um) in a 250 mL flask. The mixture was heated to approximately 60 °C and allowed to react for 5-10 minutes. The flask was removed from heat and allowed to cool then 100 mL of (< 18 MΩ) deionized water was added to the flask followed by phenolphthalein indicator. The unconsumed acid was back titrated using 1.0 M NaOH. The amount of HCl that the soil consumed (neutralized) was determined and converted to a CaCO₃ equivalent (Adams, 1984).

Total Organic Carbon: A 0.50 g of sieved sample (< 250um) was digested with K₂Cr₂O₇ and H₂SO₄ using a microwave assisted reaction system (MARS). A calibration curve using sucrose standards was prepared using the same digestion method as unknown samples. The samples and standards were heated to 135°C for a total of 30 minutes. Samples and standards were diluted with (<18 MΩ) deionized water. Absorbance of a subsample of the extraction solution was measured at 600 nm using a UV-VIS spectrophotometer. Organic carbon (%) was

determined for the soils was determined from a calibration curve generated using glucose as C standards (Heanes, 1984).

Arsenic Sequential Extraction (SEP)

Arsenic in soils was fractionated according to the sequential extraction procedure (SEP) of (Wenzel et al., 2001) with slight modification as described in Whitacre et al. (2013). This SEP uses four sequential extractions to fractionate As into (F1) nonspecifically sorbed; (F2) specifically sorbed; (F3) amorphous and poorly crystalline oxides of Fe and Al; (F4) well-crystallized oxides of Fe and Al and residual As phases. The extraction solution, temperature, and extraction time were: (F1) 0.05M $(\text{NH}_4)_2\text{SO}_4$, 20°C/4 h; (F2) 0.05M $\text{NH}_4\text{H}_2\text{PO}_4$, 20°C/16 h; (F3) 0.2M oxalate extraction, pH 3.0, 20°C/4 h; (F4) 0.2M oxalate + ascorbic acid extraction, pH 3.0, 96°C/2 h. A 1.0 g subsample of sieved soil (<250 um) was placed into a 50 mL centrifuge tube and extraction solution was added and the extraction performed. Following each extraction step samples were centrifuged at 10,000g and 20 mL of supernatant was removed for analysis via ICP – OES. A small portion of solution (5mL) was left in each tube and accounted for in the next fraction. After fractions 2, 3, and 4 25 mL of supernatant was removed for analysis to keep the soil to solution ratio constant. Supernatant was analyzed for the amount of As (mg/kg) released during each extraction step.

Task 2: Speciation of As in Soils by Advanced Spectroscopy

Exposure and potential toxicity of As from soil is limited to the species available for absorption into systemic circulation (i.e., bioaccessible) to become bioavailable. The release of As from contaminated soil to gastrointestinal fluid depends on form of solid phase As also termed “As speciation.”

There are several excellent spectroscopic methods capable of determining metal speciation, but for many elements, the most authoritative approach is through x-ray absorption spectroscopy (XAS). X-ray absorption spectroscopy is used to determine oxidation state, coordination environment, interatomic bond distances, and the identity of nearest-neighbor elements relative to the As soil contaminant. X-ray absorption spectroscopy experiments provide an *in situ* look at the current chemical form of soil metals that can be used to predict the long-term fate of the metal and its potential bioavailability based on known solubility products. Because of its need for high energy x-rays, XAS data collection can only be accomplished with a synchrotron radiation source such as the Advanced Photon Source (APS) synchrotron radiation research facility at Argonne National Laboratory.

Soils in the dataset were measured by XAS as well as Mössbauer spectroscopy to aid in Fe identification. Mössbauer spectroscopy is a technique that is considered the ‘gold standard’ for identifying and quantifying Fe oxidation states and coordination geometry in solid samples. The technique is sensitive to the nuclear environment, which depends on a number of factors including the number of electrons (i.e. oxidation state), the number of coordinating anions, the symmetry of the site, and the presence/absence of magnetic ordering. The information gained by Mössbauer spectroscopy on Fe provides the most robust identification of Fe oxidation state and coordination geometry possible. The other information describing the nuclear environment is a secondary source of species information from which to make XAS LCF models. This allows for a more accurate speciation of Fe. Iron in soil can include many species ranging from inclusion in parent material to ores to clays. Characterizing the Fe species and soil mineralogy are valuable components of predicting arsenic bioavailability and bioaccessibility from soils.

Arsenic Speciation of Soils by X-ray Absorption Spectroscopy

X-ray absorption spectroscopy was performed on all 27 soils at the Materials Research Collaborative Access Team 10-ID and 10-BM beamlines, Advanced Photon Source (Argonne National Laboratory). All of the soil samples were passed through a 250 µm sieve, fractured with a mortar and pestle, pressed into a 1-cm pellet, and mounted on Kapton tape. Data were collected using a 4-element Vortex fluorescence detector with several layers of aluminum foil shield to suppress fluorescence from other elements (such as iron) in the samples. Arsenate concentrations <20 mg As/kg were determined to be below the detection limit of the Vortex detector in our experiments. Up to five As K α (11867 eV) spectra were collected in transmission and fluorescence mode at room temperature for every soil with a sodium arsenate reference sample. Initially, only As data were collected, but it was determined iron (Fe) speciation was important to the project so the soil samples were examined for Fe speciation via XAS and Mössbauer spectroscopy. Iron concentrations <10 mg Fe/kg were determined to be below the detection limit of the Vortex detector. Up to five Fe K α (7112 eV) spectra were collected in transmission and fluorescence mode at room temperature for every soil with a metallic Fe reference sample. For Fe, only the transmission data were utilized for analysis.

Data analysis was conducted using the Athena module of Demeter software (Ravel and Newville, 2005). Each replicate scan was calibrated against the NaAs(V) (11874 eV) or metallic Fe foil (7112 eV) reference, merged, normalized, and converted to k space. Linear combination fitting (LCF) was used to identify the As or Fe species in each soil sample. The LCF models were performed using the normalized, derivative, and $\chi(k)$ spectra of the soil samples and reference standards. Lists of reference compounds used for LCF models are included for As (Table 2) and Fe (Table 3). The reference minerals include a mixture of synthetic and natural minerals received from the Smithsonian National Museum of Natural History. The LCF models predict As and Fe speciation in each soil as percentages of the reference minerals. The As x-ray absorption near-edge structure (XANES) spectra of 24 reference species are shown as normalized E and deriv E in Appendix Figure A1 and in the extended x-ray absorption fine structure (EXAFS) in chi k² space in Appendix Figure A2. The Fe XANES spectra of 29 reference species are shown as normalized E and deriv E in Appendix Figure A3.

Linear combination, least-squares fitting (LCF) provide quantitative determination of species relative abundance in samples containing multiple As or Fe species. Fit quality was judged by visual inspection and goodness-of-fit parameters such as the R-factor and reduced χ^2 values. The XANES and EXAFS regions of each spectra were both utilized for As LCF models and XANES regions for Fe LCF models.

Multiple model spectra can be fit equally well with LCF modelling, so it is important to include model compounds and select the optimal model based on a priori information available for the soils being measured. Linear combination species selection was constrained by a priori information for each soil, included contamination source, As sequential extraction, soil pH, total concentration of 3051a extractable elements, and bulk XAS spectra of both As and Fe, and Mössbauer spectra. For example, if the LCF model predicted As minerals that were not appropriate (e.g., arseniosiderite was predicted but <10 mg Ca/kg soil was reported from 3051a extractions, sample pH was very acidic and Fe XAS did not also identify arseniosiderite), then the mineral phase is very unlikely to be present and should be excluded and the LCF modelling repeated.

Linear combination fitting represents the sum of all the As or Fe present, weighted by their relative abundances to reconstruct the unknown sample. These spectral features are a function of the local bonding environment in that species, which is a function of the oxidation state, coordination number, 1st and/or 2nd shell bonding element(s), and bond distances. In complex systems (>3 species) such as soil, good model spectra covering all possible species should be used, including relevant crystalline and amorphous model phases as well as As sorbed to minerals. Natural weathering in soil creates potential for wide ranges in crystallinity and isomorphic substitution, so comparison of synthetic standards to natural samples should be understood as representing the closest approximation of the most prevalent species and not as identification in most cases. Particularly, because these soils have wide ranging soil conditions, contamination sources and measurements are taken on bulk soil samples. For these reasons, weighted model spectra from the best LC models were summed by common atomic environments (i.e., common oxidation state, 1st and/or 2nd shell bonding element(s)).

Table 2. List of natural and synthetic As-bearing minerals used for linear combination fits (LCF) to predict As phases in the soil samples.

Mineral	Molecular Formula	As Species Group	Edge (E ₀)
Loellingite	FeAs ₂	As(-III)	11867.604
Arsenopyrite	FeAsS	As(-III)	11867.487
Orpiment	As ₂ S ₃	As(III)Sulfide	11868.13
Realgar	As ₄ S ₄	As(III)Sulfide	11868.7
As (III) ads* Pyrite	FeS-As(III)	As(III) ads Sulfide	11871.12
Schneiderhohnite	Fe ²⁺ Fe ³⁺ AsO	As(III)Oxide	11870.506
Arsenolite	As ₂ O ₃	As(III)Oxide	11871.45
As (III) ads Ferrihydrite (syn**)	FeOOH•0.4(H ₂ O)-As(III)	As(III) ads Fe/Al Oxide	11870.5
As(III) ads Al ₂ O ₃ (syn)	Al ₂ O ₃ -As(III)	As(III) ads Fe/Al Oxide	11871.405
As(III) ads Montmorillonite (syn)	(Na,Ca) _{0.33} (Al,Mg) ₂ (Si ₄ O ₁₀)(OH) ₂ •nH ₂ O- As(III)	As(III) ads Fe/Al Oxide	11870.88
Arseniosiderite	Ca ₂ Fe ₃ (AsO ₄) ₃ O ₂	HFA	11874.348
Pharmacosiderite	KFe ₄ (AsO ₄) ₃ (OH) ₄ •6H ₂ O	HFA	11874.271
Beudantite	PbFe ³⁺ ₃ (AsO ₄)(SO ₄)(OH) ₆	HFA	11872.66
Scorodite	FeAsO ₄ •2H ₂ O	HFA	11873.11
Lead Arsenate	PbHAsO ₄	As(V)Oxide	11873.768
Sodium Arsenate	Na ₃ AsO ₄	As(V)Oxide	11874
Monomethylated Arsenate (syn)	MMA	As(V) ads	11874.755
Dimethylated Arsenate (syn)	DMA	As(V) ads	11874.521
As (V) ads Goethite (syn)	α- FeO(OH)-As(V)	As(V) ads	11874.182
As (V) Ads Ferrihydrite (syn) (low As)	FeOOH•0.4(H ₂ O) As(V)	As(V) ads	11874.431
As (V) ads Ferrihydrite (syn)	FeOOH•0.4(H ₂ O) As(V)	As(V) ads	11874.238
As (V) ads Hematite (syn)	Fe ₂ O ₃ -As(V)	As(V) ads	11874.343
As (V) ads Birnessite (syn)	MnO ₂ -As(V)	As(V) ads	11874.434
As(V) ads Gibbsite (syn)	Al(OH) ₃ -As(V)	As(V) ads	11874.355

*ads adsorbed

**syn synthetic

Table 3. List of natural and synthetic Fe-bearing minerals used for linear combination fits (LCF) to predict Fe phases in the soil samples.

Mineral	Chemical Formula	Fe Species	Edge (E ₀)
Fe metal	Fe (0)	Metal	7120.134
Marcasite	FeS ₂	Fe(II) Sulfide	7119.873
Loellingite	FeAs ₂	Fe(II) Sulfide	7121.559
Pyrite	FeS	Fe(II) Sulfide	7117.689
Arsenopyrite	FeAsS	Fe(II) Sulfide	7117.756
Fe Silicate	FeSi	Fe(II) Silicate	7123.385
Fayalite	Fe ₂ SiO ₄	Fe(II) Silicate	7117.689
Biotite	K(Mg,Fe) ₃ (AlSi ₃ O ₁₀)(F,OH) ₂	Fe(II) Silicate	7118.433
Fe(II) Acetate	C ₂ H ₃ O ₂ -Fe(II)	Fe(II) Organic Complex	7121.431
Fe(II) Chloride	Fe(II)Cl	Fe(II) Organic Complex	7118.951
Fe(II) Oxalate	C ₂ O ₄ -Fe(II)	Fe(II) Organic Complex	7116.89
Fe(II) Sulfate	Fe(II)SO ₄	Fe(II) Organic Complex	7124.44
Magnetite	Fe ²⁺ Fe ³⁺ ₂ O ₄	Fe (II/III) Oxide	7120.857
Siderite	FeCO ₃	Fe Carbonate	7121.105
Haematite	Fe ₂ O ₃	Fe(III) Oxide	7124.074
Maghemite	γ-Fe ₂ O ₃	Fe(III) Oxide	7124.521
Ferrihydrite (syn*)	(Fe ³⁺) ₂ O ₃ •0.5H ₂ O	Fe(III) Hydroxide	7121.621
Goethite (syn)	α- FeOOH	Fe(III) Hydroxide	7123.967
Akaganeite	β-FeO(OH)	Fe(III) Hydroxide	7123.422
Lepidocrocite	γ-FeO(OH)	Fe(III) Hydroxide	7122.382
Fe Substituted Montmorillonite	(Na,Ca) _{0.33} (Al,Mg) _{2-x} (Fe) _x (Si ₄ O ₁₀)(OH) ₂ •nH ₂ O	Fe(III) Clay	7121.042
Vivianite	Fe(II)PO ₄	Fe Phosphate	7117.537
Arseniosiderite	Ca ₂ Fe ₃ (AsO ₄) ₃ O ₂	HFA	7128.226
Pharmacosiderite	KFe ₄ (AsO ₄) ₃ (OH) ₄ •6H ₂ O	HFA	7122.937
Yukonite (syn)	Ca ₇ Fe ³⁺ ₁₂ (AsO ₄) ₁₀ (OH) ₂₀ •15H ₂ O	HFA	7127.243
Scorodite	Fe ³⁺ AsO ₄ •2H ₂ O	HFA	7124.484
Amorphous Ferric Arsenate (syn)	Fe ³⁺ AsO ₄ •2H ₂ O	HFA	7123.928
Fe(III) Phytate	C ₆ H ₁₈ O ₂₄ P ₆₋ Fe(III)	Fe(III) Organic Complex	7123.551
Fe(III) Phosphate	PO ₄ ⁻ Fe(III)	Fe(III) Organic Complex	7121.041
Fe(III) Citrate	C ₆ H ₈ O ₇ -Fe(III)	Fe(III) Organic Complex	7123.988
Fe(III) Sulfate	Fe(III)SO ₄	Fe(III) Organic Complex	7124.44

*syn synthetic

Arsenic and Fe Speciation by Mössbauer Spectroscopy

Study Mössbauer spectra on all 27 soils were collected on a WEB Research Co. Mössbauer Spectrometer System at the EPA ORD LRPCD Center Hill Lab. All soil samples were prepared for measurement by passing through a 250- μm sieve, fracturing with a mortar and pestle, pressed into a 3-cm pellet, and mounted on Kapton tape. A 50 mCi ^{57}Co source was used for gamma ray generation and mounted on a velocity transducer in a transmission orientation. Data were collected in transmission using a Krypton gas proportional counter and W302 WEB Research Gamma-Ray Spectrometer. The velocity transducer moved at 10 mm/sec for room temperature measurements and 12 mm/sec for 4 K measurements. Measurements are recorded for multiple cycles of transducer movement with counts accumulating over time. Samples with lower concentration of Fe required a longer time for measurement, on the order of days per sample. Iron concentrations <20 g Fe/kg were determined to be below the detection limit due to prohibitively long measurement times.

Samples were cooled using a Janis cryostat insulated by a vacuum sleeve. The vacuum sleeve was reduced to ultra-high vacuum using a high vacuum turbo pump system. The cryostat is cooled using a Sumitomo closed-cycle He refrigerator system and temperature controlled with a WEB research WTC102 temperature controller. System performance was gauged by monitoring the full-width-half-maximum of lines 3 and 4 in an α -Fe foil with 7 μm thickness. The value should be 0.21 mm/s +/- 0.01 mm/s at room temperature. System stability is checked by collecting a calibration file with the α -Fe foil at the same velocity and conditions as the samples every couple of days. The Fe foil calibration measurement serves as a zero position for any isomer shift in the sample.

Data analysis was conducted with MossA v1.01a software (Prescher et al., 2012). MossA was used for sample calibration and identification of site parameters such as isomer shift (IS), quadrupole splitting (QS) and hyperfine splitting (Bhf). Calibration files measured immediately prior to the sample were used for calibration and sample isomer shift is relative to Fe foil zero position. Reference values of parameters for mineral standards were sourced from the Mössbauer Mineral Handbook 2005 and the online library of Mössbauer spectra at (www.mtholyoke.edu/courses/mdyar/database). Reference values for parameters used in identification of oxidation state and coordination geometry were sourced from the review by Dyar et al. (2006). Components were fit to each unknown spectra while restraining IS, QS and Bhf values to chemically possible values (e.g. $0 < \text{IS} < 1.5$)

Task 3: In Vivo Bioavailability

Quantifying exposure in contaminated areas is performed via human health risk assessment (HHRA). Often, ingestion of arsenic contaminated soil is the primary risk driver. Using total concentration of soil arsenic in the HHRA will overestimate bioavailability because not all of the arsenic will be soluble in the gastrointestinal system and available for absorption into systemic circulation (i.e., bioaccessible).

In HHRA, RBA is used to modify exposure due to bioavailability. Each soil has a different RBA and accounting for the relative bioavailability can help provide more accurate human health risk assessments. Recently the U.S. EPA conducted a comprehensive study of RBA As (U.S. EPA, 2012). U.S. EPA issued guidance set a new default value of 60% RBA As for human health risk assessments regarding arsenic contaminated soil (U.S. EPA, 2012). This was a change from using only total concentration or assuming the soil arsenic has an RBA of 100%. Using the new default value of 60% provides a more accurate risk assessment and removes the overestimation of risk that often occurs when just the total concentration is used.

Animal models used to determine site specific RBA As for HHRA are shown below in Table 4. The animal studies include the use of juvenile swine, adult mice, *Cynomolgus* monkey, and *Cebus* monkey.

Table 4. Animal models utilized for the assessment of As relative bioavailability in contaminated soil.

Animal model	Biomarkers of As exposure	Reference
Juvenile Swine	Steady state urinary excretion	Rodriguez et al. 1999; Casteel 2005, 2009a,b,c, 2010a,b,c; Basta et al. 2007a; Denys et al. 2012; Brattin and Casteel 2013
Juvenile Swine	Single dose blood AUC	U.S. EPA 1996; Juhasz et al. 2007, 2008
Mice (C57BL/6)	Steady state urinary excretion	Bradham et al. 2011
Monkeys (<i>Cebus</i> , <i>Cynomolgus</i>)	Single dose urinary excretion	Roberts et al. 2002, 2007

Animal models involving monkeys have been used in pharmacokinetic studies and are similar to humans with respect to absorption and excretion of sodium arsenite (Basta and Juhasz, 2014). To determine As RBA using monkey models is essentially not an option because of the prohibitive high cost, in addition ethical issues regarding the use of primates have been raised. Instead of monkey models determining RBA As using swine has been deemed the “gold standard” due to their similarity to humans regarding; growth rate, gastrointestinal physiology, bone density, and eating patterns (Casteel et al., 2006; Weis and LaVelle, 1991). In addition juvenile swine have been utilized because they simulate children which is considered one of the

most sensitive populations when performing human health risk assessments. However, swine are also very costly and determining RBA As using swine can be outside of the price range of site managers when looking to get site specific RBAs. Recently the U.S. EPA has developed a method to determine RBA As using mice which is less cost prohibitive and faster than using the juvenile swine model.

For this study the adult mouse model and juvenile swine model were used to determine As RBA for the 27 study soils. Nineteen of the 27 soils were dosed to mice, 22 of the 27 soils were dosed to juvenile swine, and 14 of the 27 soils were dosed to both animals. Using two animal methods allows for a comparison between the two methods.

Mouse In Vivo Bioassays

The in vivo adult mouse model was used to evaluate the RBA of study soils (Bradham et al., 2011 and 2013). Nineteen of the 27 test soils were evaluated in the mouse assay, which were collected from sites where mining, smelting activities, pesticide application resulted in As contamination. In addition the three soils that were spiked with soluble arsenic and aged were evaluated using the mouse assay. The mouse assay for As bioavailability in soil included four- to six-week-old female C57BL/6 mice. The basal diet for bioavailability assays was powdered AIN-93G purified rodent diet obtained from Dyets (Bethlehem, PA). Amended diets were prepared by blending of test soil or reference arsenicals (arsenate) with basal diet.

Mice were housed in an American Association for the Accreditation of Laboratory Animal Care-accredited facility and animal procedures were approved by the Institutional Animal Care and Use Committee of the U.S. EPA's National Health and Environmental Effects Research Laboratory. Mice had free access to AIN-93G purified rodent diet and tap water that contained <11 µg As/L. During assays, 3 mice were housed together for 10 days in a single metabolic cage that separated urine and feces, with unlimited access to test diet and drinking water. Urine and feces were collected daily and food consumption was measured daily. For sample collection and data analysis, the unit of observation was the cage (i.e., combined excreta of three mice). Typically, an assay included 4 cages of animals (12 mice total) that received the same amended diet. Urine and feces from each individual cage were pooled over the course of the assay and processed for As analysis. Daily urine or feces collections for each cage were stored at -20°C until processed to produce a single cumulative urine sample and single cumulative feces sample. After thorough mixing, multiple aliquots of the cumulative urine sample for each cage were taken for determination of As concentration. Cumulative urinary excretion of As was calculated as the product of As concentration in the cumulative urine sample and the volume of the cumulative urine sample. Cumulative feces samples were homogenized with a freezer/mill (model 6850; Spex CertiPrep, Metuchen, NJ). Multiple aliquots of cumulative feces sample were taken for determination of As concentration. Cumulative fecal excretion of As was calculated as the product of As concentration in the cumulative feces sample and the mass of the cumulative feces sample.

Data from mouse assays were used to calculate the urinary excretion fraction (UEF) of As from ingestion of an amended diet as the ratio of cumulative excretion of As in urine (µg) to cumulative dietary intake of As (µg) (Equation 2):

$$UEF\% = 100 \cdot \frac{\text{Cum Urinary As}}{\text{Cum As Dose}} \quad (2)$$

Relative bioavailability (RBA) was calculated as the ratio of the UEF for As in a specific soil-amended diet to the ABA for As in a diet containing a reference arsenical (e.g., sodium arsenite, NaAsO₄) (Equation 3):

$$RBA\% = \frac{UEF\% \text{ Soil}}{UEF\% \text{ NaAsO}_4} \quad (3)$$

Juvenile Swine In Vivo Bioassays

The juvenile swine model was used to determine RBA As in contaminated soils (Brattin and Casteel, 2013). Juvenile swine were selected for use because they are considered to be a good physiological model for gastrointestinal absorption in children (Weis and LaVelle, 1991; Casteel et al., 1996). Details in the Study Design used in the bioassay are summarized in Appendix A.3.

The RBA for each test material was calculated as a ratio of the UEF for the test material and the UEF for the sodium arsenite reference material (Equation 4).

$$RBA\% = 100 \times \frac{UEF \text{ (test)}}{UEF \text{ (reference)}} \quad (4)$$

Uncertainty for both the mouse and swine RBA values was calculated using Fieller's Theorem (Fieller, 1954) to produce 90% confidence intervals (CI).

Task 4: In Vitro Arsenic Bioaccessibility

In order to overcome the difficulties and expenses associated with animal dosing trials used to assess bioavailability of contaminants in soil, extensive research efforts have been directed toward development of in vitro gastrointestinal methods that simulate the gastrointestinal environment. A summary of gastrointestinal conditions are presented in Table 5. The main conditions that most in vitro methods simulate are phase (gastric or intestinal), pH, solution constituents, and time.

Table 5. Human gastric and intestinal physiological parameters including pH, Time in hours (h), soil:solution ratio (g:mL), ascorbic acid (AA) secretion rate, as well as sodium chloride (NaCl), pancreatin, and bile concentrations.

Parameter	Physiological Gastric	Reference
pH	1.5-2	Malagelada et al., 1976
pH	1.7 (1.5-2)	Charman 1997
pH	1.3 (1 - 2)	Horter 1997
Time	1h	Schwartz et al., 1982
Time	2 h	Culp et al., 1973
Soil:Solution	1:800mL	Malagelada et al., 1976
Pepsin	1% (10 mg/mL)	Crews et al., 1983
NaCl	0.15M	Crews et al., 1983
AA	0.42 - 1.65 mg/h	O'Connor et al., 1989
	Intestinal	
pH	5-6.5	Horter 1997
pH	7.5	Crews et al., 1983
pH	6.5	Malagelada et al., 1976
Time	3-5h	Guyton et al. 1981
Pancreatin	0.04%	Crews et al., 1983
Bile	0.38%	Crews et al., 1983

As a result, several in vitro methods of varying complexity have been developed to determine As bioaccessibility, but only five methods that are widely used internationally were selected for this study. The general parameters for the Glycine method, the Physiologically Based Extraction Test (PBET), Unified Bioaccessibility Method (UBM), The Ohio State University In vitro Gastrointestinal method (OSU IVG), and the California Bioaccessibility method (CAB) are presented in Table 6.

Table 6. Extraction parameters for in vitro bioaccessibility methods used in this study.

Method	S:S ratio	Gastric Phase			Intestinal Phase			Reference	
		Constituents g/L	pH	Time h	Constituents g/L	pH	Time h		
Glycine	1:100	30.03 g glycine	1.5	1	1:100	1.75 g bile, 0.5 g pancreatin	7	4	Juhasz et al 2009
PBET	1:100	1.25 g pepsin, 0.5 g sodium malate, 0.5 g sodium citrate, 420 µl lactic acid, 500 µl acetic acid	1.8	1	1:100	0.175 g bile, 0.5 g pancreatin	7	4	Meunier et al. 2010a
		Saliva: 0.896 g KCl, 0.888 g NaH ₂ PO ₄ , 0.2 g KSCN, 0.57 g Na ₂ SO ₄ , 0.298 g NaCl, 1.8 ml of 1 M NaOH, 0.2 g urea, 0.145 g amylase, 0.05 g mucin, 0.015 g uric acid			Duodenal phase: 7.012 g NaCl, 5.607 g NaHCO ₃ , 0.08 g KH ₂ PO ₄ , 0.564 mg KCl, 0.05 g MgCl ₂ , 0.18 ml of 37% HCl, 0.1 g urea, 0.2 g CaCl ₂ , 1 g bovine serum albumin, 3 g pancreatin, 0.5 g lipase				
UBM	1:37.5	Gastric Phase: 2.752 g NaCl, 0.266 g NaH ₂ PO ₄ , 0.824 g KCl, 0.4 g CaCl ₂ , 0.306 g NH ₄ Cl, 8.3 ml of 37% HCl, 0.65 g glucose, 0.02 mg glucuronic acid, 0.085 g urea, 0.33 g glucosaminehydrochloride, 1 g bovine serum albumin, 3 g mucin, 1 g pepsin	1.2	1	1:100	Bile phase 5.259 g NaCl, 5.785 g NaHCO ₃ , 0.376 g KCl, 0.18 ml of 37% HCl, 0.25 g urea, 0.222 g CaCl ₂ , 1.8 g bovine serum albumin, 6 g bile	6.5	4	Wragg et al. 2011
OSU	1:150	10 g pepsin, 8.77 g NaCl	1.8	1	1:150	0.56 g bile, 0.56 g pancreatin	6.1	2	Basta et al. 2007a
CAB	1:150	10 g pepsin, 8.77 g NaCl 17.6 g ascorbic acid	1.5	2	1:150	0.56 g bile, 0.56 g pancreatin	7.5	4	DTSC 2015
S:S Ratio Soil: Solution Ratio		h hours							

An essential requisite of acceptable As in vitro methods is that IVBA be strongly correlated with relative bioavailable (RBA) As determined from animal dosing trials. All five of the methods selected for this study have reported a significant correlation between IVBA As and RBA As measured from juvenile swine dosing trials (Table 7).

Table 7. Selection of in vitro bioaccessibility method for this study – parameters and published references.

Method	No. of Soils	Types of Soils	Animal Model	Regression Type	Citation
Glycine	12	Railway, Cattle Dip, Mining, and Gossans	Swine	Stepwise Multiple	Juhasz et al. 2009
PBET	3	Copper Smelting	Rabbit and Monkey	NA*	Ruby et al. Environ Sci Technol 1996 30: 422-30
UBM	11	Calcine, Iron Slags, River Sediments	Swine	Theils Method	Meunier et al. 2010a
OSU IVG	10	Calcine and Iron Slags	Swine	Simple Linear	Basta et al. 2007a
CAB	21	Gold Mining, Pesticide, Mining Slags	Swine	Simple Linear	DTSC 2015

*NA Not Applicable

In vitro methods rely on the concept that the As solubilization in GI fluid is an important determinant of As human bioavailability. These methods measure the amount As solubilized under their respective parameters that resembles human gastric and intestinal fluids and therefore potentially available for absorption in the small intestine. The fraction of As, which solubilizes in an in vitro system, is referred to as in vitro bioaccessible (IVBA), which may then be used as an estimate or correlate with RBA.

$$\% \text{ IVBA As} = [\text{IVBA extractable As (mg/kg)}]/[\text{total soil As (mg/kg)}] *100\% \quad (5)$$

The Glycine Method

This method is a 2-step sequential extraction in which 100 mL of gastric solution (0.40 M glycine, preheated to 37°C) and 1.0 g soil (<250 µm) was added to a 175 mL HDPE bottle and placed into a rotator shaker located in a 37°C incubator. Soil samples were rotated at 40 ± 2 rpm for 1 h, and solution pH was frequently checked and adjusted to 1.5 ± 0.05 using drop wise 50% NaOH and/or 6M trace metal HCl solution. After 1 h, 5 mL aliquot of suspension was collected with a syringe and filtered (0.45 µm). Contaminant extracted during the gastric phase is expressed as Glycine IVBA gastric extraction (Glycine IVBA GE). The pH of the remaining solution was adjusted to 7.0 ± 0.2 using drop wise additions of 50% NaOH solution, followed by the addition of 0.175 g of porcine bile extract and 0.050 g of porcine pancreatin. Soil samples were rotated for another 4 h, and the solution pH was adjusted hourly to 7.0 ± 0.2. After 4 h, 5 mL aliquot of suspension was collected with a syringe and filtered (0.45 µm). Contaminant

extracted during the intestinal phase is expressed as Glycine IVBA intestinal extraction (Glycine IVBA IE).

The Unified BARGE Method (UBM)

This method was modified to be a 2-step sequential extraction in which 1.2 g soil (<250 µm) was added into a 250 mL beaker with the addition of 18 mL of saliva (S) and quickly shaken by hand for 10 s. Then 27 mL of gastric fluid (37°C) was added, and the beaker placed in a 37°C water bath. The sample was thoroughly mixed with the solution, using a paddle stirrer to maintain an homogenous suspension. Solution pH was continuously adjusted to 1.20 ± 0.05 with 1M NaOH and/or 37% HCl. After 1 h extraction, 3 mL of gastric solution was pulled out, centrifuged (4500 g for 15 min), and stored in a 15 mL falcon tube. Contaminant extracted during the gastric phase is expressed as UBM IVBA gastric extraction (UBM IVBA GE). The pH of the remaining solution was adjusted to 6.30 ± 0.1 using drop wise additions of 1M NaOH and/or 37% HCl solution, followed by the addition of 54 mL of duodenal fluid and 18 mL of bile fluid. After 4 h extraction, 10 mL of intestinal solution was pulled out, centrifuged (4,500 g for 15 min), and stored in a 15 mL falcon tube. Contaminant extracted during the gastric phase is expressed as UBM intestinal extraction (UBM IVBA IE).

The Physiologically Based Extraction Test (PBET)

This method is a 2-step sequential extraction in which the gastric solution was prepared by adding the following to 1 L deionized water: 1.25 g pepsin, 0.50 g sodium citrate, 0.50 g DL malic acid disodium, 420 µL lactic acid (85%), and 500 µL acetic acid. The pH was adjusted to 1.8 ± 0.05 with concentrated HCl. Prior to starting the extraction, the solution was warmed to 37°C. 1.0 g soil (<250 µm) was added into a 250 mL beaker with the addition of 100 mL gastric solution, and the beaker was placed in a 37°C hot water bath. The soil sample was mixed with the solution and maintained homogenous by stirring at 100 rpm using a plastic pad. Solution pH was continuously adjusted to 1.80 ± 0.1 with 1M NaCO₃ and/or concentrated HCl. After 1 h extraction, 10 mL extract is immediately centrifuged (11500 g for 15 min) and then filtered (0.45 µm). Contaminant extracted during the gastric phase is expressed as PBET IVBA gastric extraction (PBET IVBA GE). The pH of the remaining solution was adjusted to 7.0 ± 0.2 using drop wise additions of a saturated Na₂CO₃ solution. 0.175 g porcine bile extract and 0.050 g porcine pancreatin were dissolved into 10 mL DI water and added into the solution. The pH was continuously monitored and adjusted to 7.0 ± 0.2 . After 4 h mixing, 10 mL of intestinal solution was pulled out, centrifuged (11500 g for 15 min), and then filtered (0.45 µm). Contaminant extracted during the intestinal phase is expressed as PBET IVBA intestinal extraction (PBET IVBA IE).

The Ohio State University In Vitro Gastrointestinal Method (OSU IVG)

This method is a 2-step sequential extraction in which gastric solution, 150 mL of 0.10 M NaCl and 1% porcine pepsin, was heated in an open extraction vessel in a 37°C hot water bath. When the solution reached 37°C, soil (1 g, <250 µm) was added. The sample was thoroughly mixed with the solution, using a paddle stirrer to maintain an homogenous suspension, and the pH was adjusted drop wise to 1.8 using 6M trace metal grade HCl. The solution pH is

continuously monitored and adjusted to 1.8 ± 0.1 . After 1 h, 10 mL of gastric solution was removed for analysis. Contaminant extracted during the gastric phase is expressed as OSU IVG IVBA gastric extraction (OSU IVG IVBA GE). The extract was immediately centrifuged (11,160 g for 15 min) and then filtered (0.45 μm). The pH of the remaining solution was adjusted to 6.1 ± 0.1 using drop wise additions of a saturated Na_2CO_3 solution followed by the addition of 0.563 g of porcine bile extract and 0.563 g of porcine pancreatin. After 2 h of mixing, 10 mL of intestinal solution was collected for analysis. The extract was immediately centrifuged (11,160 g for 15 min) and then filtered (0.45 μm). Arsenic extracted during the intestinal phase is expressed as OSU IVG IVBA intestinal extraction (OSU IVG IVBA IE).

The California Bioaccessibility Method (CAB)

This method is a 2-step sequential extraction in which 150mL of gastric solution (0.10 M NaCl, 1% porcine pepsin, 0.1M L-ascorbic acid) and 1.0 g soil (< 250 μm) was added to a 175 mL HDPE bottle and placed into a rotator shaker located in a 37°C incubator. Soil samples were rotated at 30 ± 2 rpm for 2 h, and solution pH was checked and adjusted to 1.5 ± 0.1 using drop wise addition of 6M trace metal HCl solution. After 2 h, a minimum of 10 mL of gastric solution is removed and filtered (0.45 μm) for analysis. Contaminant extracted during the gastric phase is expressed as CAB IVBA gastric extractable (CAB IVBA GE). The pH of the remaining solution was adjusted to 7.5 ± 0.1 using drop wise additions of a saturated Na_2CO_3 solution followed by the addition of 0.563 g of porcine bile extract and 0.563 g of porcine pancreatin. After 4 h of mixing, 10 mL of intestinal solution was collected for analysis. The extract was immediately centrifuged (11,160 g for 15 min) and then filtered (0.45 μm). Arsenic extracted during the intestinal phase is expressed as CAB IVBA intestinal extraction (CAB IVBA IE).

Task 5: Cross-correlation and Statistical Analysis

A variety of statistical approaches were used to produce in vivo in vitro correlations (IVIVC) to evaluate an in vitro methods ability to predict in vivo bioavailability. Regression methods that were used include simple linear regression, orthogonal regression and Bayesian linear regression. Each in vitro method contains a gastric and intestinal phase that was considered separately for IVIVC generation. In addition, each animal model (adult mouse and juvenile swine) used to determine RBA was considered separately. This produced a total of 20 different IVIVCs that were evaluated. IVIVCs were evaluated for goodness of fit using, slope, y-intercept, and prediction error against proposed acceptance criteria. Simple linear and orthogonal regressions was done using Minitab17.2.1 (2015). Bayesian linear regression was done using R (R Development Core Team, 2008) similar to the method developed in Bradham et al. (2015).

Task 6: Mechanisms and Permanence of Sequestered Pb in Soils: Impact on Human Bioavailability

Task 6.1.1: Effect of key biological processes on long-term metal permanence of Pb-contaminated soil remediated with phosphate treatments: Development and Evaluation of Soil Fungal Inoculates

Site Description and Study Soils

The study site is an abandoned small-arms shooting range located in a cleared stand dominated by oak (*Quercus* sp.), maple (*Acer* sp.), and pine (*Pinus* spp.) trees near the Oak Ridge National Laboratory (35°55'46"N, 84°19'31"W) in Oak Ridge, TN. The area designated for target and shooting practice was cleared of trees when the firing range was first established circa 1950, after which time the target area became dominated by typical old-field grasses (*Festuca* spp.) and forbs (*Lespedeza* sp.). Initially, an earthen berm was utilized as a firing backstop, which to this day remains relatively devoid of vegetation. A more formal firing backstop consisting of tires was erected along the target area slightly south of the earthen berm sometime around 1982. This resulted in three distinct vegetation types surrounding the backstop: forested areas north and west of the backstop dominated by oak, maple, and pine trees; grassy areas previously cleared for shooting and now dominated by grasses and forbs, south of the backstop; and the backstop embankment, which still remains mostly devoid of vegetation.

The grassy area south of the backstop is periodically mowed despite the fact that the shooting range ceased operation in the mid-1980s. This firing range was previously part of a study by Moseley et al. (2008) in which the soils were described (soils #7, 8 and 9) to have between 1,000 and 4,000 mg kg⁻¹ soil Pb, an average of 1.63% total carbon, 1.31% total organic carbon, pH of around 6, and an average of 20.6%, 31.7%, and 47% sand, silt, and clay, respectively. These soils were found to have high levels of Pb bioaccessibility ranging from 75.7 up to 95.7%, indicating significant proportions of Pb in these soils is likely readily exchangeable and bioavailable despite their clay-rich texture and limestone mineral origin (Moseley et al., 2008).

Soil Analyses and Sample Collection

For our study on the soil fungi in Pb-contaminated soils, in July 2010 we established one transect through each area of differing vegetation types: forested, grassy, and backstop (which was mostly devoid of vegetation). Five to 12 points along each of the three transects were analyzed in the field for total soil Pb content using a hand-held NITON® XLi/XLt 700 Series x-ray elemental analyzer (NITON® LLC, Billerica, MA). Points along the grass-dominated transect were delineated with a G (G1 through G10), points along the forest-dominated transect were delineated with an F (F2 through F14), and points to the north of the backstop in the area devoid of vegetation were delineated with a B (B4 through B8). All soil measurements and samples were collected after having first cleared the transect point of vegetation and surface debris to expose bare soil. At each point along all transects, the x-ray analyzer was placed in contact with the soil surface, and measurements were taken according to the manufacturer's instructions for the device.

Based on these field measurements, we collected one representative “low Pb” and “high Pb” soil sample from each transect. At each soil sample collection point, three soil cores were collected aseptically within 10 cm of each other to a depth of 15 cm with a standard 2.54-cm diameter soil corer; these three cores were then composited in the field. Between sampling points, the soil corer was wiped clean of soil particulates, rinsed with a 10% bleach solution, subsequently rinsed with a 70% ethanol solution, and allowed to air dry. The singular exception to this sampling procedure was when soils from two different “high Pb” points (B7 and B8) on the backstop transect were consolidated as one sample. Soil samples were aseptically transferred directly from the soil auger into Ziploc® baggies and stored on ice for approximately 2 h for transport back to the lab and further processing. At that point, each soil sample was thoroughly homogenized; sieved to 4 mm to remove rocks, intact bullet slugs, and large fragments; and partitioned into subsamples for subsequent analysis.

Gravimetric water content was determined on replicate 10 g subsamples dried at 65°C for 120 h. Soil pH was determined with a Corning pH/ion analyzer 350 in a slurry of 5 g soil to 5 ml H₂O after shaking for 30 m, then centrifugation at 3,000 rpm for 10 min. Soil total metal content was again determined on replicate 2.0 g subsamples (after soils were homogenized, sieved, and dried), using the hand-held NITON® XLi/XL_t 700 Series x-ray elemental analyzer as described above.

Soil Fungal Cultivation and Isolation

To determine total cultivable fungi on each of the soils collected, serial dilutions were performed on three replicate field-moist soil subsamples (5 g) and plated, in replicate, onto either Malt Extract Agar (MEA – Difco™ Becton Dickinson & Co, Sparks, MD) or Czapek Dox Agar (CZA – HiMedia Laboratories Pvt. Ltd., India) and adjusted to pH 5 and 7, respectively. The ability of cultured fungi to lower the media pH was visualized with the indicators bromothymol blue in the CZA and methyl orange in the MEA. Plates were incubated at 21°C for 72 h, at which point counts were determined for total and acid-producing organisms; and acid-producers with distinct morphologies were further isolated using the same media on which they were originally cultivated (cultures of each of these isolates are maintained and available upon request). Isolates were then tested for acid production on the alternate media/pH, as well as phylogenetically identified and further characterized as described below.

The type and quantity of organic acids secreted by each isolated fungus were determined by analyzing broth supernatant with high-pressure liquid chromatography (HPLC). Broth tubes were inoculated by using a 5 mm plug of each isolate into 5.0 mL of 1% ME broth or 1% CZ broth and incubated at 30°C for 120 h. After incubation, tubes were centrifuged at 4,000 rpm for 10 min, and supernatant from each tube was filter sterilized to 0.2 µm. Sterile supernatant was acidified with 200 mM sulfuric acid and analyzed on a Waters 2707 Autosampler with a 2414 Refractive Index Detector and an Aminex HPX-87H column at 0.60 mL min⁻¹ flow rate at 35°C internal temperature. Standards included oxalic acid, citric acid, malonic acid, malic acid, lactic acid, acetic acid, and formic acid at 2.5, 5.0, 10, 15, and 20 mM. Uninoculated broth of each type served as a media control and values obtained for each isolate were adjusted to account for media content.

To determine the ability of each isolated fungus to solubilize Pb at different concentrations, Pb carbonate (Alfa Aesar, Ward Hill, MA) was incorporated into MEA at the equivalent of 2.5,

10.0, and 18.5 mM concentrations, stirred continually to maintain Pb carbonate dispersal in the media, and the mixture then poured into standard 10 cm petri plates to a depth of roughly 5 mm. Three replicate Pb-carbonate plates at each concentration were each inoculated with a 7-mm-diameter plug of each isolate. Outward radius of hyphal growth and the radius of cleared Pb carbonate were measured after 120 h incubation at 21°C. *Aspergillus niger* NRRL #3 (U.S. DA ARS Culture Collection) was used as a positive control against which to measure both growth and zone of clearing around the culture plug in the Pb-amended medium.

Isolate Sequence Characterization

Tissues from each isolated fungus found to acidify both media above were aseptically collected from the surface of an agar petri dish and used in the MoBio PowerSoilTM DNA extraction kit (MoBio Laboratories, Inc., Carlsbad, CA) according to the manufacturer's instructions for 0.25 g soil. Extracted DNA was quantified with a Nanodrop ND-1000 spectrophotometer at 260 nm (Nanodrop Technologies, Wilmington, DE), and the large subunit of the fungal rRNA gene was amplified using primers LR5R and LROF (Castro et al., 2010) for subsequent sequence analysis. The PCR reactions were performed on GeneAmp® PCR System 9700 (PE Applied Biosystem, Norwalk, CT) using a 30 µL reaction volume containing 1 x PCR buffer, 2 mM MgCl₂, 200 µM of each of the dNTPs, 1 µM of each primer, 0.075 U Taq DNA polymerase, 1.0 mg mL⁻¹ BSA, H₂O, and 12.5 ng DNA template. The cycling parameters included an initial denaturation at 95°C for 2 min, followed by 25 cycles of 94°C for 45 s, 57.5°C for 50 s, and 72°C for 1 min 45 s, followed by a final extension at 72°C for 5 min. A no-template negative control and a positive control of *Aspergillus niger* DNA at 10 ng µL⁻¹ were included in each PCR. Electrophoresis was performed in 1% agarose in Tris-acetate EDTA buffer to confirm successful amplification. PCR products were then purified with Millipore multiscreen HTS PCR filter plates (Millipore Corp., Bellerica, MA).

Big Dye Terminator v3.1 (Applied Biosystems, Foster City, CA) cycle sequencing reactions were performed using primer LROF and the following master mix: 1 µl of 5X sequencing buffer, 1.7 µl of H₂O, 1 µl of BigDye, 0.3 µl of 10 pmol/µl TA primer, and 1 µl of DNA template. Products were precipitated in ethanol, resuspended in 10 µl of Hi-Di Formamide (Applied Biosystems), and run on an ABI Prism 3730 DNA analyzer (Applied Biosystems). Sequences were edited in Sequencher program version 4.7 (Gene Codes Corp., Ann Arbor, MI), where the primers and low-quality ends of the sequences were removed. Partial sequences (400 to 500 bp) were then analyzed against the NCBI database (<http://www.ncbi.nlm.nih.gov/BLAST/Blast.cgi>) using BLASTN (Altschul et al., 1997). Edited sequences were submitted to GenBank and may be found under accession numbers JQ746543 through JQ746560.

Soil Fungal Community Pyrosequence Analysis

Microbial community composition among soils at the firing range was characterized by pyrosequence analysis as described in Gottel et al. (2011). Raw fungal 28S rRNA gene sequences were trimmed and quality checked using MOTHUR. MOTHUR was also used for preclustering at 2%, rarefaction curves, distance calculations, clustering, and further analysis based on operational taxonomic unit (OTU). Fungal sequences were classified by their top

BLAST hit as compared against SILVA LSU database in MG-RAST for each representative OTU. In order to determine the extent isolated fungal species were represented in the overall fungal community, the 52,069 LSU rRNA gene sequences from 454 analyses were formatted into a local BLAST database. The Sanger sequencing generated LSU rRNA gene sequences from the top 15 Pb-solubilizing isolates and were then compared against the 454 database using BLASTN (Altschul et al., 1997).

Task 6.1.2: Effect of Key Biological Processes on Long-term Metal Permanence of Pb-contaminated Soil Remediated with Phosphate Treatments

Study Site 1: Small Arms Firing Range Site Description and Soil Treatments

A detailed description the ORNL site is presented in the previous section. Collection of soil from site G2 was used for the current study. Treatment included litter, fungus and litter+fungus. Four treatments were applied in a 4 x 2 factorial design. Sterilization was accomplished with gamma irradiation. Each soil treatment was placed in an incubation jar and was inoculated with four 5-mm diameter agar plugs from the actively growing margin of *Phanaerochaete flavidoolba*. The non-innocolated treatments received media plugs only from an empty agar plate. Litter additions were 10 mg/g of dry grass litter material.

Study Site 2: Smelter Site, Joplin MO Site Description and Soil Treatments

A detailed description the treatments to the Pb contaminated Joplin soil similar to the ORNL soil in the previous section. Treatment included biosolids compost, phosphorus (P), Fe, fungus and combinations of these treatments. Sterilization was accomplished with gamma irradiation. Each soil treatment was placed in an incubation jar and was inoculated with four 5-mm diameter agar plugs from the actively growing margin of *Phanaerochaete flavidoolba*. The non-innocolated treatments received media plugs only from an empty agar plate. Litter additions were 10 mg/g of dry grass litter material.

Determination of Bioaccessible Pb

Bioaccessible Pb was determined by using three in vitro extractions: (1) EPA Method 1340 (EPA, 2013) at pH 1.5, (2) Method 1340 with one modification where the pH of the extracting solution was 2.5 ± 0.05 instead of pH 1.5 and (3) OSU IVG pH 1.8 method. The in vitro extraction process for Method 1340 consists of mixing 1.00 ± 0.01 g of soil and 100 ± 0.5 mL of extracting solution. Samples were placed in plastic bottles, sealed, and secured on a rotating shaker in a 37 °C cabinet. Rotations were maintained at 30 ± 2 rotations per minute. Samples were pH-adjusted to 1.50 ± 0.05 pH or 2.50 ± 0.05 pH at 5 minutes using 25% trace metal grade HCl. If necessary, samples were checked and pH-adjusted at 30 minutes. After 60 minutes of rotating, samples were removed, final pH recorded, and filtered through 0.45 µm filters. Total rotation time was 60 minutes. Total extraction time did not exceed 90 minutes. Final solution pH stayed within ± 0.25 pH unit for all four in vitro extractions. This met the EPA 1340 requirement of the final solution pH being ± 0.5 pH units from the starting solution pH (EPA, 2013).

The OSU In vitro gastrointestinal model (OSU IVG) was conducted as follows. Soil (1.0 g, < 250 µm) was placed in 150 mL of gastric solution (0.10 M NaCl and 1% (w/w) porcine pepsin) and heated in an open extraction vessel in a 37° C hot water bath. The extraction solution was continuously mixed using a paddle stirrer to maintain a homogenous suspension,

and the pH was continuously monitored and adjusted to 1.8 ± 0.1 using 6 M trace metal grade HCl. After 1 h, 10 mL of gastric solution was immediately centrifuged (11,160 g for 15 min) and then filtered ($0.45 \mu\text{m}$) for analysis of supernatant.

All in vitro extractions were performed in triplicate. In-vitro bioaccessibility (IVBA) was calculated by dividing the extractable Pb from the in vitro solution by the total Pb content of the soil using U.S. EPA Method 3051A. Sample duplicates, duplicate matrix spikes (1000 mg L-1 Pb), blanks, blank spikes (1000 mg L-1 Pb), and a standard reference material, NIST 2711a Montana Soil II, were included in the analysis as part of quality assurance and quality control measures.

Determination of Relative Bioavailable Pb

Relative bioavailable Pb (RBA Pb) were determined for select soils from post-incubated ORNL and Joplin soils by using the adult mouse model. The mouse bioassay was conducted by Dr. Albert Juhasz and Dr. Euan Smith of the Centre for Environmental Risk Assessment and Remediation at the University of South Australia.

Lead-contaminated soils ($< 250 \mu\text{m}$) were dosed to adult male (Balb/c) mice. Animals were housed in groups of 3 mice and received a 12/12 light/dark cycle and access to water ad libitum. For Pb relative bioavailability assessments, a single dose of soil suspension containing 0.25 of soil in 0.5 mL of Pb free water was administered via gavage to fasting animals. Blood samples were collected at regular time intervals following cervical dislocation over a 48 h period. Blood samples (~1 mL) were stored in 7.5 mL EDTA collection tubes at -20°C prior to Pb analysis by ICP-MS. In order to quantify blood Pb concentrations, blood was digested with hydrogen peroxide (2 ml; 30%) and nitric acid (2 ml; 70%) using a CEM Mars 6 microwave according CEM's blood digestion application note. Digested samples were then diluted with MilliQ water and analyzed by ICP-MS. Lead bioavailability was assessed using pharmacokinetic analysis encompassing area under the curve (AUC) following zero correction and dose normalization.

The AUC for the Pb acetate oral treatment was used for calculating relative Pb bioavailability according to Equation 6.

$$\text{Pb RBA \%} = \left(\frac{\text{AUC}_{\text{Oral-Soil}}}{\text{AUC}_{\text{Oral-Pb Acetate}}} \times \frac{\text{DR}_{\text{Oral-Pb Acetate}}}{\text{DR}_{\text{Oral-Soil}}} \right) \times 100 \quad (6)$$

Where:

AUC Oral-Soil = area under the Pb blood concentration versus time curve for an oral Pb-contaminated soil dose.

AUC Oral-Pb acetate = area under the Pb blood concentration versus time curve for an oral dose of Pb acetate.

DR Oral-Soil = dose of orally administered soil (mg/kg).

DR Oral-Pb acetate = dose of orally administered Pb acetate (mg/kg).

Mobility of Pb

Mobility of Pb was determined by using the Synthetic Precipitation Leaching Procedure (SPLP), U.S. EPA Method 1312. In SPLP, 30mL of extraction fluid, 60/40 weight percent mixture of sulfuric and nitric acids at pH 4.20, was added to 1.5 g of soil and agitated for 18 hours. The samples then underwent centrifugation at 10,000g for 15 minutes and supernatant removed for ICP analysis (U.S. EPA, 2007c). Extracted Pb was determined by ICP.

Pb Speciation

X-ray absorption near edge structure (XANES) spectroscopy data were collected at the Materials Research Collaborative Access Team (MRCAT) beamline 10-ID, Sector 10 located at the Advanced Photon Source (APS), Argonne National Laboratory (ANL), Argonne, IL. The electron storage ring was operating at 7 GeV in top-up mode. A liquid N₂ cooled double crystal Si(111) monochromator was used to select incident photon energies and a platinum-coated mirror was used for harmonic rejection. The monochromator was calibrated by assigning the first derivative inflection point of the absorption L_{III}-edge of Pb metal at 13,035 eV and a Pb metal foil spectrum was collected congruently with each sample scan. Samples were pressed into pellets and three XANES scans were collected for each sample in fluorescence mode using a Ge multielement detector (Canberra). A suite of previously collected Pb reference spectra was utilized for data analysis. Principal component analysis (PCA) of the normalized sample spectra was used to estimate the likely number of species contained in the samples, while target transformation (TT) was used to identify relevant standards for linear combination fitting (LCF) of the sample spectra. PCA and TT identified four suitable Pb phases for LCF which included Pb sorbed to ferrihydrite, pyromorphite ($\text{Pb}_5(\text{PO}_4)_3\text{Cl}$), hydrocerussite ($\text{Pb}_3(\text{CO}_3)_2(\text{OH})_2$), and leadhillite ($\text{Pb}_4\text{SO}_4(\text{CO}_3)_2(\text{OH})_2$). PCA and TT were performed using SixPack while data normalization and LCF were performed using Athena. Fitting range was -30 to +100 eV relative to the Pb L_{III}-edge. For each sample, the combination of standards with the lowest residual parameter was chosen as the most likely set of components.

Task 6.2: Effect of Key Soil Chemical Processes on Long-Term Metal Permanence of Pb-contaminated Soil Remediated with Phosphate Treatments

Liquid solid partitioning (LSP) extraction was used to determine the stability of solid Pb complexes of soil Pb across pH 1 - 13. This was achieved by extracting at eight pH points across the pH range (U.S. EPA, 2012). Soil was extracted at a soil to solution ratio of 1:10 for one hour at each pH, followed by 0.45um filtration and ICP analysis.

Task 7: Bioavailability and Technology Transfer

Technology transfer of SERDP products will be mainly from the U.S. EPA ORD ER-1742 members. Also, the project PI (Basta, OSU) will work with SERDP to transfer technology generated from this project to the risk assessment and remediation sector.

The U.S. EPA developed a guidance document entitled *Evaluating the Oral Bioavailability of Metals in Soils for Use in Human Health Risk Assessment* (U.S. EPA, 2007b). As part of this guidance and directed by the Office of Solid Waste and Emergency Response, U.S. EPA's Technical Review Workgroup (TRW) for Metals and Asbestos Bioavailability Committee was

formed to provide technical support to those conducting human health risk assessments at contaminated sites. The Bioavailability Committee of the TRW acts as the primary point of contact, information archive, and repository of outreach materials for the methods recommended in the guidance document. They meet on a monthly basis to review site-specific applications, provide assistance to the regions, and issue additional guidance as necessary. Moreover, the committee reviews new methods for assessing bioavailability of inorganic soil contaminants (new method validation). U.S. EPA scientists from the Office of Research and Development (ORD), Drs. Scheckel (co-chair), Bradham, and Thomas are members of the Bioavailability Committee. In order to provide outreach and technology transfer, U.S. EPA's ORD scientists, with guidance and assistance from the U.S. EPA TRW Bioavailability Committee (<http://www.epa.gov/superfund/health/contaminants/bioavailability/trw.htm>) provided presentations and support for soil-metal bioavailability and bioaccessibility research to U.S. EPA Regional offices.

Results and Discussion

Task 1: Study Soils

Total content of As, Cd, Co, Cr, Cu, Ni, Pb, and Zn using microwave assisted acid digestion, U.S. EPA 3051a, are reported in Table 8. The arsenic concentration of the study soils ranged from 162 to 12,500 mg/kg with a median value of 464 mg/kg. Most soils (24) were <10,000 mg As/kg. The mean As concentration is 200 fold greater than the 90th percentile, 10.4 mg As/kg, of background soils throughout the United States (Smith et al., 2013; Venteris et al., 2014). Contamination is obviously present, however the range in As concentration is very important. Most in vitro bioaccessibility methods that are going to be evaluated in this study were developed using mining or other types of soils that contain highly elevated As (i.e., thousands of mg/kg As). Having a wide range in soil As concentration will help when evaluating if these methods can accurately predict bioavailable arsenic for all types of soils.

Many of the soils were co-contaminated with Pb (20 soils) and Zn (26 soils). Co-contamination is most likely due to the source term. Lead arsenates were commonly used as pesticides, 7 out of the 8 herbicide/pesticide/orchard soils also contain elevated levels of Pb. Other soils obtained from different source terms also had an elevated Pb concentration (mean 1360 mg/kg) compared to background levels of 33.1 mg Pb/kg (Smith et al., 2013). Elevated levels of Zn, greater than 28.1 mg/kg, were found in all but 1 of the study soils. Cd, Co, Cr, Cu, and Ni were also found in elevated levels in several of the study soils. The mean concentrations of Co and Cr in the study soils were similar to the 90th percentile of the background concentration found across the United States. Twenty and 59 mg/kg were the mean concentrations of Co and Cr in the study soils respectively, and the natural background throughout the United States was calculated to be 16.4 mg/kg and 55 mg/kg respectively. Only 6 of the 27 study soils contained elevated levels of Cr and there was not a pattern associating Cr with the source terms. Thirteen of the 27 study soils contained elevated concentrations of Co, however many of the soils were only slightly elevated compared to background found in soils throughout the U.S. The mean concentrations of Cd, Cu, and Ni in the study soils were greater than the background concentrations of soils in the U.S. This is most likely due to the mining and ore processing operations from which the study soils were obtained. Twelve of the 14 mining and ore processing contaminated soils contained elevated levels of Cd with > 0.5 mg/kg. Twelve of the 14 mining and ore processing contaminated soils contained elevated levels of Cu of > 31.4 mg/kg. Also, 7 of the 14 soils contained elevated levels of Ni with > 28.1 mg/kg. All of the soils except the sodium arsenate spiked soils (soils 14-16) and soil 6 contained elevated concentrations of many of the other contaminants (Cd, Co, Cr, Cu, Ni, Pb, and Zn), suggesting that although As is typically the risk driver in regards to human health risk assessment but several of the other contaminants may require attention as well.

Table 8. Total elemental content determined using microwave-assisted acid digestion U.S. EPA Method 3051a.

ID	As	Cd	Co	Cr	Cu	Ni	Pb	Zn
	mg/kg							
1	464	3.50	< 1.0	215	399	240	1620	1560
2	641	1.50	48.0	212	106	274	78.0	176
3	222	< 1.0	< 1.0	85.0	63.0	93.0	24.0	107
6	839	< 1.0	8.90	12.0	22.0	25.0	30.0	152
7	332	2.50	17.0	40.0	114	35.0	1820	358
8	162	3.00	13.0	50.0	401	44.0	288	266
9	521	< 1.0	5.20	21.0	13.0	16.0	19.0	85.0
10	3910	11.0	8.80	27.0	137	36.0	2060	4090
11	249	1.60	26.0	7.60	1610	11.0	312	189
12	1240	108	18.0	35.0	2470	11.0	5510	2440
13	12500	31.0	76.0	28.0	403	4.80	12200	1710
14	238	< 1.0	4.00	13.0	5.60	10.0	6.70	26.0
15	259	< 1.0	3.30	28.0	8.80	5.70	11.0	50.0
16	226	< 1.0	6.70	30.0	8.80	7.80	2.70	52.0
17	1540	12.0	5.70	14.0	3440	15.0	4790	4100
18	283	< 1.0	7.30	39.0	88.0	14.0	1100	79.0
19	353	< 1.0	19.0	61.0	129	33.0	1120	178
20	391	< 1.0	17.0	49.0	190	33.0	1250	165
21	375	1.00	18.0	46.0	90.0	31.0	1520	223
29	4550	15.0	10.0	37.0	64.0	56.0	240	1030
30	4000	3.30	8.10	316	39.0	79.0	82.0	228
33	302	1.40	15.0	48.0	97.0	32.0	37.0	73.0
34	2540	1.60	18.0	42.0	211	34.0	133	107
35	633	18.0	53.0	28.0	214	40.0	2080	585
36	10500	1.60	40.0	13.0	128	76.0	30.0	285
37	370	1.20	6.50	61.0	86.0	32.0	12.0	80.0
38	12000	3.10	45.0	29.0	242	87.0	303	215
Minimum	162	< 1.0	3.30	7.60	5.60	4.8	2.70	26.0
Maximum	12500	108	76.0	316	3440	274	12200	4100
Mean	2210	12.2	19.9	58.8	399	50.9	1360	689
Median	464	3.05	15.0	37.0	114	33.0	288	189
USGS 90th	10.4	0.500	16.4	55.0	31.4	28.1	33.1	28.1

The major elemental content of the 27 study soils was determined using a fusion technique and quantification via x-ray fluorescence are presented in Table 9. Soil is mainly composed of minerals. Aluminum containing minerals are the most common. They are primarily composed of Al, Si, and O which are the three most abundant elements in Earth's crustal rocks and soil. Aluminum (Al) is the most abundant metal and third most abundant element in the Earth's crust and in the soil. The Al content of soil averages 7.1% (i.e., 71,000 mg/kg). The Al content of world soil ranges from 10,000 mg/kg (1%) to 300,000 mg/kg (30%) (Essington, 2004). The 90th percentile for soils across the United States is 28% Al₂O₃ or 8% Al by weight (Smith et al., 2013). The study soils exhibited a range of 3-23% Al₂O₃ with a mean value of 12% Al₂O₃ which is within the natural range of soil Al. Also, most of the Al minerals within the environment are aluminosilicate mineral phases. The study soils contained on average 53% SiO₂, which is also consistent with composition expectations for natural soil.

The second most abundant metal found within the soils samples was Fe. Iron is the second-most abundant metal and fourth most abundant element in the Earth's crust and in world soils. The Fe content is on average 4.0% of overall soil make-up (i.e., 40,000 mg/kg). The Fe content of soil ranges from 2,000 mg/kg (0.2%) to 550,000 mg/kg (55%) (Essington, 2004). The 90th percentile for soils across the United States is 11% Fe₂O₃ or 3.72% Fe by weight. The mean Fe₂O₃ concentration in the study soils was 10% with a range of 2 – 40%. The study soils mimic not only the amount of Fe found in soils throughout the US, but also exhibit the range of Fe in soils throughout the world. Other major metal contents (i.e., Mn, Mg, Ca, Na, K, Ti) were consistent with the 90th percentile determined as background for soils across the U.S. These results show that the soils within the study are similar to natural soils aside from trace element/heavy metal contamination.

Phosphorous (P) is an important component within soil when considering As chemistry. Phosphate and arsenate are the most common form of these elements found in soil and they exhibit similar chemistry. Phosphate can desorb arsenate from Al and Fe oxide minerals in soil. The study soils contained <0.1 to 0.7% P₂O₅ with a mean of 0.2% which is similar to the background concentrations found within the United States of 0.5% P₂O₅. Phosphorus normally ranges from 50 to 15,000 mg/kg in soils (0.02 to 0.69% P₂O₅) (Pierzynski et al., 1994). The study soils are within the normal range and only 3 of the 27 study soils have a P₂O₅ concentration of equal to or greater than 0.5% P₂O₅.

Table 9. Soil content of major elemental constituents expressed on an oxide basis.

ID	SiO ₂	Al ₂ O ₃	Fe ₂ O ₃	MnO	MgO	CaO	Na ₂ O	K ₂ O	TiO ₂	P ₂ O ₅
	% —									
1	41.0	15.0	18.0	0.194	1.68	3.98	0.800	0.700	2.20	0.300
2	28.0	12.0	14.0	0.180	8.40	3.40	0.500	0.200	2.10	0.700
3	57.0	14.0	7.00	0.120	2.20	1.90	1.60	1.60	0.700	0.200
6	76.0	8.00	5.00	0.040	1.10	0.600	0.400	2.10	0.500	0.100
7	52.0	13.0	5.00	0.260	1.60	1.10	0.300	2.00	0.800	0.600
8	64.0	14.0	5.00	0.090	1.80	3.00	2.60	1.10	0.700	0.200
9	67.0	8.00	3.00	0.070	1.70	7.30	0.900	1.80	0.500	0.200
10	46.0	6.00	21.0	0.040	2.20	4.10	0.300	0.500	0.600	0.200
11	59.0	3.00	11.0	< 0.01	0.700	2.60	0.100	0.700	0.100	<0.001
12	49.0	6.00	23.0	0.100	2.00	11.7	1.20	1.20	0.300	0.200
13	37.0	3.00	40.0	0.060	0.90	0.400	0.200	0.800	0.200	0.100
14	50.0	7.00	2.00	0.020	0.90	18.3	0.600	1.80	0.400	0.100
15	57.0	9.00	3.00	0.050	1.50	8.30	1.00	1.30	0.500	0.200
16	68.0	12.0	4.00	0.060	1.20	1.20	1.10	2.50	0.600	0.100
17	65.0	11.0	6.00	0.260	1.20	1.30	1.00	2.50	0.500	0.200
18	66.0	11.0	4.00	0.040	0.500	0.400	0.100	1.10	1.30	0.200
19	40.0	17.0	7.00	0.110	1.90	2.30	0.500	1.30	1.10	0.400
20	52.0	14.0	7.00	0.190	1.30	1.60	0.400	0.900	1.40	0.300
21	41.0	13.0	6.00	0.210	1.50	2.30	0.500	0.900	1.20	0.500
29	44.0	11.0	4.00	0.050	1.30	12.7	1.10	0.800	0.600	0.200
30	62.0	8.00	4.00	0.060	4.00	4.70	0.600	1.30	0.500	0.200
33	46.0	23.0	13.0	0.070	1.00	1.20	0.700	1.10	1.20	0.100
34	48.0	16.0	17.0	0.090	1.60	0.600	0.500	2.20	0.800	0.300
35	57.0	15.0	9.0	0.170	1.10	0.600	0.700	1.70	0.600	0.100
36	51.0	17.0	10.0	0.150	1.80	3.30	0.400	3.80	1.00	0.100
37	51.0	20.0	11.0	0.060	0.400	0.200	0.100	0.900	1.40	0.100
38	47.0	18.0	15.0	0.280	1.30	0.900	0.300	2.70	1.00	0.200
Minimum	28.0	3.00	2.00	< 0.01	0.400	0.200	0.100	0.200	0.100	<0.001
Maximum	76.0	23.0	40.0	0.280	8.40	18.3	2.60	3.80	2.20	0.700
Mean	52.6	12.0	10.1	0.116	1.73	3.70	0.685	1.46	0.844	0.235
Median	51.0	12.0	7.0	0.090	1.50	2.30	0.500	1.30	0.700	0.200
USGS 90th		28.0	11.0	0.150	2.00	5.00	4.70	5.70	0.700	0.500

Soil properties relevant to As solubility and bioaccessibility were determined; soil pH, EC, oxalate extractable As, Fe, Al, Mn, and P, organic carbon content (%), soil texture (% sand, % silt, and % clay), as well as cation exchange capacity (CEC) and calcium carbonate equivalent (CCE). The pH of the soils ranged from very acidic (2.14) to alkaline (9.28) (Table 10).

Most had a pH in the range of 5.5 to 7.0. Considering that As is most closely associated with Fe and Al in soils having a range in soil pH is important. As pH decreases the solubility of Fe and Al mineral phases increases which could solubilize As. Also, arsenate desorption increases at soil pH than the point of zero charge of the mineral surface, usually greater than 7.0 (Essington, 2004). Having soils with lower pH values can account for impacts of pH on As solubility within the data set. Many of the materials in the study contain excess salt with EC values > 0.2 dS/m. This was to be expected considering that many of the materials are from industrial areas (mining, smelting, glass manufacturing, etc.) or were directly taken from surfaces of waste piles at these facilities.

Study soils had a wide range of soil properties needed for a robust method evaluation (Table 10). Soil properties relevant to As solubility (including As, Fe, and Al) showed a robust range from 64.2 to 12,041 mg/kg, 3.42 to 283 g/kg, and 4.33 to 77.7 g/kg, respectively; oxalate extractable As, Fe, and Al ranged from 20.3 to 10,706 mg/kg, 0.359 to 120 g/kg, and 0.214 to 35.8 g/kg, respectively; and soil pH ranged from 2.14 to 9.28.

Table 10. Soil properties relevant to As solubility and bioaccessibility.

ID	pH	EC	Reactive Phases/ Oxalate Extractable					Soil Texture					
			As	Al	Fe	Mn	P	Organic Carbon	Sand	Silt	Clay	CEC	CCE
		dS/m		mg/kg					%				
1	7.34	NM*	364	3560	32500	1040	849	2.74	37.0	49.0	14.0	NA**	4.48
2	5.61	1.00	559	35900	31200	702	2110	8.12	49.0	50.0	1.00	12.0	BDL***
3	6.67	0.35	160	1650	3900	612	288	2.87	16.0	47.0	37.0	32.2	0.250
6	6.84	0.20	499	214	5020	240	89.0	1.37	85.0	14.0	1.00	9.40	0.870
7	6.07	0.30	261	4630	4590	1730	1410	7.34	35.0	57.0	8.00	27.2	BDL
8	7.30	0.20	134	3170	4990	207	477	2.24	55.0	40.0	5.00	NA	1.24
9	9.28	0.50	182	658	770	245	296	0.730	38.0	60.0	2.00	NA	11.5
10	2.82	4.10	3220	785	36200	149	460	2.00	30.0	64.0	7.00	95.4	BDL
11	2.14	11.1	206	1990	34800	10.0	43.0	0.27	55.0	35.0	11.0	180	BDL
12	7.71	1.60	1000	4280	54500	305	384	1.30	66.0	30.0	4.00	NA	7.18
13	3.02	2.30	10700	1390	120000	335	249	0.730	45.0	48.0	6.00	6.00	BDL
14	7.75	0.40	203	701	359	59.0	186	0.910	23.0	54.0	23.0	NA	27.5
15	7.55	0.70	239	1590	1060	193	562	3.14	19.0	54.0	27.0	NA	12.4
16	7.55	0.40	211	1260	758	235	179	0.740	7.00	60.0	33.0	NA	1.87
17	4.00	NM	1290	1880	12700	1200	623	1.53	4.00	75.0	21.0	12.1	BDL
18	6.01	NM	162	2830	2370	100	281	3.42	34.0	52.0	14.0	11.7	BDL
19	5.80	NM	263	8090	5730	464	746	7.16	64.0	31.0	6.00	28.2	BDL
20	5.42	NM	269	8790	5970	906	705	5.09	49.0	44.0	8.00	10.4	BDL
21	6.22	NM	298	11800	7230	1150	1207	4.56	63.0	34.0	3.00	33.7	BDL
29	7.47	0.85	3310	4970	4970	219	331	4.66	49.0	42.0	9.00	NA	20.2
30	8.24	1.50	1470	1950	3700	254	483	2.43	43.0	44.0	12.0	NA	11.4
33	7.81	0.20	166	2920	6300	376	96.0	1.05	25.0	45.0	30.0	NA	1.01
34	4.96	0.10	1400	3900	23100	479	466	1.11	41.0	43.0	16.0	8.20	0.87
35	6.53	0.20	263	14500	18500	1050	215	2.03	37.0	55.0	8.0	6.90	1.12
36	7.63	0.50	2080	804	26000	796	187	2.14	48.0	38.0	14.0	NA	7.13
37	5.78	0.15	38	4490	2330	402	49.0	2.00	17.0	48.0	35.0	4.50	BDL
38	7.29	0.40	9450	3910	32500	1750	401	1.77	37.0	46.0	16.0	NA	0.630
Minimum	2.14	0.10	38.0	214	359	10.0	43.0	0.270	4.00	14.0	1.00	4.50	0.250
Maximum	9.28	11.1	10700	35850	120000	1750	2110	8.12	85.0	75.0	37.0	180	27.5
Mean	6.33	1.29	1420	4910	17800	563	495	2.72	39.7	46.6	13.7	31.8	6.86
Median	6.67	0.40	269	2920	5970	376	384	2.03	38.0	47.0	11.0	12.0	3.18

*NM Not Measured due to limited amount of material

**NA Not Appropriate to measure because soil pH >7.0

*** BDL Below Detection Limit

Total and Chemical Fractionation of As in soils

Total As in soil was determined by three methods: (1) acid digestion, U.S. EPA Method 3051 / ICP-OES (U.S. EPA Method 6010c), (2) analysis by INAA, and (3) direct soil analysis by XRF. Results from methods 1 and 2 are shown in Table 11 and method 3 XRF results are in Appendix A Table A1.

Table 11. Comparison of total As determined by U.S. EPA 3051a and INAA for study soils.

ID	U.S. EPA 3051a	INAA
1	464	581
2	641	767
3	222	220
7	332	340
8	162	182
10	3910	4500
11	249	280
12	1240	1330
13	12500	13300
14	238	259
15	259	265
16	226	259
17	1540	1510
18	283	322
19	353	462
20	391	401
21	375	422
33	302	372
34	2540	2620
35	633	646
37	370	427
Minimum	162	182
Maximum	12483	13324
Mean	1296	1404
Median	370	422
90th Percentile	2541	2619

Total As trend was INAA \geq U.S. EPA 3051a for study soils. Tukey's comparison of mean As found the difference between INAA and U.S. EPA 3051 values were not significant at P<0.05. However, regression analysis of INAA As vs. U.S. EPA 3051a As was highly significant with an r^2 of 0.999 and a slope of 1.07. Total As content is important because both in

vitro bioaccessible As and *in vivo* absolute bioavailability of As (ABA) are calculated using total As soil content. The most commonly reported total As value used in human health risk assessment is obtained using U.S. EPA Method 3051. However, the adult mouse ABA values were calculated from total As contents using INAA for 21 of the 27 study soils. Results of this study support adjusting the adult mouse RBA As for each soil using the ratio of total As INAA/U.S. EPA 3051a.

Chemical fraction of As results using a sequential extraction procedure (SEP) showed As was present in all four As fractions (F1 to F4) or “pools” (Fig. 4). In general, As in each fraction followed the trend F4, F3 > F2 > F1. Arsenic in each fraction for the 27 study soils were: (F1) extractable As ranging from <1.9 to 114 mg/kg; specifically sorbed (F2) extractable As ranging from 2.94 to 1,340 mg/kg; amorphous and poorly crystalline oxides of Fe and Al (F3) extractable As ranging from 15.5 to 7,575 mg/kg; and well-crystallized oxides of Fe and Al (F4) extractable As ranging from 12.14 to 1,504 mg/kg. The SEP F1+F2 and some of the F3 fraction constitutes bioaccessible As (Whitacre et al., 2013). The SEP F4 and F5 fractions are not considered bioaccessible and hence not bioavailable. The SEP F1+F2 fractions of most soils are <20% of total As. Soils 14, 15 and 16 have >50% of total As in F1+F2 and will likely have large IVBA As and RBA As values. In contrast, SEP F4+F5 are > 75% of total As in soils 30-37. We would expect a low IVBA As and RBA As for these soils. The F3 fraction constitutes a large amount of total As for many of the study soils (Fig. 4). Only part of the F3 fraction is considered bioaccessible and the actual percentage of the F3 fraction varies with soil type (Whitacre et al., 2013). Thus, the actual amount of bioaccessible As can be bracketed by SEP, F1+F2 < IVBA As < F1+F2+F3, but will likely not be as accurate as a predictor as the *in vitro* bioaccessible methods at predicting RBA As.

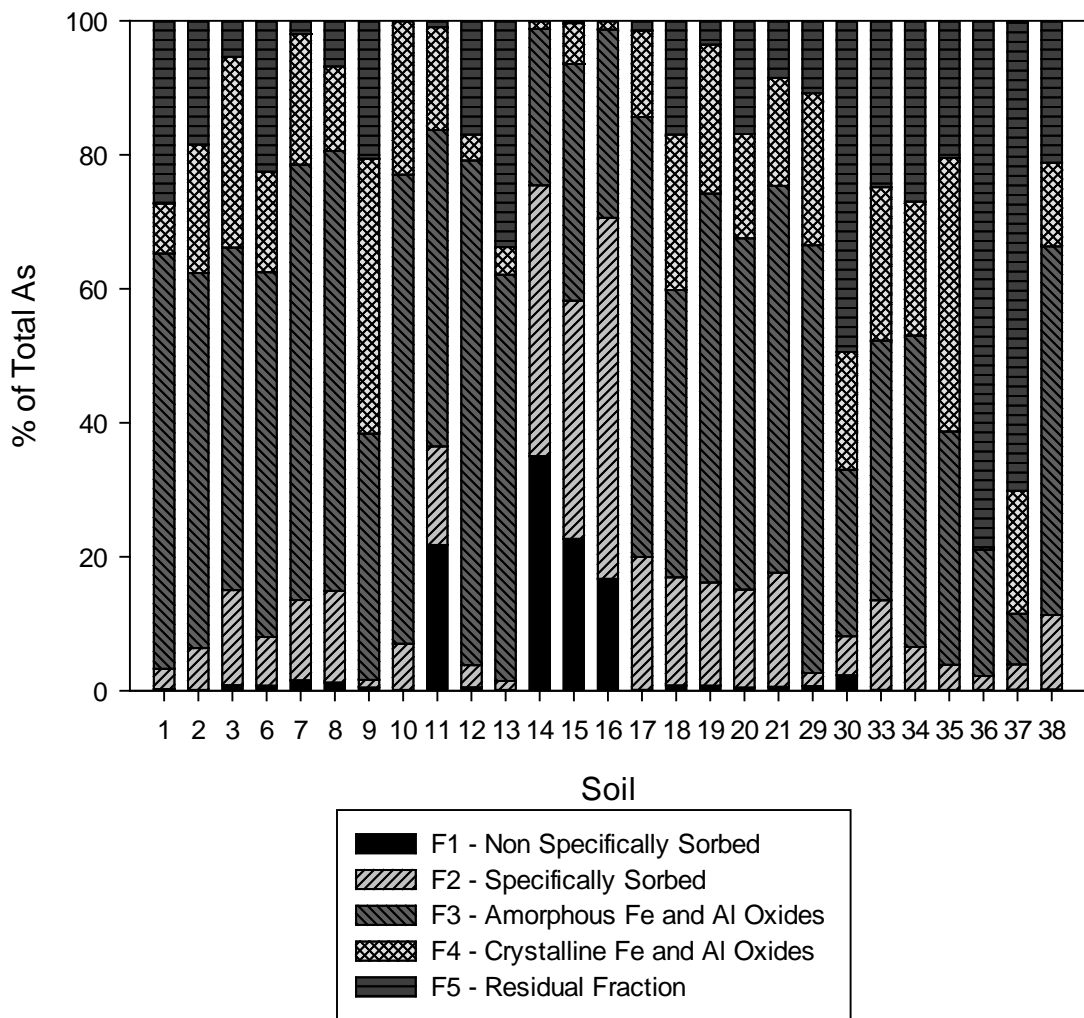


Figure 4. Arsenic fractionation by sequential extraction procedure. All results are expressed as a percentage of total soil As in each SEP fraction.

Task 2: Speciation of As in Soils by Advanced Spectroscopy

All study soils were aerobic topsoil, where oxidation of As(III) to As(V) had likely occurs, and As adsorption to mineral surfaces are the most frequent species (Deschamps et al., 2003; Manning, 2005). Iron and Al (hydr) oxides are the most abundant surfaces which retain arsenic as adsorbed species, but manganese (Mn) oxides can have a high affinity if present (Manning et al., 2002).

The geochemistry of As is commonly linked to iron (Fe) because of its strong specific bonding to arsenic as well as the abundance of Fe in most soils (Bowell et al., 2014). The geochemical association between As and Fe is well established and is mainly due to

coprecipitation of As and Fe (sulfides) and the affinity of As oxyanions for the surfaces of Fe oxides (Schwertmann and Taylor, 1989). Strong correlation coefficients between Fe and As have been reported in the soil science literature including $r = 1.0$ for US Soils, 0 to 5 cm (Smith et al., 2013) and Ohio topsoil ($r = 0.58$) and subsoil ($r = 0.70$) (Venteris et al., 2014).

Historic use of inorganic arsenic pesticides have included lead arsenate (PbHAsO_4) and arsenolite and can persist in the soil. Organo-arsenicals have been used more recently. Lead arsenate and arsenolite can be relatively insoluble and persist in soil but formation of Ca-arsenates or Ca-Fe-arsenates have been documented (Cances et al., 2008).

In mining-contaminated soil, arsenopyrite, orpiment and realgar are most commonly identified in association with sulfide minerals. Arsenopyrite is the most common chalcophile mineral of arsenic, but loellingite and coprecipitation with pyrite and other metal sulfides can also be present depending on the ore body (Hudson-Edwards et al. 2005). Arsenolite is the most common As(III) oxide and forms in neutral to alkaline and oxidizing weathering conditions. Acid mine drainage releases large amounts of aqueous arsenic and iron, which precipitates first as a hydrous ferric arsenate (HFA) and can crystalize into scorodite, arseniosiderite, form Fe oxides or other minerals depending on the weathering conditions (Filippi et al. 2015).

Arsenic Speciation

Arsenic XAS measurements of the soils are listed in Appendix Figure A5 and the EXAFS in Figure A6. The detailed list of LCF results are listed in charts in Appendix Tables A2-4, which includes percentage (%) of the standard spectra used in the best fit LC model and the reduced chi-squared value. Arsenic XAS spectra for all soils are displayed as norm(E), deriv(E) and chi space data.

Oxidation State

Oxidation state identification is the simplest analysis derived from As XAS spectra. Oxidation state identification provides clear results using only the XANES region even with low quality spectra due to the edge energy increase with increasing oxidation state. The oxidation states of an element differ in the number of valence shell electrons, with higher oxidation (i.e. less valence electrons) increasing the binding energy of the core-level electrons that are excited in K-edge XAS. Higher binding energy of core electrons need more energy (eV) to excite them, causing an increase in the K-edge (e_0) of the spectra. Figure 5 shows that the pure As sorption and mineral species used in this investigation, grouped by *a priori* information of oxidation state and 1st and/or 2nd shell bonding elements, plotted as the average e_0 energy position within standard group with error +/- 1 standard deviation.

Arsenic K-edge XANES show a clear separation of oxidation states with theoretical positions of e_0 : 11874 eV for As(V), 11871 eV for As(III), 11869 eV for As(III) sulfur inorganic compounds and 11867 eV for As(-III) metal sulfate species. The e_0 position was established using the 1st inflection point (2nd deriv 0), causing ~1eV offset from other reported values. The standards showed clear separation between As(V) and As(-III), while As(III) e_0 position depended on the 1st shell bonding element, with sulfur bonding having a much lower e_0 as expected from theory. The As (III) sulfide minerals have a lower e_0 than As(III) oxide species due to the As-S bond being more covalent; which was seen in the respective e_0 positions of our standards. All As(V) species had very similar e_0 positions regardless of 1st and 2nd shell neighbors.

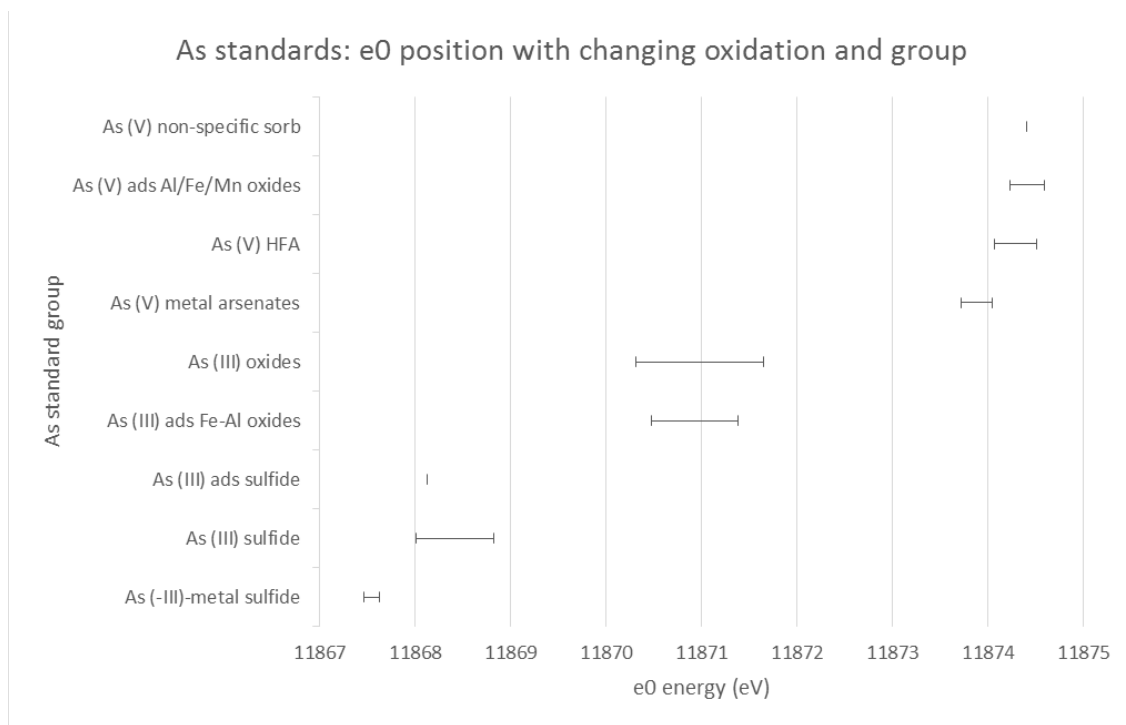


Figure 5. Energy positions of arsenic standards grouped by oxidation and coordinated elements.

A review of the e0 positions in the soil spectra showed As (V) as by-far the most abundant oxidation state in the dataset (Table 12). The abundance of As(V) oxidation state is expected because as the deposited As weathers in the oxidized topsoil environment. As(V) is more stable in this environment and where the soils were collected. Some amount of reduced arsenic (oxidation state < 5) was present in 14 of the 27 soils in the dataset, evidenced by an additional As K-edge peak position <11872 eV. Of the soils with reduced arsenic, 6 soils either had arsenic (III) sulfides or As < 3 valence. Table 12 indicates the position(s) of As K-edge(s). The percentages of these oxidation states are calculated by the LC fits summary of species LC fit to samples shown in the next section.

Table 12. Arsenic K-edge e0 positions and % of oxidation from LCF.

ID	As(-III)	As(III)-S	As(III)	As(V)	As(-III)	As(III)-S	As(III)	As(V)
	eV				%			
1			11870.28	11874.98			76	24
2				11874.53				100
3				11874.23				100
6		11868		11874.32		3	9	88
7				11874.46				100
8			11870.76	11874.5			47	53
9				11874.35				100
10			11870.38	11874.39		7	4	89
11		11869.7		11874.76		10		90
12			11871.43	11874.26			9	91
13				11874.06				100
14				11873.99				100
15				11873.92				100
16				11873.95				100
17			11871.73	11874.56			8	92
18				11874.1				100
19				11874.1				100
20				11874.22				100
21				11874.11				100
29				11874.04				100
30				11873.9				100
33		11868		11874.28		10		90
34				11874.48				100
35				11874.42				100
36	11867.41			11874.41	78			22
37		11868.4		11874.34		3		97
38	11867.61			11874.37	22			79

Arsenic Linear Combination Models of K-edge XAS

For interpretation, results from some of the species were summed with other species sharing high spectral similarity in both XANES and EXAFS, as it was unreasonable to distinguish further detail with bulk measurements in a soil matrix. The groups are as follows in Table 13 below. Data is discussed in this section referencing Table 14, which contains *a priori* chemical information available on soils and weighted groupings.

Table 13. As species groupings determined via LCF for As EXAFS and XANES.

Group	As Species
As(-III) Metal Sulfides	Arsenopyrite, Loellingite
As(III) Sulfides	Orpiment, Realgar
As(III) Oxides	Arsenolite, Schniderhohnite
As(III) ads* Sulfide	As(III) ads Pyrite
As(III) ads Fe-Al oxides	As(III) ads Ferrihydrite, As(III) ads Montmorillonite, As(III) Al ₂ O ₃
Lead Arsenate	PbHAsO ₄
Hydrous Ferric Arsenates	Arseniosiderite, Pharmacosiderite, Scorodite
As(V) ads Hydrous Ferric Oxides (HFO)	As(V) ads Ferrihydrite, As(V) ads Ferrihydrite (low As)
As(V) ads Al/Fe/Mn Oxides	As(V) ads Goethite, As(V) ads Hematite, As(V) ads Birnessite, As(V) ads Gibbsite, As(V) ads Kaolinite

* ads adsorbed

The major species across all soils regardless of contamination source were sorption to Al/Fe/Mn oxides and HFO, as would be expected from soil contamination. When looking at species by contamination source, some trends were observed. Arsenic spiked soils were found with highly-available, non-specific sorption and surface adsorbed species. In pesticide-contaminated soils (1, 2, 3, 7, 18, 19, 20, and 21) six of eight soils had a ~20% fraction of lead arsenate. The remaining arsenic in the pesticide-contaminated soils was adsorbed to Fe/Al/Mn oxide surfaces or adsorbed to HFO. Almost all of the arsenic existed as +5 oxidation, with the exception of soil 1 with an unusual ~70% fit as As(III) adsorbed to Fe and Al oxide surfaces.

The mining-contaminated soils (6, 8 - 13, 17, 33 - 38) had more variety in As oxidation state as well as in minerals found. Arsenic (III) was present in eight of fourteen soils either as As(III) sulfides or sorbed to mineral surfaces. Soils 36 and 38 were the only soils where As(-III) was identified. The most common mineral, arsenopyrite could only be identified in soil 36, by fitting both As and Fe species as sulfides. Although soil 38 had a As(-III) peak, no Fe sulfide phase was detected so it is possible that this soil contains an As(-III) metal sulfide with a cation other than Fe.

Hydrous ferric arsenates (HFA) were also only identified in mining-contaminated soils. The Fe arsenates and Ca-Fe arsenates have particular importance in many natural systems and are important in mining-impacted environments. HFAs can have significant substitution with anions (PO₄, SO₄, CO₃) and cations (Ca, K, Fe, Mg). Many HFAs are very similar in the XANES region and have only slight differences in the EXAFS region but they can have widely dissimilar solubilities and formation conditions. In soils 9, 12, 17, 35, and 38, As XAS were fit as HFA but Fe XAS were fit as HFO suggesting the As species may be adsorbed/coprecipitated with HFO without altering the HFO structure. Soils 10, 11, and 13 were the only soils where HFAs were

identified in both As and Fe XAS. Combined with the sequential extraction data, soil 11 is more likely to be a soluble HFA such as arseniosiderite and soils 10 and 13 are more likely to be an insoluble HFA mineral such as scorodite.

None of the soils were well-fit by realgar, schniderhohnite, loellingite, beudantite, MMA, DMA or sodium arsenate. A few soils were unable to be well-modelled using our standard library: soils 10, 29, and 30. Soil 10 was a mining-contaminated soil, with misfit in the As(V) e0 position. Soils 29 and 30 both were contaminated by glass manufacturing and were both best fit with As(V) non-specific sorption. The missing phase in soil 29 is likely to be an amorphous calcium arsenate because of the high soil pH, high As solubility and only weakly-defined scattering pathways in the EXAFS. Soil 30 has more defined scattering pathways in EXAFS and low As extractability, suggesting a slightly-soluble, crystalline arsenic mineral phase.

Table 14. Results of LCF from As EXAFS and XANES.

As(-III) minerals		As(III) minerals		As(III) sorption		As(V) minerals		As(V) sorption	
ID	As - Metal Sulfides	As(III) Sulfides	As(III) Oxides	As(III) ads* Sulfides	As(III) ads Fe/Al Oxides or Aluminosilicate	Lead Arsenate	Hydrous Ferric Arsenates	As(V) ads Hydrous Ferric Oxide	As(V) ads Al/Fe/Mn Oxides
%									
1					76			24	
2						21		18	61
3								100	
6		9	3					14	74
7						16		13	71
8					47			21	32
9							56	44	
10		11					57	33	
11		10					51	38	
12					9		78		13
13								33	67
14								100	
15								100	
16								100	
17					8		82	10	
18						25		9	66
19						23		7	71
20						15			86
21						23		6	71
29								100	
30								100	
33		100						23	67
34								37	63
35							44	11	45
36	78							12	10
37			3						97
38	22						35		44

*ads adsorbed

The As mineral species groups and data obtained from LCF fitting of As EXAFS and XANES results were used to determine which soils were most similar to one another using principle component analysis (PCA). The principle components are listed below in Table 15, coefficients greater than 0.5 were deemed important regardless of sign. Figure 6 below shows the score plot of principle component two vs principle component one for the As XAS data set. These two principle components described about 82% of the variance within the As LCF EXAFS and XANES data. As(V) adsorbed to hydrous ferric oxides and As(V) adsorbed to Al/ Fe/Mn oxides were also identified as dominant As species by principle component analysis with principle component one coefficients of -0.732 and 0.672 respectively. Principle component two had one significant coefficient for hydrous ferric arsenates of -0.780. There were three major soil groupings within the data set comprised of soils that were 100% As(V) adsorbed to hydrous ferric oxides (3, 14, 15, 16, 29, 30), soils that As mineralogy was dominated by As(V) adsorbed to Al/Fe/Mn oxides (2, 6, 7, 13, 19, 19, 20, 21, 33, 34, 37), and soils that contained a range of hydrous ferric arsenates (9, 10, 11, 12, 17, 35, 38).

Many of the pesticide contaminated soils that contained lead arsenate grouped together with other soils that also contain arsenic adsorbed to soil minerals of Al, Fe, and Mn, suggesting that the source type (lead arsenate pesticides) are not the phase containing most of the As in these soils. Soil 1 was the only pesticide contaminated soil to not be in the larger group. This is most likely due to the high amounts of adsorbed As(III) in soil one. Using a Grubbs outlier test soil 1 was removed from the data set as an outlier with a p value (<0.001 for $\alpha = 0.05$). The strong sorption to Fe/Al oxides or aluminosilicates and the identification of Fe substituted aluminosilicates and Fe silicates in this sample as well as its geographic location suggest that allophane may be present. Allophane is an aluminosilicate that can have a varied structure and is generally amorphous, typically it can be found with volcanic type materials, which is logical for soil 1 considering that it was obtained from Hawaii.

Soils that did not contain As(V) adsorbed to hydrous ferric oxides or Al/Fe/Mn oxides contained hydrous ferric arsenates as a major or dominant mineral form and are grouped together and shown in Figure 6. Soils 12 and 17 contained hydrous ferric arsenates as dominant phase whereas soils 9, 10, 11, 35, and 38 contained hydrous ferric arsenates as a major As mineral phase. Although about 54% of the variance within the As mineralogy was explained with the first principle component (As (V) adsorbed to either hydrous ferric oxides or Al/Fe/Mn oxides) as would be expected because As in soil closely associates with these types of soil minerals. Adding in principle component two the amount of variance accounted for increases to 82%, suggesting principle component two, As(V) adsorbed to hydrous ferric arsenates, is also an important species when looking at As mineralogy in soils.

Table 15. Principle component coefficients for As EXAFS and XANES species groups

Principle Component	1	2	3	4	5	6	7	8	9
As(-III)-Metal Sulfides	0.015	-0.06	-0.33	0.84	-0.119	0.151	-0.166	0.101	-0.326
As(III) Sulfides	-0.004	-0.027	0.03	-0.005	-0.034	-0.92	-0.186	0.09	-0.33
As(III) Oxides	0.007	0.006	0.004	-0.002	-0.061	-0.02	0.864	0.384	-0.319
As(III) ads Sulfides	0.006	0.004	0.004	-0.002	-0.049	0.005	0.246	-0.886	-0.39
As(III) ads Fe/Al Oxides or Aluminosilicates	-0.015	-0.084	-0.739	-0.513	-0.128	0.147	-0.168	0.102	-0.327
Lead Arsenate	0.101	0.074	0.04	-0.021	-0.923	0.107	-0.086	0.071	-0.327
Hydrous Ferric Arsenates	-0.046	-0.78	0.423	-0.113	-0.115	0.202	-0.166	0.103	-0.326
As(V) ads Hydrous Ferric Oxide	-0.732	0.446	0.266	-0.071	-0.127	0.166	-0.17	0.103	-0.326
As(V) ads Al/Fe/Mn Oxides	0.672	0.42	0.304	-0.284	-0.284	0.173	-0.196	0.113	-0.325

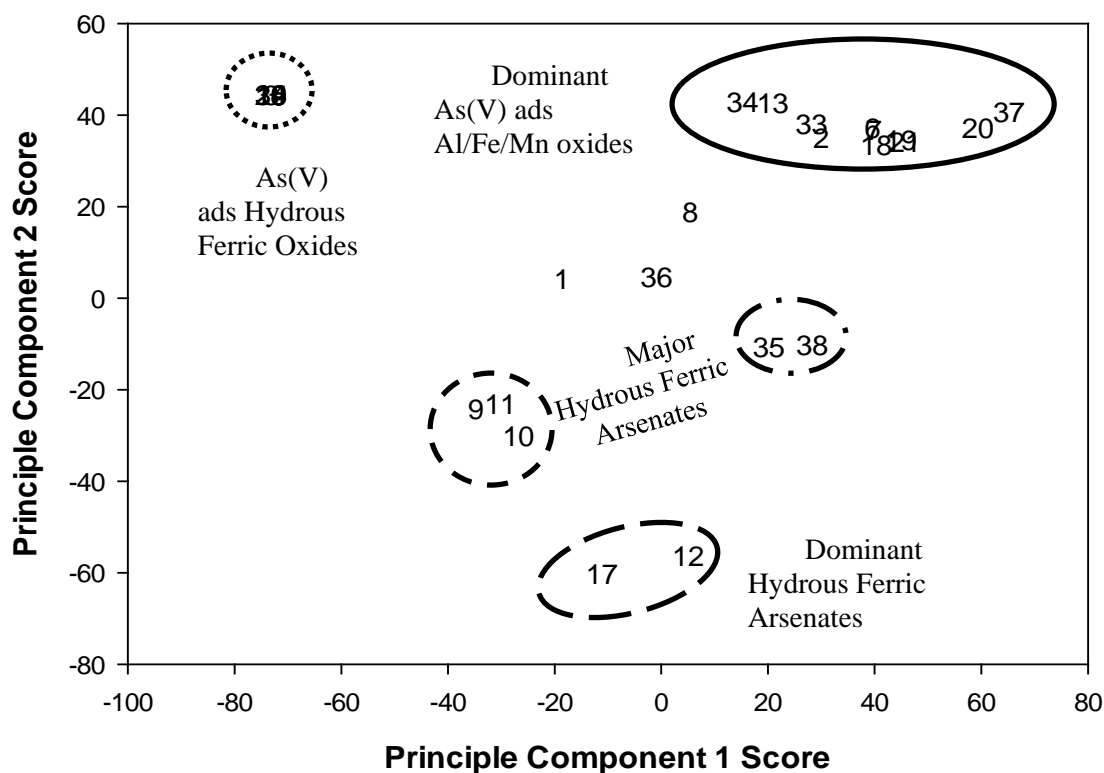


Figure 6. As soil groupings determined via PCA analysis.

Iron Speciation

Iron XAS measurements of the soils are listed in Appendix Figure A7 and the EXAFS in Figure A8. The detailed list of LCF results are listed in charts in Appendix Table A5 to A7, which includes percentage (%) of the standard spectra used in the best fit LC model and the reduced chi-squared value. Iron XAS spectra for all soils are displayed as norm(E), deriv(E) and chi space data.

Soil spectra for Mössbauer (298K and 4K), Fe XAS, and As XAS can all be found in the appendix as well as the details of their modelling. Mössbauer spectra from each soil (298 K and selected soils at 4 K) can be found in Appendix Figures A9 to A17 and details of model fits in appendix Tables A8 to A11 for each temperature respectively. These tables include IS, QS, and B_{hf} values with their intensities and error associated.

Oxidation State

Iron can have a valence of 0, +2 or +3, but Fe (II) and (III) are typically present in the soil environment. For XAS, oxidation state will increase the e_0 energy with higher oxidation as well as an intensifying of the pre-edge peak, but using LCF over the whole XAS spectrum (XANES and EXAFS) is the most accurate analysis (Prietz et al., 2007). However, using LCF will have at least the standard error (+/-10%) attached to oxidation state prediction and higher error has been reported depending on the types of Fe species or minerals in the sample (Prietz et al., 2007). Fe oxidation state can also be determined readily from Mössbauer spectra by the isomer shift (IS) of doublet peaks. The ranges for Fe(II) and (III) are very distinct; IS for Fe(III) lie between 0.1 and 0.5 and Fe(II) between 0.9 and 1.4 with a standard error of +/- 0.03. Only in the case of a mixed (II/III) mineral will IS have a value in the loosely defined region between 0.5-0.9.

After all Fe XAS and Mössbauer modelling were complete, the sum of oxidation states were compared to each other as displayed in Table 16. The two techniques matched within error of the less sensitive XAS (~10%), but there are exceptions. Some of the deviation occurred because Mössbauer can detect components as low as 1% and XAS could only detect ~5% and fit with 10% error. The small Fe(II) components may be Fe(II) inclusions in the parent material, because Fe in crustal rocks typically start as Fe(II) and oxidize to Fe(III) as they weather (Stucki, 1988). Mining contaminated soils had the highest ratio of Fe(II):Fe(III) than soils from other contamination sources.

Soil 10 was unusual because it showed much more Fe (II) in XAS than was found with Mössbauer, the reason for this may simply be heterogeneity in the sample matrix. Soil 13 appears to be fit with a much larger XAS Fe(II/III) fraction, but this is a result of fitting with maghemite, which is a Fe(II) deficient magnetite/hematite intermediate, inflating the value of the XANES (II/III) percentage (%) component.

Table 16. Comparison of oxidation state from Mössbauer and Fe XAS LCF models.

ID	Mössbauer			XANES			Difference		
	Fe (II)	Fe (III)	Fe (II/III)	Fe (II)	Fe (III)	Fe (II/III)	Fe (II)	Fe (III)	Fe (II/III)
	%								
1	20	80		15	85		5	-5	
2	39	61		44	56		-5	5	
3	10	90		13	87		-3	3	
6	57	43		61	39		-4	4	
7	18	82		28	72		-10	10	
8	46	48	6	44	56		2	-8	6
9	14	86			100		14	-14	
10	14	86		44	56		-30	30	
11	2	98			100		2	-2	
12	68	32		76	24		-8	8	
13		91	9		66	34		25	-25
14	5	95			100		5	-5	
15	8	92			100		8	-8	
16	4	96			100		4	-4	
17	6	90	4	19	81		-13	9	4
18		95	5	7	93		-7	2	5
19	4	94	2	10	90		-6	4	2
20	5	91	4	9	91		-4		4
21		97	3		100			-3	3
29	7	93			100		7	-7	
30	10	90			100		10	-10	
33	8	92		12	88		-4	4	
34	23	77		33	67		-10	10	
35	22	78		22	78				
36	44	56		58	42		-14	14	
37	19	81		14	86		5	-5	
38	11	89			100		11	-11	

Iron Coordination Geometry

Room temperature Mössbauer spectra can also identify coordination number and symmetry with changes in the isomer shift (IS) and the quadrupole splitting (QS) in the doublet peak pattern(s) of the sample. By combining the IS and QS parameters from the Mössbauer modelling, we could identify the coordination geometry and their relative percentage of the total Fe in each soil (Table 17).

Most Fe (II) or (III) compounds in the environment have octahedral (6n) coordination. For Fe(II), 6n has the most stable crystal field energy and additional stabilization if the octahedral site is distorted. Cubic, or 8-coordination (8n) is slightly less favorable than octahedral and tetrahedral (4n) is even less favorable (Stucki, 1988). As expected in the dataset, most coordination was in the 6n geometry for both Fe(II) and Fe(III), including all of the Fe(III) in the soils.

The 8n coordinated Fe(II) was found in four soils; soil 2 from Hawaii and soils 33, 34, and 35 from the same gold mining site in California. Molten Fe will first form body-centered cubic packing structure which is 8n (Stucki, 1988). It is possible that the parent material in the Hawaiian soil is volcanic and a small amount of Fe is still in an igneous material with this chemistry. The ore material from the gold mining site may have this Fe in the contaminating ore body. The rare tetrahedrally-coordinated (4n) Fe(II) was found in three soils of the dataset; two from pesticide contamination in Hawaii and one from a copper mine. The 4n Fe(II) has been known to form in Fe sulfides when they are admixed with other calcophile minerals (Goldschmidt, 1954), so it is possible that this occurred in the mined copper deposits from this site. The two Hawaiian soils (1 and 2) may have this unusual coordination from the weathered volcanic parent material, similar to the origin of the 4n Fe(II) fraction found in soil 2.

The Fe(II/III) fitting for soils 8, 17, 18, 19, 20, 21 in such small amounts is interesting. Only the 9% component in soil 13 is near the fitting limit of Fe XAS LCF (~10%). Soils 8 and 17 are mining soils, but the others are all from a single orchard site. It is known that numerous microorganisms can reduce Fe(III) during the metabolism of organic matter and precipitate Fe(II/III) such as magnetite (Lovley, 1987). The orchard soils have 3-7% organic carbon, so this is a possible source of the Fe(II/III) mixture.

Table 17. Mössbauer room temperature (298K) oxidation and coordination results

ID	Fe(II)			Fe(II/III)		Fe(III)	
	4n	6n	8n	4n/6n	4n	6n	
1	20					80	
2	12	14	13			61	
3		10				90	
6		57				43	
7		18				82	
8		46		6		48	
9		14				86	
10		14				86	
11		2				98	
12	68					32	
13				9		91	
14		5				95	
15		8				92	
16		4				96	
17		6		4		90	
18				5		95	
19		4		2		94	
20		5		4		91	
21				3		97	
29		7				93	
30		10				90	
33			8			92	
34			13			91	
35			16			84	
36		44				56	
37		19				81	
38		11				89	

Magnetic Ordering of Iron

Mössbauer spectra are able to detect magnetic ordering as a function of temperature. Each species of Fe has a unique Néel temperature (T_N), below which the two-peak dipole splitting normally seen at room temperature will separate into a 6-peak pattern as the thermal energy no longer inhibits the macroscopic magnetic ordering within the material.

Most Fe species are above their T_N at room temperature (298 K), but exceptions exist of common soil species (e.g. magnetite, hematite, goethite). Magnetic ordering causes a 6-peak pattern with a typical intensity ratio of 3:2:1:1:2:3. Iron is typically studied at multiple temperatures (e.g. 298, 77, 30, and 4 K) to find the T_N of the Fe in the sample. The T_N and

spacing of the 6-peaks (quantified by the B_{hf} value) can be partially-diagnostic of iron species, but this analysis alone is not typically used for identification (Dyar et al., 2006). Even a synthetic mineral may be a superposition of doublets and sextets for each of the Fe coordination sites present and some major lithic species of Fe are known to have identical spectra (Dyar et al., 2006). The data obtained in this study was used as an independent source for identification of oxidation state, coordination and certain Fe oxides using their B_{hf} in order to select appropriate species for Fe XAS LCF models.

After samples were cooled to 4 K, more magnetic ordering was observed in all soil samples than at room temperature, which can be seen in Table 18. Increased magnetic ordering was expected because 4 K will be below the T_N of most Fe species. Some Fe orbitals still remained unordered, which gave evidence for certain species of Fe to be used in LCF. For example, if an Fe (III) octahedral quadrupole splitting was remaining at 4 K, the value of the percent component matched very closely with the percent required for Fe (III) substituted montmorillonite used in XAS models. The B_{hf} values were also used to constrain Fe XAS fitting either by the presence/absence of magnetic ordering at 298 K or by the B_{hf} spacing.

Table 18. Mössbauer results showing the increase in magnetic ordering with decreasing temperature in selected soils.

ID	298 K			4 K			
	Magnetic Ordering	Unordered Fe(II)	Unordered Fe(III)	Magnetic Ordering	Unordered Fe(II)	Unordered Fe(III)	Unordered Fe (II/III)
%							
1	23	19	58				
2	23	23	54	77	16		7
3	9	10	81	38	7	55	
4	13	8	79				
5	12	20	67	40	23	37	
6		52	48				
7	13	21	66	62	12	26	
8	20	34	46				
9	19	13	68				
10		13	87	50	11	39	
11			100				
12	7	68	25				
13	12		89				
14			100	35		65	
15		8	91				
16	5	5	79	30		70	
17	8	14	78	65		35	
18			95				
19			90				
20	6		90	49	16	35	
21			100	58		42	
29	34	8	59				
30	12	11	77				
33	33	9	58				
34	10	13	77	82	7	11	
35	6	16	78	79	7	14	
36	6	16	78				
37	40		58	96		4	
38	16	13	71				

Iron Linear Combination Fitting of K-edge XAS

For interpretation, results from some of the species were summed with others sharing high spectral similarity in both XANES and EXAFS, as it was unreasonable to distinguish further detail due to the variety and abundance of potential species of Fe in soils in bulk measurements

from a soil matrix. The groups are as follows in Table 19 below. Results of Fe XAS LCF are summarized in Table 20.

Table 19. Iron species groupings from iron linear combination fitting of K-edge XANES summary.

Group	Fe Species
Fe(II) Sulfides	Arsenopyrite, Pyrite, Marcasite, Loellingite
Fe(II) Silicates	Fayalite, Biotite
Fe(III) Oxides	Hematite, Goethite, Maghemite
Fe(II/III) Oxide	
Hydrous Ferrous Arsenates	Scorodite, Yukonite, Pharmacosiderite
Hydrous Ferric Oxides	Ferrihydrite, Akaganeite, Lepidocrocite
Fe(III) sub Aluminosilicate	
Fe(II) Organic Complexes	Fe(II) Acetate, Fe(II) Chloride, Fe(II) Oxalate, Fe(II) Sulfate, Vivianite
Fe(III) Organic Complexes	Fe(III) Citrate, Fe(III) Phytate, Fe(III) Phosphate

The most frequently found Fe species groups in the soil dataset were the hydrous ferric oxides (HFO), Fe oxides, and Fe(III) substituted in aluminosilicate, which is common in many soils and expected from the dataset. Hydrous ferric oxides were found in every soil except for two mining soils, 11 and 13. The room temperature and 4 K magnetic ordering from Mössbauer provided good evidence for selection between the Fe hydroxides and oxides because many common species have very different Néel temperatures. Both Fe(II) and (III) organic complexes (e.g. oxalate, citrate, etc.) were also found in many soils. These species could be thought to describe the core Fe mineralogy in each soil and are a function of the soil forming conditions, independent of the arsenic contamination.

The pesticide-contaminated soils generally had less Fe (III) in aluminosilicates, but otherwise had no trends in Fe species different from the spiked soils. The mining contaminated soils however, were the only to contain Fe(II) sulfides, magnetic species and hydrous ferric arsenate (HFA) minerals. Iron(II) sulfides were found in roughly a third of the mining soils (3 of 9 soils). Only two mining affected soils (12 and 13) were fit with magnetic species and HFAs were found in soils 10, 11, and 13. The Fe(II) sulfides found in soils 6, 8, 10, 12 and 36 were all be similar in e0 position and spectral features. Arsenic sulfide was only identified in soil 36, so the species in 6, 8 and 10 are other iron sulfides. Loellingite was best fit for soils 6, 8 and 36. Soil 36 was well-fit with arsenopyrite, so it is possible this soil has a hybrid mineral of arsenopyrite and loellingite. Soils 6 and 8 lacked any As(-III) metal sulfides or As(III) sulfides so, loellingite is likely the closest match for a missing reduced Fe(II) mineral. Organic phosphate species associated with Fe were observed in soils 2, 11, 17 and 35.

Table 20. Fe LCF of K-edge XANES summary.

ID	As Source	Fe in Oxides and Clay						Fe Minerals	Fe Organic Complexes		Reduced Chi Square
		Fe (II) Sulfides	Fe (II) Silicates	Fe(III) Oxides	Fe(II/III) Oxide	Hydrous Ferric Oxides	Fe(III) sub Aluminosilicate		Hydrous Ferrous Arsenates	Fe (II) Organic Complexes	
%											
1	Pesticide		15			55	30				9.60E-05
2	Pesticide		26	7		49			18		1.40E-05
3	Pesticide			13		36	38		13		1.10E-05
6	Mining	25				39			36		2.40E-05
7	Pesticide		14	40		31			14		8.90E-05
8	Smelter	20	25	14		41					1.80E-05
9	Tailings			26		64	10				5.10E-06
10	Tailings	26	18					56			3.50E-05
11	Mining							36		64	6.40E-05
12	Mining	20	56			24					1.90E-05
13	Mining			16	34			50			7.30E-05
14	Spiked			19		15	67				1.30E-05
15	Spiked			10		20	70				1.30E-05
16	Spiked			17		18	65				7.10E-06
17	SRM			41		40			19		3.90E-06
18	Pesticide			33		60			7		6.60E-06
19	Pesticide					45	45		10		6.80E-05
20	Pesticide	9		44		21	26				1.20E-05
21	Pesticide			21		47	32				9.90E-06
29	Glass			17		83					9.30E-06
30	Manufacturing										
	Glass			22		63	15				6.50E-06
33	Mining		12	68		19					4.90E-06
34	Mining		17			38			15	29	1.40E-05
35	Mining		22			62				16	1.10E-05
36	Mining	39		15		27			19		2.10E-05
37	Mining			41		45			14		9.50E-06
38	Mining			79		21					3.00E-06

The Fe mineral species groups and data obtained from LCF fitting of Fe XANES results were used to determine which soils were most similar to one another using principle component analysis (PCA). The principle components are listed below in Table 21, coefficients greater than 0.5 were deemed important regardless of sign. Figure 7 below shows the score plot of principle component two vs principle component one for the Fe XAS data set. These two principle components described about 54% of the variance within the Fe LCF XANES data. Hydrous ferric oxides and Fe(III) substituted in aluminosilicates were also identified as dominant Fe species by principle component analysis with principle component one coefficients of -0.606 and 0.660 respectively. Principle component two had one significant coefficient for Fe(III) substituted aluminosilicates of -0.665. Mining soils 10, 11, and 13 are grouped separately from the rest of the data set in Figure 7. The amount of Fe(III) substituted aluminosilicate in these samples was essentially cancelled in the PCA analysis. These soils are grouped together and are also the only soils that contained hydrous ferric arsenates via XANES. In addition, hydrous ferric arsenates have a principle component two coefficient of 0.462, which is on the border of the 0.5 cutoff for the analysis. Many of the pesticide contaminated soils have similar Fe mineralogy to the spiked samples (14, 15 and 16). However, the spiked samples contained more Fe(III) substituted aluminosilicates than many of the pesticide contaminated soils. This is also shown in Figure 7 with the PCA analysis. Spiked soils (14,15 and 16) which have Fe(III) substituted in aluminosilicates as their dominant form are grouped separately than most of the pesticide contaminated soils (1, 3, 19, 20, 21). Soils that did not contain Fe(III) in aluminosilicates as a major or dominant mineral form are predominantly hydrous ferric oxides and Fe(III) oxides and are grouped together and shown in Figure 7. Although about 50% of the variance within the Fe mineralogy was explained with the first two principle components if principle component three is included the variance accounted for increases to 76%. Principle component 3 adds Fe(III) oxides to the dominant mineral species with a coefficient of -0.865.

Table 21. Principle component coefficients for Fe XANES species groups.

Principle Component	1	2	3	4	5	6	7	8	9
Fe (II) Sulfides	0.004	0.192	0.117	0.449	-0.291	0.298	-0.644	-0.226	-0.33
Fe (II) Silicates	-0.071	0.186	0.203	0.552	0.601	-0.288	0.196	0.139	-0.336
Fe(III) Oxides	-0.309	-0.126	-0.865	0.005	0.113	-0.012	-0.104	0.075	-0.334
Fe(II/III) Oxide	0.058	0.098	-0.046	-0.061	-0.206	-0.245	0.403	-0.778	-0.333
Hydrous Ferric Oxides	-0.606	-0.43	0.417	-0.248	-0.127	-0.247	-0.142	0.075	-0.332
Fe(III) sub Alumino-Silicate	0.66	-0.665	0.007	0.045	0.043	-0.022	-0.048	0.075	-0.331
Hydrous Ferrous Arsenates	0.268	0.462	-0.03	-0.243	-0.363	-0.458	-0.07	0.445	-0.332
Fe (II) Organic Complexes	-0.102	0.029	0.076	0.098	-0.292	0.601	0.564	0.308	-0.337
Fe(III) Organic Complexes	0.103	0.249	0.125	-0.598	0.514	0.368	-0.168	-0.118	-0.334

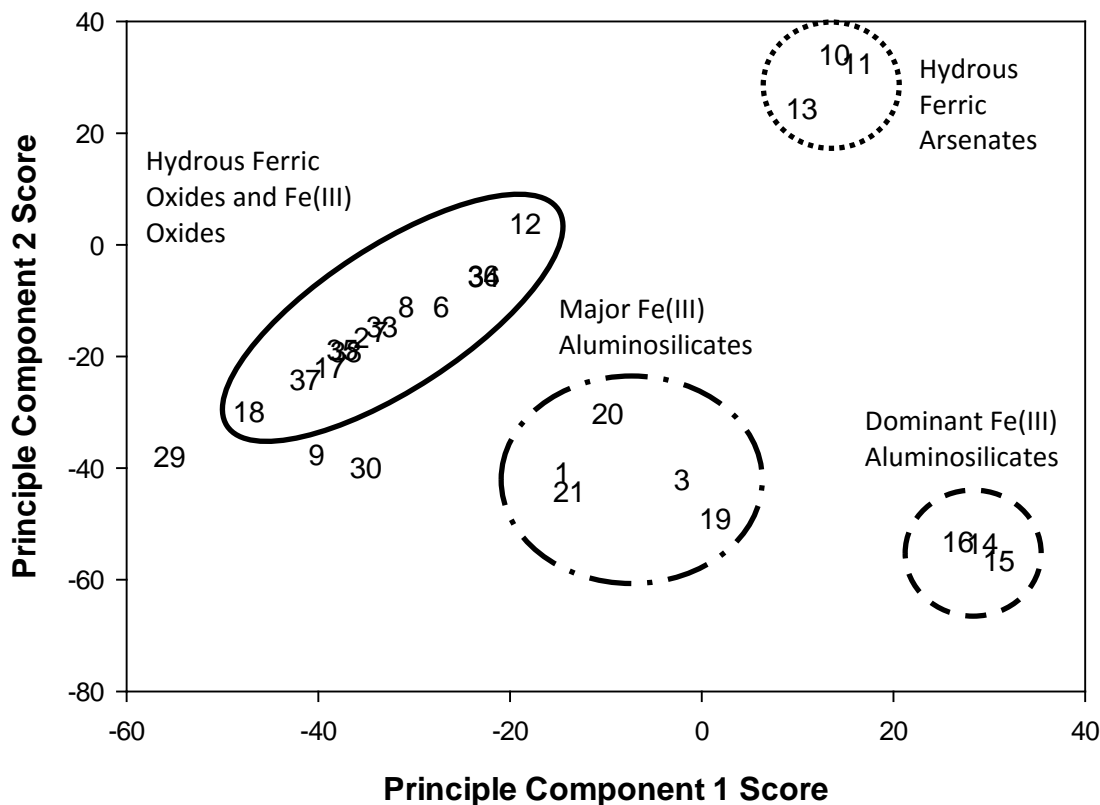


Figure 7. Principle component analysis and groupings identified using Fe XANES species groups.

Task 3: In Vivo Bioavailability

Eighteen of the 19 RBAs that were determined using the adult mouse bioassay and 3 of the 22 RBAs that were determined using the juvenile swine bioassay were calculated using total arsenic concentrations that were determined via INAA. As previously mentioned the INAA method results in a total As concentration that is on average 11% greater than the total concentration determined using an acid digestion (U.S. EPA Method 3051a). Total arsenic concentrations determined using acid digestion is more readily available than using INAA. In addition, all of the in vitro bioaccessibility (IVBA) data for this study was determined using a total As concentration determined via acid digestion. In order to allow for appropriate comparisons between all RBA and IVBA values generated for this study the RBAs that were determined based on INAA values were converted to a acid digestion basis. All of the study soils total concentration determined via acid digestion and converted RBAs are shown in Table 22. The converted RBA values will be used for the rest of the data analysis and reporting.

Total arsenic concentrations determined via acid digestion, previously described in Task 1, and ranged from 20-13,000 mg kg⁻¹ (Table 22). The in vivo mouse model and juvenile swine

model were used to determine RBA As of all 27 study soils, Mean RBA (%) and 90% confidence intervals are shown below in Table 22. RBA As determined for 19 soils via the adult mouse model ranged from 6.37 to 81.2% with an average of 34.9%. RBA As determined for 22 soils via the juvenile swine model ranged from 4.00 to 60.0% with an average of 32.5%.

Table 22. Adult mice and juvenile swine RBA values with 90% confidence intervals for all study soils.

Soil	U.S. EPA 3051a As Concentration mg/kg	Mouse RBA			Swine RBA		
		Mean	LCL*	UCL*	Mean	LCL*	UCL*
1	464	20.2 ⁺	18.1 ⁺	22.4 ⁺			
2	641	29.1 ⁺	26.0 ⁺	32.3 ⁺	39.5 ⁺	35.8 ⁺	43.1 ⁺
3	222	43.5 ⁺	37.9 ⁺	49.2 ⁺			
6	839				41.7	34.5	48.8
7	332	34.0 ⁺	29.8 ⁺	38.3 ⁺	52.3 ⁺	54.3 ⁺	58.4 ⁺
8	162	29.9 ⁺	26.6 ⁺	33.3 ⁺	54.9 ⁺	50.4 ⁺	59.4 ⁺
9	521				14.0	13.0	15.0
10	3910	12.5 ⁺	2.57 ⁺	22.4 ⁺	19.0	17.0	20.0
11	249	44.8 ⁺	41.6 ⁺	48.2 ⁺	60.0	56.0	65.0
12	1236				39.7	38.7	40.7
13	12500				7.87	4.33	11.4
14	238	79.7 ⁺	73.8 ⁺	85.9 ⁺			
15	259	69.7 ⁺	65.9 ⁺	73.6 ⁺			
16	226	81.2 ⁺	70.9 ⁺	91.7 ⁺			
17	1540	41.4 ⁺	39.1 ⁺	43.6 ⁺	41.8	39.0	45.0
18	283	30.0 ⁺	27.4 ⁺	32.7 ⁺	31.0	25.0	38.0
19	353	46.1 ⁺	41.8 ⁺	50.5 ⁺	41.0	38.0	44.0
20	391	21.5 ⁺	17.6 ⁺	25.3 ⁺	49.0	42.0	57.0
21	375	39.4 ⁺	36.1 ⁺	42.8 ⁺	53.0	49.0	57.0
29	4550				48.0	45.0	51.0
30	4000				26.0	24.0	28.0
33	302	8.55 ⁺	6.51 ⁺	10.6 ⁺	23.7	10.9	36.5
34	2540	6.37 ⁺	5.33 ⁺	7.43 ⁺	15.3	11.7	18.8
35	633	16.1 ⁺	15.2 ⁺	17.0 ⁺	19.2	16.9	21.4
36	10500				4.00	3.30	4.60
37	370	9.83 ⁺	8.82 ⁺	10.9 ⁺	11.7	8.3	15.2
38	12000				23.0	17.6	28.5

*LCL 90% Lower Confidence Limit except for soil 17 (95%)

*UCL Upper Confidence Limit except for soil 17 (95%)

⁺ Converted RBA values RBA_{INAA} x (INAA As / U.S. EPA 3051a As) = RBA_{3051a}

Figures 8 and 9 show the RBA As for the adult mouse and juvenile swine model versus the total As concentration (mg/kg) respectively. Arsenic concentrations below 1000 mg/kg are

shown in Figures 8 and 9 to aid in ease of viewing. Appendix Figures A18 and A19 show RBA As for the adult mouse and juvenile swine models vs total As concentration (mg/kg) respectively. The relationship between total arsenic concentration (<1000 mg/kg) and mouse RBA As can be expressed as Mouse RBA = -0.08 x total As concentration + 65 with an r^2 of 0.236 (Fig. 8). The slope of near zero and low r^2 suggest that total As concentration is not predictive of mouse RBA As. The relationship between total arsenic concentration (<1000 mg/kg) and swine RBA As can be expressed as Swine RBA = -0.03 x total As concentration + 49 with an r^2 of 0.092. The slope and r^2 near zero show that total As concentration is not predictive of swine RBA As. Total As concentration was not correlated with bioavailable arsenic for the 27 soils used in this study.

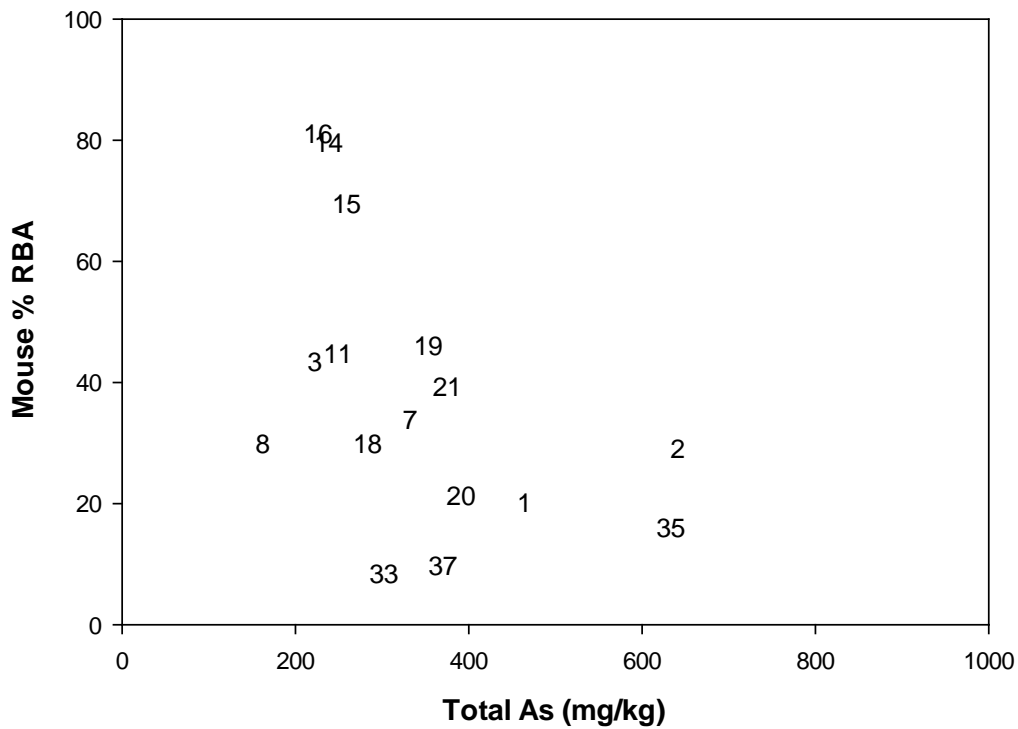


Figure 8. Relationship between mice % RBA vs total As concentration (mg/kg) for soils < 1000 mg As/kg.

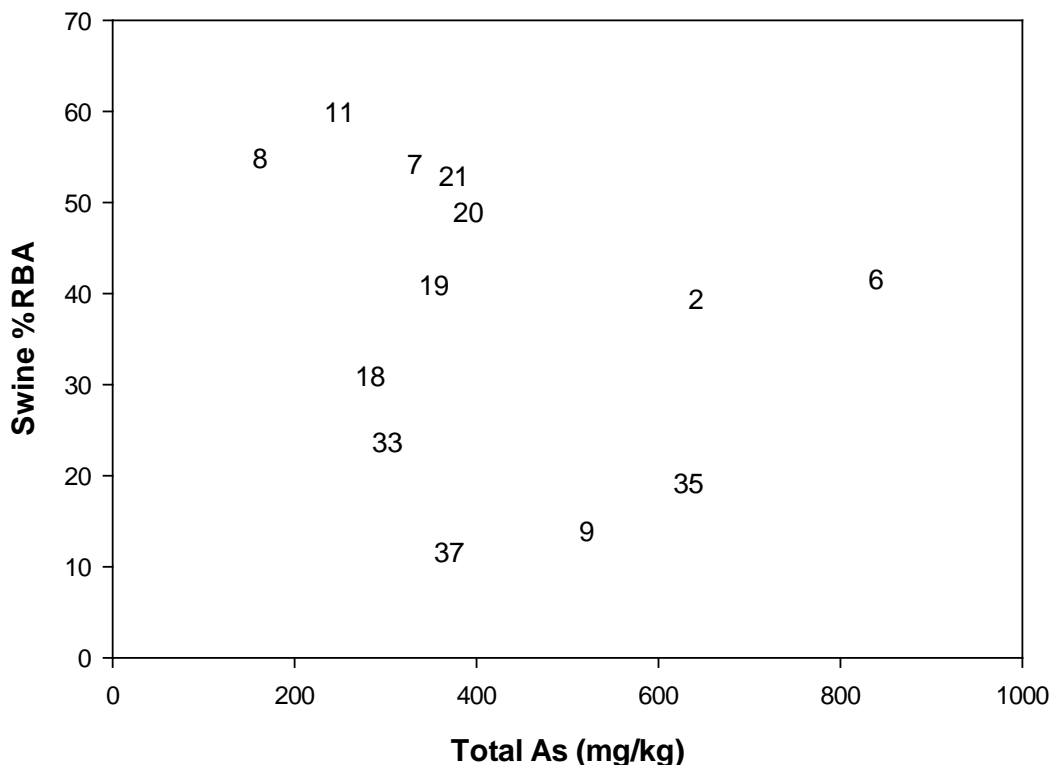


Figure 9. Relationship between swine % RBA vs total As concentration (mg/kg) for soils < 1000 mg As/kg.

Relative bioavailability was determined for 14 of the 27 study soils using both the adult mouse and juvenile swine models. The results for the 14 soils that were evaluated using both bioassays are shown below in Figure 10. Table 23 shows the summary statistics for the adult mouse and juvenile swine method. RBA for the 14 soils determined via the adult mouse model ranged from 6.37 to 46.1% with a mean of 26.4% and median of 29.5%. As RBA determined via the juvenile swine model ranged from 11.7 to 60.0% with a mean and median of 36.5% and 40.3% respectively. These results show that on average the juvenile swine model reports RBAs that are higher than the adult mouse model which was also reported by Bradham et al (2013). However, Diamond et al. (2016) concluded the swine and mouse RBA values were equal based on results from Bradham et al. (2013) and Juhasz et al. (2014). Our study shows the two model produce unequal RBA As. To date this report contains the most soils dosed to both animals for direct comparison. Bradham et al. (2013) reported 12 soils that were dosed to both animals and a review of arsenic bioavailability performed by the U.S. EPA reported 11 soils that were dosed to both mice and swine (U.S. EPA, 2012).

Research has been done to compare the RBA values determined using the adult mouse and juvenile swine models. Mouse and swine bioassays have reported similar steady state urinary excretion fractions (UEF) for As of 62 and 74%, respectively, during repeated ingestion doses of sodium arsenite, the water-soluble As form used as the reference in the calculation of RBA. Additionally, evidence was provided that the bioavailability of water soluble arsenate, As (V)

and arsenite (AsIII) is similar in mice, consistent with observations made in swine (Juhasz et al., 2007). Similar results for water soluble standards have been reported but only a few studies (Bradham et al., 2013; U.S. EPA, 2012) have been done to compare RBAs determined using both bioassays for identical soils.

The juvenile swine RBAs tend to be more variable than RBA determined using the adult mouse (Figure 11). The 90% confidence intervals for As RBA only overlap for 5 of the 14 soils (Figure 11) and the confidence intervals for the juvenile swine data are wider than that for the adult mouse model (Figure 11). Similar results were reported by Bradham et al. (2013) where the 95% CI for only 50% (6 of 12) soils overlapped. In addition the 90th percentile RBA value determine via the juvenile swine model is approximately 10% greater than the adult mouse RBA.

The mouse RBA / swine RBA ratio for the 14 soils that were dosed to using both animal models have a range of 36% to 113% with a mean of 72% (Figure 12). A simple linear regression was fit through data and compared to a 1:1 plot (Figure 13). The slope of the swine RBA As vs. mouse RBA As was 0.961 with a y intercept of 11.29. The y intercept of 11 demonstrates that mouse RBA As is less than juvenile swine RBA As. The RBAs were significantly correlated ($r = 0.81$) which corresponds to a r^2 of 0.654. These results are consistent with Bradham et al. (2013) that reported that RBA estimates for 12 identical soils assayed in mice and swine were significantly correlated ($r = 0.70$) which corresponds to a r^2 of 0.49. However correlation does not imply that they are equivalent.

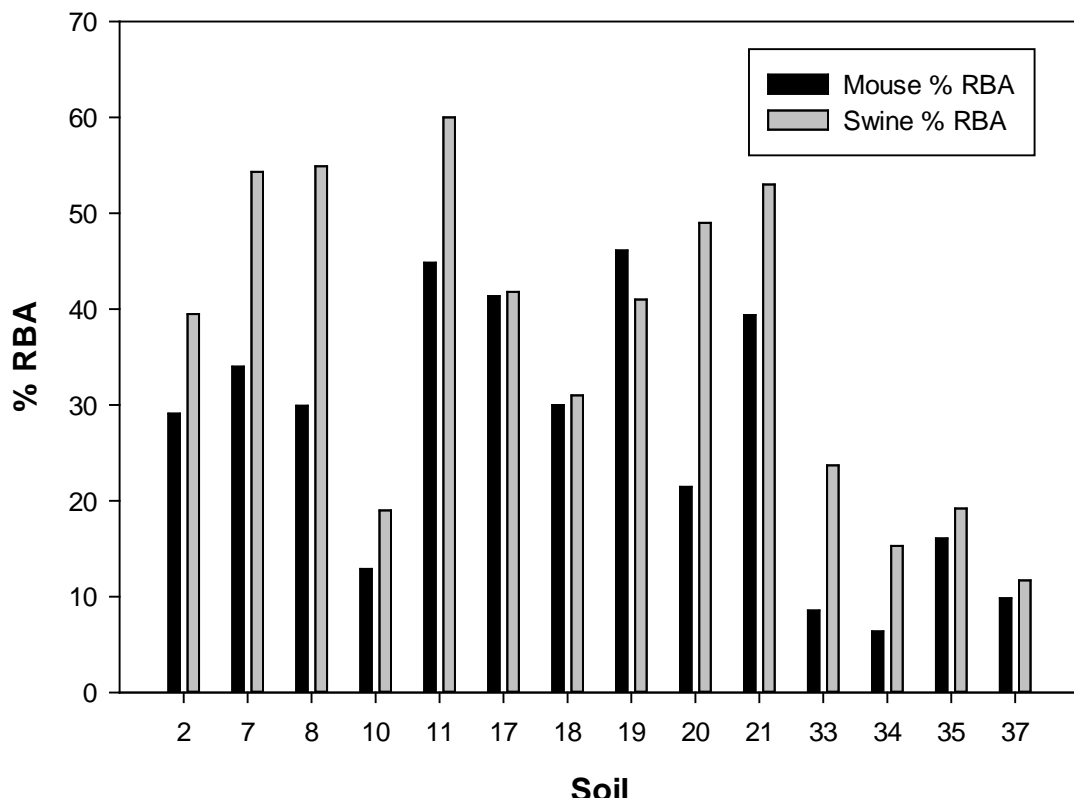


Figure 10. Percent RBA for 14 soils determined using both the adult mouse and juvenile swine models.

Table 23. Comparison of study soils that were dosed to both swine and mice.

Animal	No Dosed	RBA Summary Statistics					
		Minimum	Maximum	90th Percentile	95th Percentile	Mean	Median
		%					
Mouse	14	6.37	46.13	43.8	45.29	26.39	29.5
Swine		11.7	60	54.34	56.69	36.53	40.25

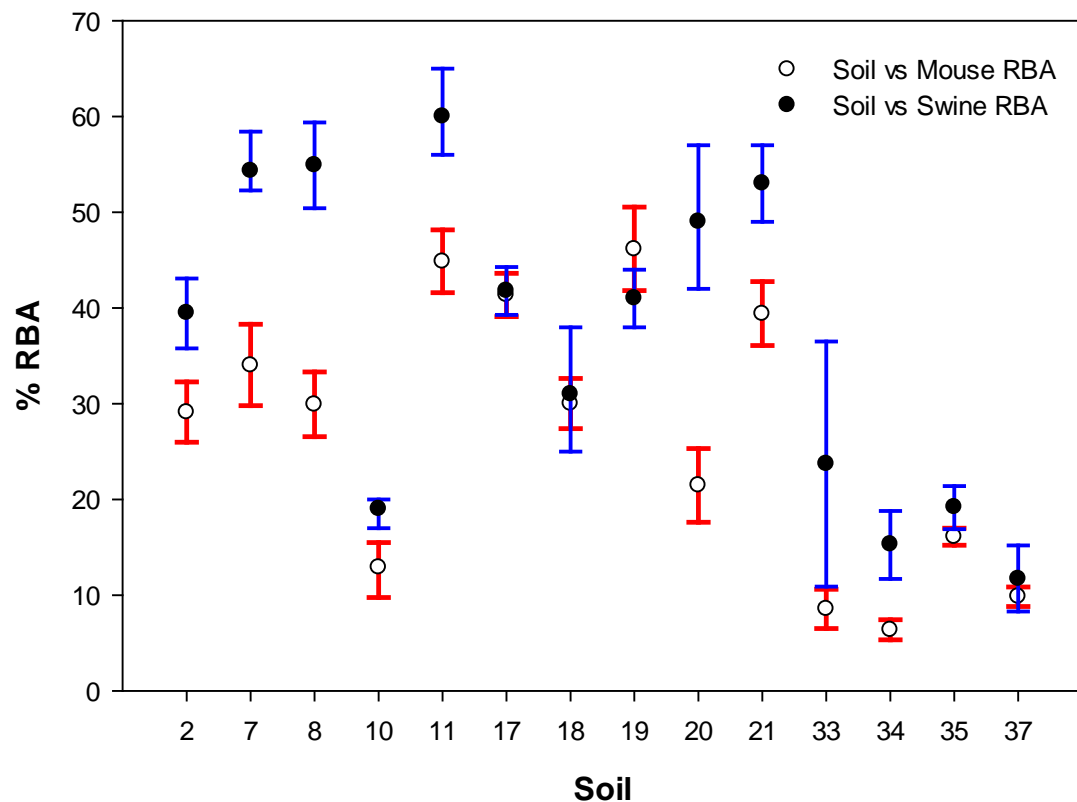


Figure 11. Comparison of 90% confidence intervals for 14 soils determined using both the adult mouse and juvenile swine bioassays.

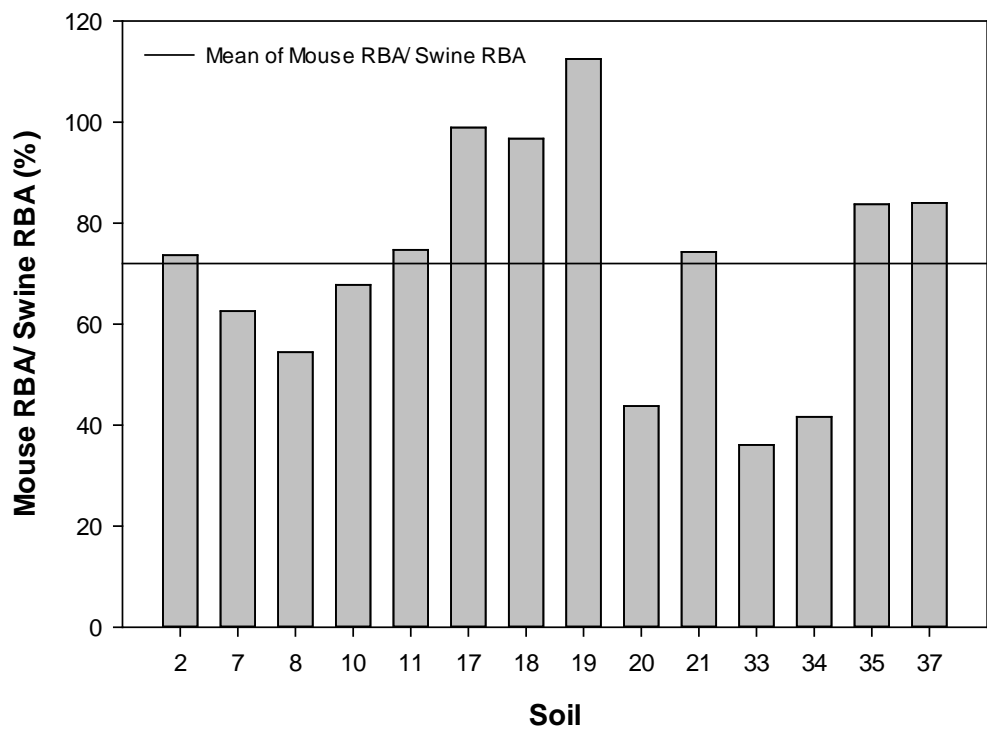


Figure 12. Percentage of juvenile swine RBA recovered by adult mouse bioassay.

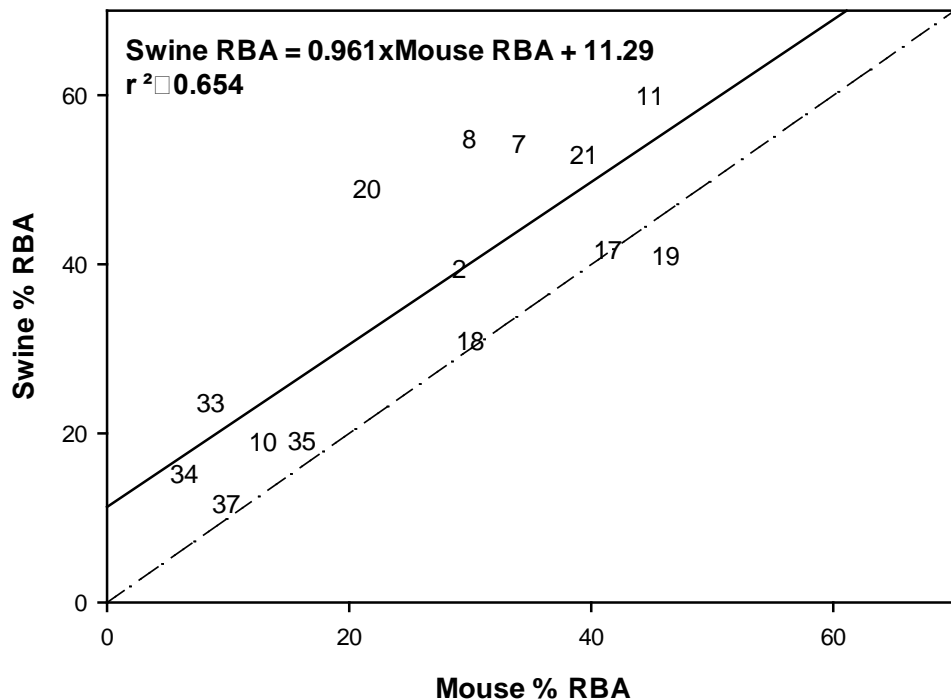


Figure 13. Simple linear regression of soils dosed to both mice and swine. Dashed line is a 1:1 unity line. Solid is Swine %RBA vs Mice % RBA linear regression.

Task 4: In Vitro Arsenic Bioaccessibility

The IVBA As results from the five methods are presented in Table 24. The results show both a wide range in IVBA As across soils as well as differences among in vitro methods for several soils. Juhasz et al. (2009) reported comparison of three of the five methods investigated in the current study on a limited number of As-contaminated soils. Their results indicated a general trend of SBRC > OSU IVG \geq PBET for four of six railway corridor soils; SBRC > OSU IVG \geq PBET for two cattle dip sites; SBRC > OSU IVG \geq PBET for two mine soils; and SBRC \geq OSU IVG > PBET for two gossan soils. Juhasz et al. (2009) concluded that IVBA As was a product of extraction pH, which was (in parentheses) SBRC (pH 1.5) > OSU IVG (pH 1.8) > PBET (pH 2.5). Although extraction pH is important, our results from the soils in the current study do not demonstrate the same trend of GLYCINE (SBRC) IVBA As always being the highest among the methods. Median and mean IVBA As followed the trend CAB (pH 1.5) > UBM (pH 1.2) \approx OSU (pH 1.8) \approx PBET (pH 1.8) \approx Glycine (pH 1.5). The UBM extraction pH of 1.2, the lowest of all four methods, did not extract the greatest amount of As. Rather, the CAB extraction pH of 1.5 extracted more, on average, than the other four methods.

Table 24. Bioaccessibility results for all soils in the study.

ID	Glycine		PBET		UBM		OSU		CAB	
	GE Mean	IE Mean								
% —										
1	40.7	14.0	28.0	23.6	28.7	22.5	37.6	26.6	52.5	49.0
2	3.20	0.400	1.90	2.30	7.80	3.90	12.0	2.30	18.1	17.7
3	22.6	14.2	19.9	24.9	28.6	55.0	20.7	22.9	72.7	70.9
6	16.8	14.4	14.0	13.7	10.3	13.2	9.70	10.9	45.8	49.4
7	36.7	25.5	33.4	32.9	43.5	41.6	35.0	36.5	32.8	34.5
8	37.8	22.9	35.3	35.7	40.2	27.9	28.4	24.3	59.5	64.3
9	8.30	7.50	8.80	8.50	9.60	9.10	10.8	9.90	20.5	20.7
10	9.30	0.90	4.50	3.10	7.90	6.90	5.40	6.10	47.1	42.2
11	63.9	8.20	56.6	36.8	41.8	10.3	35.2	2.30	73.6	70.8
12	20.0	10.6	30.9	20.7	18.3	2.30	29.7	4.00	48.0	30.8
13	3.90	0.10	0.80	1.40	0.700	1.30	0.800	1.10	26.5	28.6
14	86.3	68.6	94.3	99.2	86.9	129*	86.2	87.0	81.2	89.2
15	78.9	56.8	79.3	75.8	83.8	66.6	76.8	37.6	88.3	89.5
16	75.5	61.7	73.0	71.7	73.4	125*	75.4	82.3	104	88.7
17	31.0	4.80	22.2	21.9	32.3	22.3	25.2	23.4	83.0	78.2
18	17.8	9.10	24.0	23.2	41.4	31.6	24.6	24.8	39.0	87.0
19	12.4	6.90	15.2	15.1	25.7	14.0	23.0	24.8	40.7	90.6
20	14.9	4.00	14.5	17.7	25.1	29.0	21.1	20.9	41.4	39.6
21	22.7	3.20	20.4	18.7	21.3	22.1	29.1	25.0	50.1	45.0
29	65.8	28.5	60.0	43.7	51.7	48.1	49.1	45.0	76.7	63.4
30	27.1	15.6	23.2	19.9	21.5	26.9	21.9	22.7	39.1	37.1
33	4.70	2.30	9.00	10.0	11.5	19.3	9.40	10.0	25.1	27.9
34	1.30	0.400	1.20	1.80	3.00	4.20	3.70	4.10	22.7	26.5
35	1.60	0.400	2.30	3.10	6.00	1.90	4.60	3.40	12.4	14.5
36	2.00	0.200	1.10	1.40	1.60	1.50	1.80	0.900	12.0	11.6
37	0.500	0.300	1.90	1.90	2.40	4.10	1.50	3.00	6.10	7.80
38	14.4	4.00	8.90	9.70	10.6	11.8	9.70	10.2	50.1	46.2
Minimum	0.480	0.080	0.820	1.36	0.750	1.34	0.800	0.940	6.07	7.79
Maximum	86.3	68.7	94.3	99.2	86.9	66.6	86.2	87.0	104	90.6
Mean	26.7	14.3	25.4	23.7	27.3	19.9	25.5	21.2	47.0	48.9
Median	17.8	7.50	19.9	18.7	21.5	14.0	21.9	20.9	45.8	45.0

*Removed from in vitro in vivo correlations as an outlier.

Arsenic Bioaccessibility Measured by the Caco-2 Cell Model

Cytotoxicity of medium containing aqueous fraction generated during simulated digestion of soil

Cell morphology in wells incubated with 1:4 dilution of aqueous fractions generated during simulated digestion of control and soil 225 were similar with the appearance of domes and some small areas devoid of cells after 4 h (Figure 14).

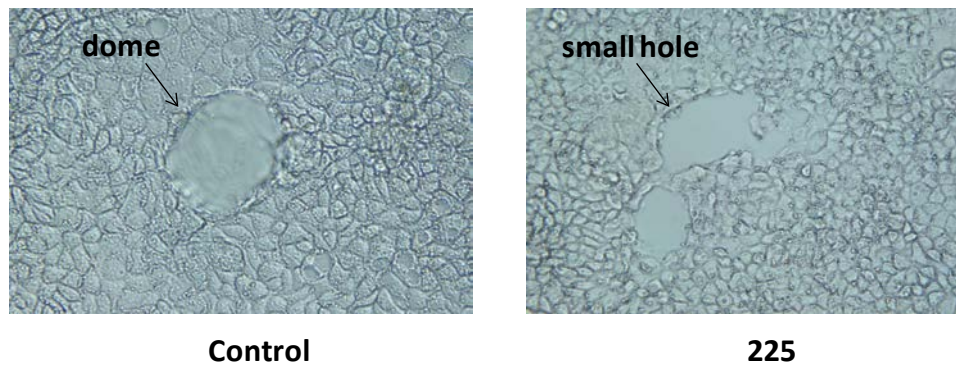


Figure 14. Representative photomicrograph (100X) of monolayer exposure to diluted aqueous fraction for 4 h. Domes and areas of detached cells in cultures incubated for 4 h with diluted (1:4) aqueous fraction from control and 225 soil.

Incubation of cultures with more diluted aqueous fraction (1:8 and 1:16) had numerous domes, and confluent monolayers remain intact. Cell protein content in wells was not adversely affected by exposure to aqueous fractions from digested control and soil 225 samples (Table 25). Results in Figure 15 show that medium LDH activity was similar in cultures exposed to all dilutions of control and test aqueous fractions. As a result, exposure of highly differentiated cultures of Caco-2 cells to diluted aqueous fraction generated during simulated gastric and small intestinal digestion of control and test soils was not toxic as indicated by the similarity of general cell morphology, protein content, and medium LDH activity.

Table 25. Protein content of wells with Caco-2 cells after exposure to diluted aqueous fraction from simulated digestion of soil. Data are mean \pm SD, n = 3 per treatment.

Dilution of aqueous fraction	Control mg protein/well	Soil 225 mg protein/well
1:4	1.7 \pm 0.2	1.7 \pm 0.1
1:8	1.8 \pm 0.1	1.8 \pm 0.2
1:16	1.9 \pm 0.1	1.8 \pm 0.2

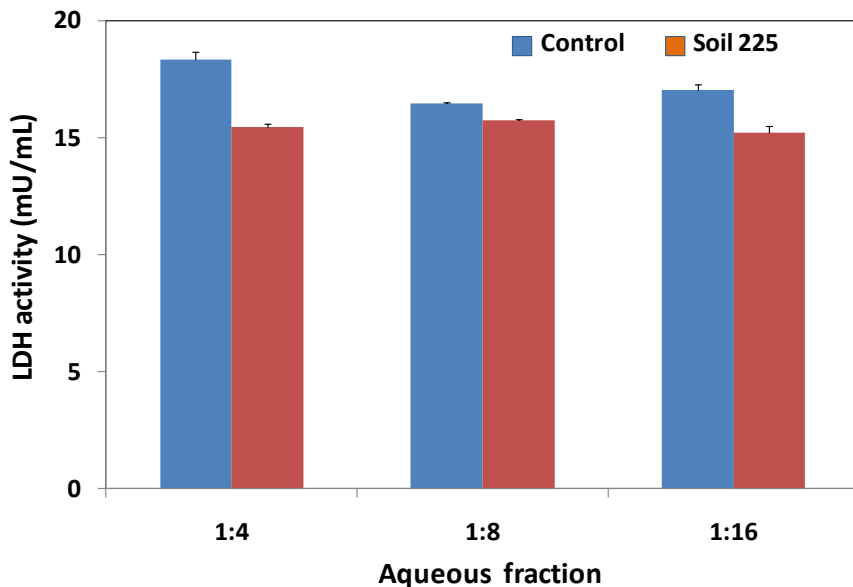


Figure 15. LDH activity in spent media after exposure to diluted aqueous fraction generated during digestion of control solution and soil 225. Data are mean \pm SD, n = 3 per treatment.

Cellular uptake of As at different stages of cell differentiation monolayers

Accumulation of As by poorly differentiated cell monolayers (2 days post-confluence) was greater than that of 70% nondifferentiated cultures (70% confluence) and highly differentiated cultures (11 days post-confluence). Cell uptake was time- and dose-dependent manner (Figure 8; Panels A and B). However, the total of As uptake by Caco-2 human intestinal cells was <1% of medium content in all cases (range of uptake, 0.22 to 0.91%).

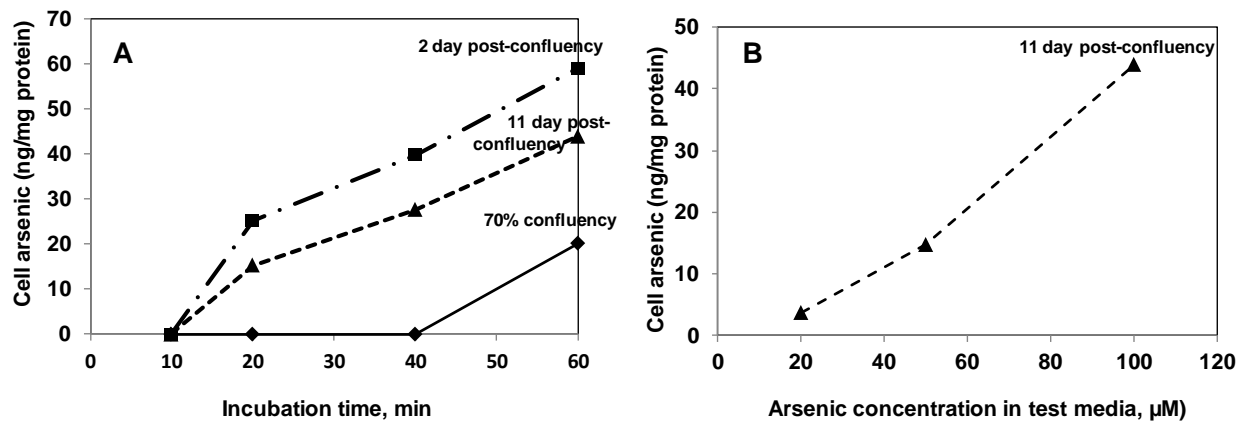


Figure 16. Monolayers of cell at 2-day post-confluence As was taken up at >70% confluence and 11-day post-confluence (panel A) and cell uptake of As during different stages of cell confluence showed time- and dose-dependent manner (panel B).

Task 5: Cross-correlation and Statistical Analysis

One of the main goals of this study was to determine which in vitro bioaccessibility methods best predict in vivo As RBA for a variety of soils. As previously described the soils used in this study have a wide range of source terms, physical properties, chemical properties, and As mineral speciation. In addition, the As RBA and As IVBA of the soils span a wide range across all of the methods and materials. The five bioaccessibility methods used have different extraction parameters impacting As IVBA. To determine the ability of an in vitro method to predict as RBA an in vitro-in vivo correlation (IVIVC) is generated. The ideal IVIVC would take into account the error associated with the RBA and IVBA measurements.

For this study three different regression techniques were used to generate IVIVCs. Orthogonal regression was initially investigated because it takes into account the error for both the x (IVBA) and y (RBA) values. However, after further evaluation this method was deemed to not be appropriate because a vital assumption with this regression technique is that the ratio of the variance between y (RBA) and x (IVBA) is 1. For RBA and IVBA data the ratio is much larger than 1. Simply stated the error for RBA measurements from animal models is much larger than the error for IVBA measurements conducted in the laboratory. IVIVCs generated using orthogonal regression are not presented for simplicity.

The variance and error for IVBA measurements is much less than that associated with RBA measurements, simple linear regression was investigated as a technique for generating IVIVCs. Simple linear regression minimizes the residual from the best fit line along the y (RBA) axis or dependent variable. Simple linear regression assumes that there is a negligible amount of error associated with the independent variable. This method is appropriate for an IVIVC and the types of measurements used to generate an IVIVC. In addition, simple linear regression is the type of regression most potential end users of IVIVCs (site managers, risk assessors, etc.) are familiar with allowing for easier explanation of the underlying assumptions associated with the IVIVCs. A total of 20 IVIVC (5 methods x 2 extraction phases x 2 animal models) were generated using simple linear regression (Fig 17 - 20). Simple linear regression also does not involve the use of complex statistical software like other methods currently used in the literature to generate IVIVCs such as the Bayesian regression method. However, to assess the robustness of the IVIVCs generated using simple linear regression an IVIVC was generated using the Bayesian approach for one of the combinations (Mouse %RBA vs Glycine GE %IVBA) (Figure 21).

When generating IVIVC, two soils (1 and 2) were removed from the data set as outliers. Soil 2 was removed from both the adult mouse IVIVC and the juvenile swine IVIVC. Soil 1 was only dosed to mice and was removed from the adult mouse IVIVC. Soil 1 was previously identified in the data set as an outlier due to the high amounts of adsorbed As(III). Soil 1 As speciation was dramatically different than all of the other soils in the study. Using a Grubbs outlier test soil 1 was removed from the data set as an outlier with a p value (<0.001 for $\alpha = 0.05$). In addition, comparing the IVBA and RBA data for soil 1 the IVBA greatly overestimated the RBA As.

Soil 2 was removed because of the high amounts of reactive Al oxide within the soil. Soil 2 reactive Al oxide concentration was 35,900 mg/kg which is more than 10X greater than the median value of 2,920 mg/kg. The IVBA for soil 2 was on average half of the RBA As. Both

Soil 2 from Hawaii has parent material of volcanic origin. These soils contain unusually large amounts of highly reactive amorphous Al as allophane mineral and are known to strongly absorbed oxyanions such as arsenate and phosphate. Figures 17 –20 show simple linear regression IVIVC without soils 1 and 2.

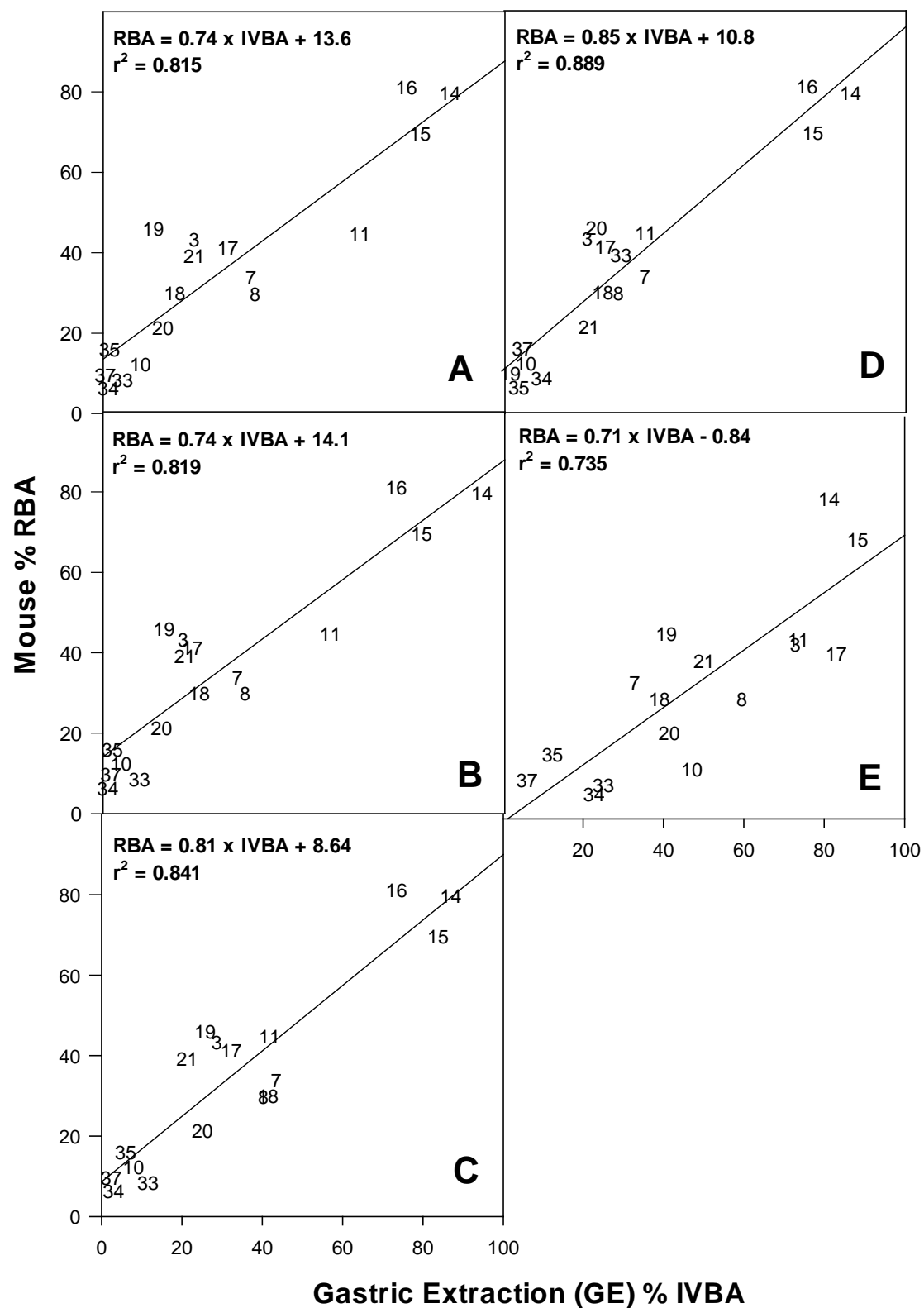


Figure 17. IVIVC for adult mouse % RBA vs % IVBA for gastric phases. IVIVC are labeled accordingly (A) Glycine (B) PBET (C) UBM (D) OSU IVG (E) CAB.

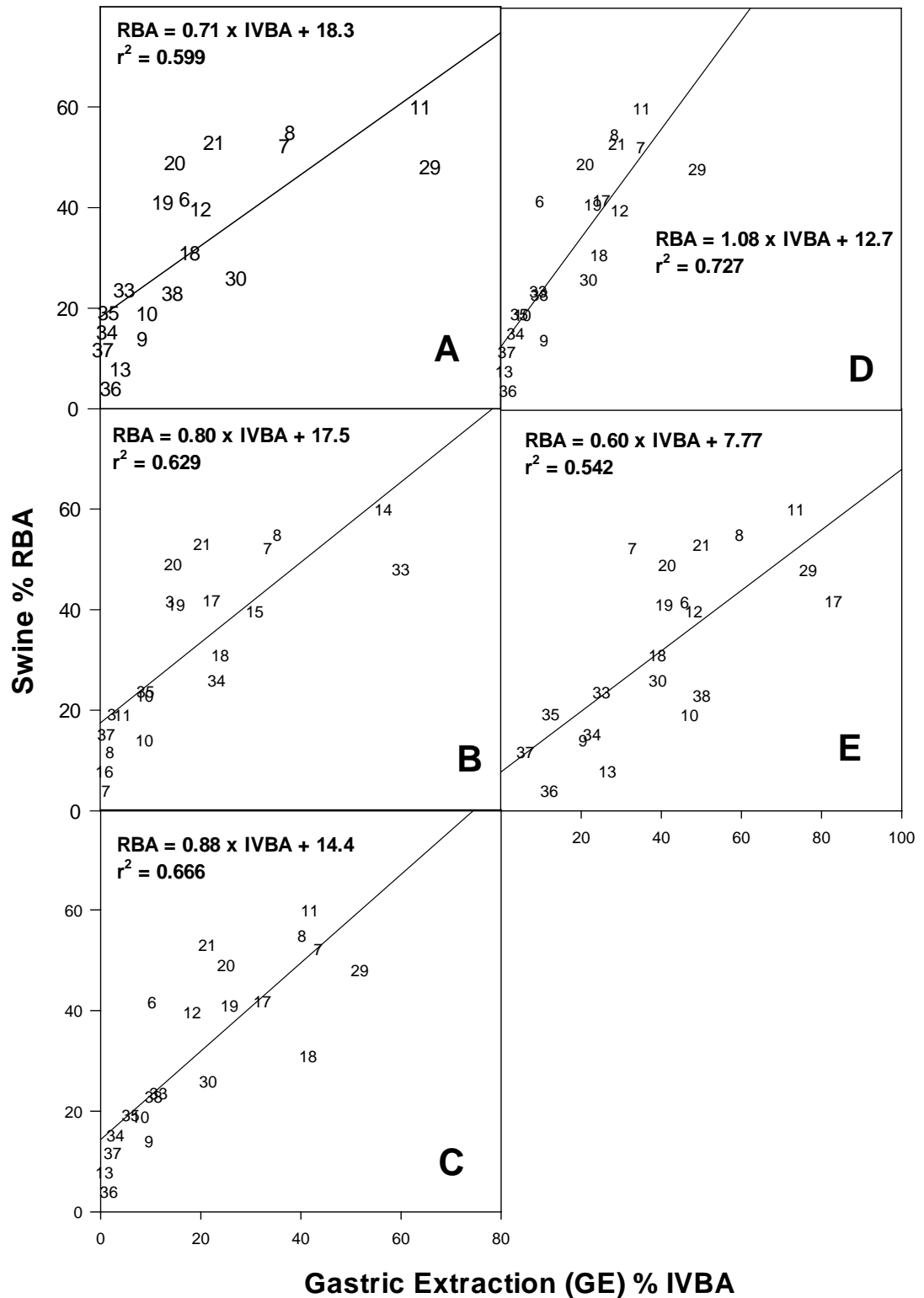


Figure 18. IVIVC for juvenile swine % RBA vs % IVBA for gastric phases. Figure label designations are the same as described in Figure 17.

Figures 17 and 18 show the simple linear regressions for the gastric extraction (GE) IVBA for the adult mouse and juvenile swine models respectively. For the IVIVC using mice RBA there was a good fit for all of the methods ($r^2 > 0.74$) and a good distribution of residuals. The slope for all of the methods was ≥ 0.71 for the IVIVC using mice RBA. The y intercepts for the mouse IVIVC had a wide range, -0.84 to 14.1. For the IVIVC using swine RBA the r^2 ranged from 0.54 to 0.73. The slope for all of the methods was ≥ 0.60 for the IVIVC using swine RBA. The y intercepts for the swine IVIVC ranged from, 7.8 to 18.3. Generally, IVIVC using mice RBA values have lower y intercepts and higher r^2 values compared to the IVIVC generated using swine RBA values. This likely due to the higher variability (Fig. 11) within the swine RBA data compared to mice RBA. The slopes of the IVIVC generated using mice RBA values are very similar to those generated using swine RBA values.

Wragg et al. (2011) adapted US FDA guidelines to evaluate regression parameters to determine acceptable IVIVC. Acceptable parameters include a slope between 0.8 and 1.2, r value >0.8 , and $r^2 >0.6$ (Wragg et al., 2011). In addition to slope and r^2 Juhasz et al. (2013), suggested the y intercept should be zero. Ideally the goal is to have a y intercept as close to zero as possible. There is a limited range for mice IVIVC slope, OSU IVG (0.85) \geq UBM (0.81) \geq PBET = Glycine (0.74) \geq CAB (0.71). There is a wide range for swine IVIVC slope, OSU IVG (1.08) \geq UBM (0.88) \geq PBET (0.80) \geq Glycine (0.71) \geq CAB (0.60). The OSU IVG and UBM meet the slope criteria for mice and swine of Wragg et al. (2011). The PBET meets the slope criteria for swine. The slopes between the mouse and swine IVIVC are similar within each method. Also, the trend is the same with OSU IVG being the largest and CAB being the smallest.

All of the mouse RBA IVIVCs meet the r^2 criteria, OSU IVG (0.89) \geq UBM (0.84), PBET= Glycine (0.82) \geq CAB (0.74) (Fig. 17). The swine RBA IVIVC r^2 were OSU IVG (0.73) \geq UBM (0.67), PBET (0.63) \geq Glycine (0.60) \geq CAB (0.54) (Fig. 18). The swine RBA IVIVC r^2 were lower than the mice r^2 but most meet the criteria of Wragg et al. (2011).

The y intercept for mice RBA IVIVC PBET (14.1) $>$ Glycine (13.6) $>$ OSU IVG (10.8) $>$ UBM (8.6) $>$ CAB (-0.84) (Fig. 17). The y intercept swine RBA IVIVC Glycine (18.3) \geq PBET (17.5) \geq UBM (14.4) \geq OSU IVG (12.7) $>$ CAB (7.8) (Fig. 18). Generally the y intercepts for the mice RBA IVIVC were lower than the swine RBA IVIVC.

In general all of the IVIVC are acceptable. A y intercept close to zero is critical for accurate prediction of RBA As for soils with low RBA (< 20-30% RBA As). For example a y intercept of 10 would account for 50% of the RBA estimate for low RBA soil.

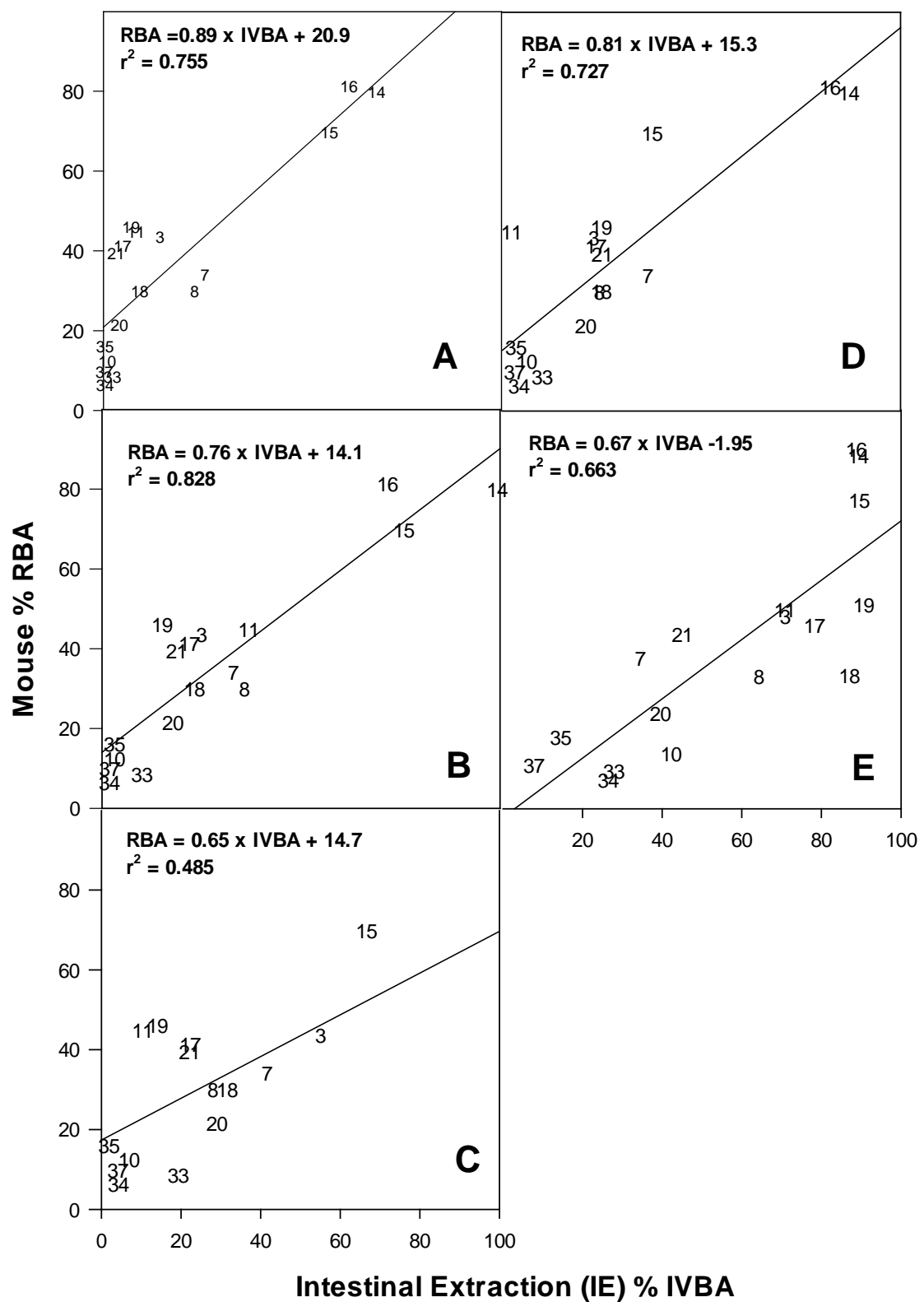


Figure 19. IVIVC for adult mouse % RBA vs % IVBA for intestinal phases. Figure label designations are the same as described in Figure 17.

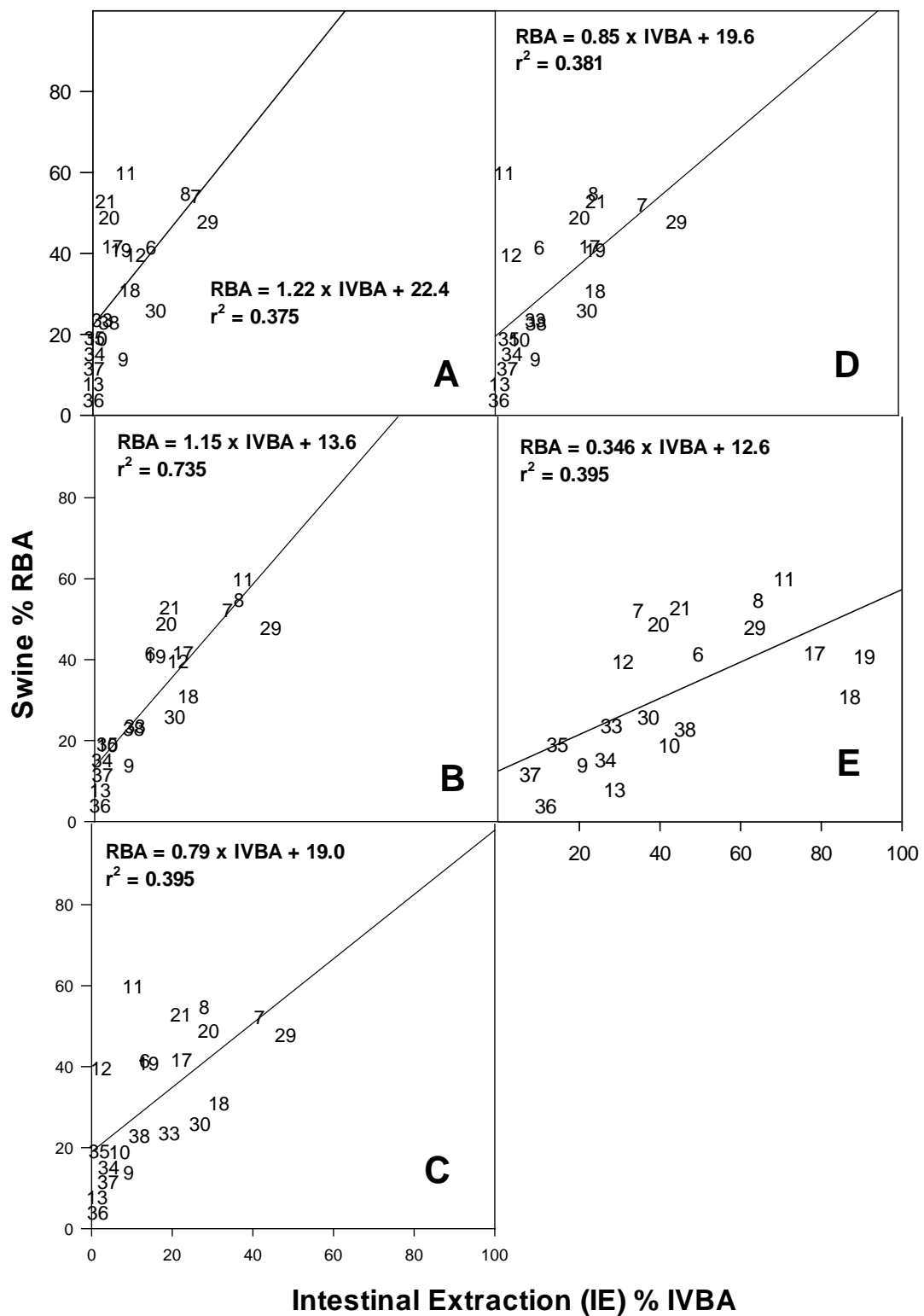


Figure 20. IVIVC for juvenile swine % RBA vs % IVBA for intestinal phases. Figure label designations are the same as described in Figure 17.

Figures 19 and 20 show the simple linear regressions for the intestinal extraction (IE) IVBA for the adult mouse and juvenile swine models respectively. In general, the IVIVC using mice RBA there was a good fit for all of the methods (Fig. 19). The slope for all of the methods ranged from 0.65 to 0.89 for the IVIVC using mice RBA. The y intercepts for the mouse IVIVC had a wide range, -1.95 to 20.9. For the IVIVC using swine RBA the r^2 ranged from 0.38 to 0.74 (Fig. 20). The slope the methods ranged from 0.45 to 1.22 for the IVIVC using swine RBA. The y intercepts for the swine IVIVC ranged from, 12.6 to 22.4. Comparison of intestinal versus gastric extractions clearly show that the gastric extraction is superior in meeting the criteria of Wragg et al. (2011) and a more accurate predictor of RBA As.

Figure 21 shows the IVIVC generated using all of the soils Glycine GE IVBA data and mice RBA data using the Bayesian regression method. The slope, r^2 , and y intercept using this more robust statistical method (Fig. 21) was not different than the IVIVC generated using simple linear regression (Fig. 17a). Simple linear regression slope (0.74), y intercept (13.6) and r^2 (0.82) (Fig 17a) is nearly identical to the Bayesian slope (0.7), y intercept (13.9) and r^2 (0.75). Simple linear regression yielded similar results as the Bayesian regression as our study.

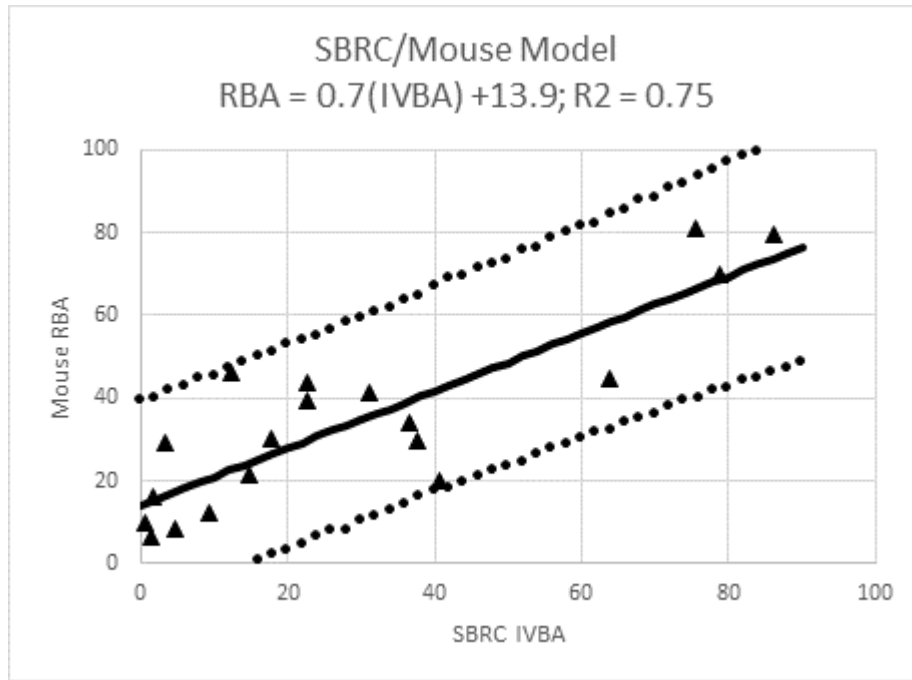


Figure 21. IVIVC for adult mouse % RBA vs % IVBA for gastric phases using the Bayesian approach. Dashed lines are 95% model prediction interval.

This study contained a variety of different types of materials that spanned a wide range of source terms, chemical properties, physical properties, and mineralogy. The methods evaluated here were predictive and appropriate for most of the soils in the study, but not all. Both soil 1 and soil 2 were from Hawaii. These soils have volcanic parent material that impacts the bioavailability/bioaccessibility of As. Further research needs to be done on these types of materials to determine if the materials in this study were unique or if it is not appropriate to estimate RBA from IVBA for these types of materials. Recently concluded research has shown CAB is an accurate predictor of RBA As using swine for soils with high oxide content including soils 1 and 2. Glycine and OSU IVG under predicted for these types of soils (DTSC, 2015).

A comparison of key considerations for selecting and IVBA method to predict RBA from this study is summarized in Table 26. All methods except CAB are better predictors for soils with high ($> 1200 \text{ mg/kg As}$). However the non-CAB methods are much less accurate for low RBA soils due to their high y-intercept values in the linear regressions used to predict RBA As. CAB is more accurate for low RBA As soils and for soils with high reactive Al and Fe oxides (i.e. soils 1 and 2 in this study).

Table 26. Considerations for applying in vitro methods to predict RBA As.

Selection Criteria	In Vitro Method				
	Glycine	PBET	UBM	OSU IVG	CAB
Rapid	x	x	x	x	x
Inexpensive	x	x	x	x	x
Commercially Available	x	x	x	x	x
High As concentration soils ($> 1200 \text{ mg/kg}$)	x	x	x	x	
High reactive Al and Fe oxide soils					x

Task 6: Mechanisms and Permanence of Sequestered Pb in Soils: Impact on Human Bioavailability

Task 6.1.1: Effect of key biological processes on long-term metal permanence of Pb-contaminated soil remediated with phosphate treatments: Development and evaluation of soil fungal inoculates

In situ field XRF analysis across the site clearly revealed increasing soil Pb content with decreasing proximity to the backstop (Figure 22). Concentrations ranged from typical background levels for U.S. soils ($\sim 26 \text{ mg kg}^{-1}$) at locations farthest away from the backstop (sites G8 and F14), to around $3,000 \text{ mg Pb kg}^{-1}$ soil at a location on the grassy transect closest to the backstop (site G2), near $5,000 \text{ mg Pb kg}^{-1}$ soil at a location directly north (behind) the backstop (site B7), and to levels $> 6,000 \text{ mg Pb kg}^{-1}$ soil at several locations on the forested transect closest to the backstop (sites F2 and F5).

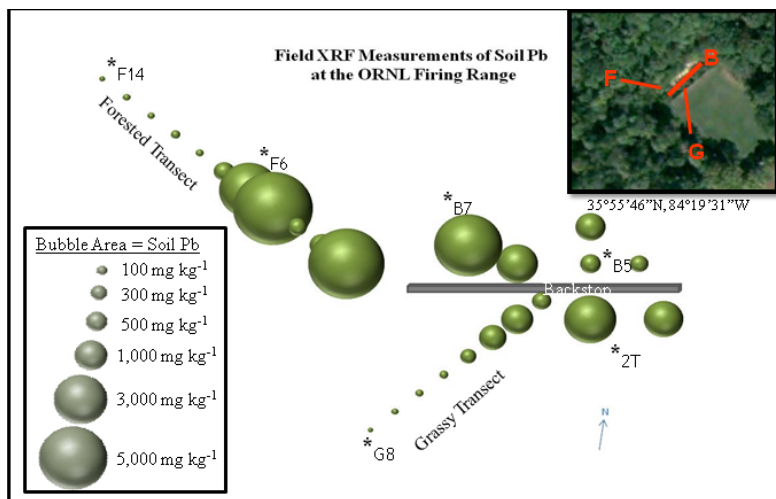


Figure 22. Approximate sampling transects of the firing range at the Oak Ridge National Laboratory with B for the firing backstop, F for the forested transect, and G for the grassy transect.

In order to obtain representative and somewhat comparable “low Pb” and “high Pb” samples from each vegetation type for microbial analysis, several soil cores were collected at sites G8, G2, F14, F6, B5, and B7 (Figure 22). Water content of the soils collected was roughly similar between all samples and ranged from around 18% to just over 24%. Soil pH was lowest on the barren eroded soils behind the firing backstop with values of 3.9 and 4.0 at sites B7 and B5, respectively; and pH was highest on the forested transect at the location farthest from the backstop (site F14) with a value of 5.8. Laboratory analysis confirmed the pattern in the field, exhibiting increasing Pb concentrations with decreasing distance to the firing backstop (Table 27, Figure 22). However, the highest values for soil Pb concentrations from laboratory

Table 27. Laboratory-determined values for moisture, pH, and heavy metals commonly found at shooting ranges for the homogenized and sieved soils collected from the abandoned ORNL firing range on 2 July 2010.

Site ID	Vegetation Cover								
		% H ₂ O	pH	Pb	As	Cu	Ni	Sb	Zn
					mg kg ⁻¹				
F14	Forested	19.5	5.8	23.6 (± 15.7)†	BD‡	BD	BD	BD	BD
F6	Forested	18.7	4.2	1450 (± 50.0)	63.8 (± 37.8)	BD	BD	BD	BD
G8	Grassy	24.4	4.9	43.3 (± 17.9)	BD	BD	BD	BD	146 (± 53.3)
G2	Grassy	19.9	5.3	2440 (± 47.1)	BD	72.5 (± 34.3)	BD	BD	66.6 (± 27.8)
B5	None	17.8	4.0	2780 (± 83.7)	309 (± 65.3)	141 (± 59.4)	BD	BD	BD
B7	None	22.6	3.9	2590 (± 92.0)	200 (± 70.6)	245 (± 76.7)	BD	BD	129 (± 58.6)

† Mean value (St Dev)

‡ Below detection limit.

analyses of homogenized, dried, and sieved soils ranged up to roughly 2,800 mg kg⁻¹ at site B5, followed by 2,600 mg kg⁻¹ at site B7, 2,400 mg kg⁻¹ at site G2, and 1,450 mg kg⁻¹ at site F6. Other heavy metals are commonly found in firing range soils, including As, Cu, Ni, Sb, and Zn. However, Ni and Sb were not found in detectable concentrations at our site using the handheld XRF system employed; and As, Cu, and Zn were found in varying concentrations ranging from typical background levels to slightly elevated levels at a few sites (Table 27). However, because of the low detection limits and higher variability associated with measuring lighter elements with the XRF system, their importance in these soils cannot be verified or discounted at this time.

Isolate identification

Forty morphologically distinct fungal isolates were obtained from the soils at the ORNL firing range that were capable of acidification of growth media in petri plates. In total, 23 of the isolates represented the *Ascomycota*, including isolates with high similarity to GenBank representatives of the genera *Eupenicillium*, *Penicillium*, *Chromocleista*, *Neosetophoma*, *Diatrys*, and *Cladosporium*, with several isolates most closely sharing identity with previously unidentified soil fungal clones. The remaining 17 isolates represented the *Basidiomycota* and included isolates similar to *Phanerochaete flavidoolba*, as well as a number of organisms within the genera *Stereum*, *Peniophora*, *Trametes*, and *Kavinia*. Within these 40 isolates, there was considerable phylogenetic overlap (i.e., eight isolates with 100% identity to *Eupenicillium* sp. O1a_PD022). Consequently, only 15 isolates that were considered representative of the various groups were further characterized for acid production and Pb solubilization. The notable exceptions to these criteria were the seven *Phanerochaete flavidoolba* isolates. In order to assess the range of abilities within an isolate type, all of the *P. flavidoolba* types were carried forward for analysis. These isolates originated from soils associated with each of the different vegetation types and with a wide range of soil Pb concentrations.

Isolate acid secretion

Organic acid secretion by 15 soil isolates as well as *A. niger* in each type of broth at 120 h incubation is given in Figure 23. Overall, isolates produced much lower levels of organic acids in Czapek Dox (CZ) broth (Figure 23A, average 4.7 mM) compared with the malt extract (ME) broth (Figure 23B, 14.8 mM). None of the *P. flavidoolba* isolates exceeded the positive control (*A. niger*) in terms of total organic acids produced while growing in CZ, but each produced small

quantities of oxalic and citric acids (<1.0 mM each) (Figure 23A). However, while growing in ME broth, all the *P. flavidoolba* isolates exceeded the acid production rate of *A. niger* (16.9 mM) with isolates #069 and #080 producing roughly 27 mM, of which nearly 20 mM was oxalic acid (Figure 23B). Among the other *Basidiomycota* (isolates #199, 044, 074, and 075), each of these isolates also yielded an increased quantity and altered mixture of organic acids during growth in ME broth over growth in CZ broth (Figure 23).

The isolates belonging to the *Ascomycota* exhibited a contrasting pattern to that of the isolates of *Basidiomycota* in the two growth media, and none produced detectable levels of oxalic acid in either medium. *Ascomycota* isolates produced roughly equivalent quantities of overall acids in each of the media; however, all four switched from a mixture of acids dominated by malonic acid, with traces of citric acid in CZ (Figure 23A), to a mixture dominated by malic acid, with traces of malonic acid in ME (Figure 23B). The *Penicillium* sp. (#033) and *Eupenicillium javanicum*-like (#078) isolates showed a more than 100% increase in overall acid production in CZ over ME broth.

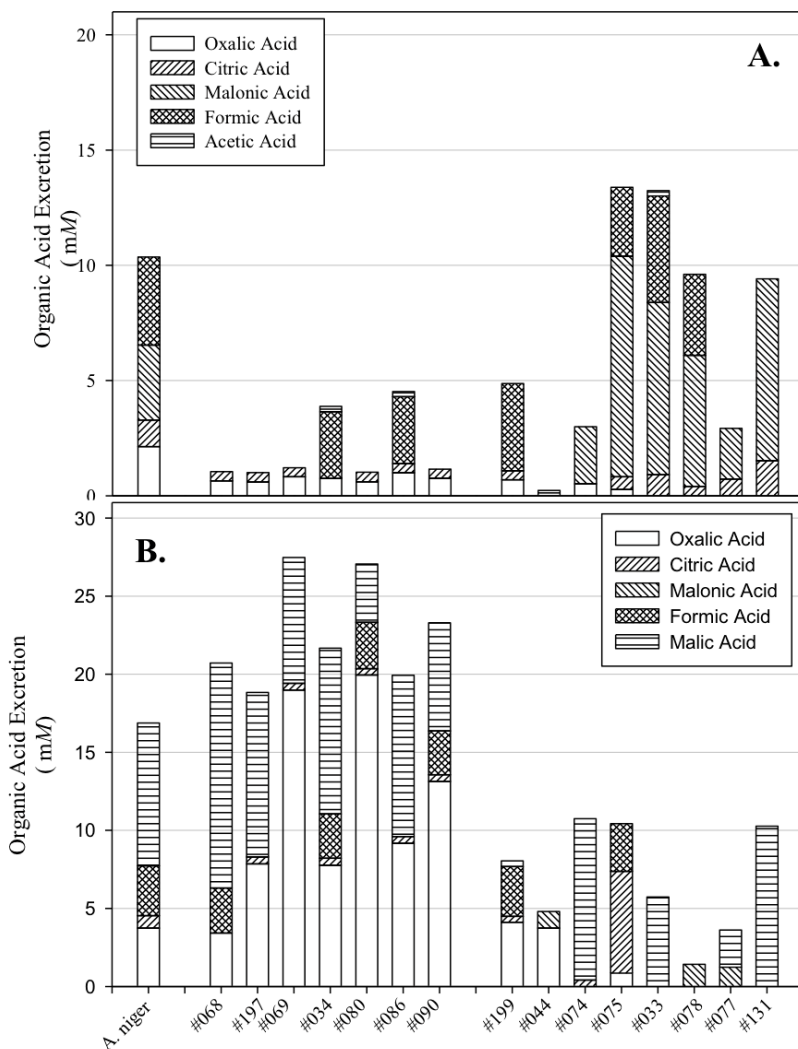


Figure 23. Organic acid secretion by *A. niger* and each soil fungal isolate into either 1% Czapek Dox broth (A) or 1% malt extract broth (B) determined via HPLC analysis of the supernatant after 120 h of incubation at 30°C on a rotary shaker.

Isolate Pb solubilization

Growth and Pb solubilization capabilities for each soil isolate and *A. niger* at multiple media Pb levels are shown in Figures 24A-C. All isolates were capable of growth, in several cases even greater than the positive control *A. niger* at all tested concentrations of Pb. Notably, however, only the *P. flavidoolba* isolates were capable of Pb solubilization at all tested concentrations. At the lowest level of Pb (2.5 mM, Figure 24A), *A. niger* showed similar growth but greater effectiveness than *P. flavidoolba* in Pb solubilization. This was demonstrated by a zone of clearing (ZOC) roughly 30 mm from the inoculating plug of *A. niger* after 120 h incubation, exceeding hyphal growth by at least 10 mm. At the intermediate concentration of Pb in the medium (10.0 mM, Figure 24B), the average growth of the *P. flavidoolba* isolates actually increased over their growth rate at the lowest level of Pb (from 21.4 to 22.7 mm, at 2.5 and 10 mM, respectively). The ZOC associated with these isolates was greater when compared to the lowest level of Pb (10.4 and 15.4 mm, at 2.5 and 10 mM, respectively). Even at the highest level of Pb in the medium (18.5 mM, Figure 24C), average growth of the *P. flavidoolba* group of isolates remained undiminished at 19.7 mm and the ZOC at 13.5 mm. The greatest rate of growth and most effective Pb solubilization among all the isolates at all tested levels of Pb was demonstrated by isolate #080. At every Pb level, *P. flavidoolba* isolates (except #034) exhibited a greater or equal growth rate compared with that of the positive control *A. niger* (Figure 24).

Amongst the remaining isolates, both *Basidiomycota* and *Ascomycota* exhibited roughly similar growth rates at different levels of Pb concentrations in the medium. Only one isolate (*Trametes versicolor*, #074) exhibited the capacity to solubilize Pb in the medium and only at the 10.0 mM concentration where the ZOC was roughly 11 mm. Within each phylum, isolate growth rate was generally lower for the isolates originating from lower or background level Pb soils than those originating from intermediate or high level Pb soils (Table 6, Figures 12A-C).

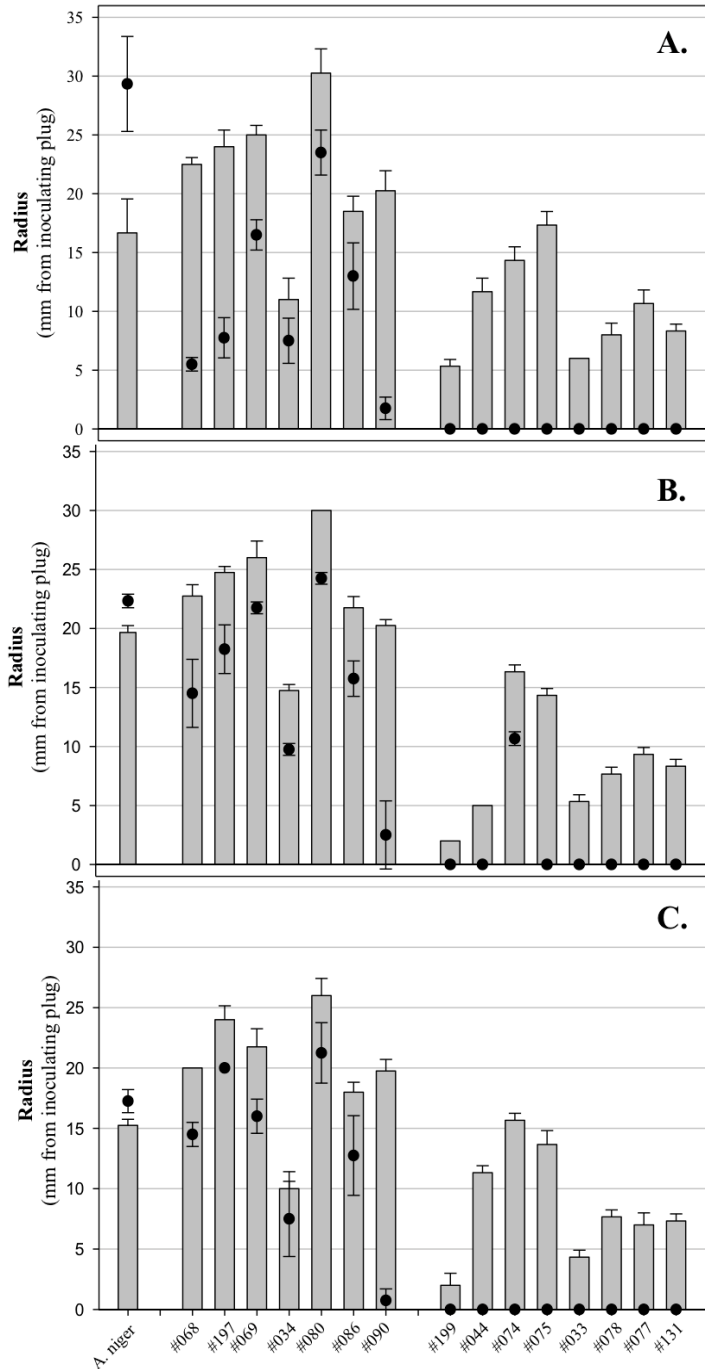


Figure 24. Hyphal growth (bars) and zone of clearing (points) for each isolate grown on malt extract agar for 120 h at 21°C with Pb carbonate incorporated into the medium at the equivalent of 2.5 mM (A), 10 mM (B), or 18.5 mM (C).

Presence and relative abundance of isolated organisms within the soil fungal community

OTUs with high identity to each of the cultured isolates were also found to be present in the soil pyrosequence libraries at varying levels. Overall, *P. flavidooalba* was found in the greatest proportion in the soils of sites F14 and B7 at 10.3 and 9.56%, respectively (Figure 25).

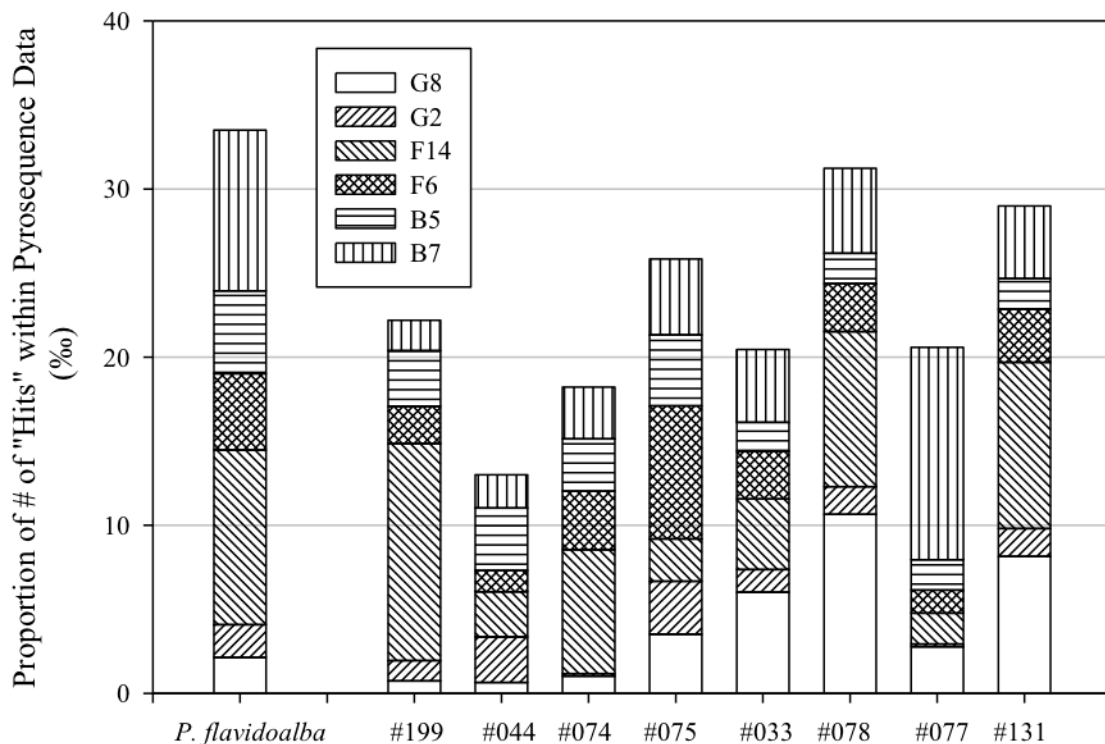


Figure 25. Proportion (%) of hits for each isolate's LSU rRNA gene sequence within the 454 pyrosequence data from each soil sample ($\geq 97\%$ identity), calculated as the number of hits for an isolate in a sample over the total number of fungal sequences for that sample.

Roughly half that level (~5%) of *P. flavidoolba* was found in the soils of sites F6 and B5 and at minimal levels (~2%) in both samples from the grassy transect (G8 and G2). The remaining *Basidiomycota* isolates were found in the greatest proportions in the soils of sites along the forested transect (F6 and F14) (Figure 25). *Stereum subtomentosum* (#199) and *Trametes versicolor* (#074) both exhibited a similar pattern to that of *P. flavidoolba*. While *Peniophora incarnata* (#044) was found in the highest proportion at site B5, the proportions at which this isolate was found in each of the sites was minimal (0.65-3.72%). The other *Peniophora* sp. (#075) was found in the greatest proportions at site F6 (7.90%) and at roughly 4% in sites B5 and B7, and only around 3% at G8 and G2.

Overall, the *Ascomycota* isolates had a greater proportion of hits in the soils at G8 than did the isolates of the *Basidiomycota*, and the *Ascomycota* isolates did not have many hits within the soils of G2 (Figure 25). *Penicillium* sp. (similar to isolate #033) and *Eupenicillium javanicum*-like sequences (similar to isolate #078) were both found in the greatest proportion (6.01% and 10.6% for #033 and #078, respectively) at site G8, but #033 was only at minimal levels in the other soils (1.33-4.33%) while #078 was also found (9.22%) at site F14. Conversely, the undescribed fungal clone (#077) had the greatest proportion of hits at site B7 (12.6%), which was also the highest proportion of hits in any one sample for the isolates of the *Ascomycota*. *Eupenicillium* sp. (#131) was found in the greatest proportions in the “low Pb” samples F14 (9.89%) and G8 (8.14%).

Task 6.1.2: Effect of key biological processes on long-term metal permanence of Pb-contaminated soil remediated with phosphate treatments

Effect of soil treatments and microbial activity on Pb solubility and mobility

The results of the ORNL and Joplin treatments on Pb solubility and mobility, as measured by SPLP, are presented in Figures 26 and 27 respectively. For ORNL, non-P treatments were not significantly ($P<0.01$) different than the untreated control (Fig. 26). Non-P treatments did not reduce P mobility (i.e., SPLP Pb). However, P-treatment resulted in a significant ($P<0.01$) reduction in SPLP Pb compared to the control. This is consistent with the scientific literature that clearly shows P treatments reduce P mobility (Scheckel et al., 2013). Sterilization of control and P treatments had no effect on SPLP Pb. Fungal inoculation did not mobile Pb in the untreated Pb-contaminated soil (control) or the P-remediation Pb-contaminated soil (P). Litter addition with fungal inoculation did not significantly increase Pb mobility.

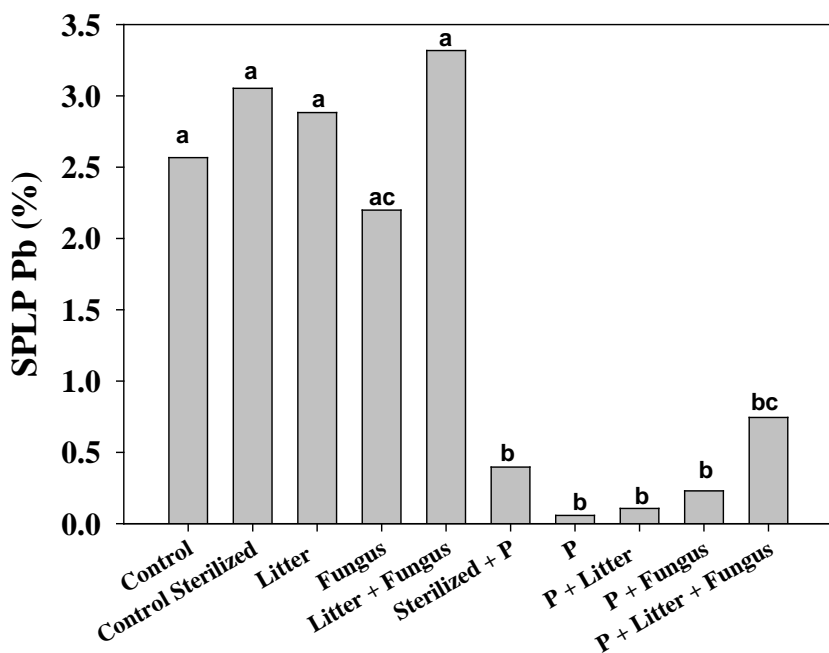


Figure 26. SPLP Pb results for ORNL treatments.

Unlike the ORNL site soil, none of the treatments for the Joplin soil resulted in SPLP Pb significantly ($P<0.1$) different than the control. None of the treatments reduced P mobility (i.e., SPLP Pb). Sterilization of control and P treatments had no effect on SPLP Pb. Fungal inoculation did not mobile Pb in the untreated Pb-contaminated soil (control) or the P-remediation Pb-contaminated soil (P). Litter addition with fungal inoculation did not significantly ($P<0.0?$) increase Pb mobility.

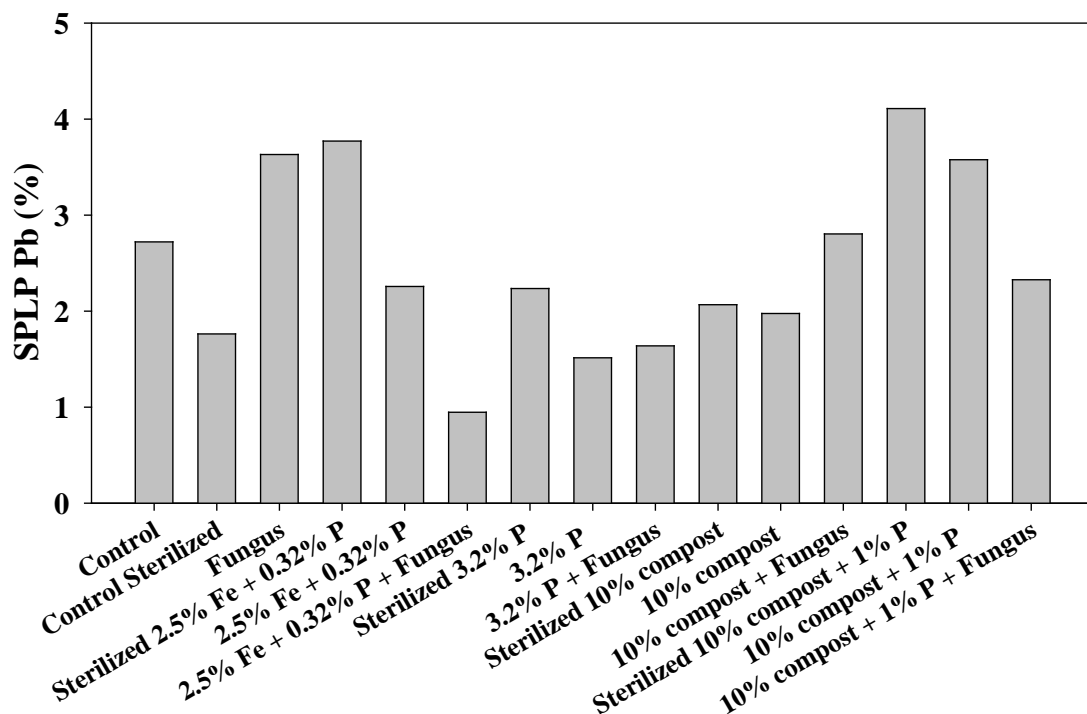


Figure 27. SPLP Pb results for Joplin treatments.

Effect of soil treatments and microbial activity on Pb bioaccessibility

The effect of ORNL and Joplin treatments on in vitro bioaccessible Pb (IVBA Pb) is presented in figures 28 and 29, respectively. For ORNL, non-P treatments were not significantly ($P<0.01$) different than the untreated control (Fig. 28). Non-P treatments did not reduce Pb bioaccessibility (i.e., IVBA Pb). However, P-treatment resulted in a significant ($P<0.01$) reduction in bioaccessible Pb compared to the control. This is consistent with the scientific literature that clearly shows P treatments reduce P bioaccessibility (Scheckel et al., 2013). Sterilization of control and P treatments had no effect on IVBA Pb. Fungal inoculation did not affect IVBA Pb in the untreated Pb-contaminated soil (control) or the P-remediation Pb-contaminated soil (P). P P treatments resulted in significantly ($P<0.01$) lower IVBA Pb than the control regardless of microbial treatment with an average of 6.06%, a 90% reduction. Litter addition with fungal inoculation did not significantly increase Pb bioaccessibility. These Pb bioaccessibility results for the ORNL soil follow the same trends as found for Pb mobility discussed earlier (Figure 26).

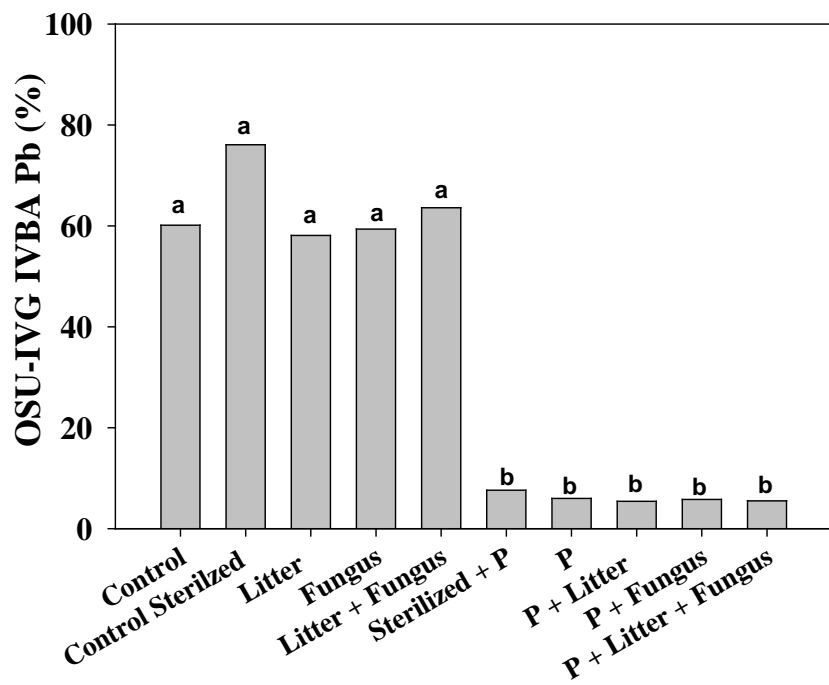


Figure 28. OSU-IVG IVBA Pb results for ORNL soil treatments.

For ORNL, with the exception of the sterilized treatment, all non-P treatments resulted in IVBA Pb that was not significantly ($P < 0.01$) different than the untreated control (48%) (Figure 29). The Joplin results were significantly more variable due to field application of treatments. However, similar to the ORNL results, the Joplin P treatments demonstrated the largest reductions in IVBA Pb relative to the control, but only the 3.2% P + Fungus treatment was significantly lower IVBA than the control ($P < 0.1$). Fungal inoculation with or without compost addition did not affect bioaccessible Pb.

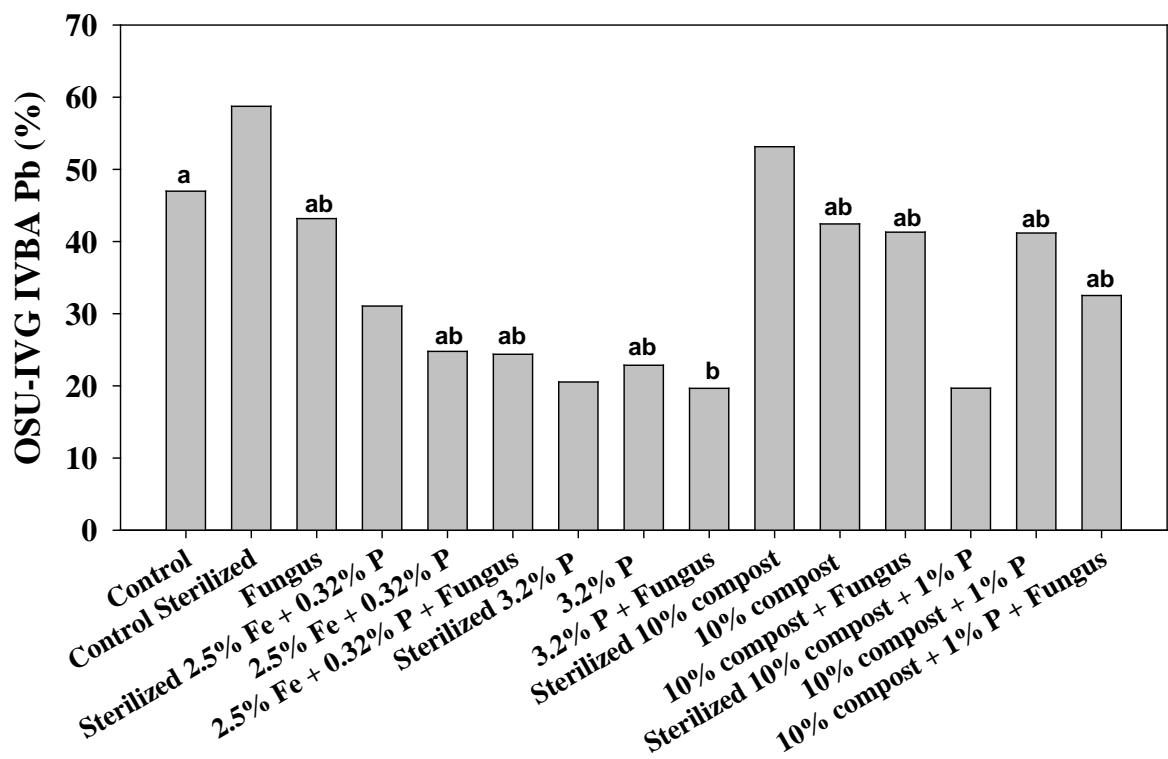


Figure 29. OSU-IVG IVBA Pb results for Joplin soil treatments.

Effect of soil treatments and microbial activity on Pb bioavailability

The effect of ORNL and Joplin treatments on in vivo relative bioavailable Pb (RBA Pb) measured using the adult mouse model is summarized in the following Table 28. Phosphorus soil treatment greatly decreased RBA Pb for both ORNL and Joplin site soils. Fungal treatments of remediated soil (i.e., ORNL + P, Joplin + Fe + P, Joplin + P) did not increase RBA Pb. Sequestered Pb remained sequestered after fungal treatment.

Table 28. Relative bioavailable Pb for ORNL and Joplin sites and treatments.

Site	Treatment	RBA Pb (%)
ORNL	Control	59.4a
ORNL	P + Fungus	2.20b
ORNL	P	2.90b
Joplin	Control	47.7A
Joplin	3.2% P + Fungus	13.2B
Joplin	3.2% P	5.40B
Joplin	2.5% Fe + 0.32% P + Fungus	9.90B
Joplin	2.5% Fe + 0.32% P	12.0B

Treatments with the same letter are not significantly different at $P < 0.05$.

Comparison should only be made within sites (a vs. b or A vs. B).

In vitro measures of Pb bioaccessibility and Pb relative bioavailability (RBA Pb)

In vitro Pb results for U.S. EPA 1340 1.5, U.S. EPA 1340 2.5, and OSU-IVG along with mouse RBA Pb for select ORNL and Joplin soils are presented in Figures 30 and 31 respectively. The results indicate that for both sites for the untreated control soil, the U.S. EPA 1340 1.5 and OSU-IVG closely approximate mouse RBA. However, in the P treated soils, the U.S. EPA 1340 2.5 and OSU-IVG closely approximate mouse RBA while U.S. EPA 1340 1.5 drastically over estimated RBA Pb.

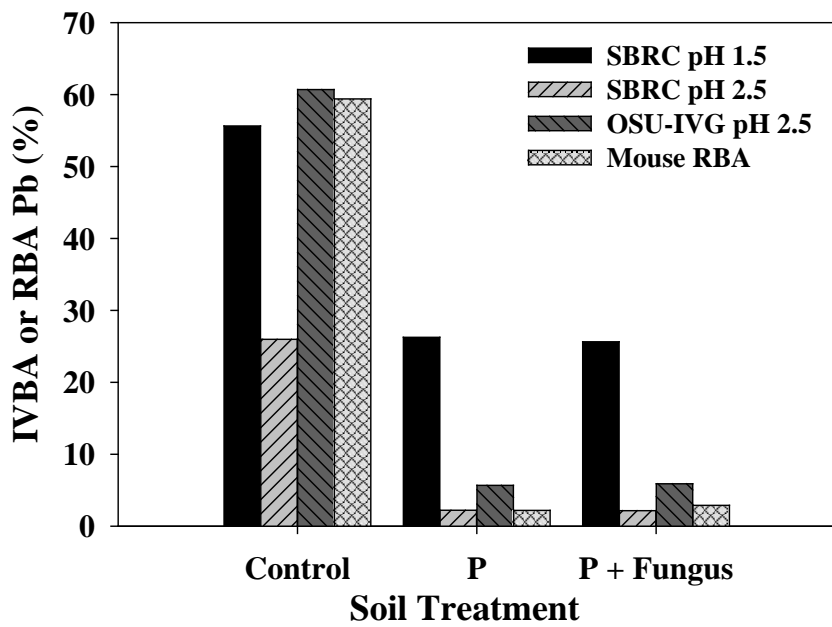


Figure 30. In vitro extractable Pb with U.S. EPA 1340 pH 1.5, U.S. EPA 1340 pH 2.5, and OSU-IVG along with mouse RBA Pb for control and P treated (with and without fungus) ORNL.

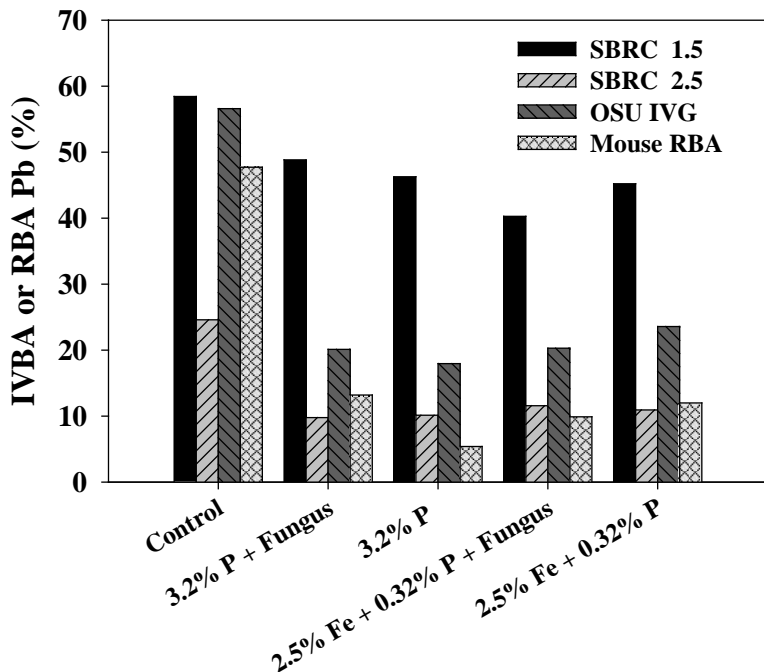


Figure 31. In vitro extractable Pb with U.S. EPA 1340 pH 1.5, U.S. EPA 1340 pH 2.5, and OSU-IVG along with mouse RBA Pb for control and P treated (with and without fungus) Joplin soils.

In order to evaluate the ability of the in vitro methods to predict mouse RBA Pb, IVIVC with U.S. EPA 1340 1.5, U.S. EPA 1340 2.5, U.S. EPA 1340 1.5 for control soils and U.S. EPA 1340 2.5 for P treatments, and OSU-IVG was evaluated (Figure 32). All IVIVCs were significant ($P<0.05$), however the two best predicting IVIVCs were U.S. EPA 1340 1.5 for control soils and U.S. EPA 1340 2.5 for P treatments (Figure 32C) and OSU-IVG (Figure 32D). This demonstrates that in vitro must applied cautiously for P treated soils. Further, the in vitro method approved by the U.S. EPA Method 1340 (SBRC 1.5) provided a good estimate of RBA Pb for both the ORNL control (-3.8%) and the Joplin control (+11%). However, U.S. EPA 1340 1.5 drastically over-extracted Pb for P treated soils (+23-41%). As a result, a regression that combines of U.S. EPA 1340 1.5 for non-P treated soils and U.S. EPA 1340 2.5 for P treated soils demonstrates a potential for the use of a 0.4M glycine extraction to evaluate P-based remedial treatments. Further development is needed to determine what defines a P treatment and if the regression (Fig. 32C) holds true over a wide range of Pb species.

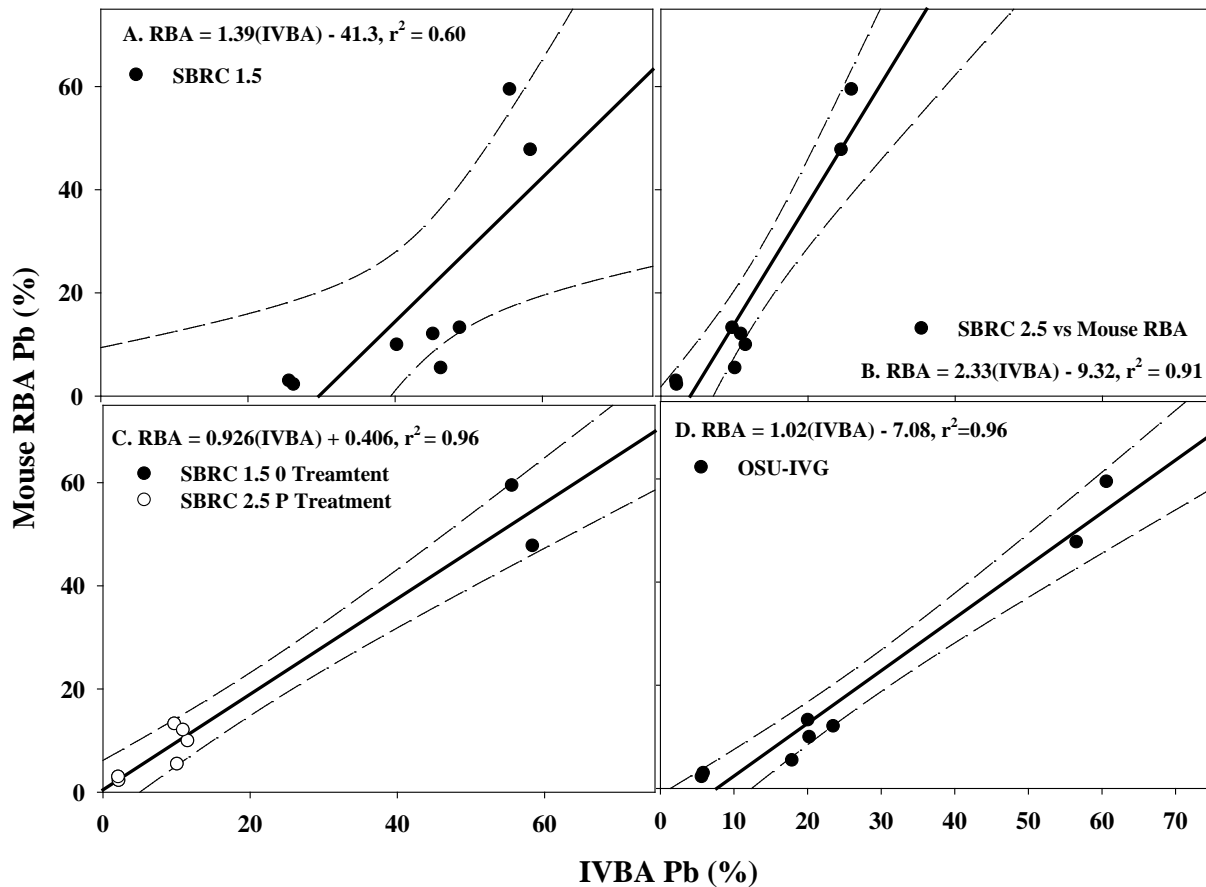


Figure 32. IVIVC (with 95% confidence intervals) of ORNL and Joplin no treatment controls and P treatments (with and without fungus) with the U.S. EPA 1340 pH 1.5 (A), U.S. EPA 1340 pH 2.5 (B), U.S. EPA 1340 pH 1.5 for control soils and U.S. EPA 1340 pH 2.5 for P treatments (C), and OSU-IVG pH 2.5 (D).

Pb Speciation

The results for Pb speciation in the ORNL control and treated soils as well as Joplin control and P-treated soils are presented in figures 33 and 34 respectively. The untreated ORNL control consisted of primarily organic bound Pb (56%), followed by Pb sulfate (19%), and then approximately equal amounts of mineral bound Pb (14%) and Pb as pyromorphite (11%). The litter, fungus, and litter + fungus treatments resulted in little shift in Pb speciation. However, all P treatments showed a large shift from the organic bound Pb pool (23-27%) to Pb as pyromorphite (31-34%) and mineral bound Pb (19-27%). This increase in Pb as pyromorphite is consistent with IVBA (U.S. EPA 1340 pH 1.5 and OSU-IVG) Pb reductions with P treatment in these soils. Fungal inoculation with or without litter addition did not affect Pb speciation (Fig. 33 and 34).

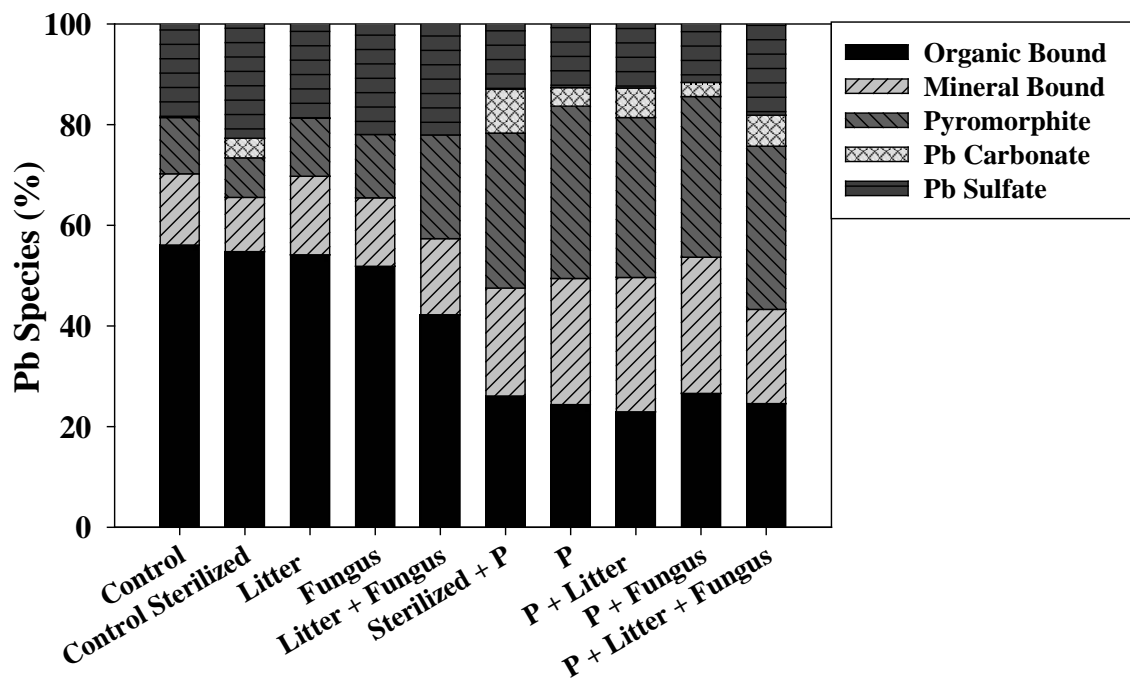


Figure 33. Pb Species in ORNL soil treatments; organic bound, mineral bound, pyromorphite, Pb carbonate, and Pb sulfate.

The untreated Joplin soil consisted of primarily of Pb sulfate (32%) and organic bound Pb (32%), followed by mineral bound Pb (22%), galena (11%), and Pb as pyromorphite (3%) (Fig. 34). Similar to ORNL, Joplin P treatments resulted in a shift from organic bound Pb (18-24%) into Pb as pyromorphite (27-37) and mineral bound Pb (23-39). However, unlike ORNL Pb sulfate was also substantially reduced in the P treatments (9-11%) and completely absent in P+Fungus treatments. Further, galena which was found in the untreated control was absent in all P treatments. Also similar to ORNL was the increase in Pb as pyromorphite is reflected in IVBA (U.S. EPA 1340 pH 1.5 and OSU-IVG) Pb reductions with P treatment. Fungal inoculation

appears to have converted Pb sulfate species into other Pb species including mineral bound and/or pyromorphite.

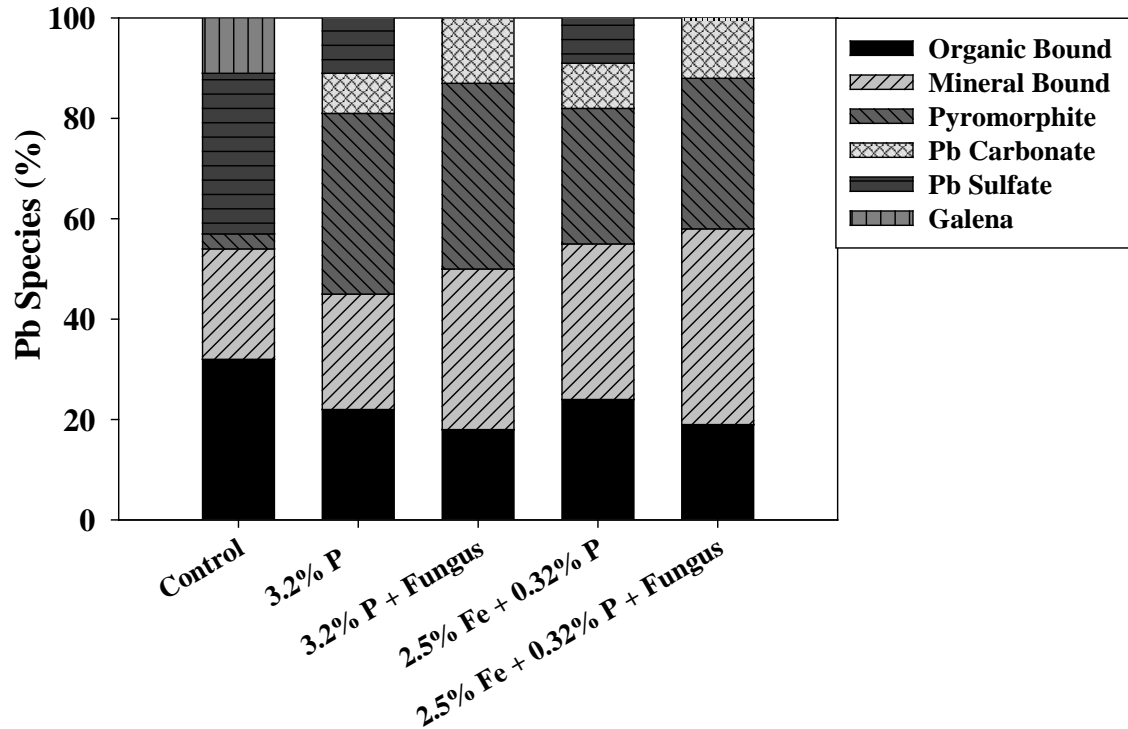


Figure 34. Pb Species in Joplin soil treatments; organic bound, mineral bound, pyromorphite, Pb carbonate, Pb sulfate, and galena.

Task 6.2: Effect of key soil chemical processes on long-term metal permanence of Pb-contaminated soil remediated with phosphate treatments

Results

The results for Pb LSP extraction for ORNL control and P-treated soils as well as Joplin control and P-treated soils are presented in figures 35 and 36 respectively. Results are consistent with Pb soil chemistry in that Pb solubility increases under acidic conditions. In general, Pb solubility at pH < 4. For both study sites, the effect of P treatment is apparent at low pH. A sharp increase in soluble Pb occurred at pH < 4 for the ORNL control soil and pH < 3 for the P-treated soil. In other words, the P-treatment extended the insolubility of Pb from pH 4 to pH 3 (Fig 35).

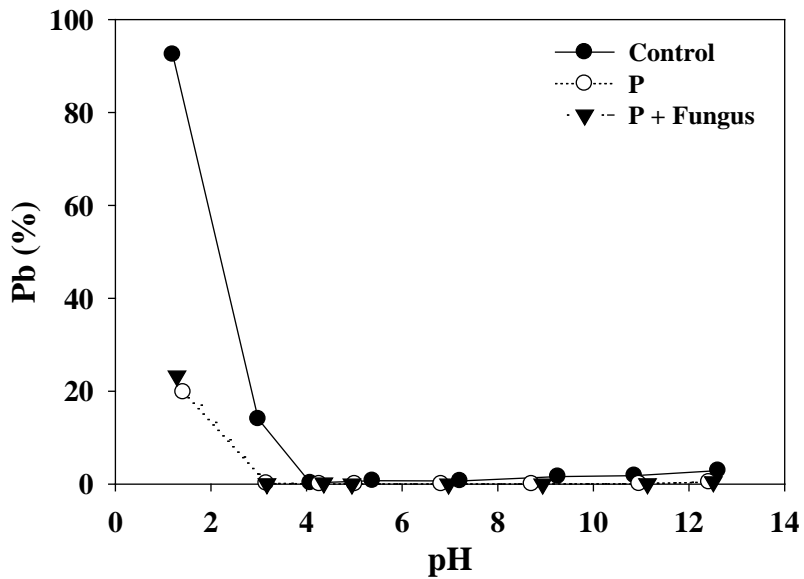


Figure 35. Pb solubility across pH for control and P-treated ORNL soil.

The control soil on the Joplin site shows increased Pb solubility at pH < 5, while the Pb in P-treated soils remains insoluble down to pH 3 (Fig. 36). The results from both sites demonstrate the stability of Pb with P-treatment, even at uncommonly low soil pH (3.0). In addition, the results suggest that in untreated soils, Pb solubility can increase at a pH around 5.0, which is a possible pH for highly weathered soils and soils that have received long term fertilizer applications. Fungal inoculation had no effect on the solubility of Pb in the P-treated soil.

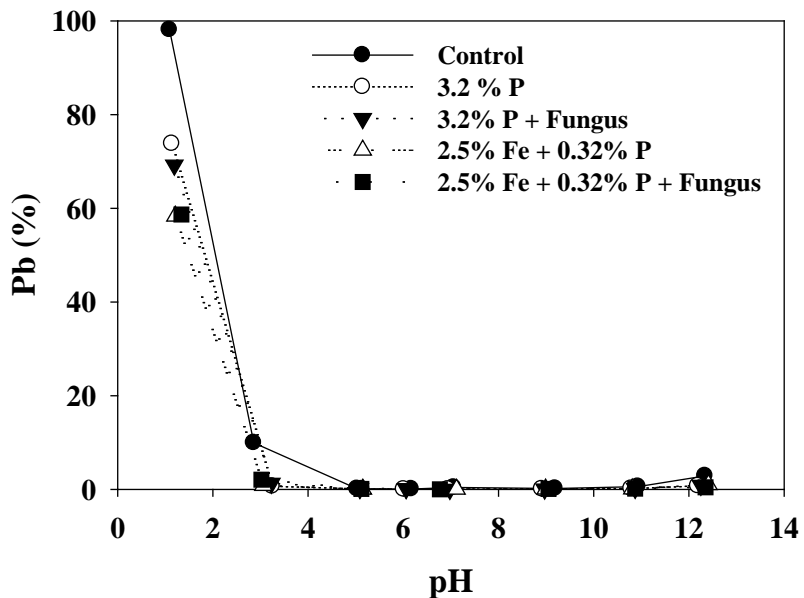


Figure 36. Pb solubility across pH for control and P-treated Joplin soils.

These LSP results are consistent with P treatments forming Pb pyromorphite that is less soluble at pH 4 than untreated soil with more soluble Pb minerals (Scheckel et al., 2013). The Pb minerals in the P treated soil are stable to acid inputs (i.e., natural or fertilizer, acid rain, etc) to very acidic soil pH \geq 3. It is improbable that acid rain, fertilizer or natural acidity inputs can reduce soil pH to levels below pH 4-5. Thus, it is highly unlikely that the long-term metal permanence of Pb-contaminated soil remediated with phosphate treatments will be affected by acidity from acid rain, fertilizer or natural sources. However, chemical processes that can produce extreme amounts of acidity and reduce the soil pH $<$ 3 will mobilize Pb. Few chemical processes, except for oxidation of reduced sulfur species, are known to produce levels of acidity capable of lowering the pH $<$ 3. Pb contaminated soils with large amounts of sulfidic waste (i.e., mining waste) should be treated with adequate alkaline soil amendments (i.e., agricultural limestone) to neutralize excessive amounts of future acidity and maintain soil pH $>$ 4. Neither the ORNL firing range or the smelter Joplin P-treated soils contained sulfidic waste. The pH of these soils will remain at pH $>$ 4. Fungal inoculation has no effect on Pb solubility as a function of pH in the ORNL P-treated soil (Fig. 35) or the Joplin P-treated soil (Fig. 36).

Task 7: U.S. EPA Bioavailability and Technology Transfer

Technology transfer of SERDP products will be mainly from the U.S. EPA ORD ER-1742 members. Also, the project PI (Basta, OSU) will work with SERDP to transfer technology generated from this project to the risk assessment and remediation sector.

Most of the project technology transfer is expected to increase after completion of the ER-1742 final report. The following presentation describing ER-1742 was made to a national audience of DoD risk assessors at the Tri-Service Environmental Risk Assessment Working Group's 2014 winter meeting.

- Basta, N.T. 2014. State of the Science of In Vitro Gastrointestinal Metal(loid)Bioaccessibility, and Predicted Human Bioavailability from Ingestion of Contaminated Soil / Dust. Tri-Service Environmental Risk Assessment Working Group (TSERAWG) 2014 Winter meeting. Fort Sam Houston, San Antonio, TX, Feb. 25-26, 2014.

At present, 40 presentations of research findings from ER-1742 have been made at international and national scientific conferences including:

- 18th International Conference on Heavy Metals in the Environment, Ghent, Belgium Sept 12-15, 2016.
- Goldschmidt 2014 Conference, Sacramento, CA.
- ACS National Meeting & Exposition, New Orleans, LA.
- Soil Science Society Annual Meeting, Cincinnati, OH
- 12th International Conference for Trace Element Biogeochemistry, Athens, GA
- Society of Environmental Toxicology and Chemistry, Vancouver, B.C., Canada
- 11th International Conference on the for Trace Element Biogeochemistry, Florence, Italy.
- Society of Toxicology Annual meeting
- American Society of Microbiology
- Ecological Society of America

The U.S. EPA's ORD scientists have provided over 30 presentations to U.S. EPA Regional offices, international, and national audiences on soil-metal bioavailability and bioaccessibility, which has increased the level of understanding of soil-metal bioavailability and bioaccessibility. The ORD scientists worked on the development of a new lead bioaccessibility standard operating procedure for OSWER to reflect changes in NIST reference materials, refine procedures, and develop a data reporting format. Dr. Bradham has provided training on this in vitro bioaccessibility assay to many of the EPA Regional offices. Dr. Bradham and OSWER's Dr. Burgess, provided in vitro bioaccessibility training at the 18th Annual Laboratory and Technical Information Group (LTIG) Conference, Boston, MA, which is a training conference specifically for Regional laboratory scientists. Drs. Scheckel and Bradham developed a short course designed for Regional Program Managers and On-scene Coordinators. A brief course description: Innovative Characterization and Remediation Technologies for Metals Contaminated Soils is a half-day introductory to intermediate training course that focuses on specific technologies/techniques that RPMs and OSCs can use when managing sites with metals-contaminated soils, including characterization, bioavailability, and remediation. As a result of the U.S. EPA scientist's efforts, several EPA Regional offices have set up laboratory capabilities to conduct in vitro bioaccessibility assays for their contaminated sites and their Regional scientists are using the results in making site-specific risk adjustments. The presentations and support provided by the U.S. EPA's scientists resulted in an improved understanding and predictive capability of soil-metal bioavailability and bioaccessibility and increased the confidence levels of the site managers to incorporate site-specific bioavailability measurements into management decisions.

Conclusions and Implications for Future Research/ Implementation

The specific objectives of ER-1742 were to (1) conduct a comprehensive study to link the binding mechanism of As in soil (i.e., speciation) with in vitro and in vivo methods used to predict current and potential future bioavailability of soil As to humans, and (2) evaluate the effect of key biological and chemical processes on the permanence of binding and bioavailability of Pb in untreated and treated (i.e., remediated) soils. Conclusions from the two objectives of ER-1742 are presented as follows.

Conclusions for Objective 1: Conduct a comprehensive study to link the binding mechanism of As in soil (i.e., speciation) with in vitro and in vivo methods used to predict current and potential future bioavailability of soil As to humans

The most important part of Objective 1 was a comprehensive evaluation of the ability of different in vitro methods to predict RBA As (Task 5). Conclusions from this part of Objective 1 are:

- Total soil As concentration was not correlated with RBA As determined by the adult mouse ($r^2 = 0.24$) or the juvenile swine ($r^2 = 0.09$) bioassays.
- All of the IVBA methods were predictive of RBA for both the mice and swine bioassays.
- A y intercept close to zero is critical for accurate prediction of RBA As for soils with low RBA (< 20-30% RBA As).
- The simple linear regression technique produced IVIVC that are of equal quality to those produced using more complex statistical techniques (i.e., Bayesian regression method).
- IVBA As from the gastric extraction is a better predictor than IVBA As from the intestinal extraction. Using the GE may also provide more conservative RBA As because the IVBA values are greater for the GE than for the IE (i.e. the As is more soluble) representation a worst case scenario for the estimating As RBA for soil ingestion.
- All methods, except CAB, are better predictors for soils with high (> 1200 mg/kg As) for swine RBA. However the non-CAB methods are much less accurate for low RBA soils due to their high y-intercept values in the linear regressions used to predict RBA As. CAB was more accurate for low RBA As soils and for soils with high reactive Al and Fe oxides (i.e. soils 1 and 2 in this study).
- Results show Caco-2 As uptake studies with sodium arsenate do not corroborate with in vivo studies. Caco-2 may be a useful model to study As uptake mechanisms, but will not likely improve bioavailability estimates for soil.

The relationship between As speciation, bioaccessibility and bioavailability of As was determined. The study was comprehensive with 27 soils representing a wide range of properties and a wide range of As contaminant sources. Conclusions from this part of Objective 1 are:

- Results of the As SEP followed the trend F4, F3 > F2 > F1 for As in each fraction, indicating the As in most study soils in an insoluble fraction.

- As expected from theory and from sequential extractions, As chemistry was closely tied to Fe chemistry in the soils evidenced by the most abundant As species being As(V) adsorbed to HFO or Fe oxides. Other identified As species includes; As (-III) metal sulfides, As (III) sulfides, As (III) oxides, As (III) adsorbed to sulfides, As (III) adsorbed to Fe/ Al oxides, lead arsenates, and hydrous ferric arsenates (HFA).
- Mössbauer and Fe EXAFS confirmed the most frequently found Fe species groups in the soil dataset were the hydrous ferric oxides (HFO), Fe oxides, and Fe(III) substituted in aluminosilicate clays, which is common in many soils and expected from the dataset.
- The RBA As for As species followed the trend Pb As pesticide > adsorbed As (V) > As sulfides.
- Despite As(V) adsorbed to mineral surfaces being a major component of most soils (>50%), these soils ranged from ~20-80% in IVBA As and widely ranged in RBA As. Arsenic speciation alone is not predictive of IVBA or RBA As. However, As speciation is very important to provide information on IVBA or RBA As results.

Significant findings regarding IVBA and RBA methods that should be considered when using them in HHRA were discovered by ER-1742. Conclusions of these findings relevant to Objective 1 are:

In Vivo Bioavailability (Task 3)

The soils evaluated in the study using the adult mouse model and juvenile swine model have produced a wide range in RBAs showing how physical and chemical properties of each soil impact As RBA.

- RBA As determined for 19 soils via the adult mouse model ranged from 6.37 to 81.2% with an average of 34.9%. RBA As determined for 22 soils via the juvenile swine model ranged from 4.00 to 60.0% with an average of 32.5%. The U.S. EPA recommended suggested that when development of site-specific bioavailability estimates are not feasible (e.g., screening-level assessments), the default value of 60% can be used. Data in this study also confirms that a default value of 60% is not likely to be exceeded at most sites.
- Relative bioavailability was determined for 14 of the 27 study soils using both the adult mouse and juvenile swine models with mouse model tending to provide lower RBA values than swine model. The mouse RBA / swine RBA ratio for the 14 soils that were dosed to using both animal models have a range of 0.36 to 1.13 with a mean of 0.72.

In Vitro Arsenic Bioaccessibility (Task 4):

- IVBA As ranged for the 27 study soils <1% to 100% across all methods with mean (by method) IVBA As of study soils ranging from 25.4% to 47.0%.
- Median and mean IVBA As followed the trend CAB (pH 1.5) > UBM (pH 1.2) ≈ OSU (pH 1.8) ≈ PBET (pH 1.8) ≈ Glycine (pH 1.5). Although extraction pH is important, our results from the soils in the current study do not corroborate with previous studies that suggest extraction fluid pH is the dominant variable to explain differences in IVBA As between different IVBA methods. IVBA results vary for individual soils depending on

the method applied and that certain extraction parameters including; soil:solution ratio, and ascorbic acid addition can be more important in determining IVBA As than simply extraction pH.

- In general, the CAB IVBA As was greater than all other methods. The median results across all methods except for CAB were similar but results within individual soils across methods differed.

Implications for Future Research / Implementation for Objective 1

Arsenic is one of the most common contaminants of concern exceeding risk criteria because soil ingestion is the primary human health risk driver at many DoD sites. Many studies have shown that As bioavailability and not total content determines human risk from soil ingestion. However, the current regulatory paradigm for human health risk assessment (HHRA) of contaminated soils does not include the use of bioavailability measures. Use of contaminant total content instead of bioavailability is often overly conservative and can result in costly and unnecessary soil remedial action.

A primary impediment to the use of bioavailability data in risk assessment and decision-making by DoD and other site managers is the absence of rapid and inexpensive tools for reliable human bioavailability estimates. Results from this study can be implemented to provide reliable estimates of human bioavailability by DoD site managers and risk assessors. Key implications of ER-1742 to assist site managers and risk assessors in implementing bioavailability in their site assessment are summarized below.

Selecting an IVBA Method for Predicting RBA As

- All of the IVBA methods were predictive of RBA for both the mice and swine bioassays. The CAB was more accurate for low RBA As soils and for several soils with high reactive Al and Fe oxides in this study. Non-CAB methods underpredicted RBA As for these soils. However, other studies have reported accurate prediction of RBA As using U.S. EPA 9200 for soils with high Fe contents (Diamond et al. 2016). More research is needed in this area before recommending a specific method.
- Pick a method that has a IVIVC with a y intercept close to zero for accurate prediction of RBA As for soils with low RBA (< 20-30% RBA As).
- Use the IVBA As from the gastric extraction (GE) of the method. GE often provides a more conservative RBA As because the IVBA values are greater for the GE than for the intestinal extraction.

Considerations When Using As Speciation Data for Site Assessment

- Speciation of As provides information on RBA As. Our study shows Pb As pesticide > adsorbed As (V) > As sulfides. This is useful information to decide whether to consider adjusting for bioavailability in a risk assessment. Arsenic species associated with low RBA As are excellent candidates for assessment of their RBA by either in vitro (i.e., IVBA) or in vivo (RBA) methods.

- Arsenic speciation alone is not predictive of IVBA or RBA As. However, As speciation is very important to provide supporting information to corroborate IVBA or RBA As results.

Future Research for Objective 1

A number of studies have reported a strong correlation between RBA As and As IVBA As, including ER-1742. There is uncertainty in the ability of IVBA methods to predict RBA As for soil for a specific site. Then uncertainty is greater when the soil properties, As speciation, and/or arsenic contamination sources are different than those reported in ER-1742. Demonstration studies to “validate” (Juhasz et al., 2013) that specific IVBA method can accurately predict RBA As for specific sites is needed to provide confidence to DoD site managers and risk assessors. Future research to demonstrate and validate results from ER-1742 for several high-priority DoD cleanup sites is a logical next step to build confidence to DoD site managers in application of bioavailability and IVBA technology for site cleanup.

Objective 2: Conduct a comprehensive study to link the binding mechanism of As in soil (i.e., speciation) with in vitro and in vivo methods used to predict current and potential future bioavailability of soil As to humans (Task 6).

The key biological and chemical processes were evaluated for soils from two contaminated sites; A firing range at the Oak Ridge National Laboratory and a Pb-smelter impacted site in Joplin, MO. The soils at both of these sites had that had received phosphorus containing P-amendments.

The untreated and treated soils were subjected to low molecular weight organic acid (LMWOA) producing fungus as a key biological process that has the potential to increase Pb bioavailability and mobility. The untreated and treated soils were subjected to soil acidification as a key chemical processes that has the potential to increase Pb bioavailability and mobility.

Fungi isolated from soil produced low molecular weight organic acids (LMWOA) including oxalic acid in non-soil laboratory conditions (i.e., broth). The LMWOA was capable of dissolved PbCO_3 that was added to laboratory medium. However, the LMWOA-isolated fungus inoculated into study soils (ORNL, Joplin) has little effect on Pb solubility, mobility and bioavailability. Soil treatment with P produced Pb minerals, including Pb pyromprophite, that are much more stable to LMWOA or acid produced by fungus than PbCO_3 .

The following conclusions can be made for both ORNL and Joplin sites:

- P treatment resulted in stable reduction in soluble Pb (measured by SPLP), and potential human bioavailability measured by IVBA methods.
- The P treatments of Joplin contaminated soil has remained stable over a long period of time (> 10 y).
- Fungal treatments did not affect Pb speciation in soil which suggests the sequestered Pb by soil amendment of P were stable

- Fungal treatments did not affect Pb bioaccessibility and potential Pb bioavailability in treated soils.
- Pb minerals in the P treated soil are stable to acid inputs at pH > 3
- A sharp increase in soluble Pb occurred at pH < 4 for the untreated control soil and pH < 3 for the P-treated soil. In other words, the P-treatment extended the insolubility of Pb from pH 4 to pH 3.

Implications for Future Research / Implementation for Objective 2

Bioavailability based in situ remediation of Pb-contaminated soil by using inexpensive and widely available phosphorus soil amendments is a proven technology. Bioavailability of Pb is greatly reduced by formation of very insoluble Pb-P minerals such as Pb pyromorphite. This technology has been used to remediate Pb contamination on firing ranges of DoD sites. Research has shown that Phosphate-induced Metal Stabilization (PIMS) reduces Pb bioavailability and risk in contaminated soils from firing ranges at U.S. Army Camp Stanley (ESTCP ER-0020).

Concern over the long-term permanence of low bioavailability Pb minerals formed in soils amended with P is a barrier for implementation of this successful technology. Information is needed on the long-term effect of key biological and chemical processes bioavailability of sequestered Pb. Will the sequestered Pb be stable and prevent increased Pb bioavailability over time? ER-1742 provided an answer to this question.

In short, the answer is “yes.” Our results show sequestered Pb in P-treated soil is stable. Neither biological fungal treatments or chemical acidification affected Pb mobility, bioaccessibility or bioavailability in P-treated soils. Low bioavailability Pb minerals formed from P treatment in Joplin contaminated soil has remained stable over a long period of time (> 10 y). The Pb minerals in the P treated soil are stable to acid inputs (i.e., natural or fertilizer, acid rain, etc) to very acidic soil pH \geq 3.

It is improbable that acid rain, fertilizer or natural acidity inputs can reduce soil pH to levels below pH 4-5. Thus, it is highly unlikely that the long-term metal permanence of Pb-contaminated soil remediated with phosphate treatments will be affected by acidity from acid rain, fertilizer or natural sources. However, chemical processes that can produce extreme amounts of acidity, such as except for oxidation of reduced sulfur species in mining waste, can reduce the soil pH < 3 and mobilize Pb. Pb-contaminated soils with large amounts of sulfidic waste (i.e., mining waste) should be treated with adequate alkaline soil amendments (i.e., agricultural limestone) to neutralize excessive amounts of future acidity and maintain soil pH > 4.

A major finding of our study is U.S. EPA method 1340 is not suitable for evaluating the bioaccessibility and bioavailability of P treated soils. A modified Method 1340, extracting solution of pH 2.5 instead of 1.5, or another method (i.e., OSU IVG) should be used to evaluate IVBA and RBA Pb in soil treated with P. These results are consistent with findings reviewed by Henry et al. (2015). Limited studies have reported U.S. EPA method does not accurately measure reduction in IVBA Pb or RBA Pb in P-treated soil and recommend changing the extraction pH from 1.5 to 2.5 in U.S. EPA Method 1340. While developing the RBALP, the precursor of Method 1340, researchers tested different in vitro conditions using untreated Pb

contaminated soils. The researchers selected pH 1.5 instead of pH 2.5 because of less variability at pH 1.5, although pH 1.5 and 2.5 both were highly correlated with RBA Pb (r^2 of 0.85 and 0.75, respectively). They did not test RBALP with phosphate-amended Pb soils. The ability of U.S. EPA Method 1340 with an extraction pH of 2.5 to predict RBA Pb in soils treated with phosphorus and other soil amendments known to reduce RBA Pb should be researched. Research should be conducted with procedures outlined by the U.S. EPA Technical Review Workgroup (U.S. EPA, 2007a) and other committees focused on acceptable methodologies for regulatory acceptance including the Interstate Technology and Regulatory Council (ITRC) “Bioavailability in Contaminated Soil” workgroup.

Literature Cited

- Adams, F. 1984. Soil acidity and liming. American Society of Agronomy: Madison, WI.
- Altschul S.F., T.L. Madden, A.A. Schaffer, J. Zhang, Z. Zhang, W. Miller, and D.J. Lipman. 1997. Gapped BLAST and PSI-BLAST: A new generation of protein database search programs. *Nucleic Acids Res.* 25:3389–3402.
- Basta, N.T. and A. Juhasz. 2014. Chapter 9: Using in vivo bioavailability and/or in vitro gastrointestinal bioaccessibility testing to adjust human exposure from soil ingestion. In: R.J. Bowell, J. Majzlan, and C. Alpers, editors. *Geochemistry, mineralogy and microbiology of arsenic in environment. Reviews in Mineralogy and Geochemistry*, Mineral. Soc. Am., Chantilly, VA.
- Basta, N.T., J.N. Foster, E.A. Dayton, R.R. Rodriguez, and S.W. Casteel. 2007a. The effect of dosing vehicle on arsenic bioaccessibility in smelter-contaminated soils. *J. Environ. Health Sci. Part A*. 42:1275–1281.
- Basta, N.T., J.N. Foster, and K.G. Scheckel. 2007b. Arsenic speciation using extended X-ray absorption fine structure and chemical extraction methods to assess oral bioavailability. Paper presented at SSSA Annual Meeting, New Orleans, LA. 4-8 Nov. Paper 91–6.
- Bowell, R. J., C.N. Alpers, H.E. Jamieson, D.K. Nordstrom, and J. Majzlan. 2014. Arsenic: Environmental geochemistry, mineralogy, and microbiology. In: R.J. Bowell, J. Majzlan, and C. Alpers, editors, *Geochemistry, Mineralogy and Microbiology of Arsenic in Environment*. Mineral. Soc. Am., Chantilly, VA.
- Bradham, K.D., K.G. Scheckel, C.M. Nelson, P.E. Seales, G.E. Lee, M.F. Hughes, B.W. Miller, A. Yeow, T. Gilmore, S. Harper, and D.J. Thomas. 2011. Relative bioavailability and bioaccessibility and speciation of arsenic in contaminated soils. *Environ. Health Perspect.* 119:1629–1634.
- Bradham, K.D., G.L. Diamond, K.G. Scheckel, M.F. Hughes, S.W. Casteel, B.W. Miller, J.M. Klotzbach, W.C. Thayer, and D.J. Thomas. 2013. Mouse assay for determination of arsenic bioavailability in contaminated soils. *J. Toxicol. Environ. Health Part A* 76:815–826.
- Bradham, K.D. C. Nelson, A.L. Juhasz, E. Smith, K. Scheckel, D.R. Obenour, B.W. Miller, and D.J. Thomas. 2015. Independent data validation of an in vitro method for the prediction of relative bioavailability of arsenic in contaminated soils. *Environ. Sci. Technol.* 49:6312–6318.
- Brattin, W., and S. Casteel. 2013. Measurement of arsenic relative bioavailability in swine. *J. Toxicol. Environ. Health Part A* 76:449–457.
- Calatayud, M., J. Gimeno, D. Vélez, V. Devesa, and R. Montoro. 2010. Characterization of the intestinal absorption of arsenate, monomethylarsonic acid, and dimethylarsinic acid using the Caco-2 cell line. *Chem. Res. Toxicol.* 23(3):547–556.
- Canavos, C.G. 1984. Applied probability and statistical methods. Little, Brown and Co., Boston.

- Cancès, B., F. Juillot, G. Morin, V. Laperche, D. Polya, D. Vaughan, and G. Calas. 2008. Changes in arsenic speciation through a contaminated soil profile: A XAS based study. *Sci. Total Environ.* 397(1-3):178–189.
- Casteel, S. 2005. Relative bioavailability of arsenic and vanadium in soil from a superfund site in Palestine, Texas. Report prepared for U.S. EPA Office of Superfund Remediation Technology Innovation. Prepared by Univ. of Missouri, Columbia, and SRC.
- Casteel, S., and SRC. 2009a. Relative bioavailability of arsenic in Barber Orchard soils. Report prepared for U.S. EPA Office of Superfund Remediation Technology Innovation. Prepared by Univ. of Missouri, Columbia, and SRC.
- Casteel, S., and SRC. 2009b. Relative bioavailability of arsenic in NIST SRM 2710 (Montana soil). Report prepared for U.S. EPA Office of Superfund Remediation Technology Innovation. Prepared by Univ. of Missouri, Columbia, and SRC.
- Casteel, S., and SRC. 2009c. Relative bioavailability of arsenic in a Mohr Orchard soil. Report prepared for U.S. EPA Office of Superfund Remediation Technology Innovation. Prepared by Univ. of Missouri, Columbia, and SRC.
- Casteel, S., and SRC. 2010a. Relative bioavailability of arsenic in an Iron King soil. Report prepared for U.S. EPA Office of Superfund Remediation Technology Innovation. Prepared by Univ. of Missouri, Columbia, and SRC.
- Casteel, S., and SRC. 2010b. Relative bioavailability of arsenic in an ASARCO and Hawaiian soil. Report prepared for U.S. EPA Office of Superfund Remediation Technology Innovation. Prepared by Univ. of Missouri, Columbia, and SRC.
- Casteel, S., and SRC. 2010c. Relative bioavailability of arsenic in NIST SRM 2710a (Montana soil). Report prepared for U.S. EPA Office of Superfund Remediation Technology Innovation. Prepared by Univ. of Missouri, Columbia, and SRC.
- Casteel, S.W., C.P. Weis, G.W. Henningsen, and W.J. Brattin. 2006. Estimation of relative bioavailability of lead in soil and soil-like materials using young swine. *Environ. Health Perspect.* 114:1162–1171.
- Castro H., A. Classen, E. Austin, R. Norby, and C. Schadt. 2010. Soil microbial community response to multiple experimental climate change drivers. *Appl. Environ. Microbiol.* 76:999–1007.
- Chaney, R.L., N.T. Basta, and J.A. Ryan. 2008. Element bioavailability and bioaccessibility in soils: What is known now, and what are the significant data gaps? SERDP and ESTCP Workshop on Research and Development Needs for Understanding and Assessing the Bioavailability of Contaminants in Soils and Sediments, Annapolis, MD, 20-21 Aug.
- Charman, W.N., C.J. Porter, S. Mithani, J.B. Dressman. 1997. Physicochemical and physiological mechanisms for the effects of food on drug absorption: The role of lipids and pH. *J. Pharm. Sci.* 86:269–282.
- Crews, H.M., J.A. Burrell, and D.J. McWeeney. 1983. Preliminary enzymolysis studies on trace element extractability from food. *J. Sci. Food Agric.* 34:997–1004.
- Culp, R.A., and A.B. Rawitch. 1973. Solubilization of lead from an alkyd paint matrix by simulated gastric and intestinal digestive fluids. *J. Paint Technol.* 45:38–41.

- Denys S., J. Caboche, K. Tack, G. Rychen, J. Wragg, M. Cave, C. Jondreville, C. Feidt. 2012. In vivo validation of the unified BARGE method to assess the bioaccessibility of arsenic, antimony, cadmium, and lead in soils. *Environ. Sci. Technol.* 46:6252–6260.
- Deschamps, E., V.S. Ciminelli, P.G. Weidler, and A.Y. Ramos. 2003. Arsenic sorption onto soils enriched in Mn and Fe minerals. *Clays and Clay Minerals* 51(2):197–204.
- Diamond, G.L., K.D. Bradham, W.J. Brattin, M. Burgess, C.A. Hawkins, A.L. Juhasz, J.M. Klotzbach, C. Nelson, Y.W. Lowney, K.G. Scheckel, D.J. Thomas. 2016. Predicting oral relative bioavailability of arsenic in soil from in vitro bioaccessibility. *J. Toxicol. Environ. Health Part A* 79:165–173.
- Department of Toxic Substance Control (DTSC). 2015. Final technical report EPA Brownfields Training, Research and Technical Assistance Grant: Arsenic characterization/bioavailability on mine-scarred lands (study). DTSC, Sacramento, CA.
- Draper, N.R., and H. Smith. 1998. Applied regression analysis. 3rd ed. John Wiley & Sons, New York.
- Drexler, J.W., and W.J. Brattin. 2007. An in vitro procedure for estimation of lead relative bioavailability: With validation. *Human Ecol. Risk Assess.* 13:383–401.
- Dyar, M.D., D.G. Agresti, M.W. Schaefer, C.A. Grant, and E.C. Sklute. 2006. Mössbauer spectroscopy of earth and planetary materials. *Annu. Rev. Earth Planet. Sci.* 34(1):83–125.
- Essington, M.E. 2004. Soil and water chemistry: An integrative approach. CRC Press, Boca Raton, FL.
- Fieller, E.C. 1954. Some problems in interval estimation. *J. Royal Stat. Soc. Ser. B (Methodological)* 16(2):175–185.
- Filippi, M., P. Drahota, V. Machovič, V. Böhmová, and M. Mihaljevič. 2015. Arsenic mineralogy and mobility in the arsenic-rich historical mine waste dump. *Sci. Total Environ.* 536:713–728.
- Finney, D.J. 1978. Statistical method in biological assay. 3rd ed. Charles Griffin and Co., London.
- Gadd, G.M. 1999. Fungal production of citric and oxalic acid: importance in metal speciation, physiology and biogeochemical processes. *Advances in Microbial Physiology* 41: 47–92.
- Gee, G.W., and J.W. Bauder. 1986. Particle-size analysis. In: editors. *Methods of soil analysis: Part 1—Physical and mineralogical methods*. ASA, Madison, WI, p. 383–411.
- Goldschmidt, V.M. 1954. *Geochemistry*. Oxford University Press, London.
- Gottel, N.R., H.F. Castro, M. Kerley, Z. Yang, D.A. Pelletier, M. Podar, T. Karpinets, E. Überbacher, G.A. Tuskan, R. Vilgalys, M.J. Doktycz, C.W. Schadt. 2011. Distinct microbial communities within the endosphere and rhizosphere of *Populus deltoides* roots across contrasting soil types. *Appl. Environ. Microbiol.* 77:5934–5944.
- Griffin, S., and Y. Lowney. 2012. Validation of an in vitro bioaccessibility test method for estimation of bioavailability of arsenic from soil and sediment. Final Report ESTCP Project ER-200916. Alexandria, VA.

- Guyton, A.C. 1981. Textbook of medical physiology. W.B. Saunders, New York.
- Han, Y., H.J. Joosten, W.L. Niu et al. 2007. Oxaloacetate hydrolase, the C-C bond lyase of oxalate secreting fungi. *J. Biol. Chem.* 282:9581–9590.
- Hendershort, W.H., and Duquette, M. 1986. A simple barium chloride method for determining cation exchange capacity and exchangeable cations. *Soil Sci. Soc. Am. J.* 50:605–608.
- Heanes, D.L. 1984. Determination of total organic-C in soils by an improved chromic acid digestion and spectrophotometric procedure. *Commun. Soil Sci. Plant Analysis* 15:1191–1213.
- Henry, H., M.F. Naujokas , C.Attanayake , N.T. Basta , Z.Cheng, G.M. Hettiarachchi , M. Maddaloni , C. Schadt , and K.G. Scheckel. 2015. Bioavailability-based in situ remediation to meet future lead (Pb) standards in urban soils and gardens. *Environ. Sci. Technol.* 49 (15), p. 8948–8958.
- Hettiarachchi, G.M., and G.M. Pierzynski. 2004. Soil lead bioavailability and in situ remediation of lead-contaminated soils: A review. *Environ. Prog.* 23(1):78–93.
- Horter, D., and J.B. Dressman. 2001. Influence of physiochemical properties on dissolution of drugs in the gastrointestinal tract. *Adv. Drug Delivery Rev.* 46:75–87.
- Hudson-Edwards, K.A., H.E.Jamieson, J.M. Charnock, and M.G. Macklin. 2005. Arsenic speciation in waters and sediment of ephemeral floodplain pools, Ríos Agrio–Guadiamar, Aznalcóllar, Spain. *Chem. Geol.* 219(1-4):175–192.
- Juhasz, A.L., E. Smith, J. Weber, R. Naidu, M. Rees, A. Rofe, T. Kuchel, and L. Sansom. 2008. Effect of soil ageing on in vivo arsenic bioavailability in two dissimilar soils. *Chemosphere* 71:2180–2186.
- Juhasz AL, E. Smith, J. Weber, M. Rees, A. Rofe, T. Kuchel, L. Sansom, R. Naidu. 2007. Comparison of in vivo and in vitro methodologies for the assessment of arsenic bioavailability in contaminated soils. *Chemosphere* 69:961–966.
- Juhasz, A.L., J. Weber, E. Smith, R. Naidu, M. Rees, A. Rofe, T. Kuchel, L. Sansom. 2009. Assessment of four commonly employed in vitro arsenic bioaccessibility assays for predicting in vivo relative arsenic bioavailability in contaminated soils. *Environ. Sci. Technol.* 43:9487–9494.
- Juhasz,A.L., N.T. Basta, and E. Smith. 2013. What is required for the validation of in vitro assays for predicting contaminant relative bioavailability? Considerations and criteria. *Environmental Pollution* 180:372-375.
- Juhasz, A.L., E. Smith, C. Nelson, D.J. Thomas, and K. Bradham. 2014b. Variability associated with As in vivo–in vitro correlations when using different bioaccessibility methodologies. *Environ. Sci. Technol.* 48:11646–11653.
- Kilmer, V.J., and L.T. Alexander. 1949. Methods of making mechanical analyses of soils. *Soil Sci.* 68:15–24.
- Lovley, D.R. 1987. Organic matter mineralization with the reduction of ferric iron: A review. *Geomicrobiol. J.* 5(3-4):375–399.

- Magigelada, J.R., G.G. Lonstreh, W.H.J. Summerskill, V.L.W. Go. 1976. Measurement of gastric functions during digestion of ordinary solid meals in man. *Gastroenterology* 70:203–210.
- Manning, B. 2005. Arsenic speciation in As(III)- and As(V)-treated soil using XANES spectroscopy. *Microchim. Acta* 151(3-4):181–188.
- Manning, B.A., S.E. Fendorf, B. Bostick, and D.L. Suarez. 2002. Arsenic(III) oxidation and arsenic(V) adsorption reactions on synthetic birnessite. *Environ. Sci. Technol.* 36(5):976–981.
- McClure, R.D. 2001. A statistical model to evaluate analyte homogeneity for a material. *J. AOAC Int.* 84:947–954
- McConnell, E.L., A.W. Basit, and S. Murdan. 2008. Measurements of rat and mouse gastrointestinal pH, fluid and lymphoid tissue, and implications for in – vivo experiments. *J. Pharm. Pharmacol.* 60:63–70.
- McKeague, J.A., and J.H. Day. 1966. Dithionite- and oxalate-extractable Fe and Al as aids in differentiating various classes of soils. *Can. J. Soil Sci.* 46:13–23.
- Meunier, L., J. Wragg, I. Koch, K.J. Reimer. 2010a. Method variables affecting the bioaccessibility of arsenic in soil. *J. Environ. Sci. Health, Part A: Toxic/Hazard. Subst. Environ. Eng.* 45:517–526.
- Meunier, L., S.R. Walker, J. Wragg, M.B. Parsons, I. Koch, H.E. Jamieson, and K.J. Reimer. 2010b. Effects of soil composition and mineralogy on the bioaccessibility of arsenic from tailings and soil in gold mine districts of Nova Scotia. *Environ. Sci. Technol.* 44(7):2667–2674.
- Moseley, R., M. Barnett, M. Stewart, T. Mehlhorn, P. Jardine, M. Ginder-Vogel, S. Fendorf. 2008. Decreasing lead bioaccessibility in industrial and firing range soils with phosphate-based amendments. *J. Environ. Qual.* 37:2116–2124.
- Norrish, K., and Hutton. 1969. An accurate x-ray spectrographic method for the analysis of a wide range of geological samples. *Geochim. Cosmochim. Acta* 33:431–453.
- Obrycki, J.F., N.T. Basta, K. Scheckel, A. Juhasz, B.N. Stevens, and K.K. Minca. 2016. Phosphorus amendment efficacy on soil Pb depends upon bioaccessible method conditions. Special Issue: Soil in the City *J. Environ. Qual.* 45(1):37-44.
- O'Connor, H.J., C.J. Schorah, N. Habibzedah, A.T.R. Axon. 1989. Vitamin C in the human stomach: Relation to gastric pH, gastroduodenal disease, and possible sources. *Gut* 30:436–442.
- Pierzynski, G.M., J.T. Sims, G.F. Vance. 1994. Soils and environmental quality. Lewis Publishers, Boca Raton, FL, 108 p.
- Prescher, C., C. Mccammon, and L. Dubrovinsky. 2012. MossA: A program for analyzing energy-domain Mössbauer spectra from conventional and synchrotron sources. *J. Appl. Crystallogr.* 45(2):329–331.

- Prietzl, J., J. Thieme, K. Eusterhues, and D. Eichert. 2007. Iron speciation in soils and soil aggregates by synchrotron-based X-ray microspectroscopy (XANES). *Eur. J. Soil Sci.* 58(5):1027–1041.
- Ravel, B., and M. Newville. 2005. ATHENA , ARTEMIS , HEPHAESTUS: Data analysis for X-ray absorption spectroscopy using IFEFFIT. *J. Synchrotron Rad.* 12(4):537–541.
- Rhodes, J.D. 1996. Salinity: Electrical conductivity and total dissolved solids. In: D.L. Sparks, editor, *Methods of Soil Analysis*. Part 3 - Chemical Methods. SSSA Book Series 5. Soil Science Society of America, Madison, WI, p. 417–435.
- Roberts, S.M., W.R. Weimar, J.R.T. Vinson, J.W. Munson, R.J. Bergeron. 2002. Measurement of arsenic bioavailability in soil using a primate model. *Toxicol. Sci.* 67:303–310.
- Roberts, S.M., J.W. Munson, Y.W. Lowney, M.V. Ruby. 2007. Relative oral bioavailability of arsenic from contaminated soils measured in the Cynomolgus monkey. *Toxicol. Sci.* 95:281–288.
- Rodriguez, R.R., N.T. Basta, S.W. Casteel, and L.W. Pace. 1999. An in vitro gastrointestinal method to estimate bioavailable arsenic in contaminated soils and solid media. *Environ. Sci. Technol.* 33:642–649.
- Rodriguez, R.R., N.T. Basta, S.W. Casteel, F.P. Armstrong, and D.C. Ward. 2003. Chemical extraction methods to assess bioavailable As in contaminated soil and solid media. *J. Environ. Qual.* 32:876–884.
- Ruby, M.V., A. Davis, R. Schoof, S. Eberle, C.M. Sellstone. 1996. Estimation of lead and arsenic bioavailability using a physiologically based extraction test. *Environ. Sci. Technol.* 30:422–430.
- Ruby, M.V., R. Schoof, W. Brattin, M. Goldade, G. Post, M. Harnois, D.E. Mosby, S.W. Casteel, W. Berti, and M. Carpenter. 1999. Advances in evaluating the oral bioavailability of inorganics in soil for use in human health risk assessment. *Environ. Sci. Technol.* 33:3697–3705.
- R Development Core Team. 2008. R: A language and environment for statistical computing. R Foundation for Statistical Computing, Vienna, Austria. ISBN 3-900051-070, URL <http://www.R-project.org>.
- Ruijter, G.J.G., P.J.I. van de Vondervoort, and J. Visser. 1999. Oxalic acid production by *Aspergillus niger*: An oxalate-non-producing mutant produces citric acid at pH5 in the presence of manganese. *Microbiology* 145:2569–2576.
- Ryan, J.A., K.G. Scheckel, W.R. Berti, S.L. Brown, S.W. Casteel, R.L. Chaney, J. Hallfrisch, M. Doolan, P. Grevatt, M. Maddaloni, and D. Mosby. 2004. Reducing children's risk from lead in soil. *Environ. Sci. Technol.* 38:19A–24A.
- Sayer, J.A., S.L. Raggett, and G.M. Gadd. 1995. Solubilization of insoluble compounds by soil fungi: Development of a screening method for solubilizing ability and metal tolerance. *Mycol. Res.* 99:987–993.
- Sayer, J.A., J.D. Cotter-Howells, C. Watson, S. Hillier, and G.M. Gadd. 1999. Lead mineral transformation by fungi. *Curr. Biol.* 9:691–694.

- Scheckel, K.G., and J.A. Ryan. 2004. Spectroscopic speciation and quantification of lead in phosphate-amended soils. *J. Environ. Qual.* 33:1288–1295.
- Scheckel, K.G., R.L. Chaney, N.T. Basta, and J.A. Ryan. 2009. Advances in assessing bioavailability of metal(loid)s in contaminated soils. *Adv. Agron.* 107:10–52.
- Scheckel, K.G., G.L. Diamond, M.F. Burgess, J.M. Klotzbach, M. Maddaloni, B.W. Miller, C.R. Partridge, and S.M. Serda. 2013. Amending soils with phosphate as means to mitigate soil lead hazard: A critical review of the state of the science. *J. Toxicol. Environ. Health Part B* 16(6):337–380.
- Schwartz, R., A.Z. Belko, and E.M. Wien. 1982. An in vitro system for measuring intrinsic dietary mineral exchangeability; alternative to intrinsic isotopic labeling. *J. Nutr.* 112:497–504.
- Schwertmann, U., and R. Taylor. 1989. Iron oxides. In: J.B. Dixon, S.B. Weed, editors, *Minerals in soil environments*. 2nd ed. SSSA, Madison, WI. p. 379–438.
- Smith, D.B., W.F. Cannon, L.G. Woodruff, F. Solano, J.E. Kilburn, and D.L. Fey. 2013. Geochemical and mineralogical data for soils of the conterminous United States. U.S. Geological Survey Data Series 801, 19 p., <http://pubs.usgs.gov/ds/801/>.
- Strasser, H., W. Burgstaller, and F. Schinner. 1994. High-yield production of oxalic acid for metal leaching processes by *Aspergillus niger*. *FEMS Microbiol. Lett.* 119:365–370.
- Strategic Environmental Research and Development Program (SERDP). 2008. Workshop Report. SERDP and ESTCP Expert Panel Workshop on Research and Development Needs. City, ST.
- Stucki, J.W., B.A. Goodman, and U. Schwertmann. 1988. Iron in soils and clay minerals. D. Reidel, Dordrecht, The Netherlands.
- Sullivan, T.S., N.R. Gottel, N. Basta, P.M. Jardine, and C.W. Schadt. 2012. Firing range soils yield a diverse array of fungal isolates capable of organic acid production and Pb mineral solubilization. *Appl. Environ. Microbiol.* 78(17):6978–6086.
- Thomas, G.W. 1996. Soil pH and soil acidity. In: D.L. Sparks, editor, *Methods of Soil Analysis*. Part 3 - Chemical Methods. SSSA Book Series 5. Soil Science Society of America, Madison, WI, p. 475–490.
- U.S. Environmental Protection Agency (U.S. EPA). 1989. Risk assessment guidance for superfund (RAGS), Vol. I, Human Health Evaluation Manual (Part A). Office of Emergency and Remedial Response, Washington, DC. EPA/540/1-89/002.
- U.S. Environmental Protection Agency (U.S. EPA). 1996. Bioavailability of arsenic and lead in environmental substrates. EPA, Region 10, Seattle, WA. EPA910/R-96-002.
- U.S. Environmental Protection Agency (U.S. EPA). 2007a. Guidance for evaluating the oral bioavailability of metals in soils for use in human health risk assessment. 9285.7-80, U.S. EPA OSWER, Washington, DC.
- U.S. Environmental Protection Agency (U.S. EPA). 2007b. Method 3051a. Microwave assisted acid digestion of sediments, sludges, soils, and oils. SW-846, U.S. EPA, Washington, DC.

- U.S. Environmental Protection Agency (U.S. EPA). 2007c. Method 1312. Synthetic precipitation leaching procedure. SW-846, U.S. EPA, Washington, DC.
- U.S. Environmental Protection Agency (U.S. EPA). 2012a. Recommendations for default value for relative bioavailability of arsenic in soil. 9200.1–113, U.S. EPA OSWER, Washington, DC.
- U.S. Environmental Protection Agency (U.S. EPA). 2012b. Method 1313. Liquid–solid partitioning as a function of extract pH using a parallel batch extraction procedure. U.S. EPA, Washington, DC.
- U.S. Environmental Protection Agency (U.S. EPA). 2013. Method 1340. In vitro bioaccessibility assay for lead in soil. SW-846, U.S. EPA, Washington, DC.
- Venteris, E.R., N.T. Basta, J.M. Bigham, and R. Rea. 2014. Modeling spatial patterns in soil As to estimate natural baseline concentration. *J. Environ. Qual.* 43:936–946.
- Weis, C.P., and J.M. LaVelle. 1991. Characteristics to consider when choosing an animal model for the study of lead bioavailability. *Chem. Speciation Bioavailability* 3:113–119.
- Wenzel, W.W., N. Kirchbaumer, T. Prohaska, G. Stigeder, E. Lombi, D.C. Adriano. 2001. Arsenic fractionation in soils using an improved sequential extraction procedure. *Anal. Chim. Acta* 436:309–323.
- Whitacre, S.D., N.T. Basta, and E.A. Dayton. 2013. Soil controls on bioaccessible arsenic fractions. *J. Environ. Health Sci. Part A*. 48(6):620–628.
- Wragg, J., M. Cave, N. Basta, E. Brandon, S. Casteel, S. Denys, C. Gron, A. Oomen, K. Reimer, K. Tack, T. Van de Wiele. 2011. An inter-laboratory trial of the unified BARGE bioaccessibility method for arsenic, cadmium and lead in soil. *Sci. Total Environ.* 409:4016–4030.
- Zia, M.H., E.E. Codling, K.G. Scheckel, and R.L. Chaney. 2011. In vitro and in vivo approaches for the measurement of oral bioavailability of lead (Pb) in contaminated soils: A review. *Environ. Pollut.* 159(10):2320–2327.

Appendix A

Supporting Data

Appendix A.1 Tables and Figures Cited in Results and Discussion

Table A1. Elemental analysis determined via XRF

ID	K	Ca	Ti	Cr	Mn	Fe	Ni	Cu	Zn	As	Cd	Ba	Pb
mg/kg													
1	2134	19051	15681	253	1340	156046	229	335	1023	325	< LOD	729	1394
2	338	17871	16252	637	1434	120400	227	110	183	708	< LOD	601	93
3	7352	7132	3500	95	829	44256	99	54	86	229	< LOD	389	24
6	10439	3218	1966	40	299	24540	22	14	134	681	< LOD	216	34
7	8294	5299	3326	58	1582	37133	33	129	404	390	< LOD	356	2303
8	4352	12368	3151	104	540	34767	60	466	314	195	< LOD	290	350
9	9102	40435	1885	31	374	15078	< LOD	18	68	441	< LOD	281	26
10	3532	18376	3360	< LOD	377	175244	< LOD	102	3382	3911	10	199	2265
11	4669	18084	618	< LOD	< LOD	89477	< LOD	981	406	223	< LOD	< LOD	348
12	9216	55009	1707	37	712	161719	107	2377	2403	1381	92	627	5306
13	5720	< LOD	1028	< LOD	418	472678	< LOD	297	1533	11514	23	560	9964
14	9063	129321	1360	22	152	9974	< LOD	< LOD	25	226	< LOD	185	12
15	6191	44799	1828	36	333	14793	20	13	49	235	< LOD	233	17
16	9835	4186	2452	43	317	22909	23	18	61	253	< LOD	303	26
17	10890	3956	2245	31	1703	49249	< LOD	3602	4490	1665	13	387	5800
18	5091	912	5972	53	230	34578	< LOD	109	92	378	< LOD	340	1478
19	6551	7807	5876	93	851	59466	29	157	197	443	< LOD	629	1521
20	5508	3442	7021	85	1261	61081	42	238	205	514	< LOD	540	1600
21	5103	8588	5939	80	1499	57215	36	120	280	530	< LOD	538	2031
29	5215	87782	3055	83	366	26051	61	68	1429	5241	19	243	294
30	8011	29709	2383	1305	451	23004	87	31	278	4031	4	305	103
33	4950	3554	7144	50	547	100948	26	83	49	329	< LOD	588	46
34	13053	< LOD	4933	50	809	174610	< LOD	172	84	2451	< LOD	500	146
35	8966	909	3156	63	1208	76127	52	201	525	604	16	443	2075
36	21495	17973	4782	23	1050	71668	< LOD	103	80	6392	< LOD	521	33
37	4324	< LOD	8273	81	426	83083	25	75	42	349	< LOD	500	20
38	14572	3390	5792	33	1946	135342	< LOD	199	178	10723	< LOD	516	290
LOD		100		10	100		10	10			1	100	
Mean	7554	22632	4618	141	809.8	86349	69.39	387.4	667	2013	25.38	423.9	1393

LOD Limit of Detection

TABLE A2. ARSENIC LCF RESULTS SOILS 1-10

ID	1	2	3	6	7	8	9	10
%								
ORPIMENT (AS ₂ S ₃)	0	0	0	0	0	0	0	0
ARSENITE COPPT WITH PYRITE	0	0	0	0	0	0	0	0
ARSENOPYRITE (FEASS)	0	0	0	4	0	0	0	7
ARSENOLITE (AS ₂ O ₃)	0	0	0	0	0	0	0	4
AS 3 ADS PYRITE	0	0	0	0	0	0	0	0
AS 3 ADS FERRIHYDRITE	0	0	0	0	0	0	0	0
AS 3 SIDERITE (FECO ₃)	85	0	0	0	0	28	0	0
AS 3 MONT	0	0	0	0	0	23	0	0
YUKONITE (CAFeASO ₄ OH)	0	0	0	0	0	0	0	0
ARSENIOSIDERITE (CAFe(ASO ₄)O ₂)	0	0	0	0	0	0	41	0
PHARMACOSIDERITE (KFeASO ₄ OH)	0	0	0	0	0	0	59	0
SCORODITE (FeASO ₄)	0	0	0	0	0	0	0	57
PB-ARSENATE PESTICIDE (PBHASO ₄)	0	25	0	0	16	0	0	0
DMA	0	0	0	0	0	0	0	0
AS 5 ADS GOE 25	0	0	77	96	71	0	0	0
AS5 ADS HEMATITE	0	0	0	0	0	0	0	0
AS 5 ADS BIRNESSITE	15	0	23	0	0	0	0	0
AS 5 ADS FH	0	19	0	0	13	49	0	33
AS 5 ADS KAO	0	0	0	0	0	0	0	0
AS 5 ADS GIBBS	0	56	0	0	0	0	0	0
TOTAL	100	100	100	100	100	100	100	100
NO. OF COMPONENTS	2	3	2	2	3	3	2	4
REDUCED χ^2	0.001366	0.0044	0.000783	0.000387	0.000563	0.000712	0.00043	0.000263

TABLE A3. ARSENIC LCF RESULTS SOILS 11-30

ID	11	12	13	14	15	16	17	18	19	20	21	29	30
	% -----												
ORPIMENT (AS ₂ S ₃)	9	0	0	0	0	0	0	0	0	0	0	0	0
ARSENITE COPPT WITH PYRITE	0	0	0	0	0	0	0	0	0	0	0	0	0
ARSENOPYRITE (FEASS)	0	0	0	0	0	0	0	0	0	0	0	0	0
ARSENOLITE (AS ₂ O ₃)	0	0	0	0	0	0	0	0	0	0	0	0	0
AS 3 ADS PYRITE	0	0	23	0	0	0	0	0	0	0	0	0	0
AS 3 ADS FERRIHYDRITE	0	12	0	0	0	0	5	0	0	0	0	0	0
AS 3 SIDERITE (FECO ₃)	0	0	0	0	0	0	0	0	0	0	0	0	0
AS 3 MONT	0	0	0	0	0	0	0	0	0	0	0	0	0
YUKONITE (CAFeASO ₄ OH)	0	0	0	73	75	4	0	0	0	0	0	75	100
ARSENIOSIDERITE (CAFe(ASO ₄)O ₂)	0	0	0	0	0	0	0	0	0	0	0	25	0
PHARMACOSIDERITE (KFeASO ₄ OH)	0	48	0	0	0	0	0	0	0	0	0	0	0
SCORODITE (FEASO ₄)	73	0	0	0	0	0	80	0	0	0	0	0	0
PB-ARSENATE PESTICIDE (PBHASO ₄)	0	0	0	0	0	0	0	25	23	15	23	0	0
DMA	0	0	0	0	0	0	0	0	0	0	0	0	0
AS 5 ADS GOE 25	0	40	77	0	0	0	0	0	0	0	0	0	0
AS5 ADS HEMATITE	0	0	0	0	0	0	0	0	0	0	0	0	0
AS 5 ADS BIRNESSITE	0	0	0	0	0	0	14	0	0	0	0	0	0
AS 5 ADS FH	19	0	0	27	25	26	0	9	7	0	6	0	0
AS 5 ADS KAO	0	0	0	0	0	0	0	0	0	0	0	0	0
AS 5 ADS GIBBS	0	0	0	0	0	0	0	66	71	86	71	0	0
TOTAL	100	100	100	100	100	100	100	100	100	100	100	100	100
NO. OF COMPONENTS	3	3	2	2	2	2	3	3	3	2	3	2	1
REDUCED χ^2	0.0004	0.0001	0.0004	0.0003	0.0002	0.0003	0.0002	0.0001	0.0002	0.0003	0.0002	0.0006	0.0002

TABLE A4. ARSENIC LCF RESULTS SOILS 33-38

ID	33	34	35	36	37	38
ORPIMENT (AS ₂ S ₃)	8	0	0	0	0	0
ARSENITE COPPT WITH PYRITE	0	0	0	0	3	0
ARSENOPYRITE (FEASS)	0	0	0	73	0	22
ARSENOLITE (AS ₂ O ₃)	0	0	0	0	0	0
AS 3 ADS PYRITE	0	0	0	0	0	0
AS 3 ADS FERRIHYDRITE	0	0	0	0	0	0
AS 3 SIDERITE (FECO ₃)	0	0	0	0	0	0
AS 3 MONT	0	0	4	0	0	0
YUKONITE (CAFeASO ₄ OH)	30	0	0	0	0	0
ARSENOSIDERITE (CAFe(ASO ₄)O ₂)	0	0	0	0	0	0
PHARMACOSIDERITE (KFeASO ₄ OH)	0	0	0	23	0	35
SCORODITE (FEASO ₄)	0	0	0	0	0	0
PB-ARSENATE PESTICIDE (PBHASO ₄)	0	0	0	0	0	0
DMA	0	0	20	0	0	0
AS 5 ADS GOE 25	63	67	63	0	75	24
AS5 ADS HEMATITE	0	17	0	0	0	0
AS 5 ADS BIRNESSITE	0	16	0	0	0	20
AS 5 ADS FH	0	0	13	4	0	0
AS 5 ADS KAO	0	0	0	0	0	0
AS 5 ADS GIBBS	0	0	0	0	21	0
TOTAL	100	100	100	100	100	100
NO. OF COMPONENTS	3	3	4	3	3	4
REDUCED χ^2	0.000115	0.000231	0.000282	7.16E-05	0.000407	2.66E-05

TABLE A5. IRON LINEAR COMBINATION FITTING OF FE K-EDGE XAS SPECTRA FOR SOILS 1-10

ID	1	2	3	6	7	8	9	10
%								
HEMATITE	25	0	13	0	0	0	26	0
FERRIHYDRITE	14	49	0	0	0	0	18	34
GOETHITE	0	7	0	0	40	14	0	0
AKAGANEITE	0	0	0	0	0	0	0	0
LEPIDOCROCITE	0	0	36	39	31	0	0	0
FE SUBED MONTMORILLONITE	20	0	38	0	0	0	10	0
MAGHEMITE	0	0	0	0	0	0	0	0
MAGNETITE	0	0	0	0	0	0	0	0
VIVIANITE	0	11	0	0	0	0	0	0
MARCASITE	0	0	0	0	0	0	0	0
LOELLINGITE	0	0	0	25	0	20	0	0
FAYALITE	0	26	0	0	0	18	0	26
BIOTITE	0	0	0	0	14	7	0	0
PYRITE	0	0	0	0	0	0	0	23
ARSENOPYRITE	0	0	0	0	0	0	0	0
SCORODITE	0	0	0	0	0	0	0	17
PHARMACOSIDERITE	41	0	0	0	0	41	46	0
YUKONITE	0	0	0	0	0	0	0	0
FE(II) ACETATE	0	0	0	36	14	0	0	0
FE(II) CHLORIDE	0	0	8	0	0	0	0	0
FE(II) OXALATE	0	7	0	0	0	0	0	0
FE(II) SULFATE	0	0	6	0	0	0	0	0
FE(III) CITRATE	0	0	0	0	0	0	0	0
FE(III) PHYTATE	0	0	0	0	0	0	0	0
FE(III)PHOSPHATE	0	0	0	0	0	0	0	0
TOTAL	100	100	100	100	100	100	100	100
REDUCED χ^2	0.0000075	0.0000140	0.0000107	0.0000239	0.0000889	0.0000176	0.0000051	0.0000351

TABLE A6. IRON LINEAR COMBINATION FITTING OF FE K-EDGE XAS SPECTRA FOR SOILS 11-20

ID	11	12	13	14	15	16	17	18	19	20
	% ——————									
HEMATITE	0	0	16	19	10	17	18	33	0	44
FERRIHYDRITE	0	0	0	0	0	0	0	0	18	21
GOETHITE	0	0	0	0	0	0	23	0	0	0
AKAGANEITE	0	0	0	0	0	0	0	0	0	0
LEPIDOCROCITE	0	0	0	15	0	0	0	60	28	0
FE SUBED	0	0	0	67	70	65	0	0	45	26
MONTMORILLONITE										
MAGHEMITE	0	0	34	0	0	0	0	0	0	0
MAGNETITE	0	15	0	0	0	0	0	0	0	0
VIVIANITE	0	0	0	0	0	0	19	0	0	0
MARCASITE	0	17	0	0	0	0	0	0	0	0
LOELLINGITE	0	0	0	0	0	0	0	0	0	0
FAYALITE	0	32	0	0	0	0	0	0	0	0
BIOTITE	0	0	0	0	0	0	0	0	0	9
PYRITE	0	0	0	0	0	0	0	0	0	0
ARSENOPYRITE	0	19	0	0	0	0	0	0	0	0
SCORODITE	36	0	0	0	0	0	0	0	0	0
PHARMACOSIDERITE	0	0	0	0	20	18	40	0	0	0
YUKONITE	0	0	50	0	0	0	0	0	0	0
FE(II) ACETATE	0	17	0	0	0	0	0	0	0	0
FE(II) CHLORIDE	0	0	0	0	0	0	0	0	0	0
FE(II) OXALATE	0	0	0	0	0	0	0	0	0	0
FE(II) SULFATE	0	0	0	0	0	0	0	7	10	0
FE(III) CITRATE	40	0	0	0	0	0	0	0	0	0
FE(III) PHYTATE	0	0	0	0	0	0	0	0	0	0
FE(III) PHOSPHATE	24	0	0	0	0	0	0	0	0	0
TOTAL	100	100	100	100	100	100	100	100	100	100
REDUCED χ^2	0.00006	0.00002	0.00007	0.00001	0.00001	0.000007	0.000004	0.000007	0.00007	0.00001

TABLE A7. IRON LINEAR COMBINATION FITTING OF FE K-EDGE XAS SPECTRA FOR SOILS 21-38

ID	21	29	30	33	34	35	36	37	38
%									
HEMATITE	21	17	22	28	0	0	15	26	44
FERRIHYDRITE	28	54	14	19	38	21	0	45	9
GOETHITE	0	0	0	41	0	0	0	15	35
AKAGANEITE	19	0	0	0	0	0	0	0	0
LEPIDOCROCITE	0	0	0	0	0	40	0	0	0
FE SUBED	32	0	15	0	0	0	0	0	0
MONTMORILLONITE									
MAGHEMITE	0	0	0	0	0	0	0	0	0
MAGNETITE	0	0	0	0	0	0	0	0	0
VIVIANITE	0	0	0	0	0	0	0	0	0
MARCASITE	0	0	0	0	0	0	0	0	0
LOELLINGITE	0	0	0	0	0	0	39	0	0
FAYALITE	0	0	0	12	17	22	0	0	0
BIOTITE	0	0	0	0	0	0	0	0	0
PYRITE	0	0	0	0	0	0	0	0	0
ARSENOPYRITE	0	0	0	0	0	0	0	0	0
SCORODITE	0	0	0	0	0	0	0	0	0
PHARMACOSIDERITE	0	28	49	0	0	0	27	0	12
YUKONITE	0	0	0	0	0	0	0	0	0
FE(II) ACETATE	0	0	0	0	15	0	19	14	0
FE(II) CHLORIDE	0	0	0	0	0	0	0	0	0
FE(II) OXALATE	0	0	0	0	0	0	0	0	0
FE(II) SULFATE	0	0	0	0	0	0	0	0	0
FE(III) CITRATE	0	0	0	0	29	0	0	0	0
FE(III) PHYTATE	0	0	0	0	0	16	0	0	0
FE(III) PHOSPHATE	0	0	0	0	0	0	0	0	0
TOTAL	100	100	100	100	100	100	100	100	100
REDUCED χ^2	0.000010	0.0000093	0.0000065	0.0000049	0.0000144	0.0000106	0.0000206	0.0000095	0.0000030

Table A8. Best model fits and parameters for 298 K measurements for soils 1-14

ID	Model Component	CS	error	FWHM	error	Int	error	QS	error	BHF	error
1	1	0.3207	0.0243	0.8458	0.0954	24.2251	2.1263	-0.132	0.0482	49.6955	0.163
1	2	0.3453	0.0036	0.4702	0.0089	58.9401	1.8505	0.5884	0.0066	NaN	NaN
1	3	1.0383	0.0408	1.0245	0.0958	16.8347	1.2501	1.8781	0.0744	NaN	NaN
2	1	0.3884	0.0026	0.4405	0.0068	49.4366	2.1351	0.6489	0.0045	NaN	NaN
2	2	0.397	0.043	1.4341	0.1823	26.1877	3.028	-0.1607	0.0809	48.0103	0.279
2	3	0.8958	0.011	0.342	0.038	7.8421	0.9044	2.5267	0.0223	NaN	NaN
2	4	1.2179	0.0074	0.4035	0.0253	16.5336	1.0773	2.8486	0.0137	NaN	NaN
3	1	0.3647	0.0024	0.5617	0.0066	80.1053	3.5897	0.6453	0.0037	NaN	NaN
3	2	0.4452	0.1106	1.4584	0.5008	10.2389	3.9798	-0.1537	0.209	49.7142	0.7205
3	3	1.1244	0.0103	0.4048	0.0309	9.6559	0.7233	2.7261	0.0202	NaN	NaN
6	1	0.226	0.013	0.481	0.037	43.267	2.217	0.849	0.026		
6	2	1.166	0.015	0.655	0.052	56.733	2.217	2.269	0.031		
7	1	0.2982	0.003	0.5057	0.0092	61.6911	3.6092	0.7891	0.0055	NaN	NaN
7	2	0.3743	0.0775	1.5242	0.3414	20.0409	4.6226	-0.1672	0.1441	49.2995	0.5275
7	3	1.2923	0.0058	0.3563	0.0187	18.268	1.257	2.3502	0.0116	NaN	NaN
8	1	0.3462	0.0364	0.7237	0.1501	11.1372	2.1686	0	NaN	50.0258	0.2794
8	2	0.3934	0.0048	0.4692	0.0146	36.7863	1.5928	0.6349	0.0086	NaN	NaN
8	3	0.5838	1.3357	0.5461	0.0915	10.4166	1.5556	1.5308	2.6813	NaN	NaN
8	4	0.6677	0.0573	0.6628	0.2244	6.2962	2.0681	0	NaN	45.4661	0.4246
8	5	1.1113	0.387	0.5406	0.0209	35.3637	1.541	2.5835	0.775	NaN	NaN
9	1	0.3631	0.023	0.6127	0.0818	22.9347	2.2199	-0.1811	0.0458	51.0295	0.1557
9	2	0.3679	0.0071	0.6157	0.0206	62.9328	2.0643	0.6704	0.0113	NaN	NaN
9	3	1.1382	0.029	0.6137	0.0811	14.1324	1.3712	2.6263	0.0553	NaN	NaN
10	1	0.3478	0.0036	0.4496	0.0095	86.3667	0.9618	0.7479	0.0064	NaN	NaN
10	2	1.1672	0.0109	0.2873	0.0302	13.6333	0.9618	2.6532	0.0217	NaN	NaN
11	1	0.3851	0.0019	0.3789	0.0052	98.024	0.8264	1.0383	0.0037	NaN	NaN
11	2	1.3886	0.0334	0.194	0.1027	1.976	0.8264	2.3986	0.0668	NaN	NaN
12	1	0.29	0.044	0.714	0.153	7.105	3.083	0		50.9	0.316
12	2	0.45	0.012	0.623	0.022	25.064	1.989	0.894	0.035		
12	3	1.046	0.008	0.837	0.013	67.831	2.836	2.02	0.013		
13	1	0.2929	0.0119	0.5538	0.0604	24.3151	4.0176	-0.0503	0.0244	50.1595	0.1779
13	2	0.3457	0.0054	0.4132	0.0302	30.9601	3.3721	-0.18	0.011	52.1975	0.0698
13	3	0.3603	0.0032	0.4924	0.0089	35.5828	2.4769	1.0656	0.006	NaN	NaN
13	4	0.6537	0.0398	0.7032	0.1477	9.142	1.9192	-0.0481	0.0748	46.2292	0.2757
14	1	0.3625	0.0053	0.5746	0.0156	80.9679	2.3489	0.5804	0.008	NaN	NaN
14	2	0.3657	0.0259	0.4417	0.0855	14.3416	2.0661	-0.2681	0.0517	51.3837	0.1771
14	3	1.112	0.0641	0.5002	0.1956	4.6905	1.55	2.6721	0.1245	NaN	NaN

Table A9. Best model fits and parameters for 298 K measurements for soils 15 - 33

ID	Model Component	CS	error	FWHM	error	Int	error	QS	error	BHF	error
15	1	0.3687	0.0037	0.5726	0.0109	91.7158	0.8592	0.4923	0.0057	NaN	NaN
15	2	1.1556	0.0123	0.2993	0.0372	8.2842	0.8592	2.6705	0.0244	NaN	NaN
16	1	0.3611	0.025	0.5433	0.0863	14.3542	1.764	-0.1855	0.0499	50.9226	0.1709
16	2	0.3619	0.0038	0.5756	0.0114	81.1513	1.8771	0.5711	0.0057	NaN	NaN
16	3	1.1375	0.0396	0.4445	0.1196	4.4944	1.0151	2.6443	0.0772	NaN	NaN
17	1	0.3472	0.0349	0.6427	0.1233	9.4146	1.6211	-0.1708	0.0704	51.479	0.2458
17	2	0.3549	0.0029	0.4294	0.0128	47.2502	1.928	0.6343	0.0122	NaN	NaN
17	3	0.3559	0.0028	0.3292	0.0124	33.2813	1.8133	1.2212	0.0086	NaN	NaN
17	4	0.7692	0.0763	0.5636	0.2486	3.6385	1.4471	-0.1775	0.1536	45.8657	0.5141
17	5	1.1613	0.0242	0.436	0.0649	6.4154	0.6828	2.5812	0.0483	NaN	NaN
18	1	0.3702	0.0021	0.3986	0.0058	88.2255	2.7224	0.6079	0.0038	NaN	NaN
18	2	0.3711	0.0865	0.6356	0.3017	6.3725	2.6199	-0.1713	0.1725	50.3085	0.5715
18	3	0.6077	0.0165	0.2146	0.0529	3.9042	0.8379	1.6137	0.0334	NaN	NaN
18	4	0.8038	0.1103	0.4069	0.3422	1.4978	0.9581	3.2002	0.2282	NaN	NaN
19	1	0.3561	0.0032	0.3293	0.0345	33.8437	7.514	0.5781	0.0226	NaN	NaN
19	2	0.3726	0.0039	0.5518	0.0242	59.8381	7.3898	0.9992	0.0569	NaN	NaN
19	3	0.8544	0.019	0.2204	0.064	2.4781	0.7301	3.0558	0.0381	NaN	NaN
19	4	1.078	0.0163	0.194	0.0348	3.8402	0.8303	0.6029	0.0318	NaN	NaN
20	1	0.3584	0.003	0.4528	0.009	66.1074	3.7954	0.6687	0.0071	NaN	NaN
20	2	0.4244	0.0987	1.4641	0.4762	12.5269	4.4303	0	NaN	48.6657	0.6915
20	3	0.4703	0.0156	0.5243	0.0767	12.7819	2.2067	1.5596	0.0535	NaN	NaN
20	4	0.8906	0.017	0.2746	0.0548	3.6276	0.684	3.1807	0.0342	NaN	NaN
20	5	1.1645	0.0144	0.2429	0.035	4.9562	0.6847	0.5426	0.0257	NaN	NaN
21	1	0.3714	0.0035	0.487	0.0127	81.9281	2.5371	0.7224	0.0084	NaN	NaN
21	2	0.4745	0.0205	0.5389	0.0827	15.524	2.4988	1.5947	0.0557	NaN	NaN
21	3	0.8826	0.0282	0.2185	0.0874	2.5479	0.862	3.1295	0.0563	NaN	NaN
29	1	0.3424	0.0214	0.5081	0.0837	18.8291	5.7197	-0.1956	0.0391	50.465	0.3483
29	2	0.3672	0.0051	0.5482	0.0143	57.5386	5.2704	0.6892	0.0085	NaN	NaN
29	3	0.3866	0.0109	0.3005	0.0572	16.337	4.9689	-0.2051	0.0202	51.9409	0.1146
29	4	1.0193	0.0536	0.6869	0.1715	7.2953	1.577	2.4534	0.102	NaN	NaN
30	1	0.3552	0.0034	0.521	0.0095	77.9787	1.8121	0.6245	0.0053	NaN	NaN
30	2	0.386	0.0304	0.5466	0.1051	12.2915	1.867	-0.1955	0.0608	50.8984	0.2082
30	3	1.1304	0.0132	0.356	0.0397	9.7298	0.858	2.6208	0.026	NaN	NaN
33	1	0.2325	0.0864	0.5166	0.162	11.5131	5.7867	-0.4539	0.1807	49.1361	0.1691
33	2	0.3379	0.0028	0.4719	0.0083	61.7432	6.0196	0.6449	0.005	NaN	NaN
33	3	0.459	0.074	0.628	0.1204	20.9104	5.8976	-0.0955	0.1216	49.2432	0.1251
33	4	1.3362	0.0102	0.2429	0.0314	5.8333	0.8203	2.3096	0.0205	NaN	NaN

Table A10. Best model fits and parameters for 298 K measurements for soils 34 - 38

ID	Model Component	CS	error	FWHM	error	Int	error	QS	error	BHF	error
34	1	0.3322	0.0035	0.4914	0.0101	73.5061	5.7623	0.7547	0.0062	NaN	NaN
34	2	0.4245	0.125	1.48	0.5384	17.0136	6.4652	-0.2867	0.2335	49.1529	0.8476
34	3	1.3183	0.0076	0.2233	0.0234	9.4803	1.0622	2.3643	0.0153	NaN	NaN
35	1	0.3642	0.004	0.5048	0.011	72.1287	6.1915	0.7531	0.0068	NaN	NaN
35	2	0.3981	0.1516	1.5408	0.6493	15.794	7.1748	-0.1777	0.2801	48.7263	1.024
35	3	1.1254	0.009	0.2846	0.0275	12.0773	1.3587	2.7071	0.0178	NaN	NaN
36	1	0.3601	0.0332	0.7732	0.1568	14.4391	3.3925	0	NaN	46.3766	0.3876
36	2	0.3647	0.0026	0.4131	0.007	56.8379	2.9145	0.5777	0.0044	NaN	NaN
36	3	0.3777	0.0113	0.5652	0.0508	27.3886	2.5887	-0.205	0.0235	50.0784	0.106
36	4	1.1458	0.0332	0.194	0.0922	1.3344	0.4926	1.1437	0.0659	NaN	NaN
37	1	0.3624	0.0216	0.7406	0.1015	21.4257	3.4968	-0.2257	0.043	47.3766	0.292
37	2	0.3644	0.0021	0.4107	0.0056	58.4628	3.21	0.5738	0.0035	NaN	NaN
37	3	0.3646	0.0112	0.4493	0.0539	19.422	2.7911	-0.2007	0.0224	50.4464	0.1103
37	4	0.8681	0.0518	0.194	0.1558	0.6896	0.4275	3.19	0.1043	NaN	NaN
38	1	0.3656	0.0029	0.5118	0.0078	66.5881	2.8731	0.7438	0.0048	NaN	NaN
38	2	0.3976	0.0475	1.2341	0.2025	22.1303	3.313	-0.2136	0.0914	49.4298	0.3209
38	3	1.1332	0.0076	0.3265	0.0234	11.2816	0.7828	2.7512	0.015	NaN	NaN

Table A11. Best model fits and parameters for 4 K measurements of soil dataset

ID	Model Component	CS	error	FWHM	error	Int	error	QS	error	BHF	error
2	1	0.3548	0.0077	0.7502	0.0591	34.5636	4.5358	-0.1458	0.0155	47.092	0.1618
2	2	1.1322	0.0303	0.9729	0.071	15.7189	1.7038	2.8897	0.0456	NaN	NaN
2	3	0.6134	0.0358	0.9293	0.1979	6.9549	2.0224	0.8792	0.1276	NaN	NaN
2	4	0.3548	0.0146	1.3062	0.0725	32.5464	4.4168	-0.1315	0.0264	42.748	0.3158
2	5	0.3522	0.0169	0.6214	0.0735	10.2162	2.3955	-0.0902	0.0334	50.5171	0.1565
3	1	0.3519	0.022	0.7579	0.0973	32.3515	3.9305	0	NaN	47.978	0.2548
3	2	0.4679	0.0479	0.3803	0.2062	5.3287	3.4439	0	NaN	50.8899	0.3946
3	3	1.1334	0.029	0.4495	0.084	7.4823	1.252	2.8175	0.0563	NaN	NaN
3	4	0.3582	0.0094	0.7147	0.029	54.8375	3.7097	0.6511	0.0144	NaN	NaN
7	1	0.3288	0.0167	0.5024	0.0965	29.349	6.5786	-0.1623	0.0333	42.7079	0.1676
7	2	0.3452	0.0352	0.537	0.1568	14.8938	5.3755	-0.0758	0.0698	45.7071	0.3672
7	3	0.4057	0.072	0.9287	0.2767	17.4828	6.6229	-0.0341	0.1383	39.3179	0.8114
7	4	1.0501	0.0142	0.3373	0.0428	12.2006	1.9441	2.4464	0.0286	NaN	NaN
7	5	0.2597	0.0409	1.0547	0.1288	26.0737	3.6709	0.9436	0.0748	NaN	NaN
10	1	0.3813	0.0102	1.157	0.0369	50.2862	2.3916	-0.2091	0.0196	46.1798	0.0699
10	2	0.2742	0.0136	1.1981	0.1008	38.9383	2.1509	0.6308	0.0357	NaN	NaN
10	3	0.9729	0.0662	1.1219	0.1944	10.7755	2.2867	2.6915	0.0965	NaN	NaN
14	1	0.367	0.0165	1.2617	0.0952	64.7548	6.0811	0.5041	0.0863	NaN	NaN
14	2	0.3286	0.0645	1.3518	0.302	35.2452	6.0811	0	NaN	50.4501	0.4581
16	1	0.3357	0.0049	0.8585	0.019	70.4592	4.5544	0.5462	0.0115	NaN	NaN
16	2	0.3981	0.0277	0.5544	0.1484	9.9967	3.6747	0	NaN	52.1833	0.3207
16	3	0.3655	0.027	0.8466	0.137	19.5441	4.1283	0	NaN	48.7744	0.4171
17	1	0.3273	0.0317	1.519	0.1628	35.4646	7.0779	0.7286	0.1217	NaN	NaN
17	2	0.3973	0.0343	0.9026	0.2268	26.7576	10.8877	0	NaN	49.243	0.6383
17	3	0.3649	0.0288	1.0058	0.158	37.7779	10.1236	0	NaN	45.5249	0.5847
20	1	0.3596	0.0192	0.5628	0.1445	18.3651	6.3672	0	NaN	47.6454	0.251
20	2	0.3803	0.0206	0.6084	0.109	19.0691	4.8076	0	NaN	50.7529	0.2752
20	3	0.4267	0.0496	0.7786	0.2395	11.73	5.0245	0	NaN	44.0765	0.6432
20	4	0.3433	0.0127	0.7731	0.0453	34.9307	4.4965	0.9816	0.0199	NaN	NaN
20	5	1.7332	0.5475	4.8573	1.1853	15.905	5.0177	4.61E-06	8.05E+04	NaN	NaN
21	1	0.3351	0.0205	0.5857	0.1394	20.2474	6.0181	-0.1551	0.0411	42.2119	0.2298
21	2	0.3198	0.0199	0.4944	0.092	15.9833	3.876	-0.1469	0.0391	45.3453	0.2061
21	3	0.3519	0.0902	1.5288	0.342	21.9192	6.3752	-0.2002	0.1563	37.3042	1.2875
21	4	0.3512	0.0096	0.7618	0.0265	41.85	4.8001	0.8838	0.016	NaN	NaN
34	1	0.3802	0.0066	0.7419	0.0303	67.9479	3.2624	-0.1925	0.0138	48.3187	0.0714
34	2	1.2469	0.0476	0.6588	0.1159	7.3847	1.1322	2.6837	0.0902	NaN	NaN
34	3	0.4786	0.0313	0.3557	0.1121	2.9856	0.9716	2.47	0.0587	NaN	NaN
34	4	0.201	0.053	0.7981	0.1885	7.9417	1.2144	0.9536	0.1113	NaN	NaN
34	5	0.3767	0.0315	0.7577	0.1484	13.7401	3.4718	0	NaN	44.5697	0.3769
35	1	0.5818	0.0615	0.5354	0.1383	11.5633	4.4241	0.181	0.1371	48.0882	0.1892
35	2	0.3167	0.0259	0.7174	0.0533	51.9895	4.5601	-0.2192	0.0408	48.0131	0.0778

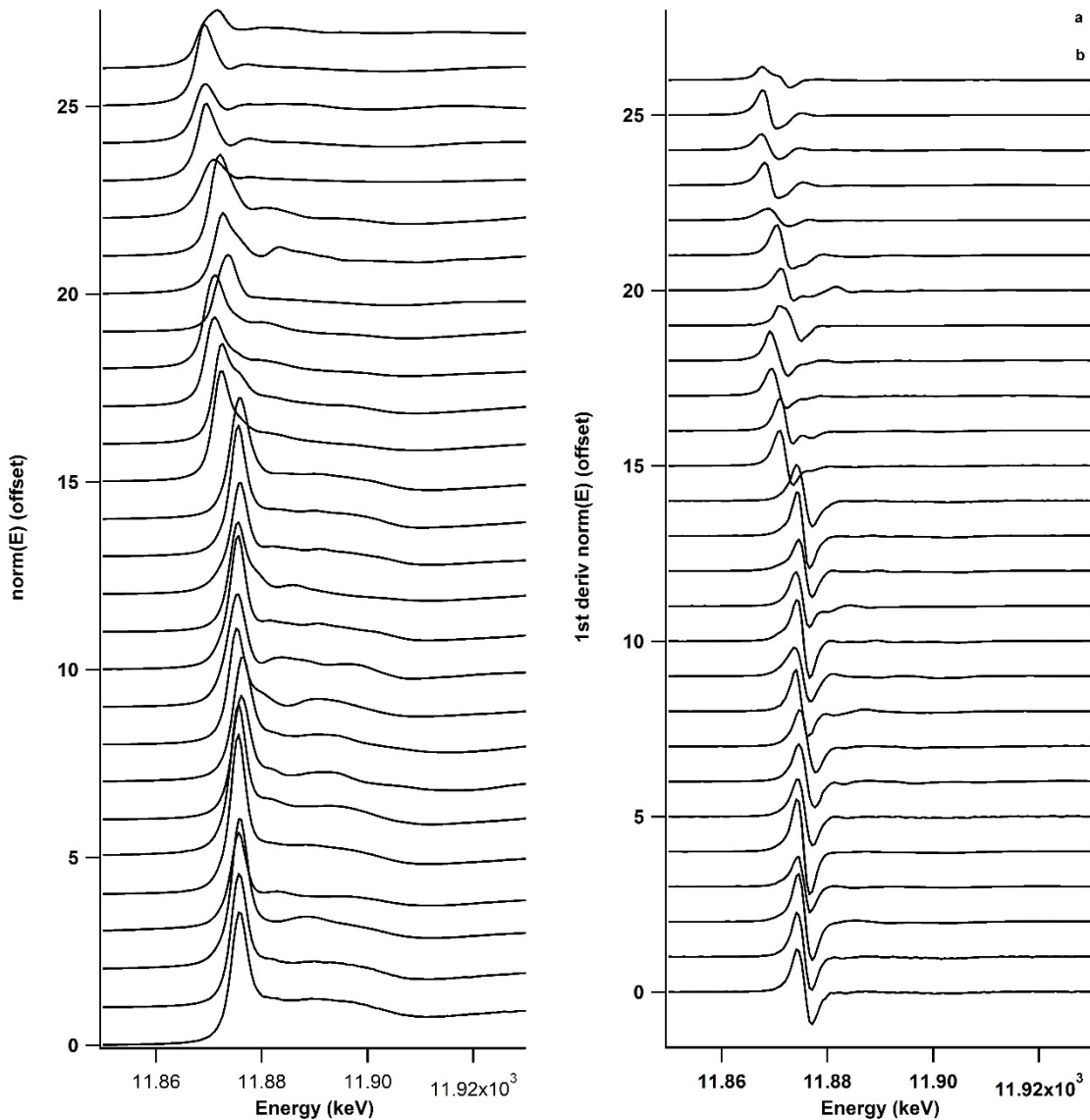


Figure A1. As Standards in order from top to bottom for both normalized and derivative data (left and right): Orpiment (As_2S_3), Realgar (As_4S_4), Loellingite (FeAs_2), Arsenite Coppt with pyrite, Arsenopyrite (FeAsS), Schneiderhohnite ($\text{Fe}_2\text{Fe}_3\text{AsO}$), Arsenolite (As_2O_3), As 3 ads pyrite, As 3 ads ferrihydrite, As 3 siderite (FeCO_3), As 3 mont, Yukonite ($\text{CaFeAsO}_4\text{OH}$), Arseniosiderite ($\text{CaFe}(\text{AsO}_4)\text{O}_2$), pharmacosiderite (KFeAsO_4OH), Scorodite (FeAsO_4), Beudantite ($\text{PbFeSO}_4\text{AsO}_4\text{OH}$), Pb-arsenate pesticide (PbHAsO_4), NaAs(V) salt, MMA, DMA, As5 ads goe, As5 ads hematite, As 5 ads birnessite, As 5 ads kao10, As 5 ads gibbs 3, As 5 ads FH, As 5 ads Kao, As 5 ads gibbs

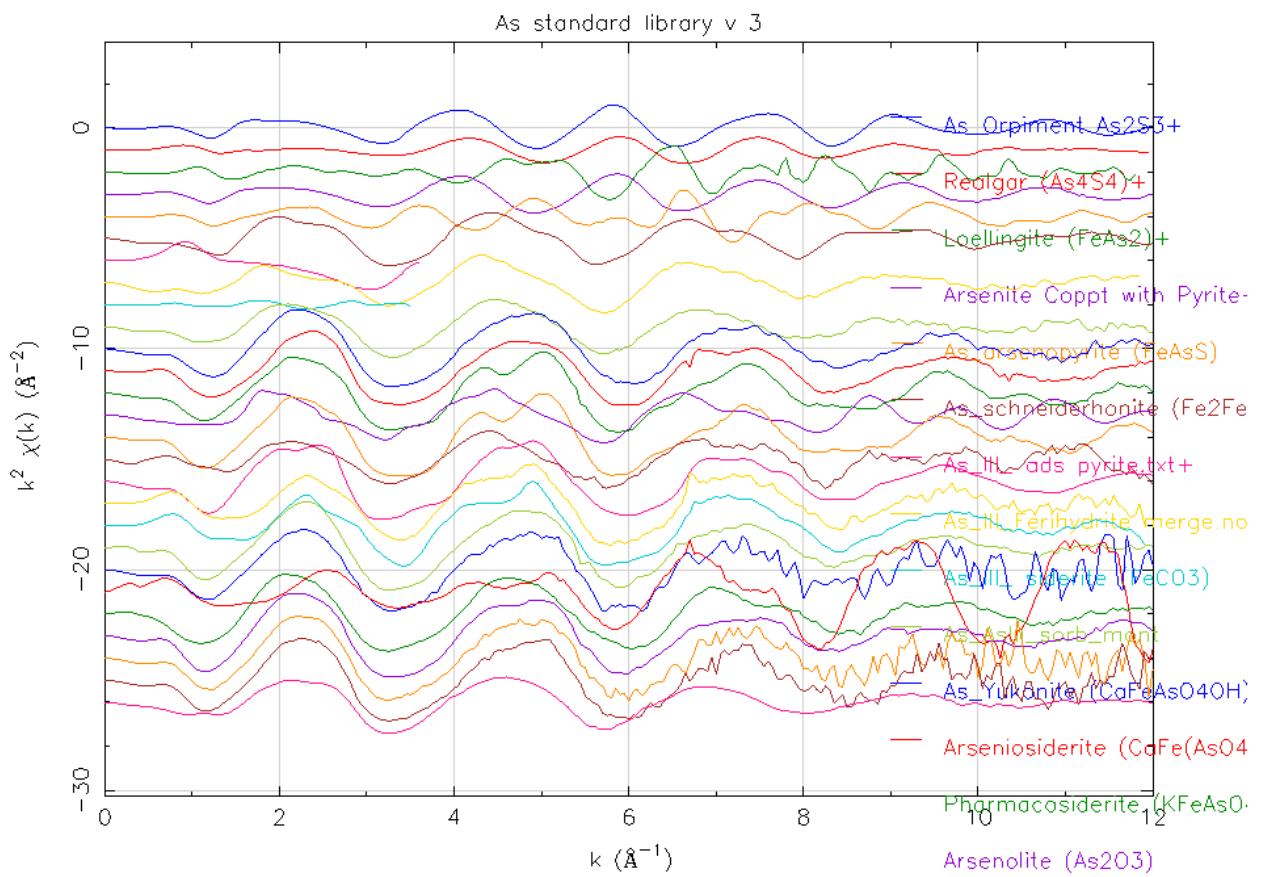


Figure A2. As χ^2 EXAFS region As Standards in order from top to bottom: Orpiment (As₂S₃), Realgar (As₄S₄), Loellingite (FeAs₂), Arsenite Coppt with pyrite, Arsenopyrite (FeAsS), Schneiderhohnite (Fe₂Fe₃AsO), Arsenolite (As₂O₃), As 3 ads pyrite, As 3 ads ferrihydrite, As 3 siderite (FeCO₃), As 3 mont, Yukonite (CaFeAsO₄OH), Arseniosiderite (CaFe(AsO₄)O₂), pharmacosiderite (KFeAsO₄OH), Scorodite (FeAsO₄), Beudantite (PbFeSO₄AsO₄OH), Pb-arsenate pesticide (PbHAsO₄), NaAs(V) salt, MMA, DMA, As5 ads goe, As5 ads hematite, As5 ads birnessite, As5 ads kao10, As5 ads gibbs 3, As5 ads FH, As5 ads Kao, As5 ads gibbs

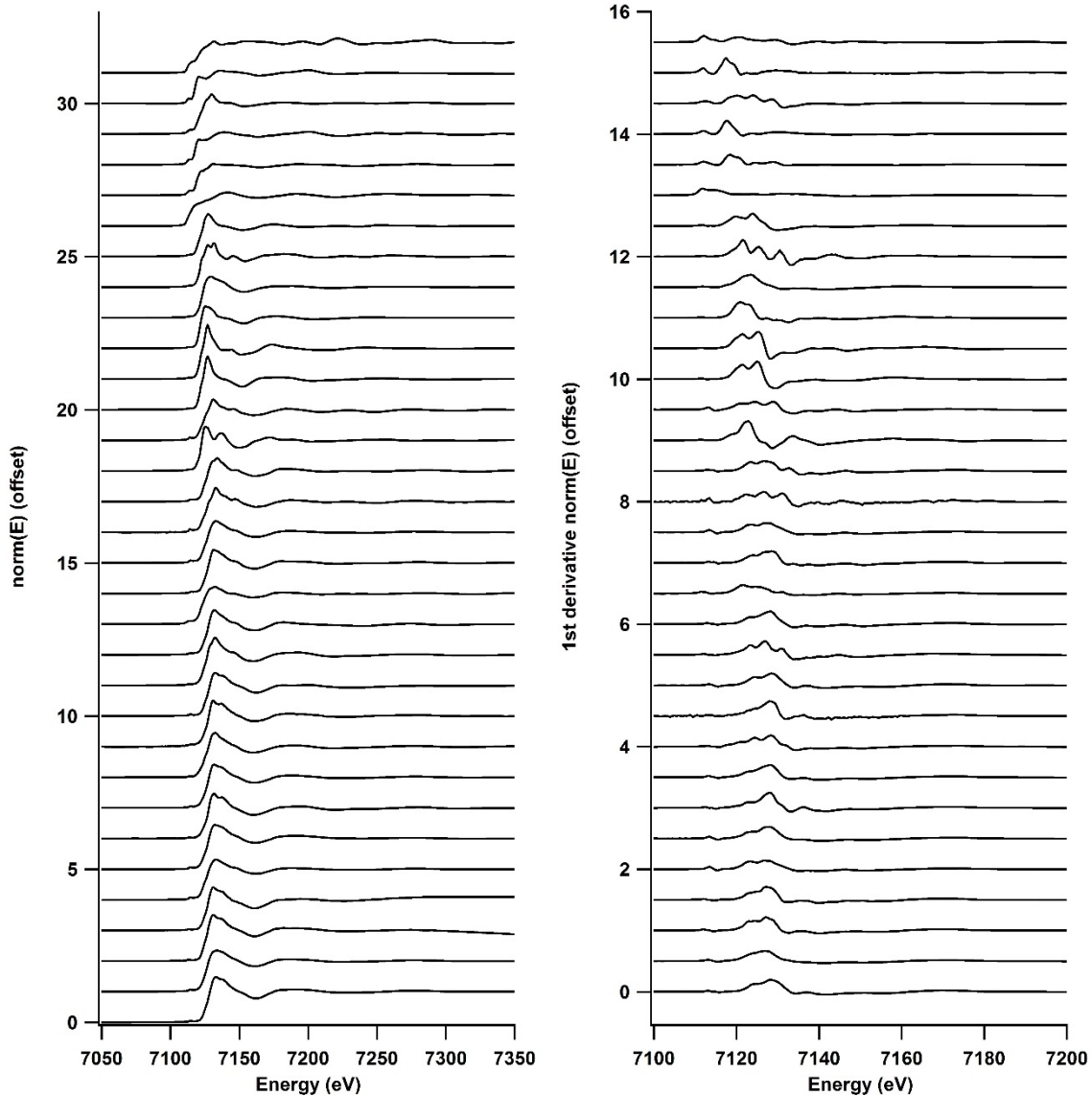


Figure A3. Fe Standards in order from top to bottom for both normalized and derivative data (left and right): hematite, ferrihydrite, goethite, Akaganeite, lepidocrocite, Fe subbed Montmorillonite, maghemite, magnetite, vivianite, fe metal, marcasite, loellingite, fayalite, biotite, pyrite, arsenopyrite, pyrrhotite, fe monosulfide, siderite, scorodite, arseniosiderite, pharmacosiderite, yukonite, fe(II) acetate, fe(II) chloride, fe(II) oxalate, fe(II) oxide, fe(II) selenide, fe(II) sulfate, fe(III) citrate, fe(III) sulfate, fe (II) phytate, fe(III) phytate, fe(II) phosphate, fe(III)phosphate, FeSi, As substituted FH

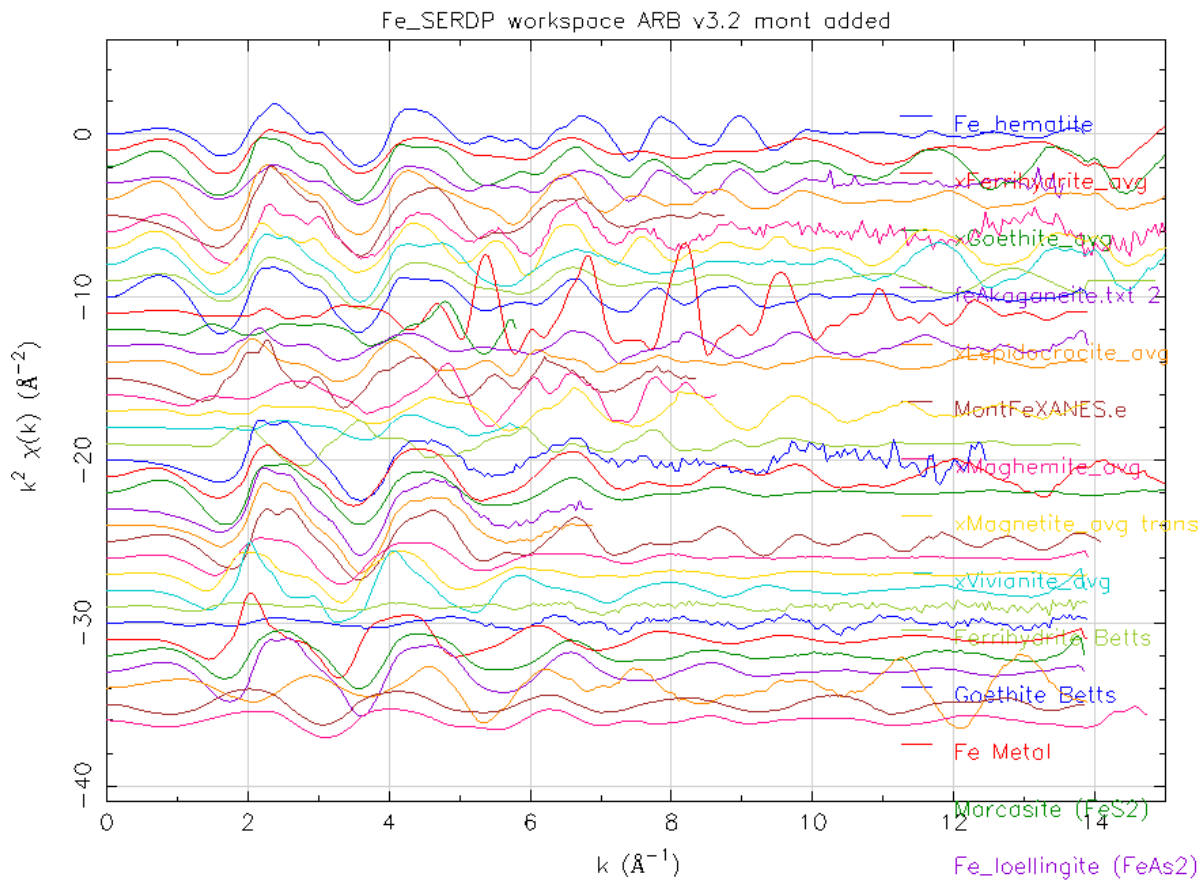


Figure A4. Fe Standards in order from top to bottom EXAFS χ^2 data: hematite, ferrihydrite, goethite, Akaganeite, lepidocrocite, Fe subed Montmorillonite, maghemite, magnetite, vivianite, fe metal, marcasite, loellingite, fayalite, biotite, pyrite, arsenopyrite, pyrrhotite, fe monosulfide, siderite, scorodite, arseniosiderite, pharmacosiderite, yukonite, fe(II) acetate, fe(II) chloride, fe(II) oxalate, fe(II) oxide, fe(II) selenide, fe(II) sulfate, fe(III) citrate, fe(III) sulfate, fe (II) phytate, fe(III) phytate, fe(II) phosphate, fe(III)phosphate, FeSi, As substituted FH

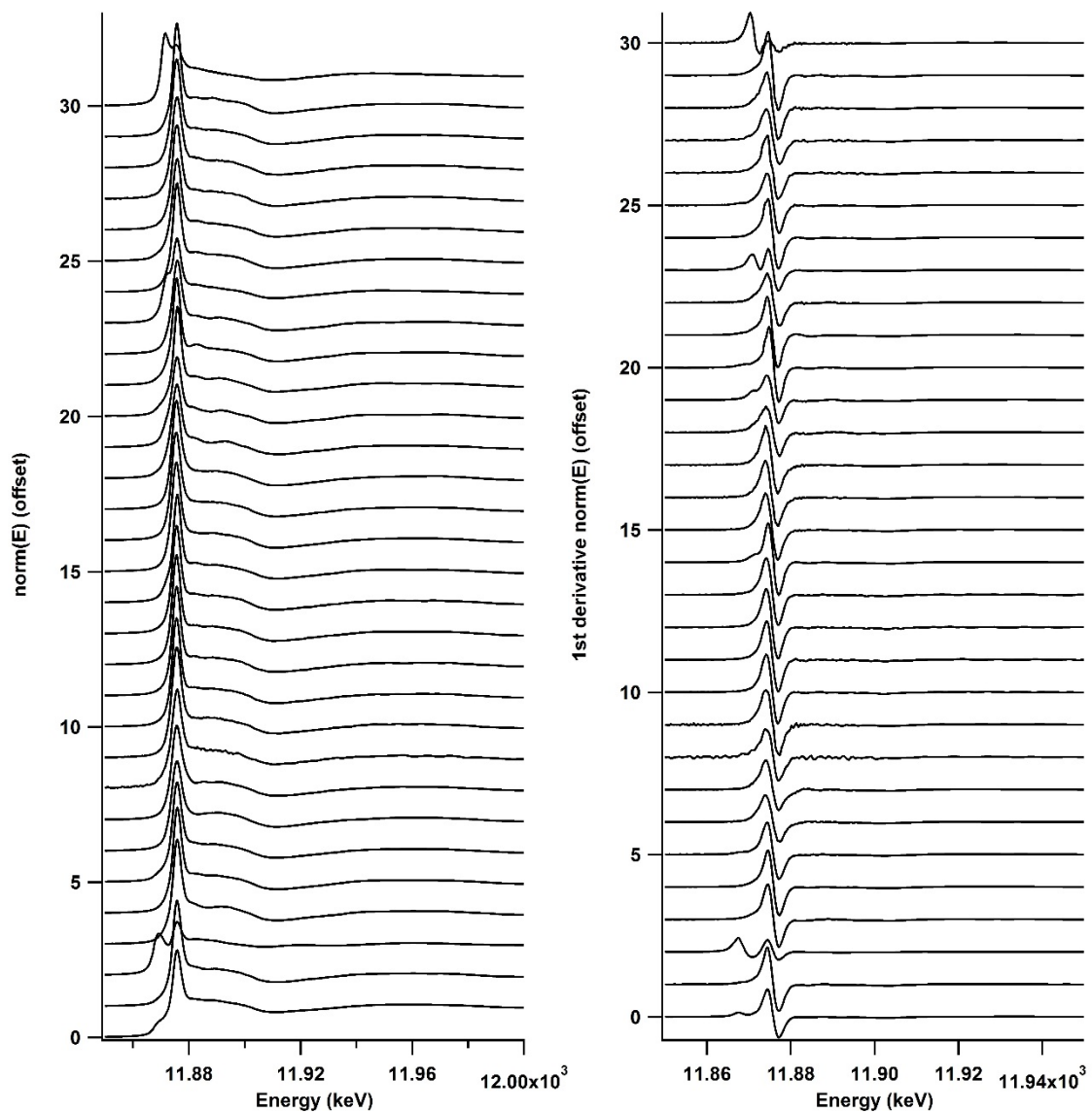


Figure A5: Soils in order from top to bottom for both normalized and derivative data (left and right): 1, 2, 3, 4, 5, 6, 7, 8, 9, 10, 11, 12, 13, 14, 15, 16, 17, 18, 19, 20, 21, 29, 30, 33, 34, 35, 36, 37, and 38

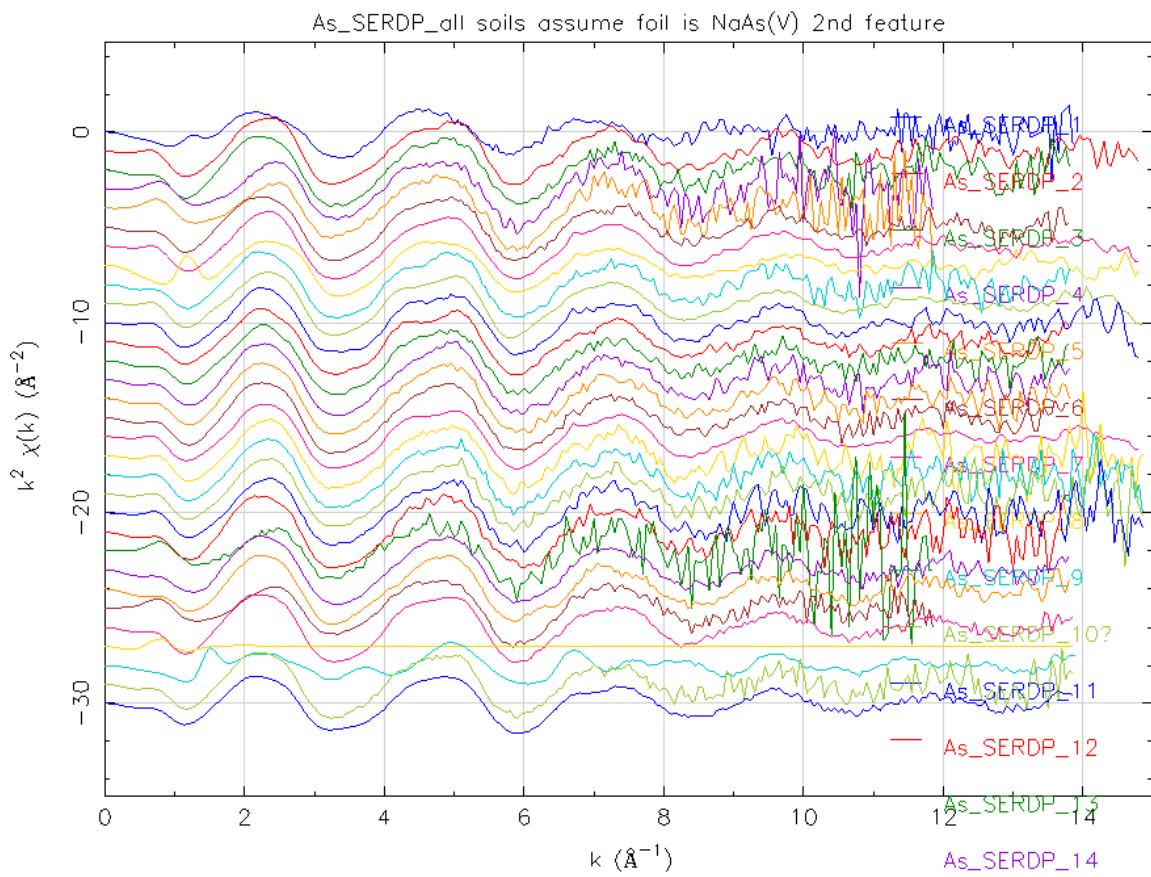


Figure A6: Soils As K-edge EXAFS χ^2 weighted from top to bottom: 1, 2, 3, 4, 5, 6, 7, 8, 9, 10, 11, 12, 13, 14, 15, 16, 17, 18, 19, 20, 21, 29, 30, 33, 34, 35, 36, 37, and 38

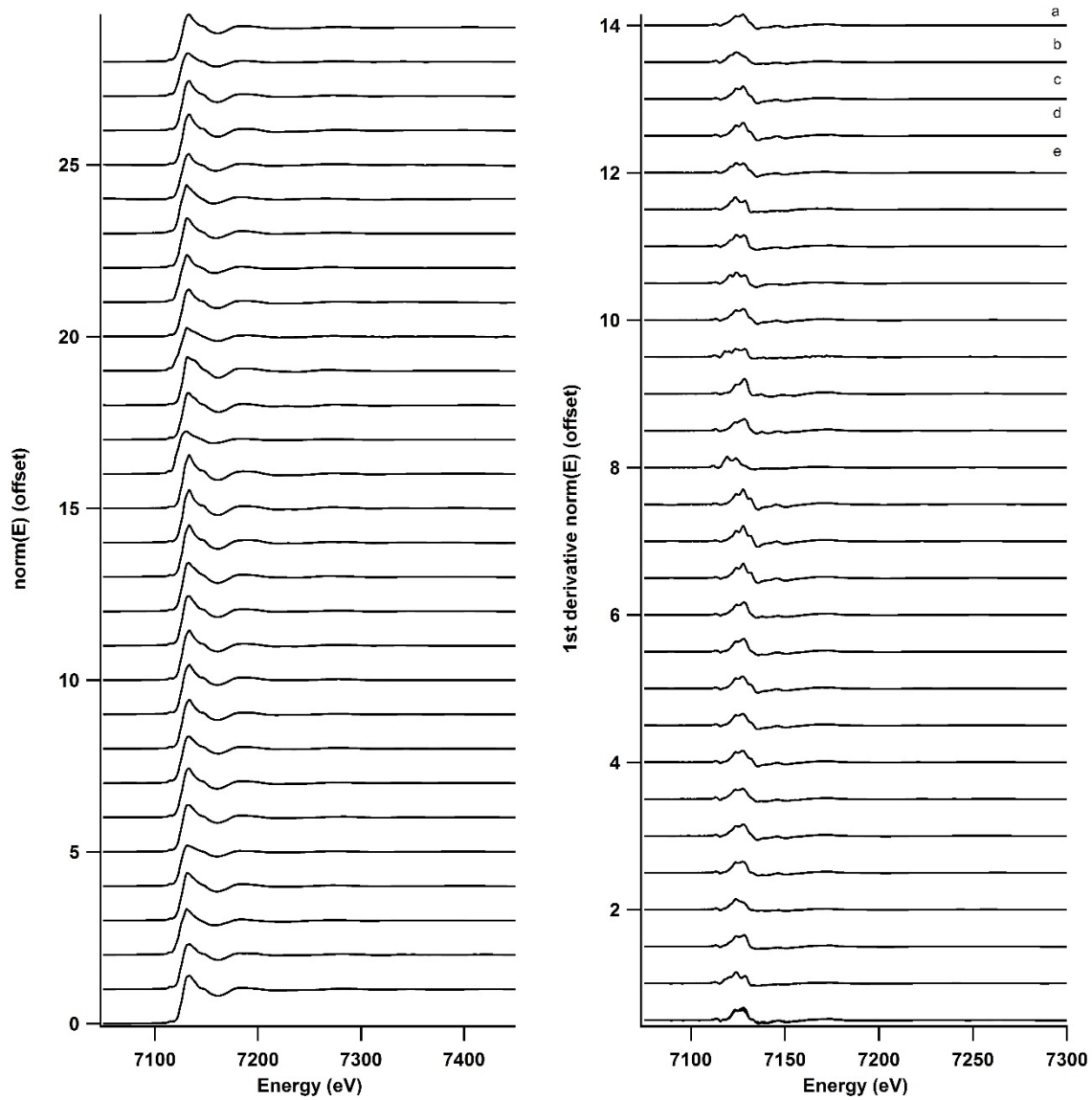


Figure A7: Fe soils in order from top to bottom for both normalized and derivative data (left and right): 1, 2, 3, 4, 5, 6, 7, 8, 9, 10, 11, 12, 13, 14, 15, 16, 17, 18, 19, 20, 21, 29, 30, 33, 34, 35, 36, 37, and 38

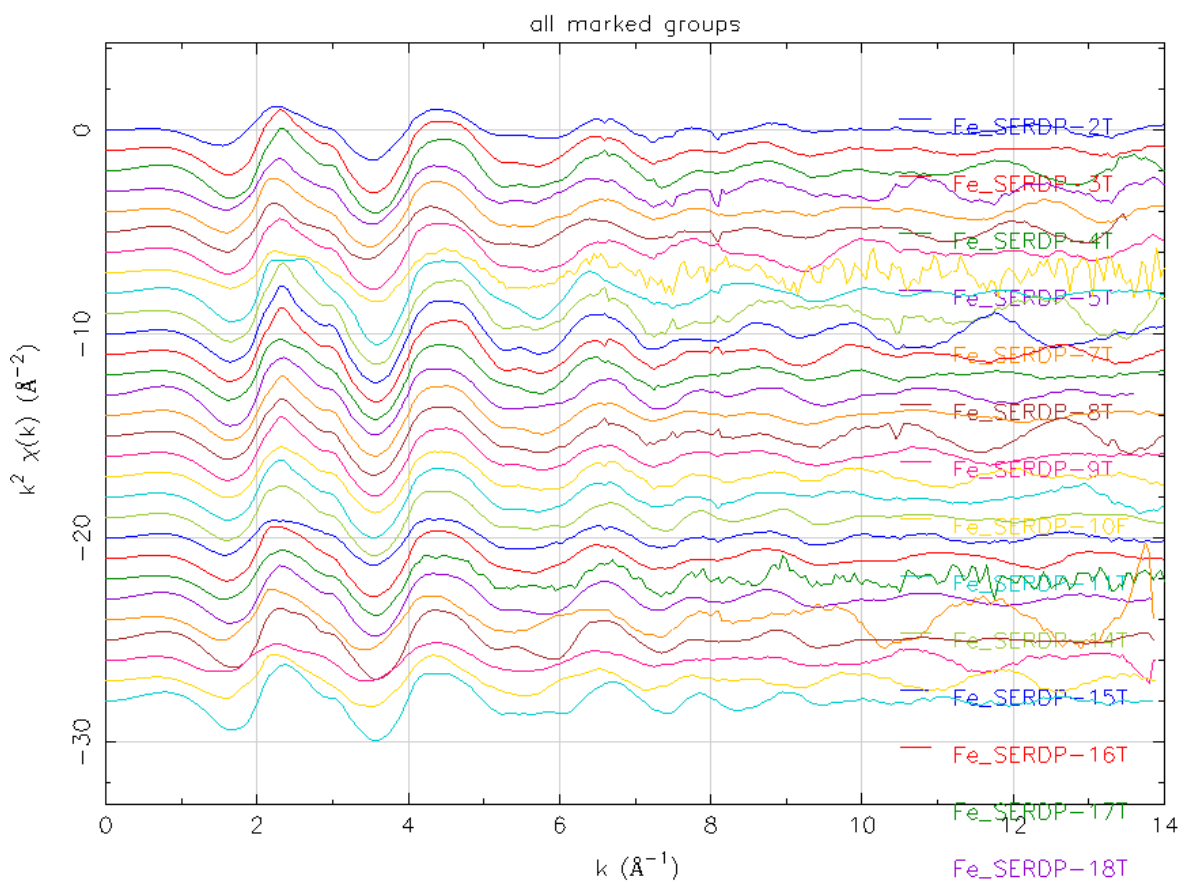


Figure A8: Fe soils EXAFS region χ^2 from top to bottom: 1, 2, 3, 4, 5 ,6 ,7 ,8 ,9 ,10, 11, 12, 13, 14, 15, 16, 17, 18, 19, 20, 21, 29, 30, 33, 34, 35, 36, 37, and 38

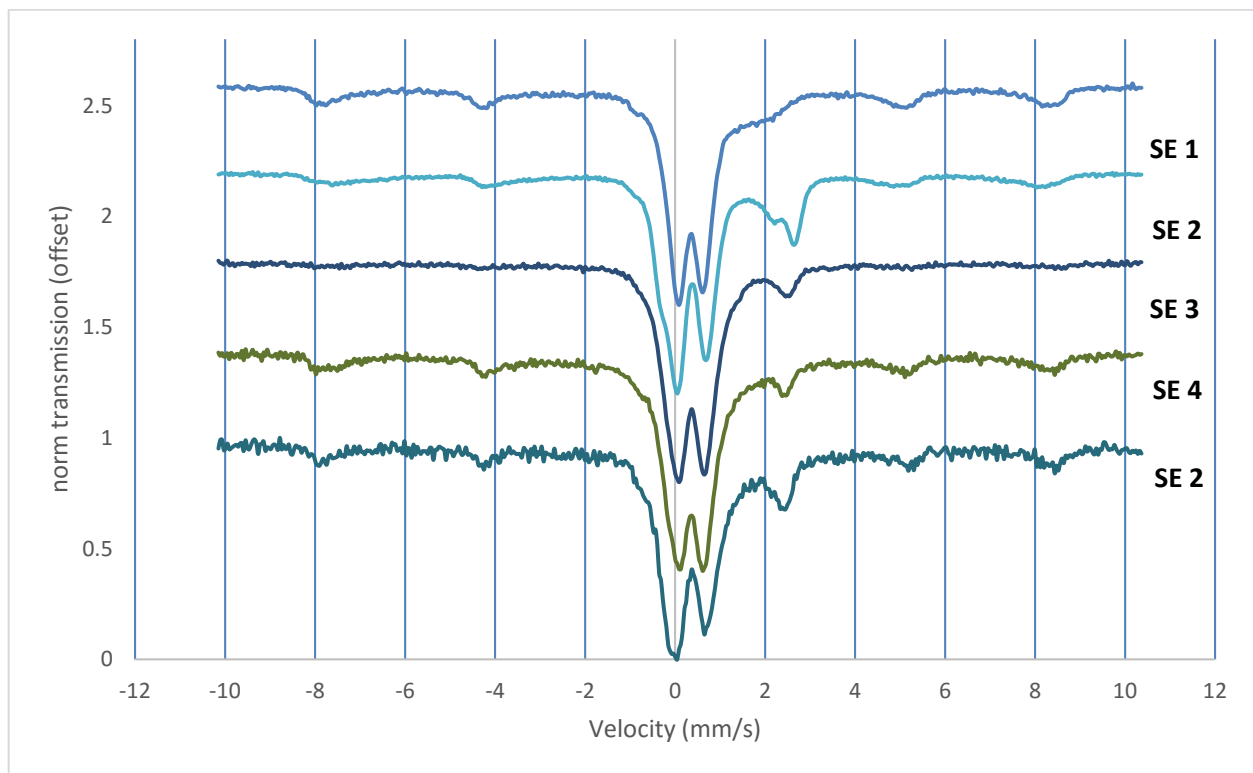


Figure A9. Mössbauer 298K samples 1-5

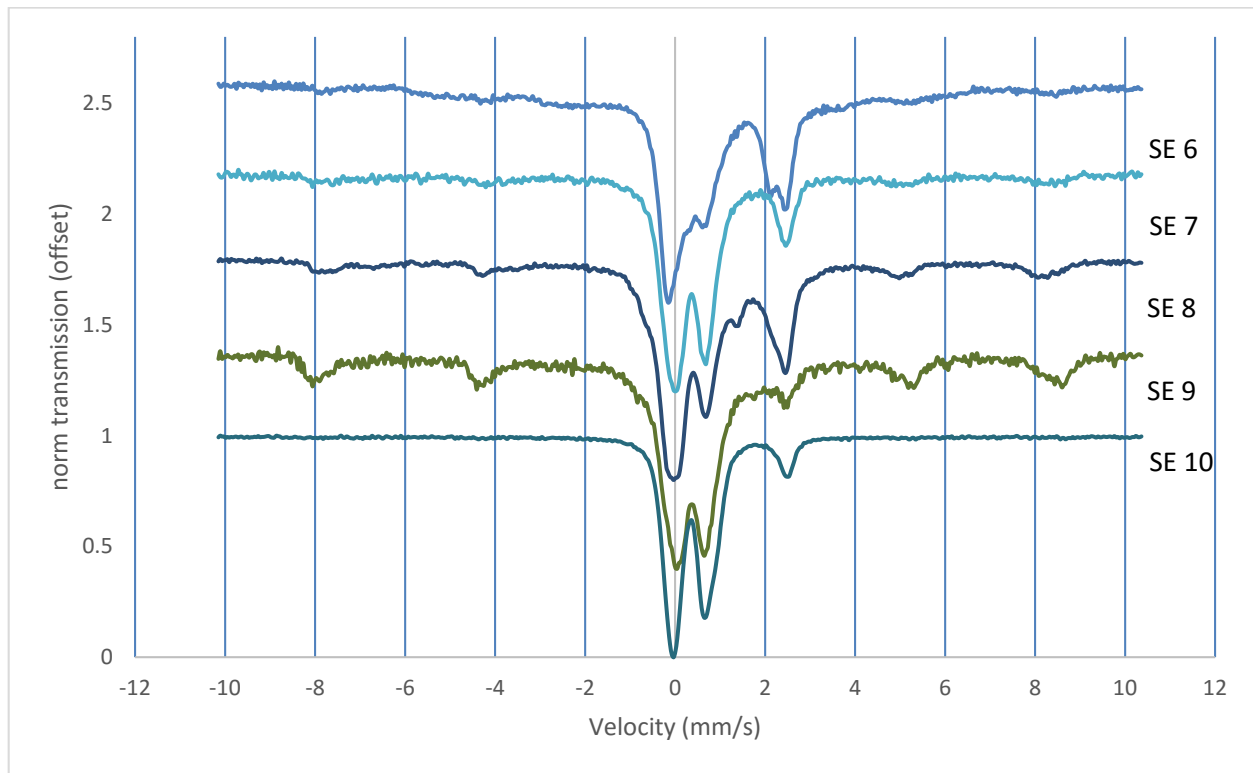


Figure A10. Mössbauer 298K samples 6-10

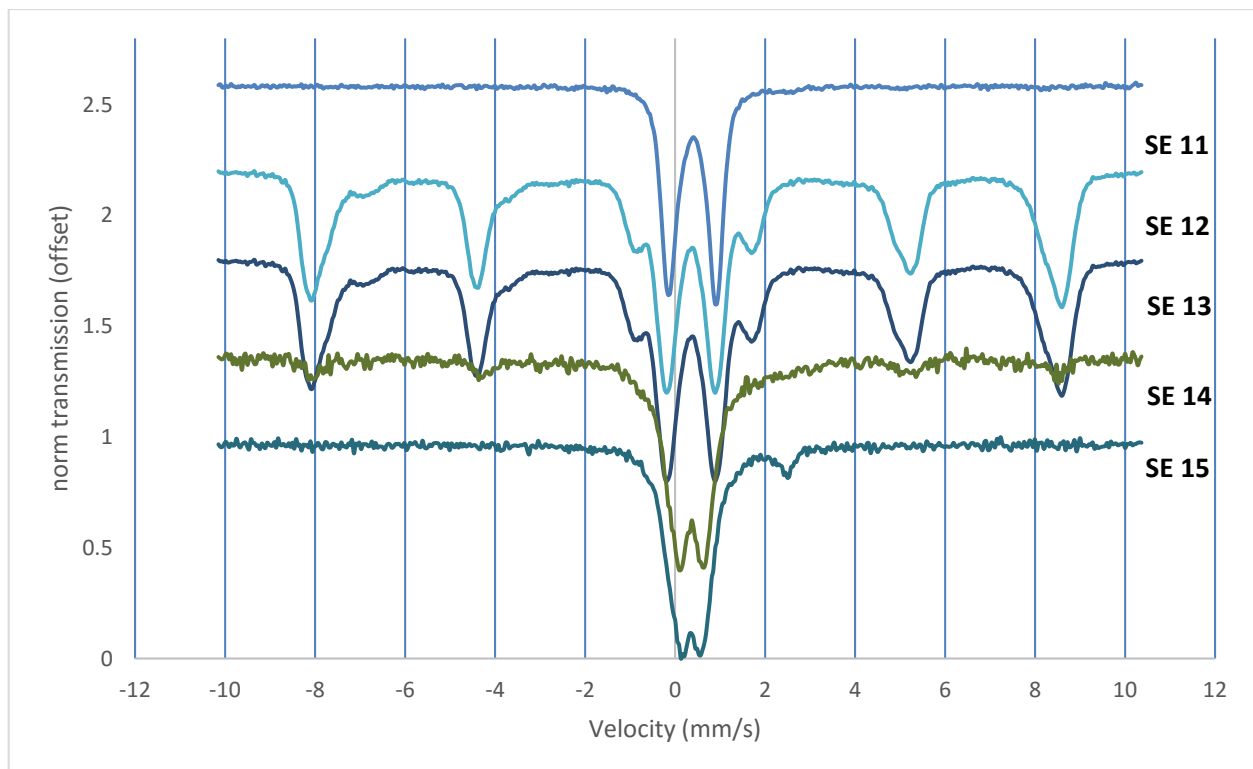


Figure A11. Mössbauer 298K samples 11-15

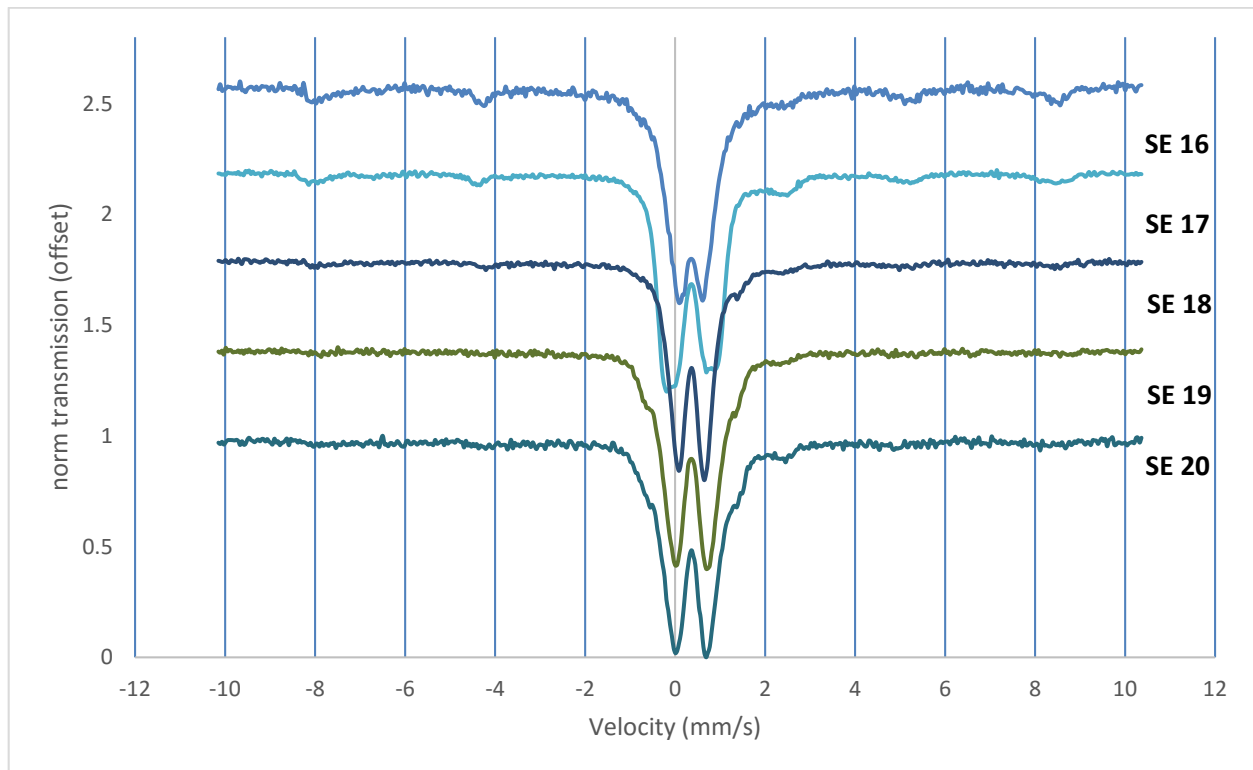


Figure A12. Mössbauer 298K samples 16-20

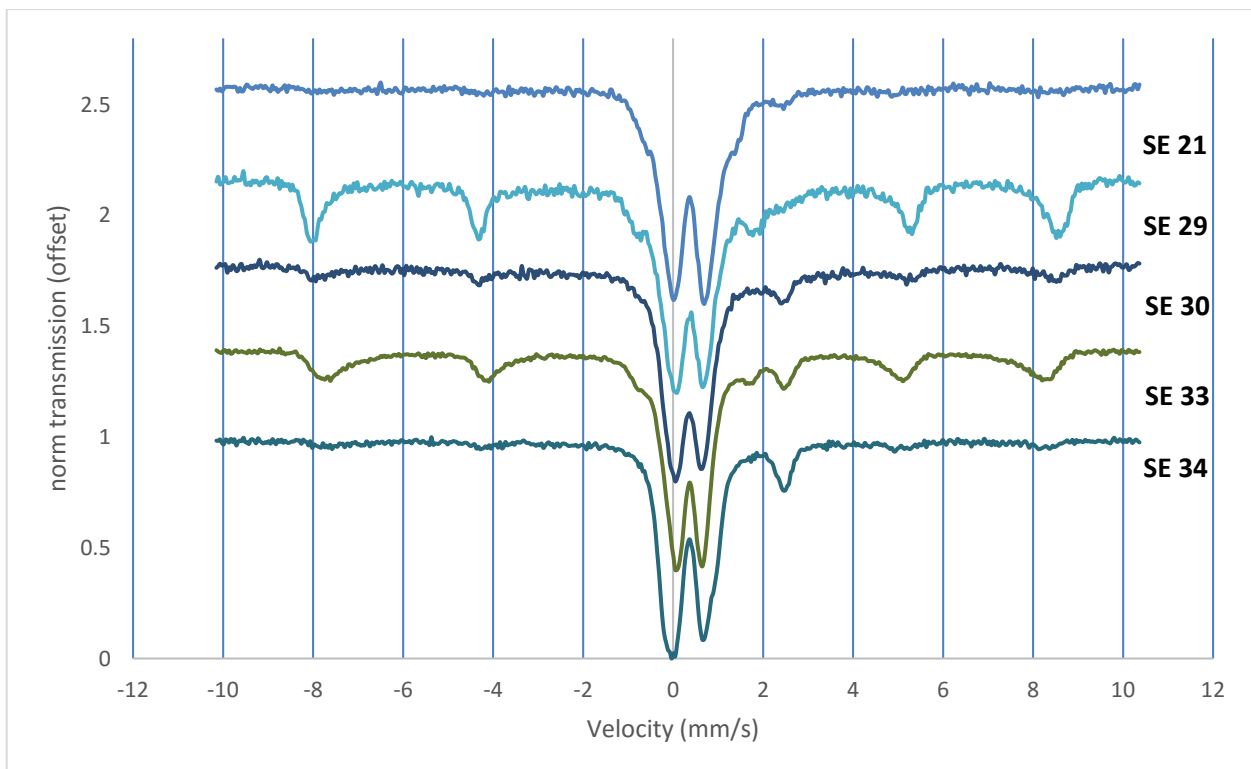


Figure A13. Mössbauer 298K samples 21-34

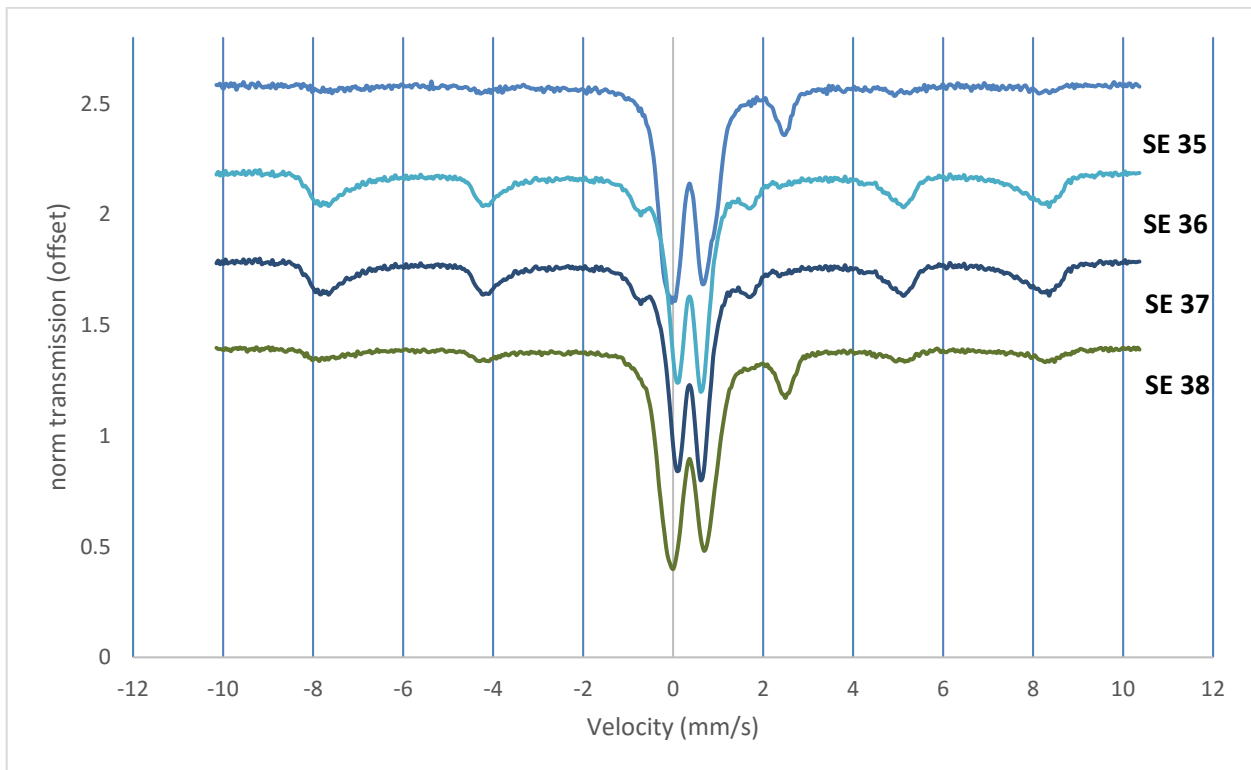


Figure A14. Mössbauer 298K samples 35-38

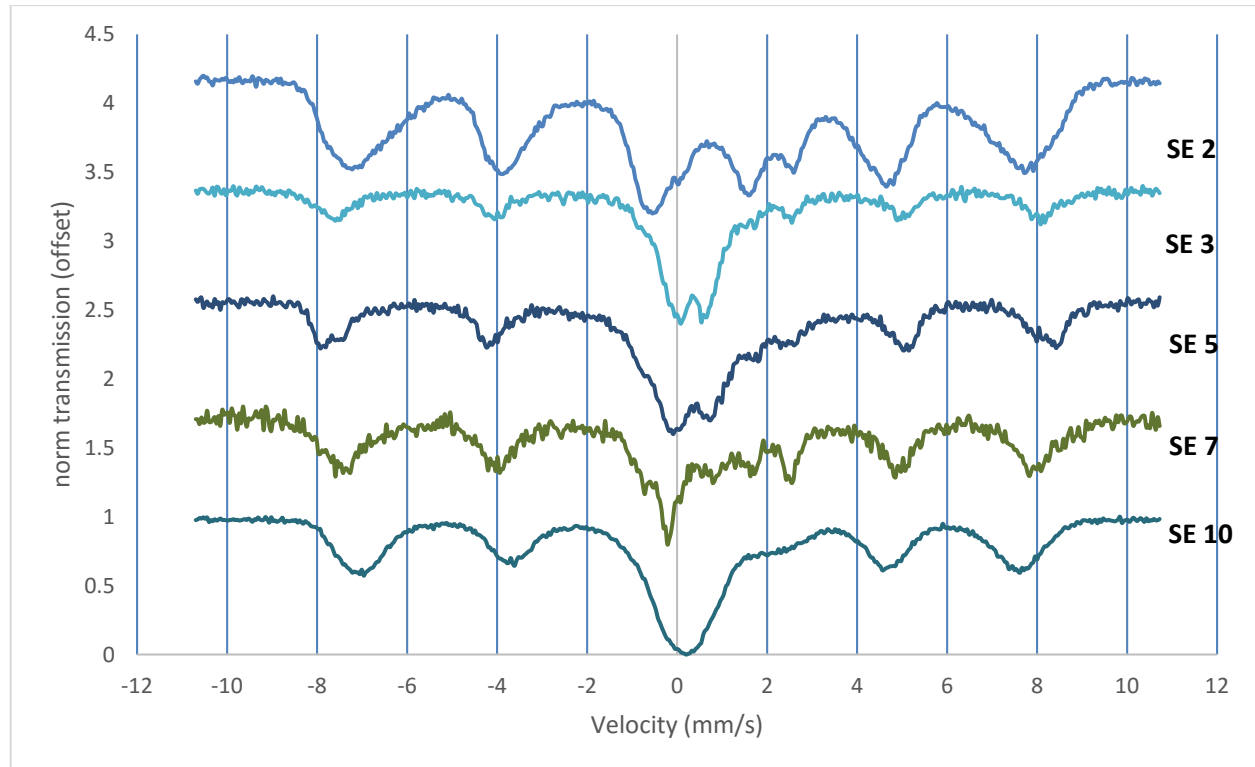


Figure A15. Mössbauer 4K measurement of samples 2-10

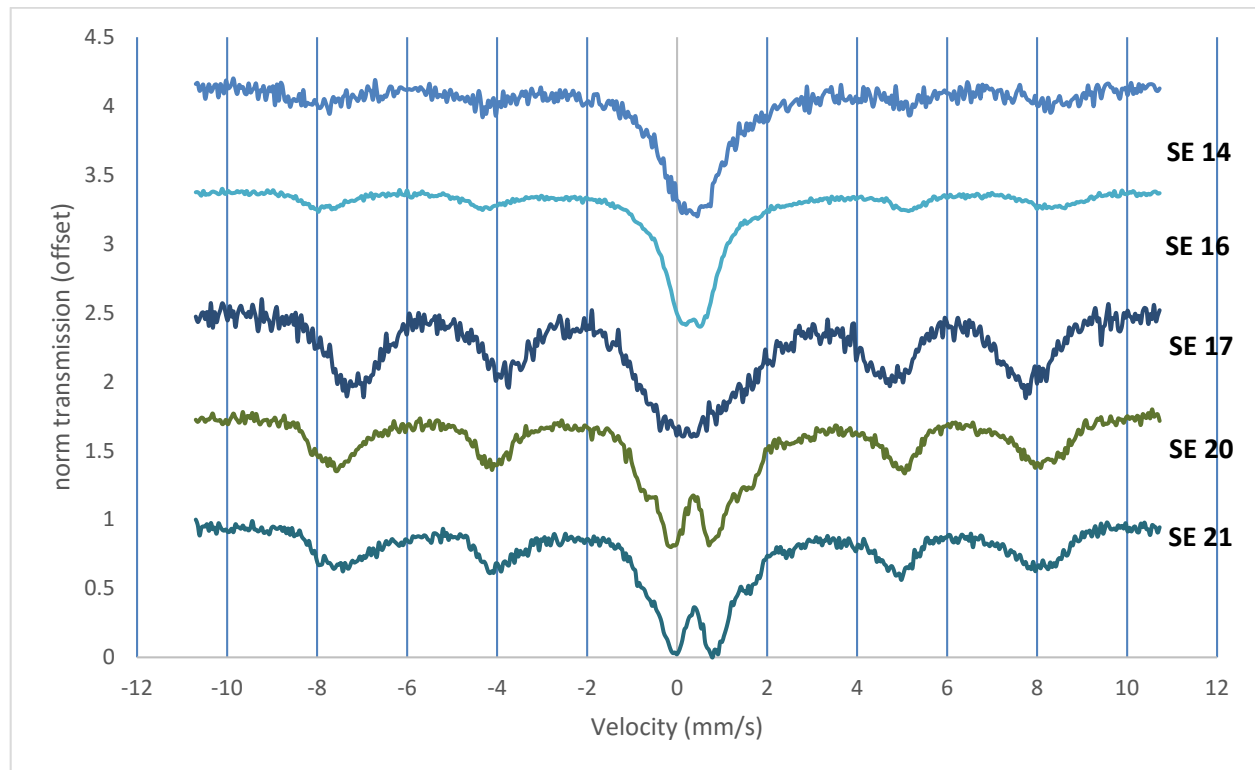


Figure A16. Mössbauer 4K measurement of samples 14-21

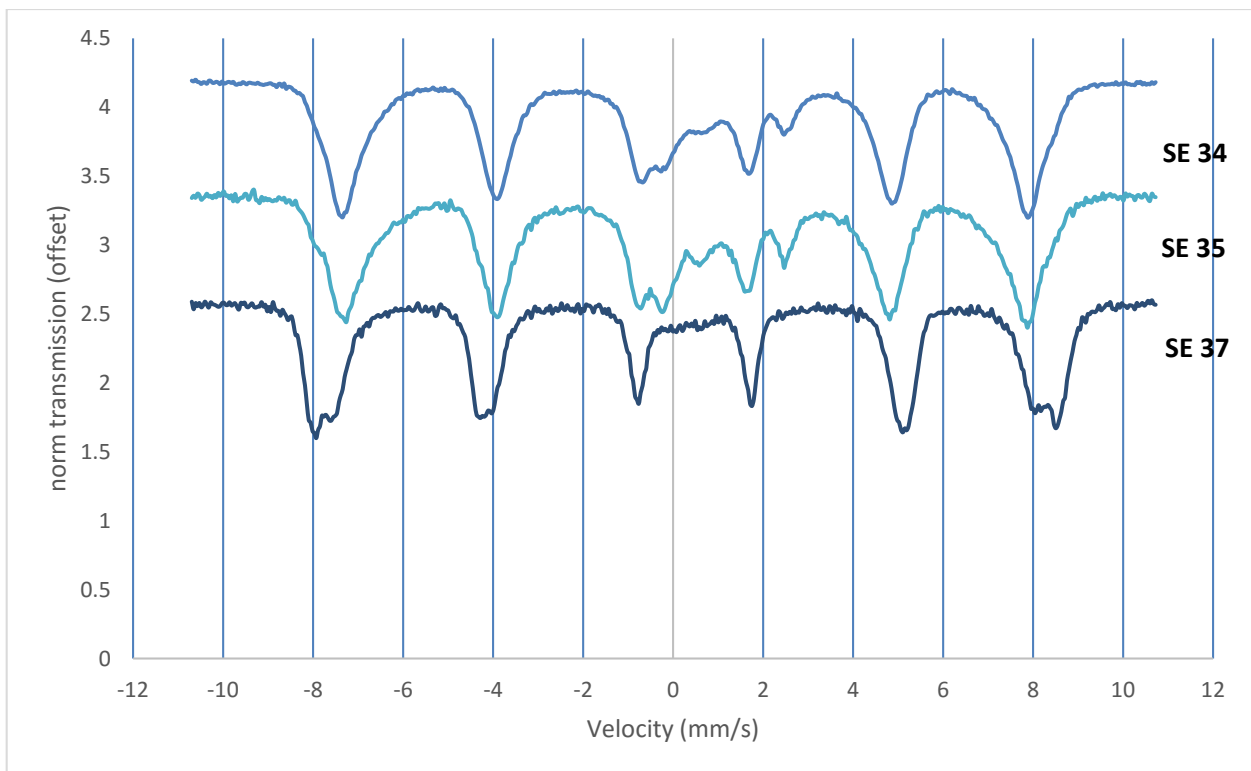


Figure A17. Mössbauer 4K measurement of samples 34-37

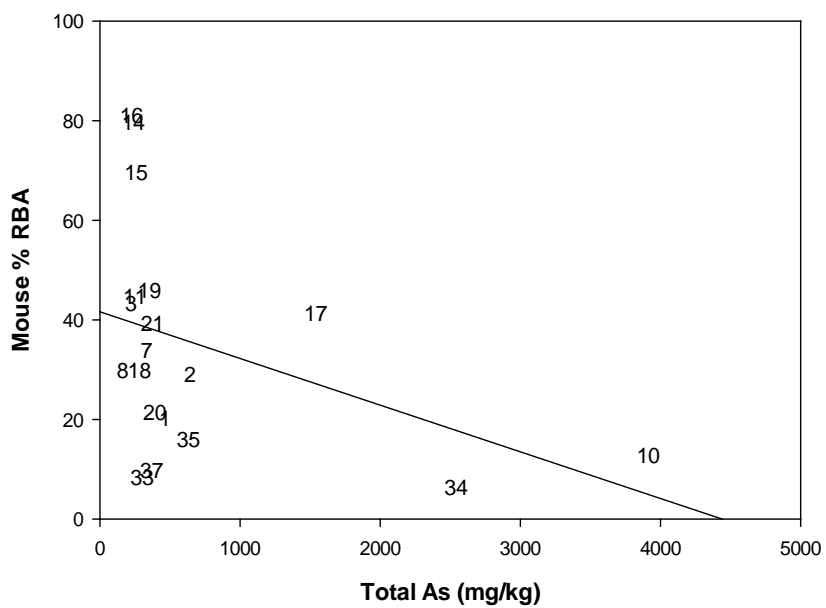


Figure A18. Mouse % RBA vs total As concentration (mg/kg) for all soils.

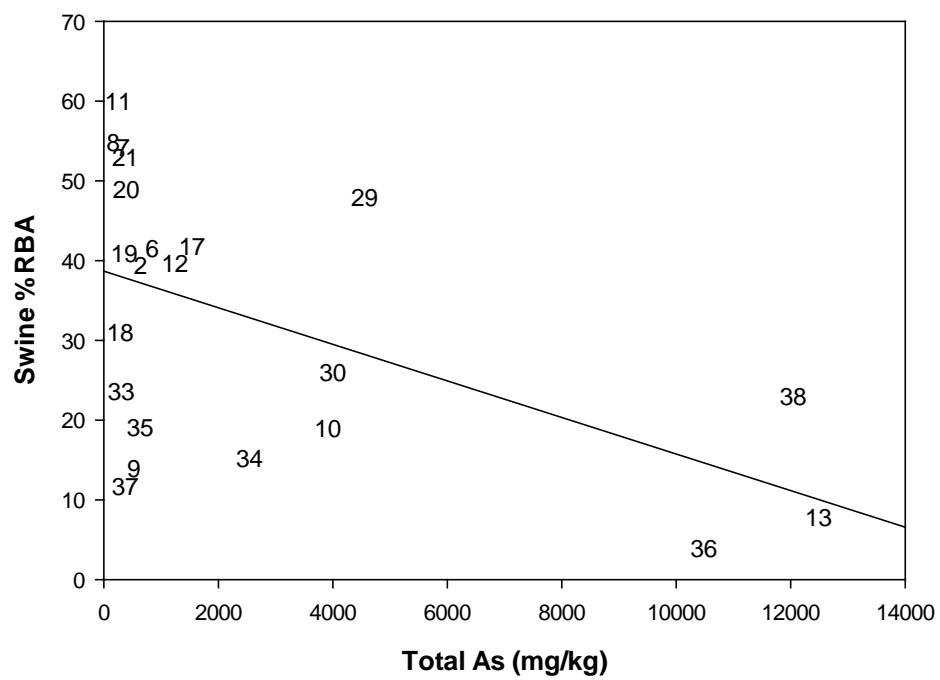


Figure A19. Mouse % RBA vs total As concentration (mg/kg) for all soils.

Appendix A.2 Typical Experimental Design for Juvenile Swine Bioassay to Determine RBA As

The study design was patterned after the standardized study protocols for measuring relative bioavailability of arsenic using the juvenile swine model. The study was performed as nearly as possible within the spirit and guidelines of Good Laboratory Practices (GLP: 40 CFR 792). Each material was administered to groups of four animals at three different dose levels for 15 days. Additionally, the study included a non-treated group of three animals to serve as a control for determining background arsenic levels. All doses were administered orally.

The soil samples were sieved through a 250 micrometer (μm) sieve prior to test substance analysis and characterization. Only material that passed through the sieve (corresponding to particles smaller than about 250 μm) were used in the bioavailability study. The study was limited to this fine-grained soil fraction because it is believed that soil particles less than about 250 μm are most likely to adhere to the hands and be ingested by hand-to-mouth contact, especially in young children.

The animals were intact males of the Pig Improvement Corporation genetically defined Line 26, and were purchased from Chinn Farms, Clarence, Missouri. The number of animals purchased for the study was several more than required by the protocol. These animals were purchased at an age of about 5-6 weeks (weaning occurs at age 3 weeks) and housed in individual stainless steel cages. The animals were then held under quarantine for one week to observe their health before beginning exposure to dosing materials. Each animal was examined by a certified veterinary clinician (swine specialist) and any animals that appeared to be in poor health during this quarantine period were excluded from the study. To minimize weight variations among animals and groups, extra animals most different in body weight (either heavier or lighter) six days prior to exposure (day -6) were also excluded from the study. The remaining animals were assigned to dose groups at random.

When exposure began (day zero), the animals were about 6-7 weeks old and weighed an average of about 9.4 kilograms (kg). The animals were weighed every three days during the course of the study. On average, animals gained about 0.39 kg/day and the rate of weight gain was comparable in all dosing groups, ranging from 0.29 to 0.46 kg/day.

All animals were examined daily by an attending veterinarian while on study. All animals were also subjected to detailed examination at necropsy by a certified veterinary pathologist in order to assess overall animal health.

Animals were weaned onto standard pig chow (purchased from MFA Inc., Columbia, Missouri) by the supplier. The animals were gradually transitioned from the MFA feed to a special feed originally developed for lead RBA studies (purchased from Zeigler Brothers, Inc., Gardners, Pennsylvania), and this feed was maintained for the duration of the study. The feed was nutritionally complete and met all requirements of the National Institutes of Health–National Research Council. Each day every animal was given an amount of feed equal to 4.5% of the mean body weight of all animals on study¹. Feed amounts were adjusted every three days, when

¹ Feed portions were 4% of the mean body weight through the morning feeding of day 0; portions were increased to 4.5% beginning with the evening feeding of day 0 and this was maintained through the end of the study.

pigs were weighed. Feed was administered in two equal portions at 11:00 AM and 5:00 PM daily. Analysis of random feed samples indicated that the arsenic levels did not exceed 0.1 µg/g.

Drinking water was provided *ad libitum* (i.e., free feeding) via self-activated watering nozzles within each cage. Analysis of samples from randomly selected drinking water nozzles indicated the arsenic concentrations were below a level of detection.

Dosing

Animals were exposed to dosing materials (sodium arsenite or test materials) for 15 days, with the dose for each day being administered in two equal portions beginning at 9:00 AM and 3:00 PM (two hours before feeding), with two minute intervals allowed for individual pig dosing. In general, dose material was placed in the center of one or more small portions (about 5 grams) of moistened feed (this is referred to as a “doughball”), and this was administered to the animals by hand. If uneaten portions of doughballs were discovered, these were retrieved and offered again for consumption. Occasionally, some animals did not consume their entire dose. In these instances, the missed doses were estimated and recorded and the time-weighted average dose calculation for each animal was adjusted downward accordingly.

The dose levels administered were based on the arsenic concentration in the dosing materials and the group mean body weights. Specifically, doses were held constant based on a body weight of 12.75 kg, the expected mean weight during the exposure interval (14 days)². After completion of the study, body weights were estimated by interpolation for those days when measurements were not collected and the actual administered doses were calculated for each day and then averaged across all days.

Collection and Preservation of Urine Samples

Samples of urine were collected from each animal for a 24-hour period on day -1 (U-0) and for 48-hour periods on days 6 to 7 (U-1), 9 to 10 (U-2), and 12 to 13 (U-3) of the study. Collection began at 9:00 AM and ended 24 or 48 hours later. The urine was collected in a plastic bucket placed beneath each cage, which was emptied into a plastic storage bottle. Aluminum screens were placed under the cages to minimize contamination with feces, spilled food, or other debris. Due to the length of the collection period, collection containers were emptied periodically (typically twice daily) into a separate holding container to ensure that there was no loss of sample due to overflow³.

At the end of each collection period, the total urine volume for each animal was measured and three 60-milliliter (mL) portions were removed and acidified with 0.6 mL concentrated nitric acid. Two of the aliquots were archived in the refrigerator and one aliquot was sent for arsenic analysis. All samples were refrigerated until arsenic analysis.

² For days 0-3, doses were based on the measured group mean body weight adjusted by the addition of 1 kg to account for the expected weight gain over the time interval.

³ For pig 245, collection U-2, a small amount of urine was spilled from the urine collection bucket between 9:30 and 11am, but the amount was not thought to be significant. For pig 244, collection U-3, the urine collection bucket overflowed sometime between 12 and 3pm, possibly due to a waterer jam; the amount of urine lost is not known.

Arsenic Analysis

Urine samples were assigned random chain-of-custody tag numbers and submitted to the analytical laboratory for analysis in a blind fashion; the samples were analyzed for arsenic by L. E. T., Inc., (Columbia, Missouri). In brief, 25 mL samples of urine were digested by refluxing and then heating to dryness in the presence of magnesium nitrate and concentrated nitric acid. Following magnesium nitrate digestion, samples were transferred to a muffle furnace and ashed at 500°C. The digested and ashed residue was dissolved in hydrochloric acid and analyzed by the hydride generation technique using a PerkinElmer 3100 atomic absorption spectrometer. Preliminary tests of this method established that each of the different forms of arsenic that may occur in urine, including trivalent inorganic arsenic, pentavalent inorganic arsenic, monomethyl arsenic (MMA), and dimethyl arsenic (DMA), are all recovered with high efficiency.

Urine analytical results are presented in Appendix A, Table A-5. All responses below the quantitation limit were evaluated at one-half the quantitation limit. Quality assurance samples are described in the following section.

Quality Assurance

A number of quality assurance (QA) steps were taken during this project to evaluate the accuracy of the analytical procedures. Randomly selected samples were spiked with known amounts of arsenic (sodium arsenate) and the recovery of the added arsenic was measured. Periodically during arsenic analysis, urine samples were randomly selected by the analyst for duplicate analysis (i.e., the same prepared sample was analyzed twice). Ten results had absolute differences between the urinary arsenic duplicate and the original result that were less than the detection limit. A random selection of all urine samples generated during the study were prepared for laboratory analysis in duplicate (i.e., two separate subsamples of urine were prepared for analysis) and submitted to the laboratory in a blind fashion. A number of Performance Evaluation (PE) samples (urines of known arsenic concentration) were submitted to the laboratory in a blind fashion. The PE samples included several different concentrations each of four different types of arsenic (arsenite, arsenate, MMA, and DMA). Laboratory control standards (samples of reference materials for which a certified concentration of specific analytes has been established) were tested periodically during sample analysis. The standard used (NIST 2670a H) consists of freeze-dried human urine that has been spiked with selected metals so as to contain elevated arsenic levels. Note that the arsenic concentration in this material is provided by NIST as a reference value, not a certified value. Reference values are non-certified values that are the best estimate of the true value but do not meet the NIST criteria for certification; they are provided with associated uncertainties that may not include all sources of uncertainty.

Data Analysis

The basic method used to estimate the RBA of arsenic in a particular test material compared to arsenic in a reference material (sodium arsenate) is as follows:

1. Plot the amount of arsenic excreted in the urine ($\mu\text{g}/\text{day}$) as a function of the administered amount of arsenic ($\mu\text{g}/\text{day}$), both for reference material (sodium arsenate) and for test material.

2. Find the best fit linear regression line through each data set. The slope of each line ($\mu\text{g/day excreted per }\mu\text{g/day ingested}$) is the best estimate of the urinary excretion fraction (UEF) for each material.
3. Calculate RBA for each test material as the ratio of the UEF for test material compared to UEF for reference material:

$$RBA(\text{test vs ref}) = \frac{UEF(\text{test})}{UEF(\text{ref})}$$

All model fitting was performed in Microsoft Excel® using matrix functions.

Dose-Response Model

Simultaneous Regression

The techniques used to derive linear regression fits to the dose-response data are based on the methods recommended by Finney (1978). As noted by Finney (1978), when the data to be analyzed consist of two dose-response curves (the reference material and the test material), it is obvious that both curves must have the same intercept, since there is no difference between the curves when the dose is zero. This requirement is achieved by combining the two dose response equations into one and solving for the parameters simultaneously, as follows:

Separate Models:

$$\mu_r(i) = a + b_r \cdot x_r(i)$$

$$\mu_t(i) = a + b_t \cdot x_t(i)$$

Combined Model

$$\mu(i) = a + b_r \cdot x_r(i) + b_t \cdot x_t(i)$$

where $\mu(i)$ indicates the expected mean response of animals exposed at dose $x(i)$, and the subscripts r and t refer to reference and test material, respectively. The coefficients of this combined model are derived using multivariate regression, with the understanding that the combined data set is restricted to cases in which one (or both) of x_r and x_t are zero (Finney, 1978).

All model fitting was performed in Microsoft® Office Excel using matrix functions.

Weighted Regression

Regression analysis based on ordinary least squares assumes that the variance of the responses is independent of the dose and/or the response (Draper and Smith, 1998). It has previously been shown that this assumption is generally not satisfied in swine-based RBA studies, where there is a tendency toward increasing variance in response as a function of increasing dose

(heteroscedasticity). One method for dealing with heteroscedasticity is through the use of weighted least squares regression (Draper and Smith, 1998). In this approach, each observation in a group of animals is assigned a weight that is inversely proportional to the variance of the response in that group:

$$w_i = \frac{1}{\sigma_i^2}$$

where:

w_i = weight assigned to all data points in dose group i

σ_i^2 = variance of responses in animals in dose group i

When the distributions of responses at each dose level are normal, weighted regression is equivalent to the maximum likelihood method.

There are several alternative strategies for assigning weights. The preferred method estimates the value of σ_i^2 using an “external” variance model based on an analysis of the relationship between variance and mean response using data consolidated across many different swine-based arsenic RBA studies. Log-variance increases as an approximately linear function of log-mean response:

$$\ln(s_i^2) = k1 + k2 \cdot \ln(\bar{y}_i)$$

where:

s_i^2 = observed variance of responses of animals in dose group i

\bar{y}_i = mean observed response of animals in dose group i

Values of $k1$ and $k2$ were derived using ordinary least squares minimization. The resulting values were -1.10 for $k1$ and 1.64 for $k2$.

Goodness of Fit

The goodness-of-fit of each dose-response model was assessed using the F test statistic and the adjusted coefficient of multiple determination (Adj R^2) as described by Draper and Smith (1998). A fit is considered acceptable if the p-value is less than 0.05.

Assessment of Outliers

In biological assays, it is not uncommon to note the occurrence of individual measured responses that appear atypical compared to the responses from other animals in the same dose group. In this study, endpoint responses that yielded standardized weighted residuals greater than 3.5 or less than -3.5 were considered to be potential outliers (Canavos, 1984). When such data points were encountered in a data set, the RBA values were calculated both with and without the

potential outlier(s) excluded, and the result with the outlier(s) excluded was used as the preferred estimate.

Calculation of RBA Estimates

The arsenic RBA values were calculated as the ratio of the slope term for the test material data set (b_t) and the reference material data set (b_r):

$$RBA = \frac{b_t}{b_r}$$

The uncertainty range about the RBA ratio was calculated using Fieller's Theorem as described by Finney (1978).

Appendix B

List of Scientific and Technical Publications

Peer Reviewed Journal Publications (5)

- Bradham, K. D., Nelson, C., Juhasz, A. L., Smith, E., Scheckel, K., Obenour, D. R., Miller, B. W., and Thomas, D. J. 2015. Independent data validation of an in vitro method for the prediction of the relative bioavailability of arsenic in contaminated soils. Environ. Sci Technol. 49(10): 6312-6318.
- Bradham, K. D., Scheckel, K. G., Nelson, C. M., Seales, P. E., Lee, G. E., Hughes, M. F., Miller, B. W., Yeow, A., Gilmore, T., Serda, S.M., Harper, S., and Thomas, D. J. 2011. Relative bioavailability and bioaccessibility and speciation of arsenic in contaminated soils. Environmental Health Perspectives 119 (11): 1629-1634
- Bradham, K.D. , Diamond, G.L. , Scheckel, K.G. , Hughes, M.F. , Casteel, S.W., Miller, B.W., Klotzbach, J.M., Thayer, W.C., and Thomas, D.J. 2013. Mouse Assay for Determination of Arsenic Bioavailability in Contaminated Soils, Journal of Toxicology and Environmental Health, Part A: Current Issues, 76:13, 815-826
- Juhasz,A.L., N.T. Basta, and E. Smith. 2013. What is required for the validation of in vitro assays for predicting contaminant relative bioavailability? Considerations and criteria. Environmental Pollution 180:372-375.
- Sullivan, T.S., N.R. Gottel, N. Basta, P.M. Jardine and C.W. Schadt. 2012. Firing Range Soils Yield a Diverse Array of Fungal Isolates Capable of Organic Acid Production and Pb Mineral Solubilization. Applied and Environmental Microbiology 78(17):6078-6086.
- Whitacre, S.D., N.T. Basta, and E.A. Dayton. 2013. Soil Controls on Bioaccessible Arsenic Fractions. J. Environ. Health Sci. Part A. 48(6): 620-628.

Peer reviewed conference or symposium proceedings (9)

- Basta N., S. Whitacre, P.Myers, V. Mitchell, C. Alpers, A. Foster, S. Casteel and C. Kim. 2014. Using in Vitro Gastrointestinal and Sequential Extraction Methods to Characterize Site-Specific Arsenic Bioavailability. Goldschmidt 2014 Conference, Geochemical Society and European Assoc. of Geochemistry, Sacramento, CA, June 8-13, 2014.
- Basta, N.T., S. Whitacre, A. Foster, C. Alpers, V. Mitchell, and P. Myers. 2014. Characterizing Arsenic Bioavailability in Gold Mining Contaminated Soils. Bioavailability and Bioaccessibility: Critical Tools For Risk Management Decisions Session, 35th North American Annual Meeting of the Society of Environmental Toxicology and Chemistry, Vancouver, British Columbia, Canada, Nov. 9-13, 2014.

- Basta, N.T., K.G.Scheckel, K.D. Bradham, D. J. Thomas, S.W. Whitacre, and B.W. Miller. 2013 Arsenic Speciation, In Vitro Gastrointestinal Bioaccessibility, and Predicted Human Bioavailability from Ingestion of Contaminated Soil. Joint MERA/ICOBTE Sponsored Symposium: Trace Element Bioavailability for Human and Ecological Risk Assessment: Concepts and Recent Advances. Organizers: N. Basta, E. Van Genderen, and C. Schlekat. 12th International Conference for Trace Element Biogeochemistry (ICOBTE), Athens, GA, USA. June 16-20, 2013. (invited)
- Bradham, K.D., Scheckel, K.G., Nelson, C.M., Seales, P.E., Lee, G.E., Hughes, M.F., Miller, B.W., and Thomas, D.J. 2011. Relative Bioavailability and Bioaccessibility and Speciation of Arsenic in Contaminated Soils. Presentation provided at International Conference on the Biogeochemistry of Trace Elements, July 5, 2011, Italy.
- Foster, A., C. Alpers, T. Burlak, A. Blum, E. Petersen, N. Basta, S. Whitacre, S. Casteel, C. Kim, and A. Brown. 2014. Arsenic Chemistry, Mineralogy, Speciation, and Bioavailability/Bioaccessibility in Soils and Mine Waste from the Empire Mine, CA, USA. Goldschmidt 2014 Conference, Geochemical Society and European Assoc. of Geochemistry, Sacramento, CA, June 8-13, 2014.
- Juhasz, A.L., N. Basta and E. Smith. 2013. What is Required for the Validation of In Vitro Assays for Predicting Contaminant Relative Bioavailability? Considerations and Criteria. Joint MERA/ICOBTE Sponsored Symposium: Trace Element Bioavailability for Human and Ecological Risk Assessment: Concepts and Recent Advances. Organizers: N. Basta, E. Van Genderen, and C. Schlekat. 12th International Conference for Trace Element Biogeochemistry (ICOBTE), Athens, GA, USA. June 16-20, 2013.
- Nelson, C.M., T.M. Gilmore, J.M. Harrington, K.G. Scheckel, B.W. Miller and K.D. Bradham. 2013. Evaluation of a Low-cost Commercially Available Extraction Device for Assessing Lead Bioaccessibility in Contaminated Soils. 12th International Conference on the Biogeochemistry of Trace Elements, Athens, GA, June 16-20, 2013.
- Stevens, B., N. Basta, S. Whitacre, S. Naber, K. Scheckel, S. Casteel, K. Bradham, and D. Thomas. 2014. Evaluation of Bioaccessibility Methods to Predict Relative Bioavailability of Arsenic in Contaminated Soils. Goldschmidt 2014 Conference, Geochemical Society and European Assoc. of Geochemistry, Sacramento, CA, June 8-13, 2014.
- Whitacre, S., N. Basta, S. Casteel, A. Foster, P. Myers, and V. Mitchell. 2014. Bioavailability Measures for Arsenic in California Gold Mine Tailings. Goldschmidt 2014 Conference, Geochemical Society and European Assoc. of Geochemistry, Sacramento, CA, June 8-13, 2014.
- Whitacre, S.D., N.T. Basta, V.L. Mitchell, and P. Myers. 2013. Bioavailability Measures for Arsenic in Gold Mine Tailings. Joint MERA/ICOBTE Sponsored Symposium: Trace Element Bioavailability for Human and Ecological Risk Assessment: Concepts and Recent Advances. Organizers: N. Basta, E. Van Genderen, and C. Schlekat. 12th International Conference for Trace Element Biogeochemistry (ICOBTE), Athens, GA, USA. June 16-20, 2013.

Non-peer reviewed conference or symposium abstracts (14)

- Basta, N., S.D. Whitacre, K. Scheckel, B. Miller, S. Casteel. 2012. Assessing Oral Human Bioavailability of Arsenic in Soil with in Vitro Gastrointestinal Methods. Presentation 409-8, ASA, CSSA, and Soil Science Society International Annual Meeting, Cincinnati, OH. Oct. 21 to 24, 2012.
- Basta, N., K. Scheckel, K. Bradham, D. Thomas, M. Failla, R. Chaney, C. Schadt, and P. Jardine. 2011. Mechanisms and Permanence of Sequestered Pb and As in Soils: Impact on Human Bioavailability. Partners in Environmental Technology Technical Symposium & Workshop sponsored by Strategic Environmental Research and Development Program (SERDP) and Environmental Security Technology Certification Program (ESTCP), Washington, DC. Nov. 29 to Dec 1, 2011.
- Schadt, C., T. Sullivan-Guest, N. Basta, P. Jardine. 2011. Firing Range Soils Yield a Diverse Fungal Community Capable of Pb-Mineral Solubilization and Organic Acid Secretion. Partners in Environmental Technology Technical Symposium & Workshop sponsored by Strategic Environmental Research and Development Program (SERDP) and Environmental Security Technology Certification Program (ESTCP), Washington, DC. Nov. 29 to Dec 1, 2011.
- Basta, N., K. Scheckel, K. Bradham, D. Thomas, M. Failla, R. Chaney, C. Schadt, and P. Jardine. 2010. Mechanisms and Permanence of Sequestered Pb and As in Soils: Impact on Human Bioavailability. Partners in Environmental Technology Technical Symposium & Workshop sponsored by Strategic Environmental Research and Development Program (SERDP) and Environmental Security Technology Certification Program (ESTCP), Washington, DC. Nov. 30 to Dec 2, 2010.
- Betts, A. R., B. Stevens, N. T. Basta, and K.G. Scheckel. 2015. Correlating arsenic (As) and iron (Fe) speciation to as bioavailability from a collection of contaminated soils with varying contamination sources and soil properties. Presentation 262-6. ASA, CSSA, and Soil Science Society International Annual Meeting, Minneapolis, MN Nov. 15-18, 2015.
- Bradham, K., K. Scheckel, C. Nelson, and D. Thomas. 2015. Development and Application of Site-Specific Arsenic Bioavailability for Contaminated Residential Soils. Bioavailability and Bioaccessibility: Critical Tools For Risk Management Decisions Session, 35th North American Annual Meeting of the Society of Environmental Toxicology and Chemistry, Vancouver, British Columbia, Canada, Nov. 9-13, 2014.
- Bradham, K.D., Scheckel, K.G., Nelson, C.M., Seales, P.E., Lee, G.E., Hughes, M.F., Miller, B.W., and Thomas, D.J. Relative Bioavailability and Bioaccessibility and Speciation of Arsenic in Contaminated Soils. Presentation provided at the Society of Toxicology Annual meeting, San Francisco California, March 12-15, 2012.
- Hughes, M.F., Bradham, K.D., Scheckel, K.G., Seales, P. E., G. Lee, C. Nelson, A. Yeow, S. Harper, and D. J. Thomas. Relative bioavailability of arsenic contaminated soils in a mouse model. Society of Toxicology Annual meeting, Washington DC March 6-10, 2011.

- Hughes, M.F., Bradham, K.D., Scheckel, K.G., Seales, P. E., Lee, G., Nelson, C., Yeow, A., Harper, S., and Thomas, D. J. Relative bioavailability of arsenic contaminated soils in a mouse model. NC Society of Toxicology Annual meeting, RTP NC, February 17, 2011.
- Mitchell, V.L., C.N. Alpers, N.T. Basta, D.L.Berry, J.P.Christopher, D.D. Eberl, C.S. Kim, R.L. Fears, A.E. Foster, P.A. Myers, and B.M. Parsons. 2012. Identifying Predictors for Bioavailability of Arsenic in Soil at Mining Sites. Society of Toxicology Annual Meeting, San Francisco, CA. March11-15, 2011.
- Sullivan, T.S., C. W. Schadt, S. Smith, N. Basta, & P. Jardine. 2013. Mapping Soil Chemical And Microbiological Properties To Help Determine Pb-associated Risks At An Abandoned Small-arms Firing Range. 113th Annual meeting of the American Society for Microbiology, May 19-2, 2013, Denver Colorado
- Sullivan-Guest, T., C.W. Schadt, N. Basta and P. Jardine. Mapping soil lead speciation and soil microbial response at an abandoned firing range in Oak Ridge, TN. 97th Annual Meeting of the Ecological Society of America, Portland, Oregon, August 5th-10th, 2012.
- Sullivan-Guest, T., C.W. Schadt, N. Basta, and P. Jardine. 2011. Firing range soils yield a diverse fungal community capable of pb-mineral solubilization and organic acid secretion. 96th Annual Meeting of the Ecological Society of America. Austin, TX
- Whitacre, S.D., Basta, N., Mitchell, V., and Myers, P. 2012. Bioavailability Measures for Arsenic in Gold Mine Tailings. Presentation 412-1, ASA, CSSA, and Soil Science Society International Annual Meeting, Cincinnati, OH. Oct. 21 to 24, 2012.

Book Chapter (1)

Basta, N.T. and A. Juhasz. 2014. Chapter 9: Using In Vivo Bioavailability and/or In Vitro Gastrointestinal Bioaccessibility Testing to Adjust Human Exposure from Soil Ingestion. In : R.J.Bowell, J. Majzlan and C.Alpers (eds.) Geochemistry, Mineralogy and Microbiology of Arsenic in Environment, Reviews in Mineralogy and Geochemistry, Mineralogical Society of America